Plasmodium-Induced Nitrosative Stress in *Anopheles stephensi*: The Cost of Host Defense

Tina Marie Loane Peterson

Dissertation submitted to the faculty of the Virginia Polytechnic Institute and State University in partial fulfillment of the requirements of the degree of

Doctor of Philosophy

in

Biochemistry

Shirley Luckhart, Advisor

Glenda Gillaspy

Peter J. Kennelly

Timothy J. Larson

Zhijian (Jake) Tu

May 23, 2005

Blacksburg, Virginia

Key words: *Anopheles*, biochemistry, malaria, nitric oxide, nitrosative stress, peroxiredoxin, *Plasmodium*

Plasmodium-Induced Nitrosative Stress in *Anopheles stephensi*: The Cost of Host Defense

By Tina Marie Loane Peterson

Shirley Luckhart, Advisor
Department of Biochemistry

ABSTRACT

Both vertebrates and anopheline mosquitoes inhibit *Plasmodium* spp. (malaria parasite) development via induction of nitric oxide ($^{\bullet}$NO) synthase. Expression of *Anopheles stephensi* $^{\bullet}$NO synthase (*AsNOS*) is induced in the midgut epithelium beginning at 6 h following a *Plasmodium berghei*-infected blood meal. $^{\bullet}$NO reacts readily with other biocompounds forming a variety of reactive nitrogen intermediates (RNIs) that may impose a nitrosative stress. These RNIs are proposed to be responsible for the AsNOS-dependent inhibition of *Plasmodium* development.

In my studies, I identified several RNIs that are induced in the blood-filled midgut in response to *Plasmodium* infection. Stable end products of $^{\bullet}$NO (NO_3^- and NO_2^-), measured using a modified Griess assay, are elevated in infected midguts at 24 h post-blood meal (pBM). Further studies using chemical reduction-chemiluminescence with Hg displacement showed that infected midguts contained elevated levels of potentially toxic higher oxides of nitrogen (NO_x), but *S*-nitrosothiol (SNO) and nitrite levels did not differ between infected and uninfected midguts at 12.5 and 24 h pBM. Thus, nitrates contributed to elevated NO_x levels. SNO-biotin switch westerns indicated that *S*-nitrosated midgut proteins change over the course of blood meal digestion, but not in response to infection. Photolysis-chemiluminescence was used to release and detect bound $^{\bullet}$NO from compounds in blood-filled midguts dissected from 0-33 h pBM. Results showed increased $^{\bullet}$NO levels in *Plasmodium*-infected midgut lysates beginning at 8 h, with significant increases at 12.5-13.5 h and 24-25.5 h pBM and peak levels at 20-24 h. Photolyzed $^{\bullet}$NO is derived from SNOs and metal nitrosyls. Since SNO concentrations did not change in response to infection, I proposed that metal nitrosyls, specifically Fe

nitrosyl hemoglobin (nitrosylHb) based on the concentration of hemoglobin, were elevated in the infected midgut.

At 12-24 h pBM, levels of midgut RNIs in infected mosquitoes were typical of levels measured during mammalian septic inflammation. The inverse relationship between AsNOS activity and parasite abundance indicates that nitrosative stress has a detrimental effect on parasite development. However, nitrosative stress may impact mosquito tissues as well in a manner analogous to mammalian tissue damage during inflammation. Elevated levels of nitrotyrosine (NTYR), a marker for nitrosative stress in many mammalian disease states, were detected in tissues of parasite-infected *A. stephensi* at 24 h pBM. Greater nitration of tyrosine residues was detected in the blood bolus, midgut epithelium, eggs and fat body.

In the midgut, Hb remained in an oxygenated state for the duration of blood digestion. The reaction between $^{\bullet}$NO and oxyhemoglobin (oxyHb) can result in the formation of nitrate and methemoglobin (metHb). Although nitrate levels were elevated in response to parasite infection, there was little to no metHb present in the mosquito midgut. The simultaneous presence of nitrates, nitrosylHb, oxyHb, and NTYR, together with a lack of elevated nitrites and metHb, suggested that alternative reaction mechanisms involving $^{\bullet}$NO had occurred in the reducing environment of the midgut. In addition, I proposed that nitroxyl and peroxynitrite participated in reactions that yielded observed midgut RNIs.

To cope with the parasite-induced nitrosative stress, cellular defenses in the mosquito may be induced to minimize self damage. I proposed that peroxiredoxins (Prx), enzymes that can detoxify peroxides and peroxynitrite, may protect *A. stephensi* from nitrosative stress. Six Prx genes were identified in the *A. gambiae* genome based on homology with known *D. melanogaster* Prxs. I identified one *A. stephensi* Prx, AsPrx, that shared 78% amino acid identity with a *D. melanogaster* 2-Cys Prx known to protect fly cells against various oxidative stresses. AsPrx was expressed in the midgut epithelium and is encoded by a single-copy, intronless gene. Quantitative RT-PCR analyses confirmed that induction of *AsPrx* expression in the midgut was correlated with malaria parasite infection and nitrosative stress. To determine whether AsPrx could protect against RNI- and ROS-mediated cell death, transient transfection protocols were

established for *AsPrx* overexpression in *D. melanogaster* (S2) and *A. stephensi* (MSQ43) cells and for *AsPrx* gene silencing using RNA interference in MSQ43 cells. Viability assays in MSQ43 cells showed that AsPrx conferred protection against hydrogen peroxide, $^{\bullet}$NO, nitroxyl and peroxynitrite. These data suggested that the $^{\bullet}$NO-mediated defense response is toxic to both host and parasite. However, AsPrx may shift the balance in favor of the mosquito.

DEDICATION

To Annika, without whom I would have written this dissertation a lot faster but probably had a mental break down in the process. Your pleasant distractions kept me sane!

ACKNOWLEGDEMENTS

I wish to thank my advisor, Dr. Shirley Luckhart, for her guidance and support of my research. Her example of enthusiasm and perseverance helped to keep my goals in focus when I did not think I had it in me to continue. Her encouragement and frankness have made me a better scientist and made me understand what it takes to become a professional in academia. She was equal parts role model, friend and personal cheerleader. I also wish to thank my graduate committee members, Drs. Gillaspy, Kennelly, Larson and Tu, for serving on my committee. I appreciated their advice as well as the use of their lab equipment and supplies. I also wish to thank Drs. Tom Sitz and John Hess.

I am deeply grateful to Dr. Andrew Gow for all of his help with the midgut RNI analyses. His assistance with the NO-related portion of my work was invaluable. I would also like to acknowledge his technicians, Trevor Fusaro and Christiana Davis, for their help when I visited their lab.

Many thanks to my lab "mates", Dr. Andrea Crampton, Dr. Junghwa Lim, Matthew Lieber, Dr. Theresa "Tree" Dellinger and Michelle Garlic McClanan, who made my days in the lab most… interesting. A special thanks to Andrea and Ken Hurley for getting my butt out of the lab to regain my sanity, and to Tree for her help getting the cell viability studies done before I "popped". I am very appreciative of Randy Saunders for maintaining the insectary and performing the feeds. I would also like to thank the library staff for their great service sending me all of the research materials necessary for completing my writing.

And lastly, thank you to my husband Todd Peterson. I never would have pursued this degree had it not been for him. Although he didn't always understand what I was doing or why, he stuck by me. I know this was especially tough when it meant living in different states for almost two years and missing out on the day to day tribulations of our pregnancy. Nevertheless, he supported my decision to continue on.

TABLE OF CONTENTS

LIST OF FIGURES

CHAPTER ONE

CHAPTER TWO

CHAPTER THREE

LIST OF TABLES

CHAPTER THREE

LIST OF ABBREVIATIONS

aa	amino acid
Ab	Antibody
Ag	*Anopheles gambiae*
Alb	albumin
As	*Anopheles stephensi*
AhpC	alkyl hydroperoxide reductase subunit C
AP	alkaline phosphatase
AS	Angeli's salt; trioxodinitrite
ASE	an *A. stephensi* cell line
1-BAPNA	N-benzoyl-L-arginine, p-nitroanilamide
BCIP/NBT	5-bromo-4-chloro-3-indolyl-phosphate /nitro blue tetrazolium
BCP	bacterioferritin co-migratory protein
bp	base pair(s)
BSA	bovine serum albumin
BLAST	basic local alignment research tool
ºC	degree Celsius
CaM	calmodulin
cDNA	complimentary or copy DNA
C_t	critical threshold cycle
Cyc	cyclophilin
Cys-NO	*S*-nitrosated cysteine
d	day(s)
ddH_2O	distilled, deionized water
DEA-NO	diethylammonium (Z)-1-(N,N-diethylamino)diazen-1-ium-1,2-diolate; diethylamine NONOate; ($^{\bullet}$NO donor)
deoxyHb	hemoglobin without a ligand
DNA	deoxyribonucleic acid
D-NAME	N^G-nitro-D-arginine
DNIC	dinitrosyl iron complex

DNPH	2,4-dinitrophenylhydrazine
dsRNA	double-stranded RNA
DTPA	diethylenetriaminepentaacetic acid
DTT	1,4-dithiothreitol; Cleland's reagent
EDTA	ethylenediaminetetraacetic acid
EPR	electron paramagnetic resonance (spectroscopy)
FAD	flavin adenine dinucleotide
FCS	fetal calf serum
flavoHb	flavohemoglobin (Hmp)
FMN	flavin mononucleotide
g	gram(s)
GC	gas chromatography
GPI	glycosylphosphatidylinositol
GR	glutathione (disulfide) reductase
Grx	glutaredoxin
GSH	glutathione (reduced form); γ-glutamyl-cysteinyl-glycine
GSNO	*S*-nitrosoglutathione
GSSH	glutathione disulfide (oxidized form)
h	hour(s)
H4B	(6R)-5, 6, 7, 8-tetrahydro-L-biopterin
Hb(s)	hemoglobin [ferrous/Fe^{2+}]
HbNO	nitrosyl-hemoglobin
H_2O_2	hydrogen peroxide
HPLC	high pressure liquid chromatography
HRP	horseradish peroxidase
ICR	Institute of Cancer Research
iNOS	inducible NOS
kD	kilodalton(s)
L-NAME	N^G-nitro-L-arginine; (NOS inhibitor)
L-NMMA	N^G-methyl-L-arginine; (NOS inhibitor)
LPS	lipopolysaccharide

metHb	methemoglobin; hemoglobin [ferric/Fe^{3+}]
min	minute(s)
μL	microliter(s)
mL	milliliter(s)
MNC	mononuclear cells
MSQ43	an *A. stephensi* cell line
mRNA	messenger RNA
MS	mass spectroscopy
MW	molecular weight
NAD(P)H	reduced nicotinamide adenine dinucleotide (phosphate)
NEM	*N*-ethylmaleimide
NF-κB	nuclear factor-kappa B
NO or $^{\bullet}NO$	nitric oxide; nitrogen monoxide; oxidonitrogen ($^{\bullet}$)
NO^+	nitrosonium (cation); nitrosyl cation
NO^-	nitroxyl (anion); oxonitrate ($2^{\bullet}1-$)
NO_2^-	nitrite; dioxidonitrate (1-)
$^{\bullet}NO_2$	nitrogen dioxide; dioxidonitrogen
NO_3^-	nitrate; trioxidonitrate (-)
N_2O	nitrous oxide; dinitrogen monoxide
N_2O_3	dinitrogen trioxide
NOA	Siever's nitric oxide analyzer
NOR-3	(E)-Ethyl-2-[(E)-hydroxyimino]-5-nitro-3-hexeneamide; ($^{\bullet}$NO donor)
NOS	nitric oxide synthase
NO_x	collective products of NO oxidation
nt	nucleotide(s)
NTYR	3-nitrotyrosine
O_2	oxygen; dioxygen (triplet)
$O_2^{\bullet-}$	superoxide; dioxide ($^{\bullet}1-$)
O_3	ozone; trioxygen
$OH^{\bullet}$	hydroxyl radical; hydridooxygen
$ONOO^-$	peroxynitrite; oxidoperoxidonitrate (1-)

ONOOH	peroxynitrous acid; hydrogen-oxidoperoxinitrate
oxyHb	oxyhemoglobin
PAGE	polyacrylamide gel electrophoresis
pBM	post-blood meal
PBS	phosphate-buffered saline
PCC	protein carbonyl content
PCR	polymerase chain reaction
PM	peritrophic matrix or membrane
PN	peroxynitrite ($ONOO^-$ and ONOOH)
pO_2	oxygen tension, partial oxygen pressure
PPi	pyrophosphate
Prx	peroxiredoxin
qRT-PCR	quantitative real-time RT-PCR
RACE	rapid amplification of cDNA ends
RBC(s)	red blood cell(s); erythrocytes
RNA	ribonucleic acid
RNAi	RNA interference
RNI(s)	reactive nitrogen intermediate(s)
RNNO	*N*-nitroso compounds
RNS	reactive nitrogen species
ROS	reactive oxygen species
RT-PCR	reverse transcription-polymerase chain reaction
s	second(s)
S2	*Drosophila melanogaster* Schneider 2 cells
SDS	sodium dodecyl sulfate; lauryl sulfate
SE(s)	standard error(s)
SIN-1	3-morpholino-sydnonimine ($^{\bullet}NO$ and peroxynitrite donor)
SNAP	*S*-nitroso-*N*-acetylpenicillamine ($^{\bullet}NO$ donor)
SNO	*S*-nitroso compounds; *S*-nitrosothiol ($^{\bullet}NO$ or NO^+ donor)
SNO-102	4-(phenylsulfonyl)-3-((2-(dimethylamino)ethyl)thiol)-furoxan oxalate; ($^{\bullet}NO$ donor)

SNO-Alb	*S*-nitrosoalbumin
SNOHb	*S*-nitrosohemoglobin
SNP	sodium nitroprusside; sodium nitroferricyanide(III) dehydrate; ($^{\bullet}NO$ and NO^{+} donor)
SOD	superoxide dismutase
Srx	sulfiredoxin
SSC	sodium chloride-sodium citrate buffer
SSPE	sodium chloride-sodium phosphate-EDTA buffer
ssRNA	single-stranded RNA
TBS	tris-buffered saline
TBF-β	transforming growth factor beta
Trx	thioredoxin
TrxR	thioredoxin reductase
TNF-α	tumor necrosis factor-alpha
UV-Vis	ultraviolet-visible (spectroscopy)

CHAPTER ONE: Literature review

IDENTIFYING THE CAUSE OF MALARIA (reviewed in **[1, 2]**)

The first documented symptoms of malaria were described in Chinese medical texts in 2700 BC. Later the *Susruta* (Sanscrit medical texts) attributed the symptoms to certain insect bites. Several Roman writers believed that malaria was a swamp disease, caused by bad air. Hence, the name of the disease is derived from Latin 'mal aria' meaning 'bad air'. The term was used to describe the illness malaria or anything resembling malaria for more than 4,000 years.

Following the development of Louis Pasteur's theory that microorganisms cause infectious diseases, the French military surgeon Charles Louis Alphonse Laveran identified the malarial parasite in a patient's blood while stationed in Algeria in 1880. Because malaria was considered to be due to bad air of marsh lands, Laveran searched for the microbe in the air, soil and water of these marshlands. The search turned up nothing and Laveran hypothesized that mosquitoes, abundant in the area, may carry the disease agent ("Treatise on Marsh Fevers"; 1884). Laveran believed that only one species, *Oscillaria malariae*, caused malaria. Later, two Italian investigators, Giovanni Batista Grassi and Raimondo Filetti, introduced the names *Plasmodium vivax* and *Plasmodium malariae* to two species discovered in 1890. Then the American, William H. Welch, named *Plasmodium falciparum* in 1897 and John Williams Watson Stephens named *Plasmodium ovale* in 1922. These discoveries completed the identification of the four human malaria parasites that we know today.

The British Army medical officer, Ronald Ross, demonstrated that mosquitoes transmitted *Plasmodium relictum*, a bird malaria parasite, and that the sporogonic cycle takes place in the mosquito. Grassi and a team of Italian investigators showed that the four human malaria parasites complete their sporogonic cycles when *Anopheles claviger* fed on infected patients. Subsequently, Grassi and others demonstrated that infected mosquitoes could infect healthy volunteers (1899). Ross was awarded the Nobel Prize in 1902 and Laveran was recognized with this honor in 1907.

EARLY CONTROL OF MALARIA (reviewed in **[1, 2]**)

With the identification of the malaria parasite life cycle, control of mosquito populations was a focus for malaria and yellow fever control. During the construction of the Panama canal (1905-1910), control efforts were lead by William Crawford Gorgas, Joseph Augustin LePrince and Samuel Taylor Darling. Methods of mosquito control included draining pools of water and cutting grass/brush within 100 yards of all houses, adding oil to areas where drainage could not occur, killing larvae with a carboxylic acid, providing quinine to workers, screening buildings against mosquitoes and manually collecting and removing adults from tents and houses. From 1914-1942, the U.S. Public Health Service requested funds to employ similar control measures to control malaria in the southern US. Malaria existed in parts of the US from colonial times until the 1940s. More than 600,000 cases of malaria occurred in the US in 1914 **[3]**. From 1947-1951, the National Malaria Eradication Program, which consisted of the CDC and state and local health agencies, used insecticidal spraying to control malaria in the southern US. Dichloro-diphenyl-trichloroethane (DDT), a commonly used insecticide, was first synthesized in 1874 by a German Chemistry student, Othmer Zeidler, for his thesis! In 1939 Paul Muller of Switzerland discovered that it had insecticidal properties and in 1948 he received a Nobel prize for this discovery. By 1951, malaria was considered to be eradicated from the US. Of the ten species of *Anopheles* in the US, *Anopheles quadrimaculatus* in the eastern US and *Anopheles freeborni* in the western US, were of primary importance for malaria transmission. These species are still prevalent in the US, thus the risk of re-emergence is possible. In fact, autochthonous transmission of malaria in the US has been attributed to these species.

Two currently used antimalarial drugs are derived from plants whose medicinal values had been noted for centuries. These drugs include artemisinin from *Artemisia annua*, the Qinghao plant, used in China since the 2nd century BC to treat fevers of unknown origin and quinine from the bark of the Cinchona tree, discovered as an ancient local remedy in Peru by European explorers in the 17th century. Chloroquine or Resochin, a synthetic derivative of chloroquine, was discovered in 1934 by Hans Andersag at Bayer

in Germany. However, the events of World War II prevented the establishment of chloroquine as an antimarial until 1946.

RE-EMERGENCE OF MALARIA (reviewed in **[1, 2]**)

The WHO estimates that more than 40% of the world's population live in areas where malaria naturally occurs and where it is a leading cause of death and illness. Malaria afflicts an estimated 300-500 million people per year while killing over one million annually (WHO, Oct 1999); 90% of the world's malaria deaths occur in sub-Saharan Africa. However, despite the 1955 WHO initiative to eliminate malaria world wide, malaria is a re-emerging disease. The disease has returned to areas from which it had been eradicated, and has spread into new areas in central Asia and eastern Europe. Sadly, more people are dying of malaria today than thirty years ago **[4]**. Contributing to this problem are the increasing numbers of drug resistant-parasites, particularly in Asia, and mosquitoes that are resistant to the major classes of insecticides. As the world's population has grown, so has the rate of transmission. Increases in road building, mining, deforestation, new agricultural and irrigation projects have created new breeding sites for mosquitoes. Similarly, increased travel, climatic change and the creation of new habitats have increased the risk of transmission to populations with no natural immunity, resulting in disease with greater severity and higher risk of death. A symptom of this trend is the increasing number of "airport malaria" cases in which infected travelers bring malaria to non-endemic regions. In many regions, malaria control programs have deteriorated or been abandoned due to war, poor socio-economic conditions or lack of community participation.

To help control the spread of malaria, global efforts are focused on the development of new control strategies. One such strategy is the creation of transgenic mosquitoes that are incapable of parasite transmission. This strategy requires a better understanding of vector biology and insect immunity to identify targets for gene manipulation and to predict the physiological and population genetic consequences of this manipulation to control transmission.

***PLASMODIUM BERGHEI* LIFE CYCLE IN *ANOPHELES STEPHENSI* (Fig. 1-1)**

Plasmodium spp. are single-celled protozoans and obligate parasites. Only sexual stage parasites are infectious to the mosquito, the host used for the completion of sexual stage development. Parasites enter the midgut with the blood meal, and within 15 min after blood ingestion, male gametocytes undergo exflagellation. Fertilization occurs 30 min to 2 h post blood meal (pBM), forming diploid zygotes. Between 3 h and 20 h pBM, the zygotes become motile and develop into ookinetes. These mobile ookinetes leave the blood bolus and invade the midgut epithelium at 24-36 h pBM. After invasion, the ookinetes settle under the basal lamina and transform into vegetative oocysts. Oocyst maturation takes 8-11 days (d). Within the oocysts, the parasites undergo meiosis to form haploid sporozoites. After 12-14 d pBM, the oocysts deteriorate and release the sporozoites into the hemolymph. Hemolymph circulation in the open circulatory system and sporozoite movement carry the parasites to the salivary glands, where, during a subsequent blood meal, they are injected with saliva into the host. *Plasmodium berghei* is a murine parasite that develops normally in *Anopheles stephensi*, providing a useful model system for laboratory assays of parasite infection **[5]**.

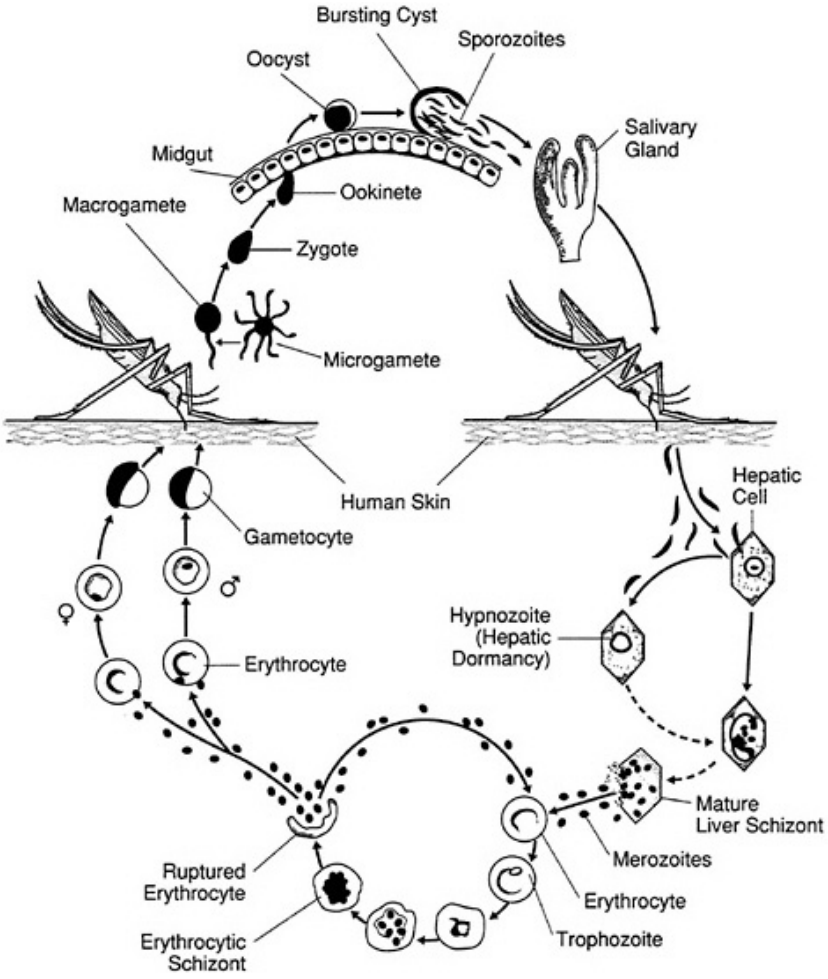

Figure 1-1: Life cycle of *Plasmodium* spp.

Malaria parasites are obligate parasites with a two-host life cycle. The erythrocytic cycle encompasses the asexual stages and occurs in vertebrate hosts such as man or mouse. The sexual stages occur in mosquito species of the genus *Anopheles*. (Ilustration by Nancy Lou Gahan Riccio **[6]**[1].)

[1] Permission to reproduce image has been granted by the illustrator: Nancy Lou Gahan Riccio.

GENERAL IMMUNE RESPONSE OF INSECTS (reviewed in **[7-9]**)

The ongoing concern with the emergence of drug resistant parasites and insecticide resistant mosquitoes has prompted the scientific community to investigate novel strategies to control the spread of malaria. The understanding of parasite-mosquito interactions is essential to develop novel strategies which impede transmission of *Plasmodium* spp. by mosquitoes. I am part of a small group of researchers investigating mosquito genes that are associated with the immune response which may be useful as targets for the development of mosquitoes with refractory phenotypes.

How do insects deal with infection? Insects do not have adaptive immunity (*e.g.* B-cells, antibodies), thus their defense system relies on an innate immune response and physical barriers that include the exoskeleton, peritrophic matrix and various tissue barriers. The innate immune responses of insects are less complex than adaptive immune responses, but upon challenge, innate responses can be activated quickly with a degree of specificity (reviewed in **[8]**). Innate immunity consists of both humoral and cellular responses that are activated following recognition of foreign molecules by receptors. Cellular responses include encapsulation and phagocytosis mediated by the circulating blood cells (hemocytes), while humoral responses include agglutination, melanization and the production of antimicrobial molecules, including bioactive peptides and nitric oxide ($^{\bullet}$NO).

At least two pathways are involved in the immune response of *Drosophila melanogater* to bacteria and fungi (reviewed in **[10]**). The Toll signaling pathway, which controls defenses against fungi and Gram-positive bacteria, and the immune deficiency pathway (Imd), which mediates defenses against Gram-negative bacteria. Antimicrobial peptides, 20-40 amino acids in length, are produced in the epithelial tissues and fat body in response to infection. Most are specific for a particular class of pathogens. Several antimicrobial peptides have been identified in *Anopheles* spp., including defensins, cecropins, attacin and gambicin **[7, 9, 11-13]**. In *A. gambiae* the defensins, crecropins and gambicin are induced in response to malaria parasite infection **[14]**. In transgenic *Aedes aegypti*, the overexpression of crecropin in the posterior midgut at 24 h pBM resulted in a 60% reduction in the number of *Plasmodium berghei* oocysts relative to control

mosquitoes **[15]**. Although defensin is induced in the *A. gambiae* midgut epithelium in response to *P. berghei* invasion **[7]**, disruption of defensin by RNAi did not increase oocyst numbers **[16]**, suggesting that antimicrobial peptides are not directly toxic to developing malaria parasites.

The immune organs of insects include the fat body, epithelial tissues, and hemolymph (reviewed in **[1]**). Fat body and hemocytes are comparable to the vertebrate liver and blood cells, respectively, and are major mediators of the systemic immune response. The gut responses are particularly important in those vectors in which pathogens complete developmental stages in this organ (*e.g. Plasmodium* spp. and *Trypanosoma* spp.). In these vectors, stage changes in parasites result in sequential losses in parasite numbers. Specifically when parasites transition from gamete to ookinete, from ookinete to oocyst, and from oocyst sporozoite to salivary gland sporozoite, significant losses in parasite numbers occur **[17]**. Two of these stage-transition losses occur in the midgut, making this organ an attractive target for efforts to further reduce or eliminate parasite development.

NITRIC OXIDE SYNTHASE (NOS) (Fig. 1-2)

Nitric oxide ($^{\bullet}$NO) is synthesized by a family of $^{\bullet}$NO synthases [NOS; L-arginine, NADPH:oxygen oxidoreductases ($^{\bullet}$NO forming); EC 1.14.23.39]. Three major vertebrate NOS isoforms have been identified: NOS-I (nNOS), a form initially associated with the brain; NOS-II (iNOS), a form most closely associated with macrophages; and NOS-III (eNOS), an isoform that is localized in epithelial cells. Neuronal NOS and eNOS are predominantly constitutively expressed whereas iNOS is an inducible immune effector **[18]**. Inducible NOS and $^{\bullet}$NO are synthesized in response to bacterial, viral, and parasitic infections in vertebrates **[19, 20]**. All three NOS isoforms require heme, flavin adenine dinucleotide (FAD), flavin mononucleotide (FMN), (6R)-5, 6, 7, 8-tetrahydro-L-biopterin (H4B), reduced nicotinamide adenine dinucleotide phosphate (NADPH), O_2, and calmodulin (CaM) to catalyze the synthesis of $^{\bullet}$NO **[21-25].** The $^{\bullet}$NO synthases are composed of two globular protein modules (domains) connected via a flexible protein

hinge region. The N-terminal oxygenase domain contains the catalytic center for •NO production, while the C-terminal reductase domain catalyzes the dehydrogenation of NADPH and supplies the electrons required for •NO synthesis. Electron transfer is activated by the binding of CaM to a site on the flexible hinge. All NOS isoforms function as homodimers and catalyze the same two-step reaction sequence. Specifically, L-Arginine is oxidized to the stable intermediate N^G-hydroxy-L-arginine, which is subsequently oxidized to form •NO and L-citrulline. Both steps in this sequence are NADPH- and O_2-dependent **[21-23]**. The nitrogen of the resulting •NO is derived from the nitrogen of the guanidino group of L-arginine **[26, 27]**, while the oxygen is derived from molecular oxygen **[28, 29]**.

Under normal conditions, the NOS domains work cooperatively to catalyze the synthesis of •NO. However, under certain conditions the oxidation reactions can become uncoupled resulting in alternate reactive species being formed. Nitroxyl (HNO/NO^-), the one electron reduction product of •NO, is a product of L-arginine oxidation by NOS when H4B or superoxide dismutase (SOD) levels are low **[30-35]**. Nitroxyl may also be produced by the oxidation of the decoupled NOS product N^G-hydroxy-L-arginine; it has been reported that up to 50% of NOS catalysis results in N^G-hydroxy-L-arginine formation **[36]**. Under conditions of L-arginine depletion, NOS reduces O_2 with the formation of H_2O_2 **[37-39]**. Alternatively, NOS can catalyze the synthesis of superoxide **[40-45]**.

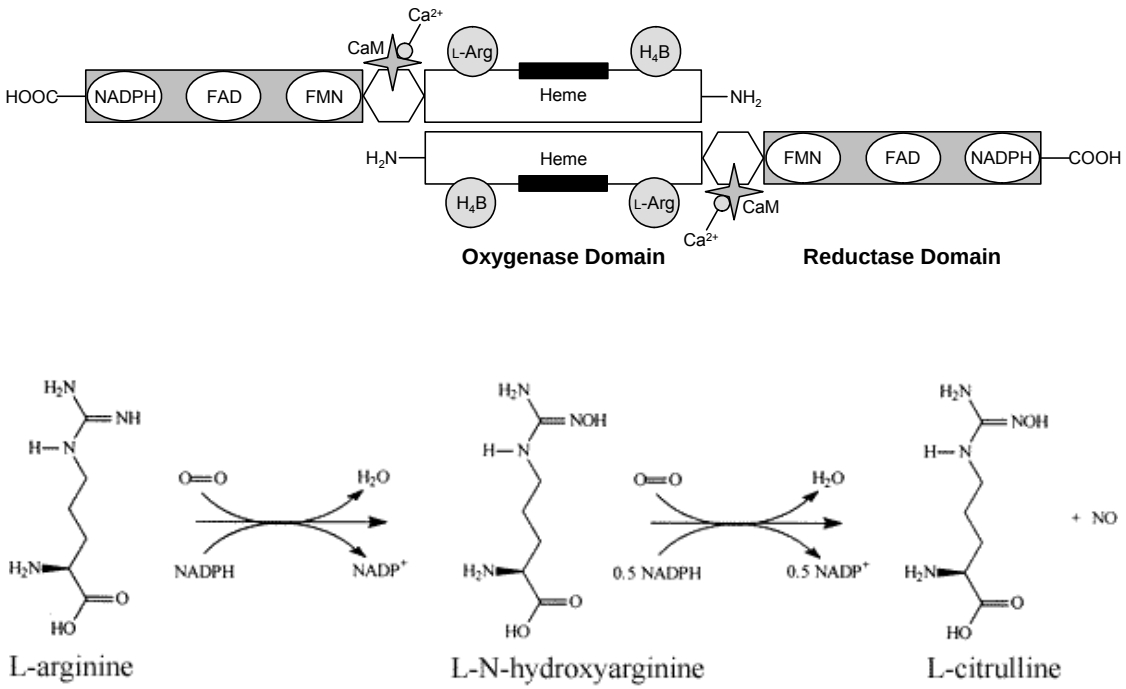

Figure 1-2: Nitric oxide synthase (NOS) [46].

Dimeric NOS catalyses the conversion of L-arginine to L-citrulline and NO.

***ANOPHELES STEPHENSI* NOS (AsNOS)**

Anopheles stephensi possesses a single copy of an inducible NOS gene (*AsNOS*; **[47] (Fig. 1-3)**. The *AsNOS* gene encodes 19 exons and is transcribed with a complex series of alternative splicing events that generate 22 transcripts; three of these transcripts are significantly induced in response to *P. berghei* infection **[48]**. As with other insect NOSs, the AsNOS protein (1,247 amino acids) shares highest homology to vertebrate nNOS **[49-52]**. From intron-exon structural analyses, it is believed that the insect and vertebrates NOS genes are derived from a common ancestor **[52, 53]**.

Drosophila melanogaster NOS (*DmNOS*) also encodes 19 exons. Transcription of *DmNOS*, like *AsNOS*, is complex and is characterized by alternate start sites and splicing to form at least ten transcripts throughout the period of fly development **[54]**. The amino acid sequence of DmNOS is 81% similar and 69% identical to the predicted amino acid sequence of AsNOS. In addition, *DmNOS* exons 4-7, 10, 12 and 13 correspond exactly to

AsNOS exons 2-5, 7, 10 and 11. *DmNOS* exon 11 is equivalent to exons 8 and 9 of *AsNOS*, and *DmNOS* exons 8 and 9 correspond to exon 6 of *AsNOS*.

To date, the alternate transcripts of *AsNOS* have not been studied in detail. As such, we have no data on whether truncated AsNOS proteins can catalyze the synthesis of •NO. Based on data from other systems, however, some truncated NOS polypeptides can form heterodimers with full length NOS to regulate NOS activity **[54]**. Several of the truncated *AsNOS* transcripts would be predicted to lack the reductase domain following translation **[48]**. If these transcripts were translated, they could form heterodimers with full-length AsNOS. Similar heterodimers from other systems have been shown to be catalytically active *in vitro*. Some isoforms of human iNOS synthesized in response to inflammatory cytokines appear to lack some encoded exon sequences **[55]**. The amino acids involved in binding to H4B are encoded by exons 6 and 8 of *AsNOS* and some transcripts appear to lack these exons **[48]**. By analogy to human iNOS, AsNOS isoforms lacking these encoded exons may be synthesized during inflammatory responses and may potentiate the production of toxic RNIs. Thus, alternative AsNOS transcripts and truncated proteins may regulate or modulate synthesis of •NO activity during an immune response.

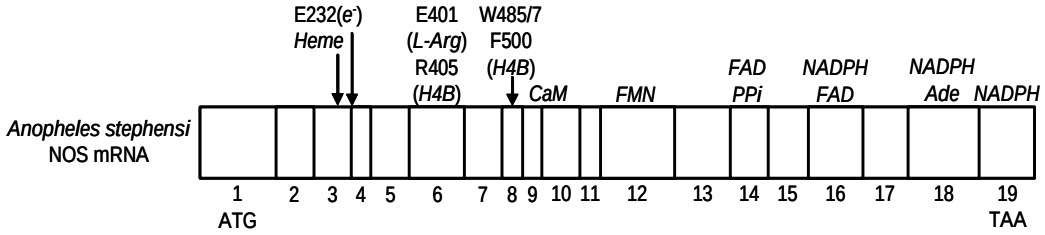

Figure 1-3: The predicted mRNA structure of *A. stephensi* NOS [48, 52].

Anopheles stephensi contains a single copy NOS gene spanning ~37 kb of genomic sequence encoding an open reading frame of 1,247 amino acids in 19 exons. Predicted conserved binding sites for amino acids believed to be involved in electron transfer (e^-), binding of L-arginine (*L-Arg*) and binding of tetrahydrobiopterin (*H4B*) are indicated. Predicted co-factor binding domains for calmodulin (*CaM*), flavins (*FAD PPi*, *FAD*, *FMN*) and NADPH/NADPH adenine (*Ade*) are also indicated. Translational start and stop codons are indicated in exons 1 and 19.

AsNOS AND *PLASMODIUM* INFECTION

Soon after blood ingestion, expression of *AsNOS* leads to •NO production that limits malaria parasite development **[52]**. *AsNOS* expression is induced by blood feeding alone, but there is greater induction in *P. berghei*-infected mosquitoes **[52]**. Quantitative, Reverse Transcription Polymerase Chain Reaction (qRT-PCR; ABI Prism® 7700, PE Biosystems) experiments revealed that the midgut of *A. stephensi* is the primary site of *AsNOS* induction following blood feeding. Significant induction in *AsNOS* expression occurs at 6 h, 9 h **[52]**, 36 h, and 48 h pBM and is indicative of a biphasic induction pattern **(Fig. 1-4; [56])**. In other work, expression of *A. gambiae* NOS was induced at 24 h pBM in response to parasite infection **[7, 11, 57]**. Similarly, NADPH-dependent diaphorase staining was more intense in *Plasmodium*-infected *A. stephensi* midguts at 24 h pBM relative to controls fed an uninfected blood meal **(Fig. 1-5)**, indicating that AsNOS protein was active at that time. Staining was more intense in the posterior midgut, an area where parasite development typically occurs. AsNOS activity, measured by the catalytic conversion of L-Arginine to L-Citrulline, was 5.3-fold higher in infected mosquitoes compared to uninfected, bloodfed controls **[52]**. Nitrites and nitrates, stable end products of •NO synthesis, were also significantly higher in the hemolymph of infected mosquitoes relative to uninfected mosquitoes at 7-14 d pBM **(Fig. 1-6)**. Dietary provision of the NOS inhibitor L-NAME to infected *A. stephensi* significantly increased the number of oocysts that developed relative to parasite numbers in mosquitoes fed inactive D-NAME **[52]**, indicating that •NO acts on parasites prior to oocyst development.

During the period from 6-48 h pBM, *Plasmodium* spp. ookinetes develop, invade the mosquito midgut epithelium and develop into oocysts. Inducible synthesis of *AsNOS* is proportional to the intensity of the parasite infection, thus induction variability is due to variation in the level of parasite infection **[58]**. In sum, induction of *AsNOS* expression parallels key stages of *P. berghei* development in the midgut. Strategies to further limit development of *Plasmodium* spp. in the midgut or at the midgut/hemocoel boundary are likely to be successful because parasite numbers are lowest at this stage of development **[59].**

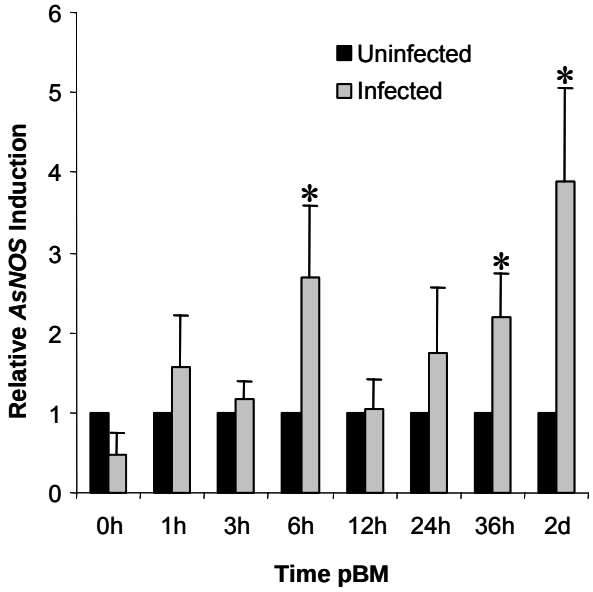

Figure 1-4: Induction of *AsNOS* in midguts from *Plasmodium*-infected mosquitoes. (Fig. 1A from **[56]**[2])

Quantitative RT-PCR was used to analyze the induction of *AsNOS* in *A. stephensi* midgut tissue following uninfected and *P. berghei*-infected blood meals. Data from six cohorts of mosquitoes were averaged and relative expression was measured; at each time point, expression levels were divided by expression in uninfected insects to show relative *AsNOS* induction in *P. berghei*-infected *A. stephensi*. Significantly enhanced levels of *AsNOS* expression in *P. berghei*-infected *A. stephensi* relative to uninfected *A. stephensi* are indicted with an asterisk (*; $p < 0.05$).

[2] Copyright © 2003, the American Society for Microbiology. All rights reserved.

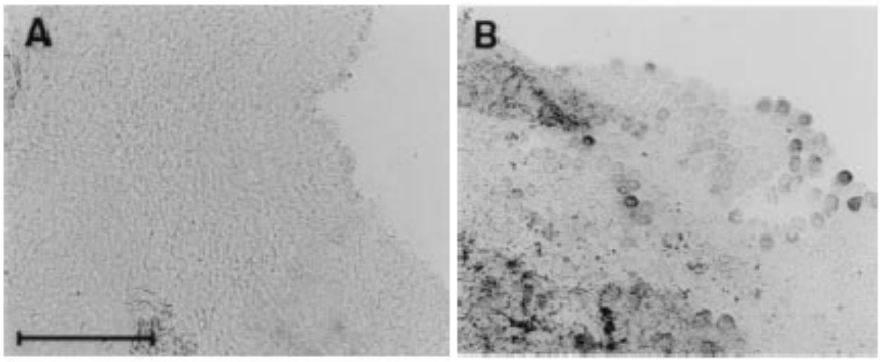

Figure 1-5: NOS activity in *A. stephensi* midguts. (Fig. 4 from **[52]**[3])

Midguts from uninfected blood fed and *P. berghei*-infected *A. stephensi* were dissected and stained for NOS activity based on the diaphorase reaction. The darker areas indicated the precipitation of diformazan resulting from NOS activity. (A) Uninfected midgut tissue at 24 h pBM. (B) *P. berghei*-infected midgut tissue at 24 h pBM. (Bar = 300 μm). NOS activity was significantly greater in posterior midgut cells, an area where midgut invasion and parasite development are concentrated **[60]**.

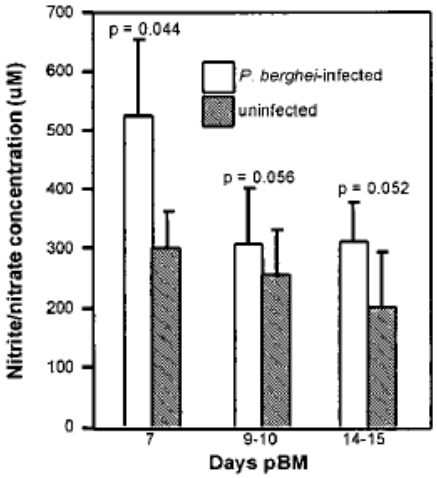

Figure 1-6: Hemolymph nitrite/nitrate levels in uninfected and *P. berghei*-infected *A. stephensi*. (Fig. 5 from **[52]**[4])

Nitrite/nitrate levels in hemolymph collected 7, 9-10, and 14-15 days pBM were determined by cadmium reduction/Griess reagent microassay **[61]**. Nitrite/nitrate levels were significantly greater in *P. berghei*-infected mosquitoes at all time points (paired *t* test). This increase correlates with the onset of sporozoite release, suggesting a role for AsNOS in the innate immune defense against this developmental stage of mosquito malaria.

[3] Copyright © 1998, National Academy of Sciences, USA. All rights reserved.
[4] Copyright © 1998, National Academy of Sciences, USA. All rights reserved.

ANOPHELES MIDGUT ENVIRONMENT

When female anopheline mosquitoes consume blood to supply proteins for egg development, they may be exposed to blood-borne pathogens including *Plasmodium* spp. To analyze the interaction between malaria parasites and mosquito-derived $^{\bullet}$NO it is necessary to understand the midgut environment. Ingested blood is stored and digested in the midgut and blood-derived nutrients are absorbed by the midgut epithelium, a single layer of ~1,500 cells with microvilli. A basement membrane called the basal lamina surrounds the midgut and faces the hemocoel. During blood feeding, the epithelial cells secrete digestive enzymes and a chitin-like material that forms the peritrophic membrane (PM). The PM is a polysaccharide matrix 1-2 μm thick that forms a protective permeable barrier between the blood bolus and the epithelium **[62]**. *Anopheles stephensi* ingests 2-10 μL of blood that is concentrated to a volume of 1-2 μL by diuresis. In general, the pH of the mosquito midgut is slightly less than 7 prior to the blood meal, but increases up to ~8 at 6-24 h pBM; the exact pH and timing of changes pBM are dependent on mosquito species **[63, 64]**. Net consumption of protein from blood is ~550 μg **[65]**, ~500 μg of which is hemoglobin (Hb) **[66]** and ~4 μg of which is soluble protein **[67]**. The midgut protein concentration remains constant for ~9 h pBM, with protein digestion commencing around 12 h **[68]**. Digestive enzymes include trypsins and aminopeptidases, with peak concentrations of these enzymes occurring at 24-33 h pBM. Over a period of 48 h, digestion occurs from the periphery of the blood bolus to the center. Intact erythrocytes have been detected in the blood bolus center up to 24 h pBM. Free heme from Hb digestion is converted to hematin that adheres to the PM. After ~48 h of digestion the remaining blood bolus and PM are excreted **[69, 70]**.

•NO AND ITS CHEMISTRY

History. From the discovery of nitroglycerin **[71]** to the development of Viagra® **[72]**, •NO has played a part in vascular biology for almost 150 years. However, the study of •NO *per se* did not begin until the late 1980s when it was discovered that •NO functions as a signaling mediator in an array of physiological processes, including regulation of blood flow/pressure, neurotransmission and immune responses. For their work in identifying •NO as endothelium derived relaxing factor (EDRF) **[73]**, Robert Furchgott, Louis Ignarro and Ferid Murad were awarded the 1998 Nobel prize in Physiology or Medicine. Until these discoveries, •NO was known only as a component of air pollution **[74]** and the mechanism of action of nitroglycerin was unknown. In 1992, •NO was named *Science* magazine's "Molecule of the Year" **[75]**. To understand the diverse physiological effects of •NO, one must first understand the biological chemistry of •NO.

General •NO reactions. At only 30 Daltons, the •NO radical is the smallest molecule that can transport an electron **[76, 77]**. •NO is lipophilic and soluble in water (1.6 mM at 37ºC) **[78]** and has a short half-life (on the order of seconds) that is dependent on concentration **[79]**.

•NO can have anti-oxidant, anti-inflammatory and tissue protective properties **[80]**. However, this free radical has also been implicated in various pathological conditions. To understand how •NO can both protect and damage cells, it is necessary to understand its chemistry. Nitric oxide has three redox related forms, nitroxyl anion (NO^-, oxonitrate(1-)), nitric oxide (•NO, nitrogen monoxide) and nitrosonium cation (NO^+, nitrosyl cation) in which the nitrogen atom has formal positive oxidation states of I, II, and III, respectively. Although •NO is a radical, it does not show a strong tendency to dimerize. Loss of the unpaired electron produces NO^+ (isoelectronic with N_2 and CO) while the gain of an electron produces NO^- (isoelectronic with dioxygen) **[81]**. •NO, NO^- and NO^+ can be interconverted and yet each species has its own unique biological affects **[78, 81, 82]**. As such, these various species must be accounted for when investigating the biological roles of nitric oxide.

Physiological levels of •NO are 10-2,000 nM, with levels >1 μM typically associated with infection **[83]**. The effects of •NO can be classified as direct or indirect **[84]**. Direct effects usually occur at low •NO concentrations (<1 μM), while indirect effects occur at high •NO concentrations (>1 μM), such as those associated with inflammation **[85]**. Direct effects derive from the interactions between •NO and biological targets. Indirect effects derive from reactions of •NO with biological molecules to form secondary compounds which can exert a variety of effects on biological targets. The indirect effects of •NO, produced through the interaction of •NO with either O_2 or superoxide ($O_2^{\bullet-}$), include nitrosation (when NO^+ reacts with an amine, thiol, or hydroxyl aromatic group), oxidation (when one or two electrons are removed from a substrate), or nitration (when NO_2^+ reacts with target group) **[85]**. Thus, concentration of •NO produced is a major determinant of whether the biological effects of •NO are regulatory or cytotoxic.

In an aqueous solution in the absence of oxidizing agents (*e.g.* oxyHb and $O_2^{\bullet-}$), •NO undergoes auto-oxidation **[reactions 1-3] [82, 86-88]**. However, in biological systems, •NO interacts/reacts readily with other molecules. Primary targets of reactions of •NO, or its redox related forms, include transition metals, oxygen species, and reduced thiols **[86, 89-91]**. In general, •NO and related compounds including SNOs, peroxynitrite (PN), nitrite and nitrate are referred to as reactive nitrogen intermediates (RNIs) **[92]**. The composition of RNIs formed depends on the local concentration of •NO and the immediate environment.

$$2\,{}^{\bullet}NO + O_2 \rightarrow 2\,{}^{\bullet}NO_2 \qquad \textbf{(1)}$$

$$2{}^{\bullet}NO_2 + 2{}^{\bullet}NO \rightarrow 2N_2O_3 \qquad \textbf{(2)}$$

$$2N_2O_3 + 2H_2O \rightarrow 4H^+ + 4NO_2^- \qquad \textbf{(3)}$$

Metal-nitrosyl. •NO can serve as a ligand for a variety of metal complexes **[93]**. Nitrosylation involves the direct binding of •NO to a metal (Fe unless otherwise specified) forming a metal-nitrosyl complex without a net change in redox state **[reaction 4] [94, 95]**. The best known example of this interaction is the reaction of •NO with the heme iron of guanylate cyclase to form Fe-nitrosyl which activates the enzyme (reviewed

in **[96]**). $^{\bullet}$NO can also inactivate enzymes, such as aconitase, by reacting with Fe in Fe-S clusters **[97]**. The nitrosyl-heme adduct is measurable in blood during inflammation (*e.g.* sepsis **[98]** and allograft rejection **[99]** but is otherwise below the limits of detection **[37, 100]**. The formation of metal-nitrosyl complexes is reversible, thus they can stabilize $^{\bullet}$NO and preserve $^{\bullet}$NO bioactivity **[101, 102]**. Metal nitrosyl complexes can also decay to yield NO^+ **[103, 104] [reaction 5]** or NO^- **[81, 105-107] [reaction 6]**. In the case of dinitrosyl iron complexes (DNIC), both NO^- and NO^+ may be released **[108]**. The ability of $^{\bullet}$NO to bind to metals in several redox forms makes it a unique ligand (reviewed in **[109]**).

$$Fe^{2+} + {}^{\bullet}NO \Leftrightarrow (Fe^{2+})\text{–}NO \qquad \textbf{(4)}$$

$$Fe^{3+} + {}^{\bullet}NO \rightarrow [(Fe^{2+})\text{–}NO^+] \rightarrow Fe^{2+} + NO^+ \qquad \textbf{(5)}$$

$$(Fe^{2+})\text{–}NO \rightarrow [(Fe^{3+})\text{–}NO^-] \rightarrow Fe^{3+} + NO^- \qquad \textbf{(6)}$$

Nitroxyl. The formation of nitroxyl can occur by several mechanisms. NOS can directly catalyze the synthesis of NO^- **[30-35, 110]** and oxidative decomposition of the NOS catalytic intermediate, N^G-hydroxy-L-arginine, can yield NO^- **[34, 110]**. It has been reported that up to 50% of the metabolism of NOS results in N^G-hydroxy-L-arginine formation **[36]**. NO^- can also be released from Fe^{2+} nitrosyl resulting in the formation of Fe^{3+} **[81, 105-107] [reaction 6]**. Another potential source of NO^- is the metal catalyzed reduction of $^{\bullet}$NO through a DNIC **[reaction 7 and 8] [108, 111-114]**. NO^- is also formed during the decomposition of SNOs in the presence of thiols **[reaction 9] [115-121]** and several researchers have reported that SOD mediates reversible conversion of $^{\bullet}$NO and NO^- **[30, 32, 122-125]**. Liochev and Fridovich **[126]** suggest that binding of $^{\bullet}$NO at the active site of SOD changes the properties of this reaction leading to production of bound NO^- followed by reaction with oxygen to yield PN. In addition PN can dissociate to NO^- and singlet oxygen **[reaction 10] [127]**.

$$Fe^{2+} + 2{}^{\bullet}NO \rightarrow Fe^{2+}(NO)_2 \qquad \textbf{(7)}$$

$$Fe^{2+}(NO)_2 + {}^{\bullet}NO \rightarrow Fe^{+}(NO^+)_2 + NO^- \qquad \textbf{(8)}$$

$$RSNO + {}'RSH \rightarrow HNO + {}'RSSR \qquad \textbf{(9)}$$

$$ONOO^- \rightarrow NO^- + O_2 \qquad \textbf{(10)}$$

Nitroxyl anion and its conjugate acid (NO^-/HNO) participate in RNS-mediated oxidative reactions **[128-130]**, but the chemistry of NO^- is significantly different than that of $^{\bullet}NO$ or PN **[128, 129, 131-133]**. For example, $^{\bullet}NO$ attenuates post-ischemic myocardial tissue damage, while NO^- aggravates it **[133]**.

NO^- reacts with a variety of targets. The release of NO^- in the absence of other reactions will result in dimerization of NO^- to yield nitrous oxide **[reaction 11] [81, 134]**. In the absence of other reactions, NO^- can also react with $^{\bullet}NO$ to form nitrous oxide and nitrite **[reaction 12] [135]**. The chemistry of NO^- and PN are directly linked because NO^- can react with dioxygen to form PN (5.7×10^7 $M^{-1}s^{-1}$) **[reaction 13] [81, 107, 129, 132, 136, 137]**. NO^- can bind to metal centers to yield two products. First, NO^- can interact with ferric heme to produce $^{\bullet}NO$ and with ferric heme to yield ferrous heme **[reverse of reaction 6] [138]** and ultimately Fe-nitrosyl **[115, 138-141] [reaction 14]**. This reaction can compete with the decomposition of NO^- to N_2O **[141]** and the reaction of NO^- with oxygen to form PN. NO^- can react with excess thiols to form hydroxylamine and the corresponding disulfide **[reactions 15 and 16] [81]**. HNO can also generate hydroxyl radical ($OH^{\bullet}$), which is produced by a variety of other reactions as well **[132, 142, 143]**.

$$2HNO \rightarrow HON{=}NOH \rightarrow N_2O + H_2O \qquad \textbf{(11)}$$

$$NO^- + 2^{\bullet}NO \rightarrow N_3O_3^- \rightarrow N_2O + NO_2^- \qquad \textbf{(12)}$$

$$NO^- + O_2 \rightarrow ONOO^- \qquad \textbf{(13)}$$

$$Fe^{3+} + NO^- \rightarrow Fe^{2+} + {}^{\bullet}NO \rightarrow (Fe^{2+})\text{–}NO \qquad \textbf{(14)}$$

$$RSH + HNO \rightarrow RSNHOH \qquad \textbf{(15)}$$

$$RSNHOH + R'SH \rightarrow `RSSR + NH_2OH \qquad \textbf{(16)}$$

Angeli's salt (sodium trioxodinitrate; $Na_2N_2O_3$; AS) is the most commonly used nitroxyl donor **[30, 144]**. Studies examining the effects of NO^- *in vitro* demonstrated that the synthetic NO^- donor AS was considerably more cytotoxic than $^{\bullet}NO$ **[130, 142]**. This cytotoxicity was dependent upon molecular oxygen and was due in part to the ability of AS to induce DNA double strand breaks and base oxidation **[130, 142, 144-148]**.

Toxicity of NO^- has also been associated with nitration of tyrosine **[149]**, and oxidation of cellular targets presumably through PN **[129, 132]** and $OH^\bullet$ formation **[132, 142, 143]**.

Peroxynitrite. The reactivity of $^\bullet NO$ with biological targets is greatly increased following the formation of $^\bullet NO_2$ **[reaction 1]** or PN **[150] [reaction 17]**. Because $^\bullet NO$ contains an unpaired electron and is paramagnetic, it rapidly reacts with $O_2^{\bullet-}$ to form PN anion ($ONOO^-$) **[89, 151, 152] [reaction 17]**. In general, for every 10-fold increase in $^\bullet NO$ and $O_2^{\bullet-}$, there should be a 100-fold increase in the rate of PN formation **[82]**. The rate constant for PN formation (0.7-1 x 10^{10} $M^{-1}s^{-1}$) is faster than that of superoxide dismutase (1-2 x 10^9 $M^{-1}s^{-1}$) **[153-157]**, thus $^\bullet NO$ can outcompete SOD for $O_2^{\bullet-}$. This favors the formation of RNIs, however, when SOD is present in micromolar concentrations, it can compete effectively for $O_2^{\bullet-}$ **[84, 158]**. Generally, the formation of PN is a diffusion-limited reaction between $^\bullet NO$ and $O_2^{\bullet-}$ **[152, 154, 156, 159]**. The half-life and diffusion properties of $^\bullet NO$ and $O_2^{\bullet-}$ differ with $^\bullet NO$ being longer lived and more diffusible than $O_2^{\bullet-}$. Thus when PN forms, it tends to form closer to the site of $O_2^{\bullet-}$ synthesis **[153]**. Alternatively NO^- can react with O_2 to form PN **[reaction 18] [137]**.

$$^\bullet NO + O_2^{\bullet-} \rightarrow ONOO^- \qquad \textbf{(17)}$$

$$NO^- + O_2 \rightarrow ONOO^- \qquad \textbf{(18)}$$

The PN anion is stable in alkaline solutions, but upon protonation the anion is converted to peroxynitrous acid, which decays to nitrate with a half-life of 1-2 sec **[160-162]**. PN is believed to decay through one of two mechanisms. The first mechanism is a rearrangement of the *cis*-PN which yields nitrate without the formation of strong oxidants **[162, 163] [reaction 19]**. The second mechanism is the homolytic fission of *trans*-PN to yield $OH^\bullet$ and nitrating $^\bullet NO_2$ species which recombine to form nitrate **[155, 161, 164] [reaction 20]**. In a pure solution, decomposition results in ~70% nitrate and ~30% nitrite **[155]**.

$$ONOO^- + H^+ \Leftrightarrow ONOOH \rightarrow NO_3^- + H^+ \qquad \textbf{(19)}$$

$$ONOO^- + H^+ \Leftrightarrow ONOOH \rightarrow [OH^\bullet + {}^\bullet NO_2] \rightarrow NO_3^- + H^+ \qquad \textbf{(20)}$$

Since PN can exist in both *cis* and *trans* configurations, it has been argued that PN formed from $^{\bullet}NO$ and $O_2^{\bullet-}$ has different properties relative to synthetic PN. For example, synthetic PN may lack the capacity to nitrate tyrosine at neutral pH *in vivo* **[165]**. PN in alkaline solution is present only in the *cis* conformation **[166, 167]**. Recent studies have shown that co-generation of $O_2^{\bullet-}$ and $^{\bullet}NO$ at physiological pH yields nearly all *cis*-PN, which was capable of nitrating tyrosine **[168, 169]**. In addition, the co-generation of $^{\bullet}NO$ and $O_2^{\bullet-}$ is equally toxic or slightly more toxic than the bolus addition of PN to bacteria and cultured cells **[170, 171]**.

Although the formation of PN can protect the host from invading organisms, high concentrations can damage host tissue as well. PN is highly reactive, forming both oxidizing and nitrating species **[161, 172]**. PN is a stronger oxidizing agent than either $^{\bullet}NO$ or $O_2^{\bullet-}$ alone **[81, 173]**. Although $^{\bullet}NO$ and $O_2^{\bullet-}$ can both limit *P. falciparum* growth in culture, neither are as effective as PN, the formation of which is largely limited by $^{\bullet}NO$ flux **[174]**. PN can directly damage DNA by inducing base modifications, mutations and single- and double- strand breaks **[175-180]**. PN can also oxidize thiols yielding thiyl radicals **[181-183]** and it can oxidize lipids **[184]**, hydroxylate aromatic amino acids and nitrate free and protein-bound tyrosines **[185-187]**.

The formation of NTYR is a marker for a number of inflammatory conditions **[188, 189]**. Reaction of PN with CO_2 produces nitrosoperoxycarbonate anion ($ONOOCO_2^-$) **[reaction 21]**, which has a shorter half-life than PN, but has a greater capacity for nitration than PN **[91, 190]**. PN can also react with thiols to produce *S*-nitrosothiols which in turn can act as $^{\bullet}NO$-donors **[172, 191-198]**. PN can therefore react with a variety of biomolecules leading to impaired function, toxicity and alterations in signaling pathways.

$$ONOO^- + CO_2 \rightarrow ONOOCO_2^- \qquad (21)$$

PN can react with both $^{\bullet}NO$ **[reaction 22]** and $O_2^{\bullet-}$ **[reaction 23]** to form nitrogen dioxide ($^{\bullet}NO_2$) **[85, 151, 172, 199]**. $^{\bullet}NO_2$ is the main component of smog and, like $^{\bullet}NO$, it is a cell permeable gas. $^{\bullet}NO_2$ dimerizes to N_2O_4 **[reaction 24]** which rapidly hydrolyzes

to nitrite and nitrate in aqueous solutions **[reaction 25]**. Thus, an overproduction of either $^{\bullet}NO$ or $O_2^{\bullet-}$ will decrease the reactivity of $ONOO^-$; accordingly, the maximum activity of PN occurs when $O_2^{\bullet-}$ and $^{\bullet}NO$ are produced in equivalent amounts. When $O_2^{\bullet-}$, levels are higher than $^{\bullet}NO$ levels, oxidative chemistry prevails. Conversely, when $^{\bullet}NO$ levels are higher than $O_2^{\bullet-}$ levels, the resulting NO_2 can then react with $^{\bullet}NO$ to produce the nitrosating agent dinitrogen trioxide (N_2O_3) **[reaction 26]**.

$$ONOO^- + {}^{\bullet}NO \rightarrow {}^{\bullet}NO_2 + NO_2^- \quad \textbf{(22)}$$

$$ONOO^- + O_2^{\bullet-} \rightarrow {}^{\bullet}NO_2 + O_2 + NO_2^- \quad \textbf{(23)}$$

$$2\,{}^{\bullet}NO_2 \rightarrow N_2O_4 \quad \textbf{(24)}$$

$$N_2O_4 + H_2O \rightarrow NO_2^- + NO_3^- + 2H^+ \quad \textbf{(25)}$$

$${}^{\bullet}NO_2 + {}^{\bullet}NO \rightarrow N_2O_3 \quad \textbf{(26)}$$

The primary reaction of N_2O_3 is nitrosation **[85]**. However, in aqueous solution N_2O_3 undergoes rapid hydrolysis to nitrite (half-life ~1 ms) **[reaction 27] [85]**. Nitrosation will occur only when substrates with a high affinity for N_2O_3 are at high concentration **[193, 198, 200, 201]**.

$$N_2O_3 + H_2O \rightarrow 2NO_2^- + 2H^+ \quad \textbf{(27)}$$

Nitrotyrosine formation. Although the mechanism(s) resulting in nitrotyrosine (NTYR) formation *in vivo* are the subject of much debate **[202-204]**, most mechanisms involve $^{\bullet}NO$ biochemistry **[188]** but are not mediated by $^{\bullet}NO$ alone **[202, 205]**. NTYR formation is mediated by RNIs including PN **[206, 207]** and $^{\bullet}NO_2$ **[206, 208, 209]**. However, physiologically relevant concentrations of ascorbate and cysteine (100 μM) have been shown to inhibit $^{\bullet}NO_2$-mediated nitration of tyrosine by 75 and 90% respectively **[208]**. Both PN and $^{\bullet}NO_2$ are formed as secondary products of $^{\bullet}NO$ reactions with $O_2^{\bullet-}$, H_2O_2, and transition metal centers.

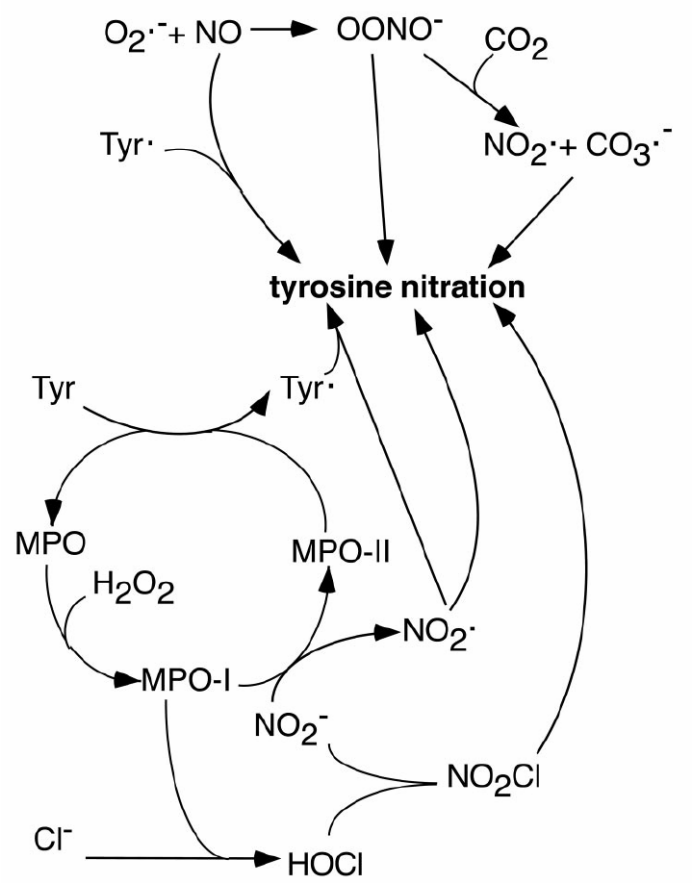

Figure 1-7: Proposed mechanisms for nitrotyrosine (NTYR) formation *in vivo*. (From **[210]**[5])

The myloperoxidase (MPO) mechanism is depicted at the bottom of the figure. The PN ($ONOO^-$) and tyrosyl radical ($Tyr^{\bullet}$) mediated mechanisms are depicted at the top of the figure.

Several mechanisms for NTYR formation have been described **(**reviewed in **[188, 210, 211]**; **Fig. 1-7)**. For some time, protein nitration was attributed exclusively to PN and considered to be a footprint for PN formation in biological systems **[206, 207, 212-214]**. PN can directly nitrate Tyr in an uncatalyzed mechanism or through reactions catalyzed by its reactions with CO_2, transition metals, and peroxidases **[213, 215, 216]**. The PN/CO_2 adduct $ONOOCO_2^-$ **[reaction 21]** can decompose to CO_2 and nitrate (~65%) or undergo hemolytic decomposition (~35%) **[153] [reactions 28 and 29]**. The decay to

[5] Reprinted, with permission, from the Annual Review of Pharmacology and Toxicology, Volume 41 © 2001 by Annual Reviews **www.annualreviews.org**

$^{\bullet}NO_2$ and $CO_3^{\bullet-}$ is believed to be responsible for the enhanced nitration by $ONOOCO_2^-$ relative to PN **[217-219]**. The reaction of PN with transition metal centers can yield NO_2^+ which reacts with Tyr to form NTYR **[185, 207]**; however, NO_2^+ reacts rapidly with water to yield nitrate. Myeloperoxidase (MPO) and horseradish peroxidase (HRP) can catalyze PN-mediated nitration **[216, 220]**. The reaction of PN with unsaturated lipids can yield nitrated lipids ($RONO_2$, $LO(O)NO_2$) **[221]**, which can nitrate tyrosine. PN nitration of Tyr can also proceed through phenoxyl radical **[185, 202, 207, 222]** and through the formation of $^{\bullet}NO_2$ and tyrosyl radicals **[206]**.

$$ONOOCO_2^- \rightarrow CO_2 + NO_3^- \quad \textbf{(28)}$$

$$ONOOCO_2^- \rightarrow CO_3^{-\bullet} + {}^{\bullet}NO_2 \quad \textbf{(29)}$$

Physiological concentrations of nitrite can be oxidized to $^{\bullet}NO_2$ by the Fenton reaction **[219]**, a Fe^{2+}-dependent reaction in which decomposition of H_2O_2 forms $OH^{\bullet}$ that oxidizes NO_2^- to nitrating $^{\bullet}NO_2$ **[223]**. Heme/iron can catalyze the nitration of Tyr with H_2O_2 and nitrite **[224]**. In addition, nitrite oxidation by H_2O_2 can be catalyzed by heme peroxidases **[204, 225, 226]** yielding $^{\bullet}NO_2$ which can nitrate Tyr. MPO can catalyze nitration of bovine serum albumin *in vitro* in the presence of nitrite and H_2O_2 **[221]**. Similarly, HRP and other cellular hemeproteins, including Hb, can catalyze biological nitration **[227, 228]**.

Although $^{\bullet}NO$ cannot directly nitrate Tyr, $^{\bullet}NO$ can react with tyrosyl radicals to yield NTYR **[205].** At very low pH, acidification of nitrite to produce nitrous acid (HNO_2) **[229, 230]** can lead to the formation of NTYR. Such a reaction may occur in the stomach after eating foods high in nitrites such as cured meats. Alternatively the direct oxidation of nitrite by hypochlorous acid **[203, 231]** can form nitryl chloride (NO_2Cl) which can nitrate Tyr or decompose to $NO_2^{\bullet}$.

Based on favorable reaction kinetics, PN-mediated reactions are the most relevant to NTYR formation in many disease states **[189]**. In addition, yields of NTYR formed by alternative nitration mechanisms are extremely small when compared to yields of NTYR formed by PN-dependent mechanism(s) **[232]**. As such, immunolocalization of NTYR remains an excellent indicator for the formation of PN *in vivo* **[232]**.

S-nitrosothiols. In mammals, SNOs are detectable *in vivo* at elevated levels during inflammation **[233, 234]**. SNOs, also known as thionitrites, are NO-adducts with the sulfhydryl groups of amino acids, peptides and proteins. Pryor *et al.* **[235]** showed that SNOs are not formed by the direct interaction of $^{\bullet}NO$ with thiols, rather they require RNIs formed during the $^{\bullet}NO/O_2$ reaction (most likely N_2O_3) **[reactions 30 and 31] [104, 201, 236-240]**. Nitrosation occurs when an RNI donates a nitrosonium ion (NO^+) to a nucleophile. Nitosation is not equivalent to nitrosylation, which occurs when a nitrosyl adduct is formed between metals and $^{\bullet}NO$. Despite this significant difference, nitrosation and nitrosylation are often misused in literature **[94, 120, 241, 242]**. NO^+ can also be formed from DNIC **[112, 243]** or PN **[172, 191-198]**. Nitrosation is a chemical reaction, not an enzymatically catalyzed one **[210]**. Although there is discussion about a consensus motif for *S*-nitrosation **[244]**, most agree that the concentration of $^{\bullet}NO$, local environment (*e.g.* $O_2^{\bullet-}$, heme protein concentration) and accessibility of Cys residues determine whether nitrosation occurs.

$$2^{\bullet}NO + \tfrac{1}{2} O_2 \rightarrow N_2O_3 \qquad \textbf{(30)}$$

$$N_2O_3 + RSH \rightarrow RSNO + NO_2^- + H^+ \qquad \textbf{(31)}$$

SNOs are significantly more stable than $^{\bullet}NO$ and, therefore, preserve the bioactivity of $^{\bullet}NO$ by increasing its half-life **[102, 108, 245-249]**. Low molecular weight (MW) SNOs are less stable than their protein counterparts (*i.e.* Cys-NO<GSNO<protein-SNO) **[120]**. The stability of SNOs is affected by metal ions and thiols **[239, 250, 251]**. SNOs can react with reduced thiols resulting in transnitrosation **[120, 252-255]** or *S*-thiolation **[115-121]**. Transnitrosation reactions, *i.e.* the transfer of a NO^+-equivalent from one molecule to another **[reaction 32]**, are a common feature of all SNOs and may account for the inhibition of Cys-dependent enzymes by *S*-nitrosated albumin (SNO-Alb) **[256]**. Transnitrosation reactions are reversible **[257]**. The *S*-thiolation reaction generates a disulfide and NO^- **[reaction 33]**. $^{\bullet}NO$ can be released from SNOs in the presence of metal ions, *e.g.* copper **[reaction 34] [111, 113, 250, 258]**. Thus, stability of SNOs in solution is enhanced by the presence of the metal ion chelator DTPA **[250].** The presence of reducing agents (*e.g.* thiols and

ascorbate), enhances metal-ion-dependent decay **[259, 260]**. As such, glutathione (GSH) has been shown to protect cells against the toxicity of RNIs formed from $^{\bullet}$NO **[201, 236]**, presumably through the initial formation of GSNO.

$$RSNO + R'SH \rightarrow RSH + R'SNO \qquad (32)$$

$$RSNO + R'SH \rightarrow RSSR' + NO^{-} + H^{+} \qquad (33)$$

$$GSNO + Cu^{+} \rightarrow GS^{-} + {}^{\bullet}NO + Cu^{2+} \qquad (34)$$

In contrast to the protective functions of some SNOs, GSNO and other SNOs can be toxic as well **[92, 261, 262]**. Cytostasis from *S*-nitrosation of intracellular proteins has been observed in *S. typhimurium* **[261]**. *S*-nitrosation of ribonucleotide reductase of *E. coli* inhibited cell proliferation **[263]**. SNOs are also toxic to *P. falciparum*. Specifically, GSNO and Cys-NO were ~1,000 times more effective at inhibiting parasite growth in culture than was nitrite **[92]**. This effect may be due to *S*-nitrosation of Cys^{25} of the plasmodial cysteine protease, falcipain **[264]**, which leads to enzyme inactivation and blocks parasite development *in vitro* **[265]**. Interestingly, treatment of infected mice with falcipain inhibitors cured infection with *Plasmodium vinckei* **[266]**.

Superoxide can react with GSNO to yield $^{\bullet}$NO **[267-269]**, but $O_2^{\bullet-}$ rapidly combines with $^{\bullet}$NO to yield PN **[118, 161]**. Superoxide can also react with GSNO to yield GSSG and equimolar concentrations of nitrite and nitrate **[reaction 35] [268]**.

$$2GSNO + O_2^{\bullet-} + H_2O \rightarrow GSSG + NO_3^{-} + NO_2^{-} + 2H^{+} \qquad (35)$$

S-nitrosation can regulate protein activity and, as such, is defined by some as a post-translational modification (reviewed in **[270]**). The binding of $^{\bullet}$NO to thiols or metals can function as a simple switch analogous to phosphorylation **[244, 271]**, but this switch must also be specific and reversible within a biologically relevant time frame **[272]**. Although SNO modification clearly can alter protein function (reviewed in **[271]**) and signaling pathways, the nature of specificity and reversibility are under investigation.

Nitric oxide in blood. A dynamic relationship exists among $^{\bullet}NO$, O_2 and Hb. Hemoglobins have ancient evolutionary origins and are found in all kingdoms of life **[273, 274]**. Recent evidence from some lower organisms suggests that the ancient function of Hb was to destroy $^{\bullet}NO$ in a manner akin to the denitrosylase activity of bacterial Hbs and that Hbs later evolved to destroy oxygen in a manner akin to the $^{\bullet}NO$-activated deoxygenase of *Ascaris* Hb **[275-277]**.

Heme proteins can limit the availability of $^{\bullet}NO$ in a manner analogous to the control of $O_2^{\bullet-}$ levels by SOD. $^{\bullet}NO$ can react with oxyHb to form nitrate and metHb **[reaction 36] [86, 278, 279]** or it can react with the heme iron to form metal nitrosyl **[reaction 3]**. Under physiological conditions in mammalian blood, the binding of $^{\bullet}NO$ to hemes and thiols of oxyHb effectively outcompetes the oxidation reaction (*i.e.* formation of metHb; **[275]**). Mammalian Hb contains several cysteine residues of which βCys^{93} has a high affinity for $^{\bullet}NO$ in the relaxed (R, oxy) state and a low affinity in the tense (T, deoxy) state **[105]**. Thus, O_2 tension (pO_2) controls *S*-nitrosohemoglobin (SNOHb) formation and decay **[105]**. Oxygen tension also plays a key role in *P. falciparum* survival: at a pO_2 of 1% O_2, the toxicity of $^{\bullet}NO$ to *P. falciparum* is enhanced **[280]**.

$$Hb(Fe^{2+})\text{-}O_2 + {}^{\bullet}NO \rightarrow Hb(Fe^{3+}) + NO_3^- \qquad \textbf{(36)}$$

Although a great deal of research has focused on the interactions between $^{\bullet}NO$ and Hb, $^{\bullet}NO$ can react/interact with a variety of other blood components, including low MW thiols (*e.g.* GSH, Cys) and albumin (Alb) **[281]**. Blood plasma contains ~0.5 mM serum Alb and ~0.3 μM Cys-NO and 0.1 μM GSNO, so SNO levels in serum are largely due to SNO-Alb (5 μM) **[82]**. In arterial plasma, SNOHb levels are ~0.3 μM whereas in venous plasma, SNOHb levels are only ~0.03 μM **[82]**. Lower intracellular thiol concentrations are correlated with greater susceptibility to $^{\bullet}NO$ *in vitro*; as such, thiols appear to scavenge and stabilize $^{\bullet}NO$ **[282, 283]**. For example, the half-life of SNO-Alb is ~24 h in neutral phosphate buffer **[82]**, facilitating diffusion of $^{\bullet}NO$ and prolonging its bioactivity **[101, 102]**.

The potential reactions of $^{\bullet}NO$ in blood are numerous (reviewed in **[77, 82]**) and are dependent on many factors including the site of production, the concentration of $^{\bullet}NO$

and the concentration of thiols, metals, and ROS. The relatively high abundance of these factors in blood dictates that very little free •NO exists, with newly synthesized •NO reacting rapidly to form nitrite (interaction with O_2), nitrate (interaction with oxyHb), PN (reaction with $O_2^{\bullet-}$), nitrosylHb (interaction with heme iron) and SNOs (interaction with thiols).

NITROSATIVE STRESS DEFENSES

Nitrosative stress refers to the stress on biological targets due to •NO/RNI concentrations that exceed the requirements for signaling. Nitrosative stress is akin to oxidative stress generated by reactive oxygen species (ROS). While oxidative stress and defense against ROS have been studied for some time, it was not until the late 1980s, when •NO was determined to be produced endogenously, that the field of nitrosative stress defense emerged. Under biological conditions, both types of stress often occur together as part of the defense arsenal against invading microorganisms. Thus, the study of nitrosative stress defense genes focused initially on microorganisms exposed to high inflammatory levels of ROS and •NO/RNIs.

Oxidative and nitrosative stress defenses are often linked, a point that is clarified by the fact that these stresses activate some of the same stress regulons in bacteria. Specifically, the SoxRS and OxyR regulons contain genes that confer protection against both ROS and RNIs. The SoxRS regulon was originally identified as a $O_2^{\bullet-}$ response regulon **[284]**. Later it was found that SoxRS could be induced by •NO **[285]** and activated by GSNO and DNIC **[286]**. Mutants of *E. coli* that lack the *soxRS* genes were more susceptible to macrophage-generated •NO **[287]**. Genes regulated by SoxRS include manganese SOD (*sodA*), which may defend against •NO by limiting PN production. The OxyR regulon was identified by its induction by H_2O_2 **[288]**. Later it was found that OxyR is activated through *S*-nitrosation and can increase the resistance of *E. coli* to Cys-SNO **[289]**. Genes regulated by OxyR include catalase/hydroperoxidase (*katG*), glutathione reductase (*gorA*) and alkyl hydroperoxide reductase (*ahpCF*).

Thiol status plays a critical role in •NO/RNI defense. Bacteria with low thiol concentrations have been shown to be more susceptible to •NO/RNIs than were bacteria with high thiol concentrations (reviewed in **[283]**). High levels of low molecular thiols such as GSH and homocysteine, or species-specific low MW thiols like mycothiol and trypanothione **[290-295]**, appear to function as •NO/RNI scavengers. For example, mutations in the *metL* gene encoding an enzyme required for homocysteine biosynthesis increased bacterial susceptibility to damage by SNOs **[282]**.

Based on these observations, enzymes involved in maintaining a reduced thiol pool contribute to nitrosative stress defense. Enzymes that maintain reduced thiol status in the cell are associated with the thioredoxin reducatase (TrxR) and GSH reductase (GR) systems. Depletion of GSH increases the sensitivity of cells to •NO **[201, 236, 296]**. To maintain a reduced GSH pool, GSH can be synthesized *de novo* (γ-glutamylcysteine synthase) or oxidized glutathione (GSSG) can be recycled to the reducing tripeptide by GR. Oxidant stress from •NO/RNI or ROS leads to the induction of GSH synthesis **[297-299]**, highlighting the role of GSH in maintaining cellular redox status. Bacterial GR is an OxyR regulated gene (*gorA*) that requires NADPH. This co-factor is supplied by the hexose monophosphate shunt, the first step of which is catalyzed by glucose-6-phosphate dehydrogenase, which is a SoxRS regulated gene (*zwf*). Insects lack GR **[300, 301]** and reduction of GSSG in *A. gambiae* was achieved only by thioredoxin (Trx) addition **[300]**. The *P. falciparum* Trx/TrxR system can reduce GSSG and efficiently turn over GSNO **[302]**. Similarly, Trx can protect human cells from the •NO donor SNAP **[303].**

In addition to their roles in redox homeostasis, cellular thiols are targets for RNI-mediated *S*-nitrosation and inactivation. For example, depletion of GSH increased *S*-nitrosation of other cellular thiols **[304]**. Through conversion to GSNO, GSH thus acts to protect other cellular thiols from *S*-nitrosation. Conversion of GSNO to GSSG is catalyzed by glutathione-dependent formaldehyde dehydrogenase (GS-FDH) **[305]**. This enzyme is highly specific for GSNO and does not act on Cys-NO or *S*-nitrosohomocysteine **[305].** Hepatocytes from mice lacking GS-FDH showed a 60-175% increase in GSNO accumulation compared to controls **[305]**. *Ex vivo* treatment of the hepatocytes with cytokines and LPS increased protein bound SNO by 50% compared to

controls **[305]**, indicating that GSNO formation can protect critical cellular targets from modification and damage due to *S*-nitrosation.

In *E. coli* SNOs induce *oxy*R which controls the regulon containing *ahpCF* **[289]**, which encodes the bacterial peroxiredoxin (Prx) AhpC. Initially characterized as a unique group of peroxidases (20-30 kD) that lack redox metals or prosthetic groups, the Prxs have recently generated interest as nitrosative defense genes **[306-319]**. Disruption of AhpC in *Mycobacterium tuberculosis* resulted in increased sensitivity to GSNO and mildly acidified nitrite (which dismutates to form $^{\bullet}NO$, NO_2, N_2O_3 and N_2O_4) relative to wild type cells **[306]**. When a human epithelial cell line was transfected with *M. tuberculosis* AhpC, resistance to GSNO increased 5-fold compared to untransfected cells **[306]**. Further, in cells co-transfected with AhpC and iNOS, AhpC prevented apoptotic cell death induced by iNOS expression **[306]**. In other studies, the tsa1Δ tsa2Δ (Prx double deletion) mutant of *Saccharomyces cerevisiae* showed hypersensitivity to PN and the $^{\bullet}NO$-donor sodium nitroprusside (SNP) **[316].** *In vitro*, Prxs can catalytically detoxify PN to nitrite, a reaction was "fast enough to forestall the oxidation of bystander molecules" **[306-309, 316-319]**.

Long before $^{\bullet}NO$ was recognized as a biologically important molecule, $^{\bullet}NO$ was used as a "non-physiological" ligand in hemoproteins studies. Now, we know that O_2 binding and release by Hb in animal vasculature is influenced by the cooperative binding of $^{\bullet}NO$ to the vacant hemes. In more primitive species, Hbs act to protect cells against nitrosative stress. Bacteria produce three types of Hbs, including single domain Hbs such as *Campylobacter* spp. Cgb, truncated Hbs such as *Mycobacterium bovis* HbN, and flavohemoglobins such as *E. coli* Hmp. The best characterized bacterial Hb is Hmp, a two domain globin which detoxifies $^{\bullet}NO$ by acting as an $^{\bullet}NO$ oxygenase or $^{\bullet}NO$ denitrosylase in a mechanism whereby NO is converted to nitrate **[320]**. Transcription of *hmp* is upregulated by $^{\bullet}NO$, SNP, SNAP and GSNO **[321-323]** and mutants lacking *hmp* are more sensitive to RNIs **[322, 324]**. *Campylobacter jejuni* Cbg resembles Hmp in that it lacks a reductase domain; *cbg* deficient mutants were hypersensitive to the nitrosating agents GSNO and SNP and the $^{\bullet}NO$ donor spermidine NONOate **[325]**. The truncated Hbs are smaller than the single domain Hbs by 20-40 residues and stoichiometrically oxidize $^{\bullet}NO$ to nitrate through an unknown mechanism **[326]**. In murine macrophages,

stimulation with with LPS and interferon-gamma not only induced the synthesis of •NO, but also induced the expression of a minor beta-hemoglobin subunit, suggesting that mammalian Hbs participate in •NO defense as well as oxygen/CO_2 transport **[327]**.

Thus, nitrosative stress defense genes can act on several levels. They can prevent nitrosative stress by inhibiting •NO formation (NOS inhibitors) or by preventing •NO interaction with ROS. For example, inhibitors of NADPH oxidase would limit $O_2^{\bullet-}$ production thereby limiting PN formation. Nitrosative stress defenses can also act on RNIs to reduce toxicity through bystander oxidation (*e.g.* of low MW thiols) or by enzymatic conversion to a less toxic RNI (*e.g.* Prx-mediated reduction of PN).

RESEARCH OBJECTIVES

The long-term goal of my project was to assess toxicity of •NO synthesis during *Plasmodium* infection of *A. stephensi.* The malaria parasite life cycle is dependent on passage through both mosquito (sexual cycle) and vertebrate (asexual cycle) hosts. Defense responses during either cycle will reduce/eliminate parasite transmission. In the vertebrate host, •NO participates in defense responses to a variety of microbial, viral, fungal, and protozoal pathogens. In A. *stephensi*, *Plasmodium* infection induces *AsNOS* expression in the midgut, resulting in elevated •NO production and decreased *Plasmodium* development **{Luckhart, 2003 #711; Luckhart, 1998 #10}{Luckhart, 1999 #11}**. These observations led to the hypothesis that *AsNOS* may be a useful target for genetic manipulation to create transgenic mosquitoes that are refractory to malaria parasite transmission.

For this strategy to be successful, we must understand how •NO limits mosquito-stage *Plasmodium* infection and whether this response is toxic to the insect host. The biochemistry of •NO is complex and includes regulatory, cytoprotective and cytotoxic effects. Minimal toxicity of free •NO suggests that killing of *Plasmodium* occurs via the formation of RNIs **{Rockett, 1991 #42}**. Thus, although previous studies demonstrated that *Plasmodium* infection induces *AsNOS* expression in the mosquito midgut, the RNIs formed in this environment have not been identified. The first part of my research,

therefore, was focused on the identification of mosquito midgut RNIs as a basis to predict how induction of *AsNOS* expression limits parasite development. My data revealed that potentially toxic RNIs are present at inflammatory levels in the mosquito midgut. These RNIs are not only potentially toxic to developing parasites, but also likely impose significant stress on the mosquito host. As such, the second part of my research focused on the role of peroxiredoxin in protecting mosquito cells against parasite-induced RNIs. The specific aims of my research were as follows,

1) How does $^{\bullet}$NO synthesis in the blood-filled *Anopheles* midgut limit *Plasmodium* development?
   a) What RNIs are elevated in the *Plasmodium*-infected midgut?
   b) Is mosquito-derived $^{\bullet}$NO the source of the elevated RNIs observed in the infected midgut?
   c) Do ingested blood constituents serve as substrates for midgut RNI formation?
   d) How might midgut RNIs limit *Plasmodium*-development in *A. stephensi*?

2) Does $^{\bullet}$NO synthesis by *A. stephensi* result in damage to host tissue?

3) Does *Anopheles* peroxiredoxin protect the mosquito from nitrosative stress?
   a) Are *peroxiredoxins* (*Prxs*) expressed in *A. stephensi*?
   b) Is *AsPrx* expression modulated by parasite infection *in vivo*?
   c) Can *AsPrx* expression be similarly modulated *in vitro* by biological/chemical stresses proposed to be present in the *Plasmodium*-infected midgut?
   d) Can *AsPrx* expression *in vitro* enhance mosquito cell viability in the presence of oxidative and nitrosative stresses?

CHAPTER TWO: Reactive nitrogen intermediates (RNIs) induced in the midgut of *Plasmodium berghei*-infected *Anopheles stephensi.*

INTRODUCTION

Anopheles stephensi possesses a single copy of an inducible •NO synthase gene (*As*NOS; **[47]**). Soon after blood ingestion, induction *of AsNOS* expression leads to •NO synthesis that limits *Plasmodium* development **[52, 56]**. During parasite infection, induction of *AsNOS* expression in the midgut is biphasic, with >2-fold inductions at 6 h, 36 h, and 48 h after feeding **(Fig. 1-4)**. Ookinete invasion takes place ~24 h pBM and invasion is temporally correlated with increased levels of NOS protein as revealed by immunofluorescence **[328]**.

•NO production can limit parasite development in the mosquito midgut, as demonstrated by dietary provision of the NOS inhibitor N^G-nitro-L-arginine methyl ester (L-NAME) relative to control insects provided with D-NAME, the inactive stereoisomer, in the infectious blood meal **[52]**. The effect of midgut RNIs on parasite viability appears to occur both prior to and during midgut invasion. In studies parallel to the work presented here, provision of L-NAME, but not D-NAME, to *A. stephensi* significantly decreased the percentage of apoptotic *P. berghei* ookinetes in the midgut lumen **[329]**. At later times during midgut invasion, ~5% of ookinetes travel 5-6 cell diameters in the epithelium, perhaps in an effort to escape the toxic diffusible •NO and RNIs **[328]**. This extensive movement may explain the observation that ~95% of ookinetes appear to escape the epithelium **[328]** yet only a few remain to survive as oocysts (reviewed by **[330]**). Thus, •NO/RNIs formed in the mosquito prior to and during parasite invasion are apparently toxic to insect-stage *P. berghei*.

To test the hypothesis that •NO/RNIs are toxic to developing mosquito-stage parasites requires detailed analyses of the •NO/RNI chemistry of insect midgut. By extension, interpretation of this chemistry requires an understanding of the role of •NO/RNIs in mammalian physiology. Although •NO has been implicated in many

regulatory processes including blood pressure control, neurotransmission, and immune processes **[73, 331-333]**, •NO also contributes to the pathology of inflammation, neurodegenerative diseases, cardiovascular disorders, and possibly cancer. The dichotomy of the cytotoxic and cytoprotective properties of •NO is explained by the level of •NO production **[85]**. At low levels, •NO function is primarily associated with regulatory processes, whereas at higher levels, •NO function is associated with toxicity **[84]**. Even at higher fluxes, however, •NO function can be cytoprotective. For example, high fluxes of •NO can scavenge superoxide ($O_2^{\bullet-}$), protecting cells from this damaging ROS **[80]**. Based on this diversity of roles, it is clear that the chemistry of this highly reactive radical is dependent on the formation of a multitude of RNIs that extend and preserve the bioactivity of •NO.

The cytotoxic and regulatory actions of •NO are dependent on RNIs that are formed from the same general reactions. Specifically, •NO participates in four reaction pathways: •NO can react with (1) $O_2^{\bullet-}$ to form peroxynitrite (PN), (2) reduced thiols to form *S*-nitrosothiols, (3) metal ions to form metal nitrosyls and (4) •NO can undergo autooxidation (reviewed in **[91]**). Metal nitrosyls can activate or inactivate Fe-S cluster-dependent enzymes and enzymes that require metal porphyrins for activity. *S*-nitrosothiols (SNOs) can alter protein function by compromising critical cysteine residues. PN and various oxides of nitrogen can mediate oxidation and/or nitration reactions, thus potentially damaging proteins, lipids and DNA (reviewed in **[82, 91, 334, 335]**). In addition, PN is highly reactive **[161, 162, 172]** and toxic to cells and microorganisms **[170, 215, 336-338]**. Thus, it is believed that PN is responsible for a variety of the pathological conditions associated with overproduction of •NO **[161, 162, 172]**. Since PN is a transient species whose biological half-life (10-20 ms) **[339]** is shorter than that of •NO (1-30 s) **[340]**, it cannot be directly measured and its presence must be inferred from a combination of analytical, pharmacological, and/or genetic approaches **[341]**. The presence of nitrated tyrosine (NTYR) is commonly used as a marker for •NO-mediated tissue damage since NTYR is a stable end product of tyrosine reaction with several RNIs including PN **[342]**. Increased levels of NTYR have been observed in certain diseased-states and have been correlated with elevated levels of other indices of oxidative stress (reviewed in **[188]**). NTYR formation also represents a shift

from the signal transducing physiological actions of •NO to oxidative and potentially pathogenic effects associated with •NO synthesis **[343]**.

In addition to direct toxic effects of RNIs, the formation of some RNIs can preserve the bioactivity of •NO. Nitrates and nitrites are stable decomposition products of •NO in aqueous solutions. However, nitrates can be cytotoxic **[92]** and nitrites can function as substrates in hydrogen peroxide (H_2O_2)/peroxidase-mediated tyrosine nitration **[225, 344]**. Nitrosyls and SNOs stabilize bound •NO **[101, 102, 108, 120, 245-249]**. The half-lives of these compounds are on the order of minutes to hours, depending on the RNI and environment of synthesis **[82, 120, 194, 234, 345]**. As such, these RNIs can facilitate •NO transport from the site of synthesis to remote sites of action.

The direct and indirect effects of RNIs on malaria parasite survival are poorly known and have been interpreted primarily from studies of asexual stage parasites **[92, 280, 346-348]**. Minimal toxicity of free •NO suggests that killing of *Plasmodium* occurs via the formation of RNIs **[92]**. Rockett *et al*. **[92]** found that *S*-nitrosothiol derivatives of cysteine (Cys-NO) and glutathione (GSNO) were toxic to *P. falciparum in vitro.* These low molecular weight (MW) SNOs were 1,000-fold more toxic than nitrate, and nitrate was 3-fold more toxic than nitrite. Susceptibility was dependent on stage of asexual development in that trophozoites were more vulnerable to the •NO/NO^+ donor SNAP than were ring stages **[348]**. Taylor-Robinson showed that the •NO donors SNP (a metal nitrosyl) and GEA 5024 had similar negative effects on *P. falciparum* development **[346]**, indicating that a variety of RNIs are toxic to malaria parasites. In addition to the toxic effects of •NO/RNIs, some compounds were cytostatic to *P. falciparum* at lower concentrations **[346, 348]**.

In this portion of my dissertation, I analyzed the RNI chemistry in the midgut of *A. stephensi* infected with *P. berghei*. Here I show results supporting parasite-induced production of higher oxides of nitrogen (NO_x) associated with an inflammatory state. Specifically, the production of PN, nitroxyl (NO^-), and nitrates are conjectured to be enhanced in *Plasmodium*-infected midguts. In addition, metal nitrosyls may be elevated in the infected midgut and are assumed to be associated with the heme iron in Hb. Understanding this chemistry will help to determine how *AsNOS* induction leads to inhibition of parasite development. This work will lay the foundation for future efforts to

manipulate the mosquito •NO-mediated immune response to create insects that are refractory to parasite development and, thus, transmission.

MATERIALS AND METHODS

Reagents. Allantoin, d-biotin, diethylaminetriamine pentaacetic acid (DTPA), N-ethylmaleimide (NEM), glutathione, N^G-nitro-L-arginine methyl ester (L-NAME), D-NAME, potassium iodide (KI), sodium dodecylsulfate (SDS), sodium nitrite ($NaNO_2$), sodium nitrate ($NaNO_3$), sodium hydrosulfite ($Na_2S_2O_4$), uric acid sodium salt (urate), and vanadium(III) chloride (VCl_3) were purchased from Sigma. Dimethyl formamide (DMF), dimethyl sulfoxide (DMSO), glycine, methanol, potassium acetate and tris (hydroxymethyl) aminomethane (TRIS) were purchased from Fisher. Mercury(II) chloride ($HgCl_2$) and copper(I) chloride (CuCl) were purchased from Acros. Peroxynitrite (PN) was purchased from Cayman Chemical. Streptavidin was purchased from Promega.

Insect rearing and parasite infection. *Anopheles stephensi* Liston (Indian wild type) mosquitoes were maintained on 10% sucrose-soaked cotton balls at 27°C and 75% relative humidity under a 12 h light/dark cycle. Mosquitoes 4-7 days (d) old were bloodfed on anesthetized naïve (uninfected) or *Plasmodium berghei*-infected (5-14% parasitemia; strain NK65) mice (Institute of Cancer Research; ICR). Following the blood meal, mosquitoes were maintained at 21°C for parasite development. For the urate study, urate and allantoin were prepared in PBS then adjusted to pH 6.7. For the L-NAME assay, the NOS inhibitor L-NAME (1 mg/mL), or the inactive stereoisomer D-NAME (1 mg/mL) were provided as dietary supplements to the mosquitoes as described **[52]**. Fresh NAME solutions were prepared daily in sterile distilled, deionized water (ddH_2O); ddH_2O was used as the control. For the supplemental diets, cotton balls were sterilized by autoclaving. Cotton balls soaked with dietary treatment solutions (changed twice daily) and sugar cubes (changed daily) were administered from three days before blood feeding until termination of the experiment. For urate and NAME feeds, *P. berghei*-infected mice were rotated among mosquito cartons (15 min per carton) to avoid mouse-to-mouse

variability in the infected blood meals. Mosquito infections were monitored by counting oocysts on midguts stained with 0.1% mercurochrome at 10 d post-infection.

Sample preparation: At various times post-blood meal (pBM), mosquitoes were collected, anesthetized (~5 min at 0°C), and midguts dissected into the appropriate buffer (9 μL per midgut) for each experiment. Samples were homogenized by sonication, centrifuged at 2,000 x g for 2 min and the supernatant collected and immediately stored at -80°C until experiments were conducted. Heme concentrations were calculated based on absorbance values of midgut samples at 300-800 nm; heme concentrations were calculated from the absorbance peaks and the respective extinction coefficients for either oxyhemoglobin (oxyHb; ε_{soret} = 125 $mM^{-1}cm^{-1}$, $\varepsilon_{\alpha\ band}$ = 14.6 $mM^{-1}cm^{-1}$, $\varepsilon_{\beta\ band}$ = 13.8 $mM^{-1}cm^{-1}$) or methemoglobin (metHb; $\varepsilon_{sore\ t}$= 124 $mM^{-1}cm^{-1}$) **[349]**.

Griess Assay. At 8, 12.5, 24 and 33 h pBM 20 midguts from *P. berghei*-infected or uninfected, bloodfed *A. stephensi* were dissected into PBS, pH 7.2. Total nitrite levels were determined using the Colorimetric Non-enzymatic Nitric Oxide Assay Kit (Oxford Biomedical Research). In brief, this procedure used a modified Griess reaction assay **[350]**. Zinc sulfate was used to precipitate proteins from the sample and cadmium (Cd) beads non-enzymatically converted available nitrate to nitrite **[61, 351-353]**. Total nitrite (nitrite and Cd-converted nitrate) was quantified using the Griess reagent (a mixture of *N*-(1-naphthyl) ethylenediamine hydrochloride and sulfanilamide) to yield a purple-azo product with absorbance at 562 nm. Total nitrite values were normalized against the heme concentration to take into account the differences in ingested blood meal volumes **(Fig. 2-1)**.

Chemiluminescent detection of RNIs. RNIs can be measured by selectively cleaving $^{\bullet}NO$ from the parent compound followed by detection of the freed $^{\bullet}NO$. Chemiluminescence detection of the liberated gas phase $^{\bullet}NO$ is possible by through the excited intermediate, nitrogen dioxide ($^{\bullet}NO_2$*), formed during its reaction with ozone (O_3) **[reaction 1]**. Decay of $^{\bullet}NO_2$* to the ground state emits a photon of light (*hv*) in the near-infrared region **[reaction 2]** and can be quantified and integrated with a photomultiplier tube/computer system.

$$^{\bullet}NO + O_3 \rightarrow {}^{\bullet}NO_2^* + O_2 \quad (1)$$

$$^{\bullet}NO_2^* \rightarrow h\nu + {}^{\bullet}NO_2 \quad (2)$$

Chemiluminescent detection is widely used in $^{\bullet}$NO analyses as it is an extremely sensitive and selective technique for quantifying pmol $^{\bullet}$NO levels **[354-358]**.

For NO_x, nitrite and SNO analyses, chemical reductions were used to liberate $^{\bullet}$NO prior to chemiluminescence detection. Mosquito midguts (50) were dissected into modified phosphate-buffered saline (PBS, 1% Nonidet P-40, 4 mM potassium ferricyanide [$K_3Fe(CN)_6$], 10 mM N-ethylmaleimide, and 0.1 mM diethylamine triamine pentaacetic acid [DTPA], pH 7.4 **[359]**). The metal ion chelator DTPA was used to improve the stability and sensitivity of the system for SNO detection **[360]**. The chemical reduction of RNIs and subsequent detection were performed in a $^{\bullet}$NO analyzer **(**NOA; Sievers Instruments, Boulder, CO.; **Appendix A) [357, 358]**. Prior to analysis, midgut lysate sample proteins were concentrated by microfiltration (10- or 100 kD Microcon; Millipore Corp., Bedford, Mass.) at ~2,000 x g for 20 min; this treatment was essential to minimize sample foaming during analysis. In addition, 100 µL diluted antifoam agent (166 µL diluted in water to 5 mL; Sievers) was added to the reaction vessel to further reduce foaming. Different classes of RNIs vary in susceptibility to chemical reduction **[356, 361]**. Sample aliquots were injected into an anaerobic (He-purged) reaction vessel containing either room temperature acidified sodium iodide (50 mg NaI in 5 mL glacial acetic acid) for NO_2^- measurements or 95°C acidified vanadium(III) chloride (5 mL of 0.8 g VCl_3 dissolved in 100 mL 1 N HCl) for NO_x measurements **[358, 361-365] [reactions 3-6]**.

$$I^- + NO_2^- + 2H^+ \rightarrow NO + \tfrac{1}{2}I_2 + H_2O \quad (3)$$

$$2NO_3^- + 3V^{3+} + 2H_2O \rightarrow 2NO + 3VO_2^+ + 4H^+ \quad (4)$$

$$VCl_3 + 2\ R\text{-}SNO + 2\ H_2O \rightarrow 2\ NO + 2\ R\text{-}SH + VO_2Cl + 2\ HCl \quad (5)$$

$$HNO_2 + V^{3+} \rightarrow NO + VO^{2+} + H^+ \quad (6)$$

Pretreatment of sample aliquots with mercuric chloride (1 part 0.2% $HgCl_2$ in water or water alone: 2 parts mosquito lysate: 3 parts PBS) for 30 min at room temperature liberated $^{\bullet}NO$ from *S*-nitrosothiols **[250, 366, 367]**; the resulting nitrites were collected in the filtrate thereby making them detectable as an increase in the measured nitrite level **[reactions 7 and 8]**.

$$RSNO + Hg^{2+} \rightarrow [RS(Hg)NO]^{2+} \quad \textbf{(7)}$$

$$[RS(Hg)NO]^{2+} + H_2O \rightarrow RSHg^{+} + HNO_2 \text{ (or } [H^{+}/NO_2^{-}]) + H^{+} \quad \textbf{(8)}$$

Values were compared to standard curves of sodium nitrate ($NaNO_3$) or sodium nitrite ($NaNO_2$), and normalized against the heme concentrations of matched sample aliquots to account for differences in blood meal volumes among mosquitoes. Four separate cohorts of uninfected and *P. berghei*-infected *A. stephensi* were used for these analyses. The levels of NO_x, nitrite and SNO induction in midguts of *P. berghei*-infected *A. stephensi* relative to those in uninfected *A. stephensi* at each time point were analyzed by using the Student's *t* test. These assays were performed in the laboratory of Dr. Andrew Gow at the Children's Hospital of Philadelphia (Philadelphia, PA).

Free and photolyzable (*S*-nitrosothiols and metal nitrosyls) $^{\bullet}NO$ were measured by photolysis-chemiluminescence detection **[102, 360]**. Midguts (10 per sample) were dissected into buffer (0.1 M phosphate buffer (pH 8) or 0.9% saline containing 100 μM DTPA) and injected into the manual injection valve of an Isco 2350 HPLC pump connected to a photolysis chamber **(**Nitrolyte, Thermedics, Inc., Woburn, MA; **Appendix B)**. Degassed (with N_2 or He), ddH_2O was used as the mobile phase (1 mL/min flow rate). $^{\bullet}NO$ was released by photolysis when the sample passed through a quartz coil surrounding a mercury arc lamp emitting broad wave band UV light (Hanovia-Colight, Inc., Newark, NJ) **[360, 368]**. The output passed through two cold traps (0°C and -75°C) to condense the liquid and less volatile gasses (such as nitrite and nitrate). In the chemiluminescence spectrometer (Model 510, Thermal Energy Analyzer (TEA), Thermedics, Inc.), ozone combined with $^{\bullet}NO$ producing the activated state $^{\bullet}NO_2$* which upon decay emitted light detected by a photomultiplier and the electrical output analyzed by an integrator (5890 series II Plus, Gas Chromatograph, Hewlett Packard). Values

obtained from the integrator were compared to a standard curve made from samples of known concentrations of GSNO. GSNO was prepared immediately prior to use by reacting equimolar concentrations (0.5 M) of GSH in water and nitrite in 1 M HCl (both solutions contained 100 μM DTPA). Formation of GSNO was indicated by a red color. Due to the stickiness of the midgut lysate samples, the machine lines were cleaned extensively with 0.1 N NaOH followed by buffer between each sample run. Concentrations of midgut bound-$^{\bullet}$NO were adjusted to the heme concentration of the sample. These assays were performed at Duke University in the laboratory of Dr. Jonathan Stamler (Durham, NC). Since most tap water contains contaminating nitrite levels, all aqueous solutions for use in the NOA and Nitrolyte were made with ultrapure water from a Milli-Q System (Millipore, Inc., Bedford, MA). Buffers used were also analyzed for RNIs; any contamination, if present, was subtracted from the sample data.

SNO-biotin switch western analyses. The SNO-biotin switch westerns were performed using a protocol adapted from Jaffrey *et al.* **[369]**. Briefly, midguts from uninfected and *P. berghei*-infected mosquitoes collected at 1, 6, 12 and 24 h pBM were dissected into buffer (69 mg NEM, 4.3 mg DTPA, 49 mg potassium acetate in 10 mL water, pH 6.5). Immediately prior to blood feeding, samples of mouse blood were obtained by tail snip and diluted 1:10 into buffer A. Heme concentration was measured and samples containing 1.5 nmol heme in 3 μL buffer were mixed with an equal volumes of 50 μM NEM containing 2.5% SDS. Samples were incubated for 30 min at 37°C. An equal volume of 1 mM CuCl was added to each sample and incubated for 30 min at 37°C. Half volume of 4 mM Biotin-HPDP (*N*-[6-(biotinamido)hexyl]-3'-(2'-pyridyidithiol) propionamide, US Alchemy, Inc.; made by diluting first to 50 mM in DMF then to 4 mM in DMSO) was added to each sample; samples were incubated for 30 min at room temperature. For controls, a duplicate sample set was processed identically except that DMSO without Biotin-HPDP was added in the last step. All reactions were performed in the dark. Sample proteins were mixed without heating with non-reducing Laemmli's sample buffer, electrophoretically separated on 10-20% Tris-HCl SDS-PAGE Ready gels (BioRad), then transferred to Immobilon™-P (Millipore) using semidry electrophoretic transfer (BioRad). Membranes were blocked with 10% milk before

exposure to 1:30,000 dilution of peroxidase-conjugated anti-biotin monoclonal antibodies (Clone BN-34; Sigma). Peroxidase activity was detected using SuperSignal® West Pico Chemiluminescent substrate (Pierce).

Hemoglobin analysis. *Anopheles stephensi* midguts (10 per sample) were dissected into PBS at 1, 12.5, and 24 h pBM from infected and uninfected bloodfed mosquitoes and from non-bloodfed mosquitoes. Mouse tail snip blood was collected immediately prior to blood feeding from the uninfected mouse used for feeding and diluted 1:10 in PBS. Heme concentration was measured and samples containing 3 nmol heme in 5 µL PBS were mixed with 5 µL loading buffer (62.5 mM Tris-HCl, pH 6.8, 40% glygerol, 0.01 bromophenol blue with or without 2% β-mercaptoethanol). Proteins were electrophoretically separated on 7.5% polyacrylamide gels under native conditions. Hemoglobins (Hbs) were visible without staining as heme-containing red-brown bands. The electrophoretically separated proteins were transferred to Immobilon™-P (Millipore) using wet electrophoretic transfer (EC140 Mini Blot Module; E-C Apparatus Corporation) and Towbin transfer buffer (25 mM Tris, 192 mM Glycine, 20% methanol, 0.1% SDS, ~pH 8.3) as described by the manufacturer. Blots were treated with 1 mM levamisole, pH 7.5 (Sigma) for 20 min to block endogenous alkaline phosphatases (AP), then blocked for 1 h in TBS containing 5% non-fat dry milk powder and 0.02% Tween-20. For detection, western blots were incubated with rabbit anti-mouse Hb (Research Plus, Inc.) antisera at a 1:100,000 dilution overnight at 4°C followed by an AP-conjugated goat anti-rabbit IgG secondary antibody (Southern Biotechnology Associates) at 1:10,000 for 2 h at room temperature. The colorimetric 5-bromo-4-chloro-3-indolyl-phosphate (BCIP)/nitro blue tetrazolium (NBT) substrate (Vector) was used to visualize bands.

Immunohistochemical staining for nitrotyrosine (NTYR). To identify tyrosine nitration within tissues of the mosquito abdomen, immunohistochemistry was performed. The immunohistochemical detection of NTYR was adapted from protocols of Ischiropoulos *et al.* **[370]**. Non-bloodfed, infected and uninfected *A. stephensi* were collected and preserved in Lillie's Neutral Buffer at 1, 3 and 6 d pBM. Ten-micron

sections of paraffin-embedded mosquitoes were prepared and mounted on poly-lysine coated slides by American HistoLabs, Inc. After sequential de-paraffinization with xylenes (twice for 10 min) and rehydration through graded alcohols (100%, 95%, and 70%; twice each for 5 min), the sections rinsed with PBS (0.5 M NaCl, 2.7 mM KCl, 4.3 mM $Na_2HPO_4 \bullet 7H_2O$, 1.4 mM KH_2PO_4; pH 7.2) and incubated 5 min in PBS containing 0.3% Triton X-100. The higher salt content of this PBS was necessary to reduce non-specific staining. Subsequent washes between treatments used PBS with 1% Tween-20 (PBST). Endogenous peroxidases were blocked using a 5% H_2O_2/95% methanol mixture. To facilitate the use of biotinylated antibodies and avidin-biotin complex (ABC) which increased the sensitivity of detection **[371, 372]**, endogenous avidin and biotin were also blocked by first incubating sections PBS supplemented with 0.1% streptavidin (30 min at 37°C) followed by PBS supplemented with d-biotin (30 min at 37°C) **[373, 374]**. The sections were incubated with 5% normal goat serum (Vector) in PBST for 30 min at 37°C to block nonspecific binding. Polyclonal anti-nitrotyrosine (αNTYR; Upstate Biotechnology) was used as the primary antibody (1:700 for 90 min at 37°C) and a biotinylated anti-rabbit (Vector Labs) was used as the secondary antibody (1:200 for 40 min at 37°C). Antibodies were diluted in PBST. The ABC (Avidin Biotin Complex) kit and VIP (Very Intense Purple) substrate (Vector Labs) were chosen for detection to amplify the signal and contrast with the brown-red color of the midgut contents. Slides were incubated with PN diluted 1:10 in PBS to create positive controls. Negative controls consisted of sections detected with αNTYR pre-absorbed overnight with NTYR or sections treated with 0.5 M sodium hydrosulfite in N_2 purged 0.01 N NaOH (3 times for 5 min). Sodium hydrosulfite converted NTYR to aminotyrosine which was not detected by the antibody.

Statistics. Statistical significance was evaluated using the Student's *t* test (Microsoft Excel). Although p values of 0.01 and 0.05 are conventionally used to define differences between means that are significant, it has been reported that with biological experiments of small sample size, $p<0.1$ can be interpreted as significant if the data support other biological observations **[375]**. I have generally indicated $p<0.05$ as significant, however, in several cases $p<0.1$ was used to designate significance.

RESULTS

Total nitrite levels. $^{\bullet}$NO can be measured directly using $^{\bullet}$NO-specific electrodes and chemiluminescence, however, the short half-life and low concentrations of $^{\bullet}$NO *in vivo* **[376]** reduce the practicality of these methods. The auto-oxidation of $^{\bullet}$NO in aqueous solutions leads to nitrite formation **[86, 377]**. As such, nitrites alone have been used to evaluate $^{\bullet}$NO production. In biological systems, however, nitrates, rather than nitrites, predominate as a result of the reactions of $^{\bullet}$NO with targets such as oxyHb and $O_2^{\bullet-}$ **[86, 172, 279, 378-380]**. Nitrites and nitrates are stable end products of $^{\bullet}$NO metabolism (they are stable in frozen plasma for at least 1 yr **[381]**) and are well established indicators of $^{\bullet}$NO production **[380]**. Because the bloodfed midgut is rich in Hb, nitrates are predicted to be a major component of the stable nitrite and nitrate end products. Thus, I evaluated both the nitrite and nitrate content. For these assays, nitrates were converted to nitrites and the "total nitrite" level was measured using the conventional Griess assay. Nitrate to nitrite conversion can be accomplished through enzymatic conversion with nitrate reductase **[382, 383]** or reduction with metallic cadmium **[351, 352]**. Nitrate reductase-catalyzed conversion of nitrates to nitrites is incomplete (30-64% yield), preventing its use for nitrate analysis in serum **[384, 385]**. As such, our method employed Cd-mediated conversion.

At 24 h pBM, total nitrite levels were significantly higher in midgut blood samples from *P. berghei*-infected mosquitoes (36.5 ± 10.5 μM) compared to midgut blood samples from uninfected *A. stephensi* **(**21.9 ± 7.1 μM; **Fig. 2-2)**. In humans, by comparison, nitrite/nitrate serum levels are elevated (>40 μM) during malaria parasite infection compared to control uninfected individuals (~25 μM) **[386, 387]**. The timing of increased nitrosative stress as measured by Griess assay coincides with the invasion of mosquito midgut epithelium by *Plasmodium* ookinetes and follows induction of *AsNOS* expression in the midgut epithelium. At 6 h pBM, *AsNOS* expression was increased in parasite-infected midguts **(Fig. 1-4)**. Although *AsNOS* was not significantly induced at 12 and 24 h, NADPH-dependent diaphorase staining revealed that AsNOS protein was elevated in infected midguts at 24 h pBM **(Fig. 1-5**; **[52])**. Elevation in RNIs, as characterized by the stable end products nitrite and nitrate, was detectable by Griess assay

some hours after *AsNOS* induction. This lag likely reflects, to some extent, the time required for protein synthesis. Catalysis, in contrast, is nearly coincident with RNI formation; •NO is highly reactive and fleeting. The rapid auto-oxidation of •NO in solution would presumably lead to increased nitrite levels shortly after synthesis. Elevated nitrite levels may also reflect the reaction of •NO with other compounds forming more stable RNIs which are less labile and can exert their effects after •NO production or further from the site of •NO synthesis. Because Griess analyses cannot discriminate among these chemical routes leading to nitrite formation, my next goal was to determine which RNIs were formed in midgut blood, and whether these compounds could aid in preserving and extending •NO bioactivity. My preliminary assays were focused on the formation of SNOs since recent investigations have shown that SNOs retain •NO activity **[79, 233, 255, 388]** and are toxic to *P. falciparum in vitro* **[92]**.

Photolyzable adducts of •NO. Measurements of nitrite/nitrate may underestimate significant changes in •NO flux because some RNIs do not decompose to these stable end products. Notably, *S*-nitrosation of thiols and NTYR formation (*e.g.* from PN derived from •NO reacting with $O_2^{\bullet-}$) are not detected by the Griess assay **[131, 151]**. •NO can also react with transition metal ions to form metal nitrosyls (*e.g.* with the Fe porphyrin of Hb; **[83, 94, 389]**). •NO that is bound to thiols and metal ions ("photolyzed-•NO") can be cleaved by ultraviolet (UV) light and reacted with ozone to form excited nitrogen dioxide which can be detected using the Nitrolyte **[102, 360]**. Although free •NO can also be detected using this technique, the time from sample collection to analysis in most systems would allow autooxidation to nitrite, decreasing the likelihood that free •NO contributes to sample measurements.

The Nitrolyte was used to measure photolyzed-•NO levels in lysates of midguts dissected from *A. stephensi* immediately after (0 h) to 33.5 h after feeding on uninfected or *P. berghei*-infected mice. In these assays, photolyzed-•NO levels in the uninfected and infected midguts did not differ at early time points **(<12 h; Fig. 2-3)**. At 12.5-13.5 h and 24-25.5 h pBM, however, the concentration of photolyzed-•NO from midgut RNIs was significantly higher in infected compared to uninfected samples **(Fig. 2-3)**. These measurements, even from uninfected mosquitoes, were significantly higher than blood

levels of photolyzed-•NO in some mammals. For example, Stamler *et al.* **[390]** reported levels of 125-250 nM •NO/mM heme in rat blood. Relative to normal rat blood, uninfected midgut blood samples contained 0.2 to 4-fold higher concentrations of •NO while infected midgut blood samples contained 2.5 to 7-fold higher concentrations of •NO. The timing of increased photolyzed-•NO in infected midguts relative to uninfected midguts was consistent with the timing of total nitrite increase as measured by the Griess assay **(Fig. 2-2)** and both patterns were consistent with the timing of ookinete invasion of the midgut epithelium.

In an initial trial, preincubation of a midgut lysate sample with $HgCl_2$ resulted in a decrease in signal output from photolysis-chemiluminescence, indicating that a portion of photolyzed-•NO existed as mercury-labile SNOs (not shown). Unfortunately, excessive sample precipitation following $HgCl_2$ reduction precluded accurate readings. Nevertheless, my observations prompted further study of midgut SNO levels. Extensive trials to identify a reagent that would selectively reduce SNOs without causing sample precipitation or incomplete SNO reduction failed (not shown). Those compounds included in testing were $HgCl_2$, dithionite, p-chloromercuribenzoic acid, cysteine/copper (Cys/Cu (I)), tris (2-carboxyethyl) phosphine hydrochloride (TCEP), and 1,4-dithio-DL-threitol (DTT). These difficulties led to the development of an alternate assay for measurement of midgut lysate SNOs.

Selective chemical reduction of midgut RNIs. Sample processing problems described above precluded the use of photolysis-chemiluminescence to evaluate midgut lysate SNOs. As such, I attempted to use the Saville assay **[367]**, which is based on $HgCl_2$-induced cleavage of RSNOs to form nitrites followed by detection of nitrites by the Griess reagent. However, excessive protein precipitation, interference from oxyHb absorption spectra, and low sensitivity prevented collection of data from midgut lysates using the Saville assay (not shown). Subsequent protocols were based on selective chemical reduction and measurement using the Sievers •NO Analyzer (NOA). These assays and instrumentation detect free •NO from reduction in a manner that is indistinguishable from that of the Nitrolyte, however, the reaction vessel is more suitable for difficult samples.

Together with NOA detection, selective chemical reduction can be used to differentiate various RNIs and SNOs **[356, 358, 361] (Appendix C)**. As such, I used three reduction treatments to measure midgut lysate nitrogen oxides (NO_x; including SNOs **[358, 362, 365]**, nitrite/nitrate and higher oxides of nitrogen), SNOs, nitrates and nitrites. Treatment with VCl_3/HCl revealed increased levels of NO_x in infected midguts compared to uninfected midguts at both 12.5 and 24 h **(**$p=0.049$ and $p=0.069$, respectively; **Fig. 2-4)**. The mean percentage increase in NO_x levels at 12.5 h was 59.5% (95% confidence interval [CI] -0.8 to 119.8), and at 24 h, the mean percentage increase was 50.8% (95% CI -56.6 to 158.2). Sample variation was, therefore, quite high, but less than sample variation reported for human plasma **[391, 392]**. Sample to sample variability may be attributable in part to the differences in infection intensities between cohorts, which affect induction of parasite-activated immune genes **[58]**.

The sample buffer for NOA analyses included ferricyanide **[359]** to stabilize midgut lysate SNOs, so that these RNIs could be distinguished from others. Ferricyanide can also release $^{\bullet}NO$ from nitrosylHb via the formation of metHb **[359]**, which would increase measurable nitrate levels in midgut lysates. At 24-25.5 h pBM, the photolyzed-$^{\bullet}NO$ concentrations were 0.87 ± 0.27 and 0.19 ± 0.08 μM/mM heme in the infected and uninfected midgut lysates, respectively **(Fig. 2-3)**. However, even if 100% of the photolyzed-$^{\bullet}NO$ was derived from metal nitrosyls which had been converted to nitrates, these values are too small to completely account for the differences in infected and uninfected NO_x levels. Hence, my data are in agreement with the observation that >80% of the total $^{\bullet}NO$-related compounds in blood can be accounted for by free nitrite/nitrate **[393]**.

Relative levels of nitrite and SNOs **(Fig. 2-5)** indicated that these RNIs likely contributed very little to the observed differences in NO_x levels between infected and uninfected midguts using VCl_3/HCl treatment **(Fig. 2-4)**. Differences detected with VCl_3/HCl and KI/acetic acid, therefore, were likely due to increased levels of nitrate and higher oxides of nitrogen. Hence, these results also suggest that the differences in photolyzed-$^{\bullet}NO$ **(Fig. 2-3)** in infected and uninfected midguts were more likely due to metal nitrosyls than to SNOs. Based on the molar concentration of Hb in the midgut, nitrosylHb would be expected to represent a major photolyzable adduct of $^{\bullet}NO$. If this

were the case, elevated levels of midgut nitrosylHb following the inflammatory response of *A. stephensi* to *P. berghei* would be consistent with observations of significant increase in nitrosylHb levels in venous blood from rats experiencing endotoxic shock **[394, 395]**.

At 24 h pBM, NO_x levels in midgut lysates from *P. berghei*-infected and from uninfected *A. stephensi* were 13.2 ± 3.9 and 8.7 ± 1.9 μM/mM heme **(Fig. 2-4)**, while nitrite levels measured by acidic iodide reduction-chemiluminescence were 3.0 ± 0.5 and 3.1 ± 0.8 μM/mM heme for infected and uninfected midguts (not shown), respectively. Griess assay data presented a different picture: at 24 h pBM, total nitrite levels in infected midgut lysate were 2.9 ± 0.5 μM/mM heme, while total nitrite levels in uninfected midguts were 1.6 ± 0.3 μM/mM heme **(Fig. 2-2)**. Data from other studies has shown that the recovery of $^{\bullet}NO$ from nitrates following acidic iodide reduction was <1.7% and often no conversion was detected **[356]**; thus the elevated nitrite levels detected using NOA analysis were not due to reduction of other RNIs. Incomplete Cd reduction of nitrates and increased sensitivity of chemical reduction-chemiluminescence may also contribute to these discrepancies.

Previous work indicated that hemolymph nitrite/nitrate levels were 10-50 μM in uninfected *A. stephensi* and up to 200 μM in *P. berghei*-infected mosquitoes **(Fig. 1-6**; **[52])**. When midgut heme concentrations are accounted for **(Fig. 2-1)**, midgut lysate NO_x concentrations were equivalent to 68.5 ± 11.3 μM and 101.7 ± 18.0 μM at 12.5 h pBM for uninfected and infected midguts, respectively, and 101.7 ± 29.0 μM and 196.2 ± 58.8 μM at 24 h pBM for uninfected and infected midguts, respectively **(Fig. 2-4)**. In sum, these values corresponded reasonably well with published hemolymph nitrite/nitrate levels **[52]**. Serum nitrite and/or nitrate levels >75 μM are consistent with levels reported in human sepsis, an often fatal inflammatory condition **[391, 392]**. Thus the NOA data revealed that the $^{\bullet}NO$-mediated defense of *A. stephensi* to *P. berghei* is an inflammatory response that is characterized by the formation of nitrates and higher oxides of nitrogen.

Potential confounding sources of RNIs. The elevated RNIs in the *P. berghei*-infected *A. stephensi* midgut could be derived from three sources: the parasite, the ingested mouse blood, and the mosquito. Although NOS-like activity was reported in *P. falciparum* asexual stages **[396]**, no prototypical NOS gene has been identified in the *P.*

falciparum genome and no further studies have corroborated these findings. As such, I assumed that the parasite does not contribute •NO to the midgut environment. ICR mice do not synthesize inducible •NO in response to *P. berghei* infection **[397]**, indicating that the ingested blood was not likely the source of *de novo* •NO production and RNI formation.

To determine the relative contribution of mosquito produced •NO/RNIs to those ingested during feeding, I provided the NOS inhibitor L-NAME (N^G-nitro-L-arginine methyl ester) or the inactive stereoisomer D-NAME as dietary supplements to *A. stephensi*. If the elevated RNIs were mosquito-derived, then L-NAME but not D-NAME or water should suppress the elevation of infected midgut RNIs. Midguts were collected at 12.5 and 24 h after feeding and the total levels of NO_x and nitrites were measured as described previously (NOA). Absolute values of these RNIs were not usable since NAME was also chemically reduced under these conditions **[358, 362, 398, 399]**. As such, it was assumed that uninfected and infected mosquitoes, on average, consumed equal amounts of NAME and relative values (infected/uninfected) of RNIs were assessed. Since L-NAME, but neither D-NAME nor water, was capable of reducing the levels of NO_x and nitrite, the increase in RNIs in the infected midgut were derived from AsNOS catalytic activity **(Fig. 2-6)**. These data are also in agreement with previous observations which showed that AsNOS activity was decreased by L-NAME to a larger degree in lysates from *P. berghei*-infected mosquitoes than in lysates from uninfected mosquitoes **[52]**. Results shown are from a single experiment, thus low induction of NO_x may be characteristic to the infection of this cohort of mosquitoes. The fact that NAME had a similar affect on nitrite and nitrate levels is indeed odd since previous results showed no induction in nitrite level in response to infection **(Fig. 2-5)**. Because NAME was also reduced, the induction values may not be accurate. As such, the experiment should be repeated and include steps to remove NAME **[399]** prior to analysis (see also Future Directions).

Biotin switch analysis of S-nitrosated proteins. Plasma nitrite/nitrate levels in rats can be increased 8-fold relative to controls following injection with LPS **[388]**. This treatment also induced a 2- to 3-fold increase in plasma SNO levels **[234, 388]**, which

included a ~24-fold increase in SNOHb **[388]**. In *P. berghei*-infected *A. stephensi*, midgut *AsNOS* expression is induced and nitrite/nitrate levels in the infected midguts were increased 2-fold relative to uninfected midguts at 24 h pBM. Although significant differences in the levels of SNOs in infected and uninfected midguts were not detected, concentrations of specific *S*-nitrosated compounds such as SNOHb may change in response to infection. Changes in the profiles of SNO-modified peptides and proteins following infection could influence the toxicity of •NO in the midgut. For example, some SNO-modified proteins and peptides release higher fluxes of •NO than others and this phenomenon has physiological relevance. **[92, 102, 194, 257, 259, 281, 283]** For example, *S*-nitrosoalbumin (SNO-Alb) measured *in vivo* has been shown to have a half-life of ~30 min **[234]** and the slow release of •NO from SNO-Alb would substantially increase the bioactivity of •NO.

To determine whether the profile of *S*-nitrosated midgut proteins differed in lysates from *P. berghei*-infected versus uninfected *A. stephensi*, I initially attempted to analyze midgut lysates by western blotting with rabbit SNOAlb/Cys-NO antiserum provided by Dr. Andrew Gow. Unfortunately, these assays were not successful. As such, I used an alternate method to detect *S*-nitrosated proteins by western blotting based on a "SNO-biotin switch" method **[369]**. In this method, •NO molecules bound to thiols were exchanged with biotin. Each biotin was predicted to add ~0.225 kD to the protein. The modified proteins were detected by western analysis using anti-biotin antisera.

SNO-biotin switch western blots of midgut lysates from *P. berghei*-infected and uninfected *A. stephensi* showed little to no differences in the profiles of SNO-modified proteins **(Fig. 2-7, A)**. As expected, digestion of midgut blood over time appeared to reduce protein complexity in the samples **(compare 24 h versus 1 h, Fig. 2-7)**. In all SNO-biotin switch blots, however, the absence of proteins <29 kD was unexpected. In general, I predicted that as digestion proceeded, smaller cross-reacting digested fragments of *S*-nitrosated proteins would become more abundant. However, even at early times post-digestion **(Fig. 2-7, A, 1 h)**, no proteins <29 kD were *S*-nitrosated. In the case of Hb, a strong cross-reacting band at ~64 kD, the molecular mass of tetrameric Hb, was evident in the SNO-biotin-switch blots, particularly so at 24 h **(Fig. 2-7, B, 24 h)**. This cross-reacting protein may be *S*-nitrosated on β-Cys^{93}, the residue that is modified in

mammalian Hbs *in vivo* **[105, 247, 390]**. As digestion proceeded in *A. stephensi*, tetrameric Hb abundance was reduced, and dimeric Hb (~32 kD) abundance was increased **(Fig. 2-7, B, panel b)** as expected. Although monomeric Hb was detected by Hb western analysis, cross-reacting bands corresponding to monomeric Hb were not evident in the SNO-biotin switch blots. This finding suggests that perhaps nitrosation of β-Cys^{93} requires cooperativity of the other subunits or that *S*-nitrosated monomeric Hb is less stable than dimeric and tetrameric forms. The lack of cross-reacting proteins <29 kD have been noted by others. For example, nitrosated species were only detected in the higher MW fraction (>20 kD) in several studies of human plasma **[194, 281, 400]**.

In addition to Hb, Alb is an abundant blood target for *S*-nitrosation. Although the level of SNOs in plasma differs between species (*e.g.* human ~7 μM and rabbit ~1 μM), ~95% of SNOs in plasma exist as *S*-nitrosoproteins, ~80% of which is SNO-Alb **[102]**. From this observation, I would predict that the some bands detected in the SNO-biotin switch blots would correspond to Alb. Since tetrameric Hb and albumin both migrate at ~64 kD, they are not clearly distiguishable by 1D western blot analysis. Although my data cannot be used to draw conclusions about Alb, some facets of blood digestion would predict that SNOHb may be more abundant than SNOAlb. First, the mosquito the blood meal is concentrated by diuresis to a heme concentration of ~18 mM immediately following blood meal ingestion **(Fig. 2-1)**. This value is closer to that reported for intact RBCs (17-22 mM; **[190, 401]**) rather than whole blood (~10 mM heme; **[402]**), which may favor an increase in SNOHb relative to SNOAlb. In addition, digestion liberates Hb from RBCs, which would significantly increase access for *S*-nitrosation.

Nitrotyrosine staining. I hypothesized that elevated AsNOS activity in response to parasite infection may damage mosquito tissues through the formation of toxic RNIs. NTYR modification is often used as a marker of nitrosative stress **[342]**. Many disease states are associated with elevated NTYR levels **[188, 232]**. $^{\bullet}$NO is indirectly capable of reacting with tyrosine residues to form NTYR **[403]**, while PN **[206, 207, 212-214]** and NO^- **[149, 404]** can directly induce NTYR formation. PN readily nitrates proteins *in vitro* and has also been proposed to be the major mediator of protein nitration *in vivo* **[206, 207, 212-214]**.

Immunohistochemical detection of NTYR **[370]** was performed on tissue sections of non-bloodfed, and infected and uninfected *A. stephensi* collected 1, 3 and 6 d pBM. Greater NTYR levels were observed in tissues of *P. berghei*-infected versus uninfected *A. stephensi* at 24 h pBM **(Fig. 2-8)**. Staining was particularly evident in the fat body, eggs, midgut epithelium and blood bolus. Staining was also more intense in the distal portion of the midgut, consistent with observations that parasite invasion and oocyst development are concentrated in this area. Together, midgut RNI levels and NTYR data suggest that nitrosative stress is enhanced in and around the infected midgut during the time of ookinete invasion of the midgut epithelium and oocyst development. At 3 and 6 d pBM, NTYR staining was low to undetectable in both infected and uninfected mosquito samples (not shown). The lack of NTYR formation is assumed to be the result of degradation of nitrated proteins **[405, 406]** and lack of new NTYR formation. Although *AsNOS* is elevated at 3 d (not shown) the elimination of the blood meal bolus at ~48 h changes the midgut environment. If NTYR formation is mediated through blood meal constituents, such as Hb-catalyzed reactions or blood meal-derived signaling factors, then NTYR formation will not occur following the completion of blood meal digestion.

Comparable recent studies by Kumar *et al.* **[407]** reported an unspecified time lag between *AsNOS* expression and protein nitration in *P. berghei* ookinete-invaded midgut epithelial cells. Although my time course of NTYR staining was not extensive enough to draw detailed conclusions about timing, I suspect that the timing behind my observations agrees with the timing reported by Kumar *et al.* **[407]**. Specifically, elevated *AsNOS* expression was noted in the infected *A. stephensi* midgut at 6 h pBM **(Fig. 1-4)** and elevated NTYR formation seen at 24 h pBM. As such, the onset of NTYR formation would have occurred between 6 and 24 h pBM. To more precisely determine the onset of NTYR formation in infected versus uninfected *A. stephensi*, I had planned to repeat NTYR analyses with sections of mosquitoes collected at 2, 8, 12.5, 24, and 33 h pBM. Although staining of 24 h samples corroborated my initial findings (not shown), technical problems with NTYR antisera prevented completion of these analyses.

Hemoglobin analyses. UV-vis spectra of midgut lysates from 1-49 h pBM revealed that Hb in infected and uninfected samples existed mainly as oxyHb during the

period of digestion **(Fig. 2-9)**. These findings were particularly notable given that mammalian Hb is readily oxidized from oxyHb to metHb following blood withdrawal from the host (personal communication, Dr. Andrew Gow). If nitrosylHb is, in fact, a major donor to photolyzed-$^{\bullet}$NO output, the oxyHb spectra would be consistent with the increased affinity of the reasonably stable nitrosylHb for oxygen under alkaline conditions **[408, 409]** like those found in the midguts of *Anopheles* spp. **[63, 64]**. The lack of metHb in the *A. stephensi* midgut blood samples suggests that the midgut is a reducing environment, deriving in part from abundant blood-derived free thiols such as GSH which limit the conversion of oxyHb to metHb **[410]**. It is also possible that oxyHb is maintained by the action of metHb reductase derived from RBCs **[411]**, although this alternative is less likely at extended times post-digestion.

In higher animals, Hbs function to transport oxygen to tissues and carbon dioxide away from them. However, it is believed that the first functions of Hbs were related to $^{\bullet}$NO detoxification **[273, 274]**. Bacterial, yeast and some plant Hbs provide protection against nitrosative stress and microbes. For example, truncated Hbs from bacteria protect against $^{\bullet}$NO damage by facilitating conversion of $^{\bullet}$NO to nitrate **[326, 412]**. Bacterial and yeast flavohemoglobins (flavoHb) catalyze the conversion of $^{\bullet}$NO to nitrates and NO^- **[274, 320, 322, 413]**, with bacterial catalysis dependent on NADPH, FAD, and O_2 **[273]**.

Preliminary results with *A. stephensi* midgut lysates suggested the mosquito midgut may alter the behavior of mouse Hb towards O_2. Incremental addition of $^{\bullet}$NO to midgut lysates resulted in $^{\bullet}$NO-primed NAD(P)H dependent oxygen consumption (data not shown). This response was similar to that seen with *E. coli* flavoHb **[273]** and also to *Ascaris lumbricoides* Hb, which consumes O_2 to maintain a low pO_2 that favors parasite viability **[276, 414]**. Lower pO_2 enhances the killing power of NO$^{\bullet}$ for *P. falciparum* **[280]**, but, paradoxically, is also required for the parasite to survive in culture **[415]**. I propose that *A. stephensi*-generated $^{\bullet}$NO may help maintain low pO_2 to which the parasite has adjusted, but which also facilitates the control of parasite development by $^{\bullet}$NO synthesis. To probe these interesting findings, midgut conditions including oxygen tension, reducing environment and thiol content should be characterized in future studies.

Hemoglobins also participate in host defense as antimicrobial toxins. Specifically, fragments of Hb termed "hemocidins" are antimicrobial **[416-418]** and have been

identified in digested bovine blood from *Boophilus microplus* and *Ornithodoros moubata* ticks **[419-421]**. Hemocidins inhibit the growth of Gram-positive and Gram-negative bacteria and yeasts **[422]** but have not been tested for activity against eukarotic parasites such as *Plasmodium* spp. To determine whether novel Hb digestion products were present in the *A. stephensi* midgut, I used native PAGE to electrophoretically separate midgut lysate proteins. Hemoglobin can be directly observed on these gels due to the red-brown color derived from heme. Although no prominent truncated Hbs were observed in midgut lysates, a protein with apparent high MW and red-brown color of heme was notable in infected midgut lysates at 12.5 and 24 h pBM and not in normal mouse blood, uninfected midgut lysates, or samples collected at 1 h pBM **(Fig. 2-10, A)**. The slow migrating protein was not evident following sample treatment with β-mercaptoethanol, indicating that disulfide bonds were responsible for reduced migration **(Fig. 2-10, B)**. To determine whether the slow migrating protein was in fact Hb, I performed anti-Hb western blots on the separated, transferred proteins. Although no cross-reacting proteins consistent with Hb fragmentation were observed (not shown), a cross-reacting protein with high apparent MW indicated that the slow migrating, disulfide-linked protein was Hb **(Fig. 2-10, C)**. The association of this slow migrating Hb with only infected midguts suggested that nitrosative or oxidative stress may be associated with its formation. Interestingly, some infected midgut lysates appeared to lack slow migrating Hb, suggesting that variation in parasite infection intensity and, hence, nitrosative stress is translated into variation in disulfide formation.

Evidence for midgut PN. The formation of PN in biological systems is mainly due to the reaction of $^{\bullet}NO$ with $O_2^{\bullet-}$ at almost diffusion controlled rates (6.7×10^9 M^{-1} s^{-1}) **[156]**. Uric acid/urate is a product of purine metabolism with limited membrane permeability and is a potent scavenger of PN **[136]**. The mechanism of protection from PN by urate is still under investigation **[423]**. However, urate administration to mice with symptoms of multiple sclerosis significantly decreased NTYR formation in brain and greatly reduced disease severity **[424]**. Peroxynitrite readily nitrates proteins *in vitro* and has also been proposed to be the major mediator of protein nitration *in vivo* **[206, 207, 212-214]**. Similarly, it is believed that iNOS upregulation in multiple sclerosis lesions

and the formation of PN leads to the formation of NTYR in brain tissues of MS patients **[424]**. In a similar manner, I proposed that midgut NTYR staining in infected midguts was due to elevated PN. Further, I hypothesized that if PN is a mosquito-derived RNI that also kills malaria parasites, then mosquitoes fed a urate-supplemented diet should have increased parasite loads relative to controls.

All mammals except higher order primates have a urate oxidase (*Uro*) gene that encodes a protein that catalyses the oxidation of urate to allantoin **[425-427]**. Interestingly, the abrupt evolutionary event that led to the lack of *Uro* in higher primates, at the risk of urate-caused disease, may be a direct result of the capacity of this molecule to inactivate PN **[424]**. *Drosophila melanogaster* has a single copy of *Uro* which is expressed only in the malphigian tubules **[428]**. A BLAST analysis using *DmUro* amino acid sequence as query yielded a single hit in *A. gambiae* genome (2e-93 on chrmomosome 3, not shown). From these observations, I predicted that *A. stephensi Uro* would catalyze the conversion of dietary urate to allantoin, a compound that lacks the antioxidant properties of urate. As a control for urate, allantoin was provided as a dietary supplement to the mosquitoes.

After confirming that mosquitoes would ingest urate as a dietary supplement, cartons of *A. stephensi* were provided supplements of 1 mM urate in PBS, allantoin in PBS or PBS alone as soaked cotton balls prior to and during infection with *P. berghei*. At 10 d pBM, midguts from each treatment group were dissected and oocysts on each midgut were counted. Using both the Student's *t* test and the more robust Student-Newman-Keuls test for data analysis, the mean oocyst counts between PBS and allantoin treatments were not different from each other but both were different from urate treatment **(Fig. 2-11)**. The significantly higher oocyst loads in urate-fed mosquitoes supported my hypothesis that PN is a midgut RNI that limits malaria parasite development.

Human plasma contains urate at concentrations up to 500 μM **[426]**, while mouse plasma contains ~20 μM urate **[424]**. If *A. stephensi* could utilize ingested urate as an antioxidant, significant differences in infection could result from feeds that utilize human versus mouse blood. To test this possibility, I repeated the urate feeding assay, but included a urate dose of 500 μM for comparison. When mosquitoes were fed 500 μM

urate, parasite loads were not significantly different from controls (**Fig. 2-11**). Thus, ingested urate alone from human blood is predicted to have a minimal impact on parasite infection in the mosquito.

DISCUSSION

Overview. In an aqueous solution, •NO undergoes auto-oxidation to nitrite **[86, 87] [reaction 9]**.

$$4NO + O_2 + 2H_2O \rightarrow 4HNO_2 \rightarrow 4NO_2^- + 4H^+ \qquad \textbf{(9)}$$

However in the blood-filled mosquito midgut, •NO is predicted to react with midgut contents to form a complex array of RNIs. During parasite infection, the expression of *AsNOS* is induced to a greater extent than during normal blood feeding **(Fig. 1-4**; **[52])**. Activity of AsNOS prevents development of parasites to the oocyst stage **[52]**, but the mechanism by which this occurs has remained unknown. I hypothesized that •NO synthesis limits *Plasmodium* development through the increased formation of certain toxic RNIs that extend and preserve the bioactivity of •NO. Specifically, parasite infection in *A. stephensi* leads to increased levels of nitrate and other higher oxides of nitrogen (NO_x), NTYR, and photolyzed-•NO adducts. Because no elevation in *S*-nitrosated compounds was detected following infection, I proposed that the photolyzed-•NO adducts were metal nitrosyls. The predominant metal nitrosyl is probably nitrosylHb based on the high mM concentration of Hb in the midgut. Like the higher oxides of nitrogen, iron nitrosylHb is an indicator of inflammation and contributes to the formation of damaging oxygen radicals **[429]**. Alternatively, iron released from Hb during digestion may react with •NO to form dinitrosyl iron complexes (DNICs) **[108, 113]**. Although DNICs, like nitrosylHb, mediate toxic effects through redox destabilization **[430]**, the presence of nitrosyls in the midgut was not confirmed directly.

In addition to contributing to the direct formation of toxic RNIs, a high Hb concentration could also explain the formation of high levels of nitrate, which can be

formed from the reaction of •NO with oxyHb **[reaction 10] [279, 431-433]**, although the expected increases in metHb were not observed. The lack of metHb may be due the action of metHb reductase or other enzymes that can catalyze reduction of metHb to oxyHb.

$$Hb(Fe^{2+})–O_2 + {}^{\bullet}NO \rightarrow Hb(Fe^{3+}) + NO_3^- \qquad \textbf{(10)}$$

Although photolyzed-•NO levels were increased in response to infection, these RNIs cannot completely account for the elevation in NO_x levels. As such, I hypothesized that other RNIs are formed under the inflammatory conditions of parasite infection in *A. stephensi*. High levels of nitrates in the midgut would be directly toxic to *Plasmodium* **[92]**. However, because NO_x formed under conditions of oxidative and nitrosative stress associated with inflammation ultimately degrade to nitrate **[434]**, I can also infer that the higher nitrate levels in the infected mosquito midgut are the result of synthesis of inflammatory NO_x that would hinder parasite development. These inflammatory and potentially toxic NO_x would include NO^- and PN, which together with nitrosylHb, would create an inhospitable environment for parasite development.

Possible mechanisms for nitrosyl Hb formation. Many researchers have pondered how •NO can regulate vascular reactivity in the presence of blood, where erythrocytic Hb should scavenge •NO **[73, 435]**. Similarly, how does •NO synthesis limit *Plasmodium* development in the blood-rich midgut of the mosquito? Classically, •NO can react with either deoxyHb to form nitrosylHb **[reaction 11] [94, 95]** or with oxyHb through a PN intermediate forming metHb and nitrate **[reaction 10]**. Alternatively the redox related form, NO^-, can react with metHb to form nitrosylHb **[reaction 12] [105, 115, 131, 134, 138-141]**.

$$Hb(Fe^{2+}) + {}^{\bullet}NO \Leftrightarrow Hb(Fe^{2+})–NO \qquad \textbf{(11)}$$

$$Hb(Fe^{3+}) + NO^- \Leftrightarrow Hb(Fe^{3+})–NO^- \Leftrightarrow Hb(Fe^{2+})–NO \qquad \textbf{(12)}$$

The levels of nitrosylHb *in vivo* are the subject of some debate and have been reported to be ~5 μM in mixed venous blood that is lowered to ~2.5 μM in arterial blood, consistent with allosteric control of intramolecular transfer of •NO in Hb [436]. In the vascular system there is a conversion between •NO on T-state (tense, deoxyHb) hemes (nitrosylHb) in venous blood and •NO on R-state (relaxed, oxyHb) thiols (SNOHb) after Hb is oxygenated by the lungs **[105, 247, 390]**. In blood both α- and β-chain nitrosyl heme in T-state Hb are formed in the microcirculation and venous system where lower oxygen and higher •NO synthesis are present. Because •NO dissociates faster from the β heme **[105]**, it has been reported that •NO binds selectively to α heme in the venous circulation **[247, 390, 437, 438]**. In the lungs, O_2 increases promoting R-state Hb causing •NO transfer from nitrosyl to β-Cys^{93}. •NO bound to the β-Cys^{93} of Hb in the R-state dissociates from the thiol when the T-state is reformed **[247, 390]**. When the mosquito ingests its blood meal, Hb is drawn from the peripheral venous blood, thus it likely contains nitrosylHb. However the observation that midgut blood contains and maintains oxyHb suggests that ingestion of the blood meal is analogous to blood entering the lungs.

In addition to the reactions outlined above, nitrosylHb may form from the reaction of •NO with oxyHb. When •NO is added to oxyHb *in vitro*, the predominant species formed is metHb as expected from the classical reaction between Hb and •NO **[reaction 10] [401]**. This oxidation reaction has been given great significance in •NO biology, but data from Gow *et al.* **[83]** suggest that under normal physiological conditions the concentration of •NO relative to Hb is low therefore vacant hemes are in excess over •NO which enables the addition of •NO to heme to compete with the oxidation reaction. Using normoxic Hb (~99% O_2 saturation as exists in arterial blood) and physiological •NO concentrations (~1 μM), they have shown that a sizeable amount of •NO will form nitrosylHb instead of nitrate/metHb; the portion of nitrosyl Hb formed increased with increasing Hb concentration (up to 6% Hb as nitrosyl Hb) **[83]**. When aerated RBC were treated with 1 μM •NO the yield was 2:1:0 of SNO:iron-nitrosyl Hb:metHb **[83]**. *In vitro*, the addition of superoxide dismutase (SOD) to Hb increased the yield of total •NO bound to approximately 100% of $[NO]_o$ **[83]**.

Alternatively the formation of nitrosylHb can result from the reduction of metHb to deoxyHb which can then bind •NO **[401]**. It has been shown that in a solution of free

Hb under high local concentrations of •NO, three sequential additions of •NO to the same Hb would result in the net formation of nitrate and nitrosylHb **[reactions 13-15]**,

$$^{\bullet}NO + oxyHb \rightarrow metHb + NO_3^- \quad \textbf{(13)}$$

$$^{\bullet}NO + metHb \rightarrow deoxyHb + NO^{+\cdot} \quad \textbf{(14)}$$

$$^{\bullet}NO + deoxyHb \rightarrow NOHb(Fe^{2+}). \quad \textbf{(15)}$$

Under such a reaction one would assume that the release of nitrosonium ions would also elevate SNOHb. However cyanide-based trapping of metHb to prevent its reduction to deoxyHb, still resulted in SNOHb formation with bolus •NO addition, thus the SNOHb formed was not a result of metHb reduction **[401]**.

All reactions of •NO with Hb in the vasculature are believed to be decreased by the RBC membrane providing a diffusion barrier **[376]** and •NO partitioning into the hydrophobic cell membrane **[439]**. It is known that the kinetics of the reaction of •NO and Hb differ when Hb is cell-free versus intraerthrocytic **[378, 401, 440, 441]**. •NO reacts at least 1,000 times faster with free Hb than with Hb contained by the RBC membrane **[441]**. At 20ºC the rate constants for these reactions **[reactions 10 and 11]** are competitive at 3.7-9 x 10^7 $M^{-1}s^{-1}$ and 2.6 x 10^7 $M^{-1}s^{-1}$ respectively **[279, 432, 442, 443]**. Thus •NO formed should react preferentially with decompartmentalized Hb forming metHb and/or nitrosyl Hb. In a sickle-cell model where ~10% of RBC are lysed daily, elevated levels of cell free ferrous Hb were shown to consume μM levels of •NO; this was accompanied by iron nitrosylation and nitrosylHb dioxygenation (metHb and nitrate formation) **[441]**. Alternatively, it has been proposed that Hb transports •NO as *S*-nitrosothiol. The •NO bound to thiols is technically a nitrosonium cation (NO^+) thus it cannot react with ferrous heme. This makes SNOHb insensitive to the reactions with heme yet it is still "active" as it can release "NO" at sites of low oxygen tension **[83, 105, 247, 390, 436]**.

The midgut conditions resemble that of a cell-free Hb system since the RBCs nearest to the midgut epithelium, the source of •NO, are actively digested and lysed. Thus, the first interaction of •NO with the blood meal will be with cell-free blood components. Rates of erythrocyte hemolysis differ in different stains of mosquitoes;

within 20 min of ingestion there is 1% hemolysis in *An. albimanus* and *An. freeborni*, but 9.6% in *An. gambiae* **[63]**. The rate and amount in *A. stephensi* has not been tested. Nevertheless with digestion there is hemolysis, resulting in •NO-chemistry that would be different from chemistry with intact blood cells in the vasculature, increasing the likelihood that •NO and Hb can react/interact. The higher concentrations of Hb in the midgut together with high local concentrations of •NO produced by the midgut epithelium, could explain the increased propensity for nitrosylHb formation as described by Gow *et al.* **[83]**, yet by this mechanism metHb and SNOHb still are formed. Although higher levels of nitrates were observed in infected mosquitoes, there is not a corresponding increase in metHb or SNOHb as one would expect with the Hb-mediated dioxygenation reaction. This could be explained either by a strong metHb reductase (or other similar enzyme) to regenerate oxyHb, or another pathway to generate nitrates.

Although midgut conditions are more consistent with the chemistry typical for cell free Hb rather than intraerythrocytic Hb, the occurrence of Hb aggregation in the midgut hinders the accessibility of Hb that would occur in a true cell-free situation. The accessibility of Hb plays a role in the proposed scenario where three •NO are needed to react with a single oxyHb resulting in nitrosylHb formation **[401]**; in a mathematical model, lower accessibility could enhance HbFe(II)NO formation by ~30% **[401]**. Thus one can speculate this sequential addition of •NO to oxyHb to form nitrosylHb may be favored in the midgut where in addition to high local •NO fluxes being produced by the epithelium, Hb is freed from RBC and sequestered by aggregation during digestion. The net result of such a scenario would be higher levels of nitrosylHb and nitrate which would agree with results of my experiments.

A simpler explanation for my observations may be that the tetrameric nature of Hb allows the majority of subunits to be ligated with O_2, thereby producing spectra with oxyHb characteristics. If a minor population of Hb hemes are in the deoxy state in the ingested blood meal, •NO can bind directly to form nitrosylHb **[reaction 11]**. Under alkaline and oxygenated conditions, such as are found in the midgut **[63, 64]**, α-nitrosylHb can bind and carry oxygen in the β subunits of Hb **[409]**. If [oxyHb] >> [nitrosylHb] or [deoxyHb], these reactions would account for the observed presence of oxyHb in the mosquito midgut following blood feeding, a balance which may also be

maintained by the availability of free thiols. In addition, the binding of oxygen to nitrosylHb creates a nitrosyl/oxyHb hybrid, which would be predicted to have a 10^3-fold decreased heme affinity for $^{\bullet}NO$ **[409]**. This characteristic would predict that nitrosylHb would release $^{\bullet}NO$ by dissociation **[409]**, thereby maintaining the bioactivity of $^{\bullet}NO$ in the context of oxygenated Hb.

Evidence for PN in the A. stephensi midgut. I propose that parasite infection elevates $^{\bullet}NO$ and $O_2^{\bullet-}$ levels promoting the formation of PN, which in addition to limiting parasite development, nitrates tyrosines in proteins of the midgut epithelium and surrounding tissues of *A. stephensi*. Numerous experiments in our laboratory and in the laboratories of our colleagues indicate that NOS is induced in the mosquito in response to *Plasmodium* **[47, 48, 52, 57, 328, 444, 445]**. Data from *A. gambiae* suggest that $O_2^{\bullet-}$ formation is also likely to occur in the *A. stephensi* midgut. Specifically, analysis of the *A. gambiae* genome predicted that 16 peroxidases are encoded; mRNA levels of six of these genes were differentially expressed in response to ookinete invasion, with five induced and one reduced in response to infection **[407]**. One of these transcripts, AgDoux (ENSANGP00000006017), was highly expressed under conditions of ookinete invasion. AgDoux is predicted to function as a dual oxidase **[407]**, with an N-terminal peroxidase domain and a C-terminal NADPH oxidase domain **[446]**. As such, the local induction of Ag-Duox could lead to high local levels of $O_2^{\bullet-}$. Additionally, *A. albimunus* inoculated by enema with *P. berghei* ookinetes produced higher $O_2^{\bullet-}$ levels than controls **[447]**. Together with the known induction of NOS in response to parasite infection and several potential sources of $O_2^{\bullet-}$ (hemolymph **[448]**, Ag-Duox **[407]**, and alternative NOS catalysis **[41-43, 449, 450]**), PN formation and PN-mediated NTYR formation can be predicted to occur in *A. gambiae* and *A. stephensi*. Furthermore, the combination of $^{\bullet}NO$ and $O_2^{\bullet-}$ has been show to kill 75% of *P. berghei* ookinetes *in vitro* **[447, 451]**, suggesting that PN formation *in vivo* would be toxic to developing parasites.

Formation of $ONOOCO_2^-$ by the reaction between PN and CO_2 can increase the yield of nitration by 30% relative to that of PN alone **[67]**. Since the rate constant of PN for oxyHb and for CO_2 are comparable (k ~1 x 10^4 and 3 x 10^4 $M^{-1}s^{-1}$ at 25°C, respectively), local concentrations of CO_2 and oxyHb dictate the reactivity of PN **[339,**

452]. At low oxyHb concentrations most PN reacts with CO_2, thereby resulting in the reaction of oxyHb with $ONOOCO_2^-$, whereas at high oxyHb concentrations, more PN interacts directly with oxyHb **[190]**. The latter situation is more likely in RBCs where the concentration of oxyHb is 17-22 mM **[190].** Because midgut blood oxyHb concentration is in the range typical of RBCs, PN is more likely to react with oxyHb rather than with CO_2, suggesting that $ONOOCO_2^-$-mediated nitration does not occur in the midgut.

The effect of urate on parasite load in *A. stephensi* further suggests that PN, rather than $ONOOCO_2^-$, is present in the midgut. Uric acid inhibits nitration reactions and has been used as a scavenger of PN *in vitro* and *in vivo* **[453]**. In addition, urate can quench dihydrorhodamine oxidation mediated by AS **[136]**, indicating that urate can alter the chemistry of NO^-, which could indirectly influence PN formation. In contrast to these effects, urate has no effect on $ONOOCO_2^-$-mediated nitration **[213]**. Urate-inhibitable parasite reduction would, therefore, be consistent with PN as a mediator of toxicity and PN-mediated NTYR formation in *A. stephensi*. PN-mediated nitration reaction is believed to occur through a reaction with these intermediates **[reaction 16-18] [153]**,

$$ONOOH \rightarrow OH^{\bullet} + {}^{\bullet}NO_2 \rightarrow NO_3^- + H^+ \quad \textbf{(16)}$$

$$OH^{\bullet} + Tyr \rightarrow Tyr^{\bullet} + H_2O \quad \textbf{(17)}$$

$$Tyr^{\bullet} + {}^{\bullet}NO_2 \rightarrow NTYR \quad \textbf{(18)}$$

Since urate can also scavenge hydroxyl radical ($OH^{\bullet}$) **[454, 455]**, it is suggested that urate supplementation could also have increased parasite load by reducing levels of the cytotoxic $OH^{\bullet}$ intermediate. In addition PN can decay to nitrate either through homolysis of PN to ${}^{\bullet}NO_2$ and $OH^{\bullet}$ followed by the reaction of these products to form nitrate **[218]** or the rearrangement of *trans*-PN **[172, 202]**. The $OH^{\bullet}$ pathway is strongly favored following recent studies showing that PN was almost exclusively generated as *cis*-PN **[168, 169].** This would contribute to the increased nitrate level seen in infected formation from PN.

In addition to PN-induced NTYR formation, NO^-**,** heme proteins, transition metals and/or peroxidases can catalyze NTYR formation. Nitroxyl may nitrate phenols through its reaction with O_2 to form PN **[137, 149].** PN can directly nitrate Tyr or react

with transition metal centers to form NO_2^+ formation which can react with Tyr to form NTYR **[185, 207]**. In contrast to my hypothesis that NTYR formation is PN-mediated, Kumar *et al.* **[407]** propose that $^{\bullet}NO$ formation results in nitrite accumulation, which then serves as a substrate for a myeloperoxidase (MPO)-mediated tyrosine nitration **[407, 456]**. In support of this hypothesis, some *Plasmodium*-infected in *A. stephensi* cells stained very strongly with DAB indicating infection-induced peroxidase activity **[407]**. Further, the addition of nitrite and H_2O_2 to midgut homogenates, resulted in the nitration of BSA, indicating that nitrite/peroxidase-mediated tyrosine nitration can occur in the midgut environment **[407]**.

My data, however, indicate that nitrites required for the NTYR chemistry described by Kumar *et al.* **[407]** do not change in response to parasite infection in *A. stephensi*. Two explanations can be presented to resolve these differences: (1) induced nitrites are rapidly consumed in the H_2O_2/nitrite reactions thereby resulting in steady state levels of nitrite in *A. stephensi* and (2) $^{\bullet}NO$ is converted to higher oxides of nitrogen such as PN which partially nitrate tyrosine while the remainder decomposes to nitrates. Thus, I propose that two mechanisms for NTYR formation occur in *A. stephensi* and include one that is dependent on PN and one that is dependent on H_2O_2/peroxidase. Given that important processes in biological systems are often redundant, it is likely that multiple nitrating pathways function simultaneously. Recent biochemical experiments support both pathways (generating nitrogen dioxide or PN) operating simultaneously *in vivo* **[344]**. Specifically, the peroxidase/nitrite/H_2O_2 system can generate NTYR formation *in vitro* through two mechanisms; the first involves $^{\bullet}NO_2$ generation and the second has the enzyme complexed to PN **[344]**. As nitrite levels were increased, the second reaction pathway was favored over the first since nitrite competitively reduces peroxidase compound I. Thus, at higher levels of nitrite the PN pathway was favored **[344]**. The level of nitrite to achieve this transition was dependent on the type of peroxidase **[344]**. For both peroxidase-catalyzed reactions, only 50% of the oxidizing equivalents from H_2O_2 were used for nitrating phenol, with the remainder decaying to nitrate **[344].** These findings suggest that chemistry of the *A. stephensi* midgut could support NTYR formation through both $^{\bullet}NO_2$- and PN-mediated reactions.

Evidence for nitroxyl in the A. stephensi midgut. My experimental data support the presence of elevated NO^- levels in midguts of *Plasmodium*-infected *A. stephensi*. Specifically, disulfide-linked Hb, present only in infected midguts **(Fig. 2-10)**, may be a footprint for high NO^- levels, since the reaction of thiols with NO^- produces a RSNHOH species which can react with reduced thiols to form disulfide-linked species **[457-459] [reaction 19 and 20]**.

$$RSH + HNO \rightarrow RSNHOH \quad \textbf{(19)}$$

$$RSNHOH + R'SH \rightarrow 'RSSR + NH_2OH \quad \textbf{(20)}$$

Nitroxyl is also capable of NTYR formation **[149];** however because NO^- is a much weaker nitrating agent than PN or peroxidase/nitrite/H_2O_2, NTYR is not considered a marker for the presence of NO^-. In addition, PN can oxidize thiols to disulfides through a variety of mechanisms **[153, 183]**; for example, disulfide-linked Hb can form when PN is reacted with Hb **[190]**. However, nitrite is a by-product of PN-mediated thiol oxidation **[183]**. Since midgut nitrite levels did not increase in response to infection, PN-mediated oxidation of Hb in the midgut is, therefore, not as likely as nitroxyl-mediated oxidation of Hb.

Oxidative stress can modify the secondary and tertiary structure of bovine serum albumin (BSA; **[460]**) and the structure and protein-protein interactions of Hb **[461-463].** Modifications include increased hydrophobicity causing protein aggregation and covalent cross-linking predominantly due to bi-tyrosine formation. However some modifications of Hb under oxidative stress have been attributed to the formation of disulfide adducts. Specifically, DTT-sensitive disulfide linkages formed between Hb and various cytoskeletal proteins as well as among Hb monomers following treatment of rat RBCs with the oxidant dapsone hydroxylamine **[463]**. Although these observations help to understand reduced mobility of Hb in infected *A. stephensi*, the role that disulfide-linked Hb may play in preserving or modifying the bioactivity of $^{\bullet}NO$ or altering oxidative conditions in the midgut will have to be clarified in future studies.

S-nitrosothiols in the A. stephensi midgut. In addition to nitration of tyrosine-containing proteins, PN can oxidize or *S*-nitrosate thiol groups **[172, 191, 192, 194-198]**. However, elevated levels of SNOs were not observed in the infected midguts at 12.5 and 24 h pBM **(Fig. 2-5)**, suggesting that SNO-related toxicity and SNO-mediated signaling are not significant factors in parasite load reduction. In addition, no changes in SNO-modified protein profiles were seen between the infected and uninfected samples at 1, 6, 12, and 24 h pBM **(Fig. 2-7)**. Despite these results, it is possible that a portion of SNOs decayed/reacted quickly during the dissection of the midguts, thus the processed lysates did not accurately account for these forms.

Toxicity of RNIs predicted to occur in the A. stephensi midgut. In the redox-active midgut, the effects of endogenously produced $^{\bullet}$NO are enhanced through the formation of various redox products. These products, including nitrate, metal nitrosyl, NO^- and PN, likely mediate the $^{\bullet}$NO-dependent reduction in *Plasmodium* development. Metal nitrosyls preserve the bioactivity of $^{\bullet}$NO, while toxic nitrates comprise the majority of *Plasmodium*-induced RNIs. Intriguingly, elevated levels of nitrosylHb and nitrotyrosine are detected during the inflammatory response of two mouse strains to the protozoan *Leishmania amazonensis* **[150, 464]**, suggesting that the chemistry of nitrosylHb formation and PN-mediated toxicity are similar to the chemistry and toxic effects of $^{\bullet}$NO synthesis in *Plasmodium*-infected *A. stephensi*. Nitroxyl and PN are strongly reactive and can oxidize thiols and amines, nitrosylate metals, induce DNA strand breaks and base oxidation **[129, 130, 142, 144-148, 465]**, oxidize lipids and proteins, deaminate DNA, oxidize sugars, and significantly alter protein activity through nitration (reviewed in **[153, 159, 162, 177, 341, 466-469]**).

There were several obstacles associated with defining *Plasmodium*-induced midgut RNIs in *A. stephensi*. Many RNIs are highly reactive and have short half-lives, thus making their detection challenging. There are a limited number of reliable analytical techniques available for measurements in complex biological matrices **[361]**. In addition my sample volumes were small, with each midgut containing only ~1-2 μL of blood. Confounding absorption spectra from the blood components often conflicted with

colorimetric detection techniques and the midgut lysates were innately viscous, clogging several instruments required for my analyses. Despite these challenges, I have attempted to shed light on the possible RNIs that exist in the mosquito midgut using a variety of techniques. These results should provide a better understanding of the $^{\bullet}$NO-related innate immune response of *A. stephensi* to *P. berghei* infection providing ground work for further studies and understanding of mosquito stage malaria and transmission.

FUTURE DIRECTIONS

Obtain accurate L-NAME inhibited RNI formation data. For our purposes, the NAME experiment provided suitable evidence that the elevated midgut RNIs were derived from AsNOS and not the ingested blood meal. However, NAME was reduced by acidified vanadium treatment and, thus, interfered with the quantification of NO_x. To eliminate the contribution of NAME, the assay should be repeated with the addition of steps to remove N^Gnitro-L-arginine analogs from the samples by solid phase extraction on cation-exchangers as described by Tsikas *et al.* **[399]**.

Determine whether alternate AsNOS catalysis occurs. Although it is generally accepted that NOS catalyzes the synthesis of $^{\bullet}$NO, a growing body of literature suggests that NOS can also catalyze the synthesis of NO^- **[30-35]**, H_2O_2 **[37-39]** and $O_2^{\bullet-}$ **[40-45, 450]**. My data suggest that PN and NO^- contribute to inflammatory levels of NO_x in the *A. stephensi* midgut following a *P. berghei* infected blood meal. To fully understand the chemistry of RNI production *in vivo*, it will be necessary to assay AsNOS catalysis directly. Specifically, these studies can help to determine whether NO^- synthesis is catalyzed directly by AsNOS, or whether this RNI is generated by downstream reactions of $^{\bullet}$NO with other chemical species. In addition, these studies can help to determine whether AsNOS catalysis is a source of $O_2^{\bullet-}$ for PN formation.

The Luckhart lab has previously shown that *AsNOS* transcription is complex, with more than 20 transcripts detected by northern analyses **[48]**. Three of these transcripts were significantly induced in the midgut in response to *P. berghei* infection **[48]**. Comparative analyses of the AsNOS predicted amino acid sequence indicate that the

residues involved in binding to the co-factor tetrahydrobiopterin (H4B) are located in exons 6 and 8; NOS proteins lacking this binding site would be predicted to catalyze the synthesis of products comparable to those synthesized by NOS at low levels of H4B **[30-35, 470]**. In *A. stephensi*, transcripts identified with these exons deleted **[48]** may be translated into functional proteins that are directly responsible for NO^- formation in the midgut. Further, if AsNOS catalyzes the synthesis of $O_2^{\bullet-}$, then PN synthesis can be predicted. If AsNOS catalyzes H_2O_2 synthesis, this product would support peroxidase-mediated nitration. Thus, alternative catalysis of AsNOS or truncated isoforms of AsNOS isoforms may potentiate the production of toxic and reactive RNIs.

To begin studies of AsNOS catalysis, I suggest that the three *AsNOS* transcripts that are induced in response to parasite infection be identified. The sequences of these transcripts can be used to generate recombinant proteins for biochemical assays of catalysis *in vitro*. H4B levels are reduced during oxidative stress **[471]**, thus in an inflammatory state, where oxidative stress is high, NOS may favor NO^- formation. Since H4B concentration determines the catalytic products of NOS activity **[450, 472]**, H4B levels should be measured in the midgut of infected and uninfected mosquitoes following protocols for biopterin measurement **[473]**.

Measure midgut superoxide levels. Based on my data, I believe that PN is formed in the *A. stephensi* midgut in response to *Plasmodium* infection and that PN plays an important role in limiting parasite development in the mosquito. The formation of PN is dependent on both $O_2^{\bullet-}$ and $^{\bullet}NO$ concentrations. Thus, to confirm that PN can form under midgut conditions, it will be necessary to determine midgut $O_2^{\bullet-}$ concentrations. The direct measurement of $O_2^{\bullet-}$ poses the same challenges as RNI measurement: short half-life, sample volumes too small to analyze and interference from Hb in many of the standard assays. Several publications describe measurement of $O_2^{\bullet-}$ levels in insects **[448, 474-477]**; however, no data have been collected from blood-filled midguts of any arthropod species. Superoxide anion has been measured in mammalian blood samples using the lucigenin-enhanced chemiluminescence method **[478-480]**, but this detection method required specialized equipment. To overcome these difficulties, I propose comparing activity or levels of enzymes that catalyze $O_2^{\bullet-}$ synthesis in dissected *P.*

berghei-infected and uninfected midguts. Alternatively, it may be possible to infer levels of $O_2^{\bullet-}$ in mosquito midguts by assaying the enzymes that are responsible for $O_2^{\bullet-}$ detoxification.

Superoxide can be generated by the one-electron reduction of molecular oxygen by NAD(P)H oxidases. To understand the potential role of NADPH oxidases in mosquito midgut RNI chemistry, initial efforts should focus on an analysis of the *A. gambiae* genome for sequences that encode oxidase homologs. One oxidase/peroxidase has been identified to date. Expression of *AgDoux*, a dual function oxidase, was strongly induced in the midgut of *P. berghei*-infected *A. gambiae* at 28 h pBM **[407]**. In addition to midgut expression, NADPH oxidase activity has been detected in salivary gland homogenates of the adult female *Anopheles albimanus* **[477, 481]**. Because mosquito saliva is injected into the host during probing, saliva and host NADPH (released by broken cells) that are ingested during blood feeding may contribute to an initial burst of $O_2^{\bullet-}$ synthesis. Finally, truncated NOS isoforms that comprise only the reductase domain can function as NADPH oxidases **[42, 45]**

To assess $O_2^{\bullet-}$ levels by analysis of enzymes responsible for $O_2^{\bullet-}$ scavenging, I would focus initially on midgut SOD activity in the mosquito. SOD catalyzes the dismutation of $O_2^{\bullet-}$ to produce O_2 and H_2O_2. SOD scavenging of $O_2^{\bullet-}$ affects RNI-mediated chemistry in two ways. Firstly, SOD scavenging of $O_2^{\bullet-}$ will prevent the formation of PN and, hence, block any PN-mediated effects **[241]**. Secondly, the formation of PN essentially scavenges $^{\bullet}NO$, possibly altering cellular signaling processes **[469]**. Analysis of blood meal-induced *SOD* expression in the midgut epithelium of parasite-resistant and susceptible strains of *A. gambiae* has been reported **[480]**. In the two susceptible strains tested, *SOD* expression was induced 0.95- and 1.94-fold at 12 h pBM and 2.1- to 2.5-fold at 24 h pBM relative to uninfected controls. The authors suggested that *SOD* expression was induced by elevated levels of $O_2^{\bullet-}$ **[480]**.

In addition to $O_2^{\bullet-}$ scavenging, SOD is of interest because the *in vitro* addition of SOD to Hb increased the yield of total bound $^{\bullet}NO$ to ~100% of $[NO]_o$ **[83]**, a mechanism which could account for the portion of midgut $^{\bullet}NO$ that is bound as heme nitrosyl. SOD can also decrease the conversion of oxyHb to metHb **[482]**, which would be consistent with the surprising lack of metHb in bloodfed midguts. SOD has also been implicated in

the reversible conversion of NO^- to $^{\bullet}NO$ **[30, 32, 122-125]** and this conversion could extend the bioactivity of NO^- that is believed to form in the infected midgut. In light of these actions of SOD, I propose that future efforts should focus on the determining the expression profile of *AsSOD* in response to parasite infection.

Quantify midgut nitroxyl content. Because NO^- is highly reactive and has a short half-life, HNO/NO^- cannot be directly quantified. Although both NO_3^- **[134, 483]** and hydroxylamine **[106, 138]** can be used as a measure of NO^- formation, other pathways can lead to the formation of NO_3^- and hydroxylamine **[363]**. The only end product derived directly from HNO is nitrous oxide (N_2O), indicating that N_2O levels should be used for estimating nitroxyl formation [**reaction 21**] **[134, 484]**.

$$2HNO \rightarrow HO\text{-}N\text{-}N\text{-}OH \rightarrow N_2O + H_2O \qquad \textbf{(21)}$$

Because elevation in nitrate levels in the *A. stephensi* midgut may be due to NO^-, I propose that measurement of midgut N_2O by either gas chromatography or GCMS as described by others **[134, 363, 484]** will help to confirm whether NO^- is formed in the mosquito midgut following parasite infection.

Continue to analyze midgut NTYR formation. *(1) Determine onset of increased NTYR formation in the infected midgut.* I have modified the protocol for NTYR staining for use with a new primary antibody. The sections from mosquitoes collected at 2, 8, 12.5 and 33 h pBM have been prepared but should be processed to determine onset of increased NTYR staining in the *P. berghei*-infected midgut.

To provide support for my hypothesis that PN can induce NTYR formation in *A. stephensi*, I suggest evaluating $O_2^{\bullet-}$ levels and *AsSOD* expression in the midgut epithelium (described above). It may also be fruitful to perform immunohistochemical analysis of NTYR formation on sections of mosquitoes collected following urate feeding. Urate scavenges PN and should prevent PN-mediated NTYR formation. Because urate does not interfere with peroxidase-mediated nitration, this experiment would determine whether PN or an alternative mechanism, such as the MPO-mediated mechanism

suggested by Kumar *et al.* **[407]**, is responsible for the bulk of the tissue nitration in infected mosquitoes.

2. Determine whether tyrosine nitration correlates with protein/DNA oxidation. Protein oxidation coincides with NTYR formation under conditions associated with nitrosative damage; NTYR formation alone is not an indicator of damage. As such, I propose that protein oxidation be evaluated to determine whether increased nitration in the *P. berghei*-infected midgut is consistent with tissue damage. Two measurements have been used to assess oxidative damage: Protein Carbonyl Content (PCC) and 8-hydroxy-deoxyguanosine (8-OH-dG) formation. PCC is an indicator of oxidative damage of proteins. A modified version of the PCC assay described by Levine *et al.* **[485-487]** can be used. In this procedure, proteins can be extracted from mosquito samples and precipitated with trichloroacetic acid. Protein carbonyls are reacted with DNPH and the pelleted protein is washed in ethyl acetate/ethanol. Pellets are then resuspended in 6 M guanidine and the absorbance read at 370 nm. Heme-containing proteins, such as Hb, can affect the assay by absorbing in the same region as DNPH **[488]**. To circumvent this, appropriate blanks (protein without DNPH) or carcass and washed gut material should be used as controls. Additionally, 8-OH-dG formation is indicative of DNA oxidation that may occur under conditions associated with $^{\bullet}$NO-mediated oxidative damage of proteins **[487, 489]**. For these assays, purified DNA isolated from mosquito tissues would be dissolved in 1 mM deforoxamine/20 mM sodium acetate then digested by nuclease P1 followed by AP. After passage through a 30 kD filter, digests can be analyzed by HPLC **[487, 490]**. Once protein and DNA damage have been assessed *in vivo*, specific RNIs can be tested against ASE cells *in vitro* assays to predict which species are responsible for tissue damage *in vivo*.

3. Identify potential protein targets of $^{\bullet}$NO *modification.* Several studies have indicated that tyrosine nitration is a selective process in that not all proteins and not all tyrosine residues are targets for nitration **[213, 491]**. The nitration of proteins may alter protein conformation and structure, catalytic activity, and/or susceptibility to protease digestion **[211, 214, 492, 493]**. For example, nitrated tyrosines cannot function as substrates for protein tyrosine kinases **[214, 494, 495]**. As such, signal transduction cascades requiring this phosphorylation would be compromised.

Although our assays have focused on the possibility that NTYR formation in mosquito tissues is a consequence of toxic effects of RNIs on parasite development, NTYR formation may also directly affect parasite development. As such, it may be of interest to determine whether NTYR can be detected in parasite proteins and whether Tyr nitration reduces parasite viability/maturation. Identification of NTYR in parasite proteins during sporogony is complicated by the presence of blood and mosquito proteins, but it may be possible to examine parasites in midgut blood smears directly with immunocytochemical staining. If parasites appear to stain positively for NTYR, it may be possible to isolate parasites from mosquito midguts for protein analysis by immunoprecipitation, gel electrophoresis and protein sequencing by Edman degradation as described by Gole *et al.* **[496]**. Alternatively, one could hypothesize that specific parasite proteins are potential targets for NTYR modification. For example, *Plasmodium* chitinase may be a target for tyrosine nitration. The peritrophic matrix (PM) is the first physical barrier faced by the parasite in the mosquito midgut. Ookinetes penetrate the PM through the release of chitinase, and chitinase inhibitors have been shown to be effective blockers of oocysts development **[497]**. An epitope found in *P. gallinaceum* ookinetes that reacts with a monoclonal antibody (MAb 1C3) raised against the *P. falciparum* chitinase, PfCHT1, has been shown to be effective in blocking oocyst development **[498]**. It is believed that MAb 1C3 interacts with a second chitinase. The epitope recognized by MAb 1C3 is tyrosine-rich (L<u>Y</u>DS<u>Y</u>A<u>YY</u>GKK<u>Y</u>D<u>Y</u>VIIMGFTL). As such, it would be interesting to determine whether these Tyr residues are be nitrated and whether this modification alters chitinase function.

If PN-mediated NTYR formation is important for modulating parasite development, then the ratio of $^{\bullet}NO$ to $O_2^{\bullet-}$ is very important. NTYR formation is optimal under conditions of $^{\bullet}NO/O_2^{\bullet-}$ flux of ~1 and excess of either radical results in the reaction with tyrosyl radicals and $NO_2^{\bullet}$ thus deactivating the NTYR process **[199, 499, 500]**. Thus the strategy to create transgenic mosquitoes with increased $^{\bullet}NO$ production, with the assumption that this modification will increase parasite killing, may fail if PN/NTYR is primarily responsible for deterring parasite development and $O_2^{\bullet-}$ synthesis is not increased proportionately.

Continue to analyze midgut SNOs. Although higher MW SNOs do not appear to differ in infected and uninfected midgut lysate samples, changes in lower molecular weight SNOs have yet to be analyzed. Low MW SNOs (*e.g.* GSNO or Cys-NO) can be isolated from midgut blood lysates using a filter with a 5kD cutoff prior to analysis by LC-MS with GSNO and Cys-NO standards. Alternatively, low MW SNOs may be quantified using the NOA with larger injection volumes and with NO-displacement using CuCl followed by reaction with DAN (2,3-diaminonaphthalene) to yield the fluorescent compound NAT (2,3-naphthyltriazole; **[9]**), or by monitoring the loss of fluorescence when di-dansyl-homocysteine is transnitrosated by *S*-nitrosothiols (Dr. Bulent Mutus, University of Windsor, Canada; personal communication).

Identify the source of photolyzed-•NO. It possible that •NO addition to oxyHb can form nitrosylHb. The source of increased photolyzed-•NO in the infected midgut was assumed to be nitrosylHb based on lack of increased SNO levels at the same times pBM. However, direct measurement of nitrosylHb is required to confirm the presence of this RNI in mosquito midgut lysates. EPR spectroscopy is a useful technique for determination of •NO in metal complexes or heme proteins **[247, 501-503]** and should be performed to verify that photolyzed-•NO is derived from nitrosylHb. If nitrosylHb is present, further studies are needed to determine why levels of SNOs and metHb are not concurrently increased in the midgut environment.

In addition to quantifying nitrosylHb, EPR spectra can be used to distinguish the form of nitrosylHb present. When •NO reacts with Hb it can form 6-coordinate α- and β-nitrosyl, indicative of the Hb in the R-state, or 5-coordinate α-nitrosyl heme associated with Hb in the T-state **[83]**. Identification of the form of nitrosylHb present would further our understanding of the midgut environment. Although EPR spectra analyses on midgut lysates were proposed, limitations in available collaborative efforts prevented completion of these experiments in a timely manner for my dissertation.

In addition to nitrosylHb, I have not addressed the possibility that a portion of photolyzed-•NO in the *A. stephensi* midgut may derive from *N*-nitroso compounds (RNNOs). Free •NO and •NO-adducts, including *S*-nitrosothiols, RNNOs, and iron–nitrosyl adducts can be detected using photolysis-chemiluminescence **[102, 360, 504].**

RNNOs can be generated endogenously in the course of infectious and inflammatory processes either via •NO-mediated nitrosation, intermediate formation of PN, or bacterial action **[400, 505]**. I proposed that PN is formed in the midgut and is a contributor to mosquito •NO-mediated inhibition of *Plasmodium* development. PN can lead also lead to the formation of RNNOs **[505]**, suggesting that RNNOs may be a component of the toxic RNIs produced in *A. stephensi*. Data from studies with *Aedes aegypti*, however, suggest that RNNOs do not have antiplasmodial activity. Specifically, when female *Aedes aegypti* were provided a sucrose solution with 0.1% *N*-nitroso compounds, *P. gallinaceum* development was not inhibited in subsequent infectious blood meals **[506]**.

Investigate contribution of bacterial metabolism to midgut RNIs. The midgut of the mosquito is colonized with bacteria and fungi. Previous studies have shown that blood feeding can increase bacterial levels 11-16,000 fold over pre-feeding levels **[507, 508]**, with the greatest changes associated with Gram-negative species **[509]**. In studies of malaria parasite infection, provision of Gram-negative, but not Gram-positive bacteria with an enriched gametocyte culture resulted in a significant decrease in oocyst development in *A. stephensi* **[510]**. Similarly, when bacteria from field-collected *Anopheles albimanus* were fed together with a *Plasmodium vivax*-infected blood meal to aseptic laboratory-reared *A. albimanus*, infections and oocyst counts were lowered by several bacterial species **[511]**. Because bacterial infections vary from year to year **[511]** and from location to location in the field **[512]**, bacterial co-infection may influence malaria parasite transmission.

Bacteria are equipped with an arsenal of •NO-modifying enzymes. Among them are the flavohemoglobins (*Hmp*) and nitrite reductases. Hmps have been identified from bacteria and yeast and function as •NO dioxygenases, converting •NO to nitrate **[273, 513]**. As such, some midgut nitrate may be derived from the action of bacterial Hmps. In addition to the Hmps, many Gram-negative bacteria are equipped with nitrite reductases. Three different nitrite reductases are found in bacteria, including cytochrome *c* which can consume •NO and reduce nitrite to ammonia and cytochrome *cd1* (*nirS*) and trimeric copper containing (*nirK*) nitrite reductases which reduce nitrite to •NO (reviewed in **[514, 515]**). Among the Gram-negative bacteria, *Pseudomonas* spp. may be of particular

relevance to both RNI chemistry and parasite infection in the mosquito. *Pseudomonas aeruginosa* has been isolated from laboratory-reared and field-collected mosquitoes **[507, 508]** and can decrease oocyst levels when provided in a blood meal with *P. falciparum* **[508, 510]**. Cd1-nitrite reductase of *P. aeruginosa* can catalyze the synthesis of •NO from nitrite and also catalyze the *N*-nitrosation of diphenylamine **[515-517]**, suggesting that this bacterium may contribute to the pool of •NO and RNNOs in the mosquito midgut.

In sum, bacterial flora of the midgut may contribute to the pool of RNIs present following bloodfeeding and infection. For example, if bacterial nitrite reductases are active in the midgut, nitrite may be recycled to •NO, which could explain the lack of increase in nitrite levels following parasite infection. Further, bacterial Hmps could catalyze the conversion of •NO to nitrate, an RNI that is present at higher levels following parasite infection. To evaluate the influence of bacterial metabolism on midgut RNIs, analyses of midgut lysates should be repeated using axenic mosquitoes, created by administration of antibiotics from three days prior to blood feeding until the conclusion of the experiment. Alternatively, expression levels of bacterial *Hmp*, *nirK* and *nirS* in dissected midguts should be evaluated to determine whether pathways involving these enzymes alter midgut RNI profiles and malaria parasite development in the mosquito.

Continue to investigate the chemical properties of Hb in the midgut. The amino acid homology of flavoHb with Hb and with metHb reductases from distantly related animals, plants, protists, helminths, and bacteria **[518-521]** has led to the hypothesis that the ancient role of Hb was •NO detoxification **[273]**. The possibility that ingested Hb may have altered function due to the new milieu and digestive proteolysis is interesting. Preliminary observations of NADPH-dependent O_2-consumption by midgut lysates suggested that ingested Hb may function, in part, as an •NO-dioxygenase. It would be of interest to continue these studies and to determine whether metHb reductase activity is detectable in midgut lysates. These studies would also help to explain the lack of metHb in the bloodfed midgut under conditions of high nitrate levels.

Test the in vitro susceptibility of mosquito stage Plasmodium to RNIs. To date, direct tests of the effects of NO-donors and RNIs have only been performed primarily

using asexual stages of the parasite **[92, 280, 346, 348, 522-524]**. As such, it is necessary to perform these assays using mosquito-stage parasites to determine whether midgut RNIs are directly toxic or whether they inhibit growth, leaving the parasite vulnerable to other mosquito defenses. One recent study demonstrated that the •NO donor SNP and the ROS donor dihydroxyphenylamine (L-DOPA) increased mortality of *P. berghei* ookinetes ~2-fold relative to controls; treatment of ookinetes with both reagents simultaneously enhanced mortality to ~3-fold relative to controls **[525]**. Advances in cultivation of the mosquito stage parasites *in vitro* **[447]** will facilitate controlled analyses of RNI toxicity *in vitro*. Based on my data, I propose that dose-response assays of parasite viability be performed using PN, NO^-, nitrosylHb and a variety of SNOs.

Determine whether species of infecting parasite is a factor in mosquito midgut RNI production. The virulence of parasite infection is dependent on the combination of host and *Plasmodium* species. The mosquito response to parasite development varies depending on the species of mosquito and on the species of infecting parasite **[526, 527]**. In addition, midgut physiology varies across *Anopheles* species. Specifically, rates of RBC hemolysis and blood compaction, changes in midgut pH during blood digestion and rates and patterns of PM formation are species-specific **[63]**. The species of parasite influences the percentage of RBCs infected and the amount of hemozoin formed, factors which are relevant to *AsNOS* expression (**[528]**; Luckhart unpubl.) and which would be predicted to alter midgut RNI formation. In the mosquito, *P. berghei* invasion of the midgut epithelium occurs intracellularly, whereas *P. falciparum* transverses through intercellular spaces **[328, 529]**; these differences, in turn, impact the midgut response to the parasite.

In addition to differences in mosquito response to parasite development, the mammalian response to parasite infection can alter blood meal composition **[530]** and levels of inflammatory mediators which can affect the formation of RNIs in the mosquito midgut **[56]**. The amounts and ratios of SNOs, RNNOs and metal nitrosyls formed in rodents and primate appear to differ significantly **[361]**. The ICR mice used in my experiments do not mount and •NO-mediated immune response to *P. berghei*, indicating that host-derived RNIs do not contribute to increased RNI levels observed in the

mosquito midgut following infection. In humans, however, malaria patients have higher concentrations of plasma nitrites/nitrates than do uninfected control subjects **[386, 387]**, suggesting that parasite development in field populations of *Anopheles* spp. may be influenced by host-derived RNIs.

In addition to variation in the mammalian immune response, parasite infection of human populations has led to the appearance of hemoglobinopathies (*e.g.* sickle cell Hb, α-thalassemia, β-thalassemia) which alter the host response to parasite infection. Sickle trait RBCs produce higher levels of $O_2^{\bullet-}$ and H_2O_2 than do normal RBCs **[531]**. Similarly, thalassemic cells produce hemichromes and other molecules that generate ROS **[532, 533]**, which are known to adversely affect growth and viability of *Plasmodium* **[534]**. Host-derived ROS may also alter the ROS/RNI balance in the mosquito midgut. Finally, sickled Hb destabilizes RBC membranes, resulting in high concentrations of cell-free Hb **[441]**, which is likely to alter the dynamics of $^{\bullet}$NO/Hb interactions in both the human and the mosquito host.

In summary, the ICR mouse, *P. berghei* and *A. stephensi* comprise a convenient natural host-parasite system for laboratory studies, but data from this system may not be extrapolated to the physiology of mosquito infection with *P. falciparum* derived from human hosts. As such, future studies should attempt to determine whether the chemistry and physiology that I have characterized are consistent with that which occurs in a host-parasite system of significant medical importance.

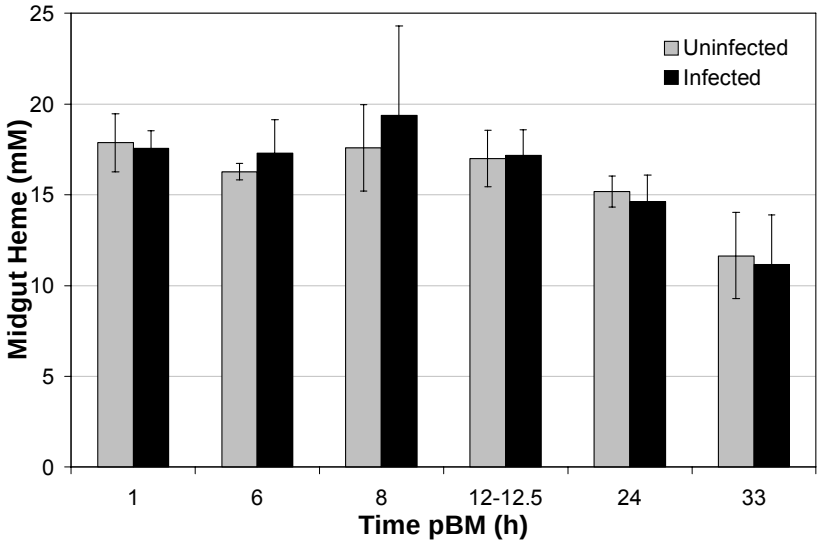

Figure 2-1: Midgut heme concentration.

To account for the variability in individual ingested blood meal volumes, midgut data were normalized to midgut heme concentration. To confirm that normalization was not falsely skewing the data, uninfected and infected midgut heme concentrations were measured and compared at various times pBM. Although heme concentration appeared to decrease beyond 12 h pBM, heme concentration in infected compared to uninfected midguts was not significantly different at all time points tested ($p>0.5$; $n=4$-12).

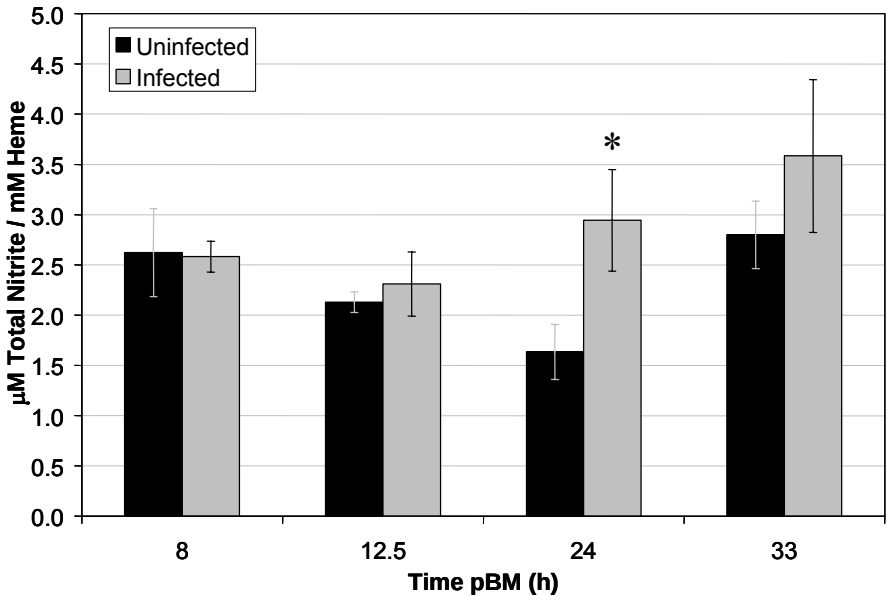

Figure 2-2: Midgut levels of total nitrite levels were increased in response to *P. berghei* infection.

Nitrite and nitrate are stable end products of •NO. Midgut lysates from four cohorts of *A. stephensi* were used for analyses. Cadmium beads were used to non-enzymatically convert nitrate to nitrite. Total nitrites were reacted with the Griess reagent yielding a product which absorbs at 562 nm. Absorbances were compared to a standard curve created with sodium nitrite. At 24 h pBM the increase in *P. berghei*-infected midgut total nitrite level compared to uninfected sample was statistically significant (Student's *t* test, *p=0.015).

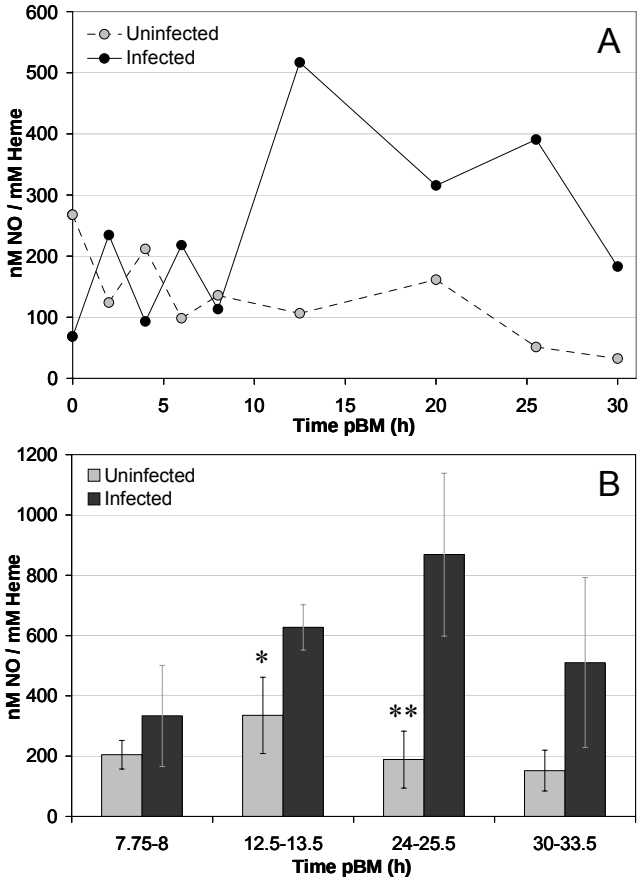

Figure 2-3: Midgut levels of photolyzed-•NO were increased in response to *P. berghei*-infection.

RNI-derived •NO was quantified using photolysis-chemiluminescence spectroscopy. Bound •NO was cleaved by UV-photolysis then reacted with ozone yielding excited nitrogen dioxide. Upon decay a photon of energy was released which was quantified. For midgut lysates, •NO concentration was normalized against sample heme concentration to account for variation in ingested blood meal volume. **(A)** A representative run demonstrates that 0 through 8 h pBM, photolyzed-•NO levels in uninfected and *P. berghei*-infected midguts were relatively consistent. In contrast, elevated photolyzed-•NO levels were detected in infected midguts between 12.5 and 30 h pBM. **(B)** Midguts were dissected from three cohorts of uninfected and *P. berghei*-infected *A. stephensi.* Parasite infection increased levels of photolyzed-•NO in midgut lysates collected from 8-33.5 h pBM. At 12.5-13.5 h and 24-25.5 h pBM, infected midgut levels were significantly higher than those from uninfected blood meals (Student's *t* test, *p=0.02 and **p=0.03, respectively).

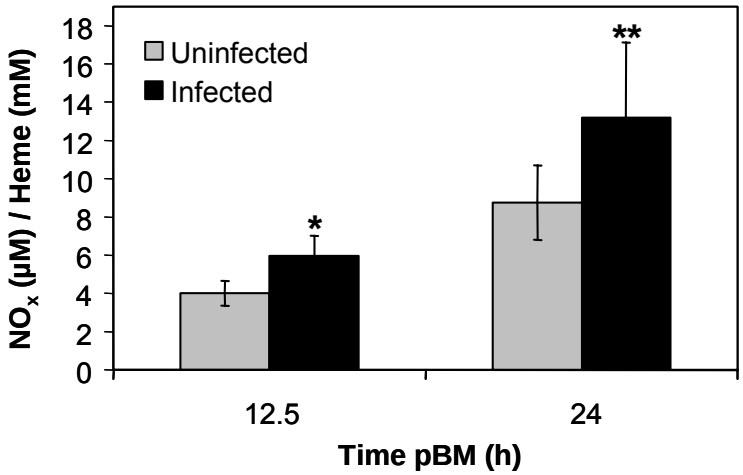

Figure 2-4: Midgut levels of higher oxides of nitrogen were increased on response to *P. berghei* infection. (Fig. 1B from **[56]**[6])

Vanadium chloride/hydrochloric acid at 95°C was used to chemically reduce nitrites, nitrates, SNOs and higher oxides of nitrogen (collectively termed NO_x) to free $^{\bullet}NO$ which was detected by chemiluminescence in the Nitric Oxide Analyzer (NOA; Sievers). Greater levels of NO_x were observed in the infected midguts at 12.5 and 24 h pBM (Student's *t* test: *p=0.049 and **p= 0.069, n=4).

[6] Copyright © 2003, the American Society for Microbiology. All rights reserved.

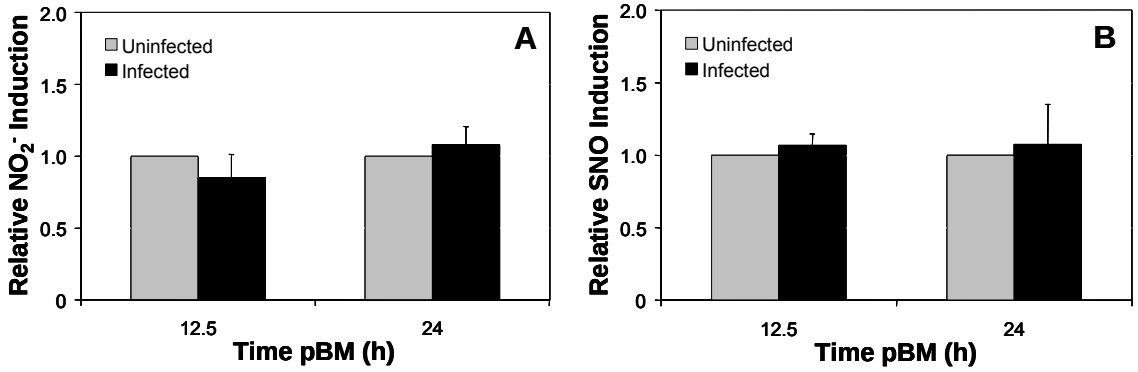

Figure 2-5: Midgut levels of nitrites (NO_2^-) and SNOs were unchanged in response to *P. berghei* infection.

Midgut lysates were prepared from four cohorts of infected and uninfected *A. stephensi* collected 12.5 and 24 h pBM. Acidified KI was used to chemically reduce nitrites to •NO. Pre-treatment of the sample with $HgCl_2$ liberated •NO from SNO in the form of nitrite, thereby increasing nitrite concentrations. •NO was measured by chemiluminescence using a Sievers Nitric Oxide Analyzer. Data from four cohorts of mosquitoes were averaged and relative RNI levels were obtained by dividing infected and uninfected means by the uninfected means; hence, uninfected means are represented as the value "1". At 12.5 and 24 h pBM neither **(A)** relative nitrite levels (p=0.19 and p=0.27) nor **(B)** relative SNO levels (p=0.19 and p=0.27) were changed due to infection.

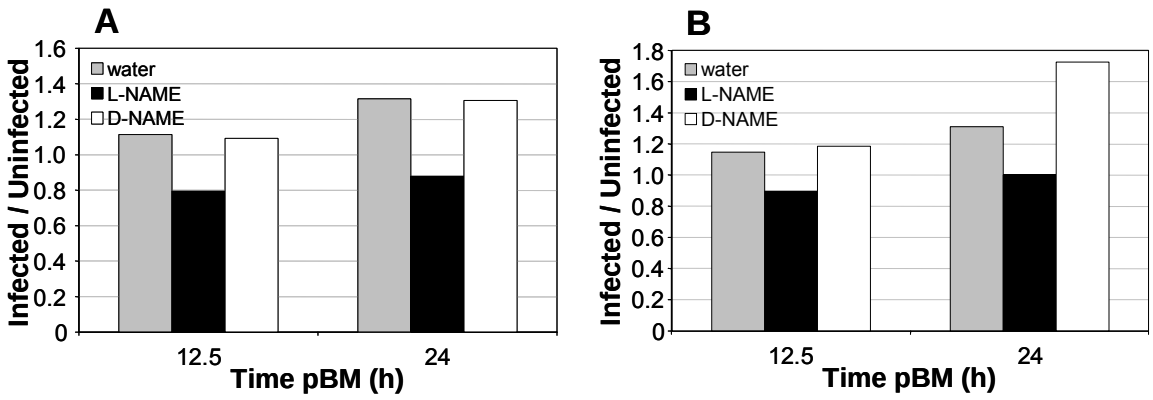

Figure 2-6: Dietary L-NAME inhibited *P. berghei*-induced AsNOS preventing an increase in midgut nitrite and NO_x levels.

The NOS inhibitor L-NAME (N^G-nitro-L-arginine methyl ester) or the inactive stereoisomer D-NAME were provided as dietary supplements to *A. stephensi*. Midguts were collected at 12.5 and 24 h pBM and the total levels of nitrites **(A)** and NO_x **(B)** were measured using the NOA as described in the Materials and Methods. Absolute values of these RNIs could not be calculated since NAME was also chemically reduced under the conditions used. As such, it was assumed that uninfected and infected mosquitoes consumed equivalent amounts of NAME and the relative values (infected/uninfected) of RNIs were measured. Since L-NAME but neither D-NAME nor water reduced the levels of both nitrite and NO_x, the increased RNIs in the infected midgut appeared to be derived from AsNOS activity.

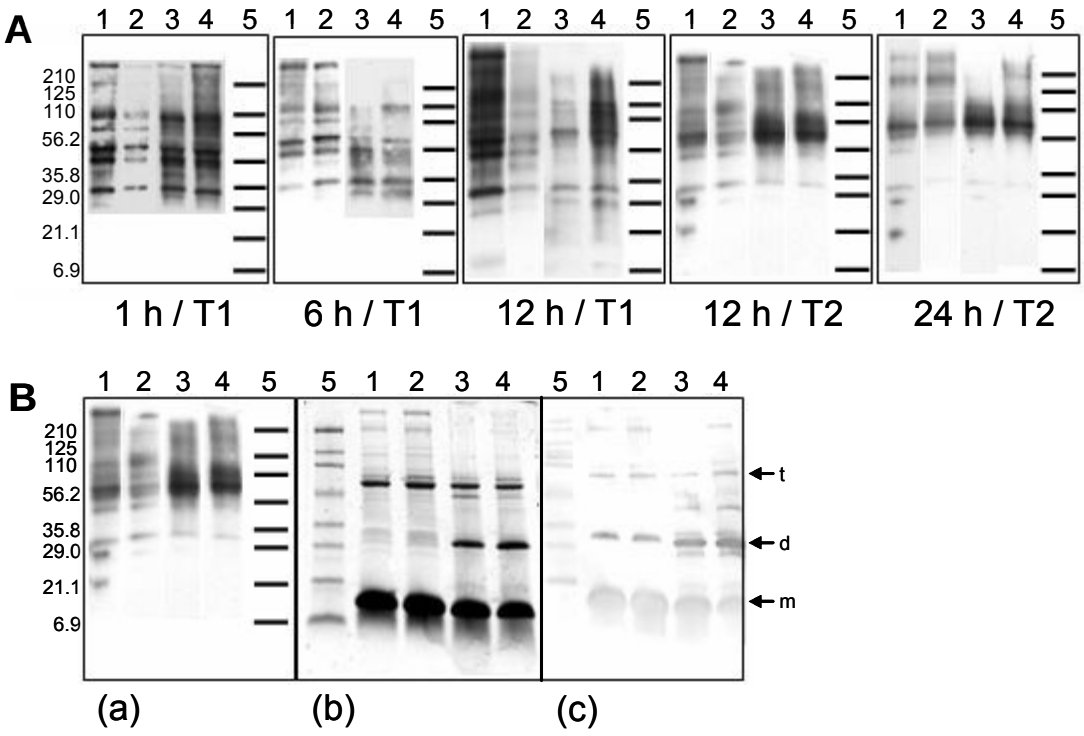

Figure 2-7: SNO-biotin switch western analysis of *S*-nitrosated proteins in the *A. stephensi* midgut.

In the SNO-biotin switch westerns •NO bound to thiols was exchanged with biotin. The modified proteins were detected by western analysis using anti-biotin antisera. **(A)** SNO-biotin-switch westerns show no major changes in *S*-nitrosated protein profiles in infected versus uninfected midgut samples. **(B)** A representative corresponding Coomassie stained gel (b) and western blot using Hb antisera (c) for a 12 h pBM SNO-biotin switch blot (a). Migration of tetrameric (t), dimeric(d) and monomeric (m) Hb are indicated by arrows. Lanes: 1=uninfected mouse blood, 2=infected mouse blood, 3=uninfected midgut lysate, 4=infected midgut lysate, and 5=molecular weight markers (kD). T1 and T2 refer to two independent trials.

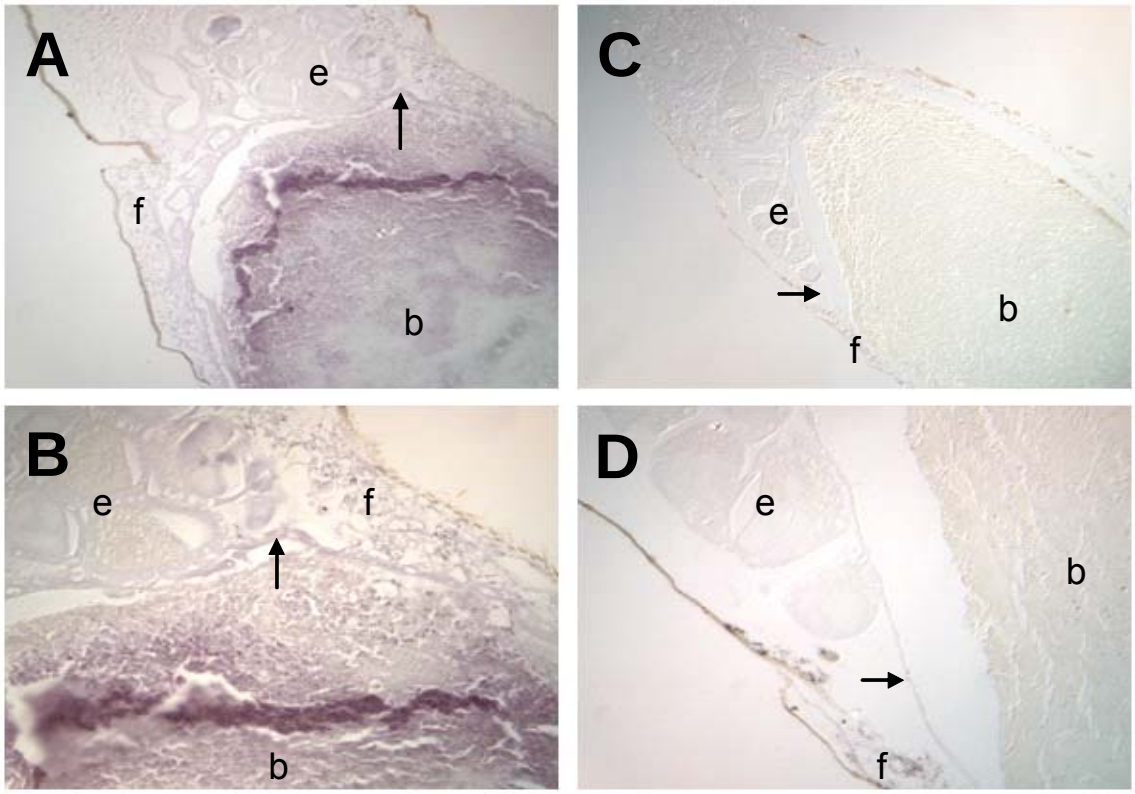

Figure 2-8: Nitrotyrosine (NTYR) levels in the midgut and abdomen were increased in response to *P. berghei* infection.

Immunohistochemical staining of 10 micron sections of bloodfed *A. stephensi* was performed using a polyclonal anti-nitrotyrosine (αNTYR) antibody and the ABC/VIP kit (Vector Labs) for detection of bound αNTYR **[370]**. NTYR is a marker for potential exposure to RNIs. At 24 h pBM, increased staining for NTYR (purple) was observed in tissues of *P. berghei*-infected **(A, B)** compared to uninfected *A. stephensi* **(C, D)**. This difference was not apparent at 3 d and 6 d post-blood meal (not shown). Staining was observed in the (b) blood mass, (e) eggs, (f) fat body and (→) midgut epithelium). The most pronounced staining occurred in blood meal bolus in the posterior of the midgut. Tissue samples were observed under 100x **(A,C)** and 400x **(B, D)** magnification.

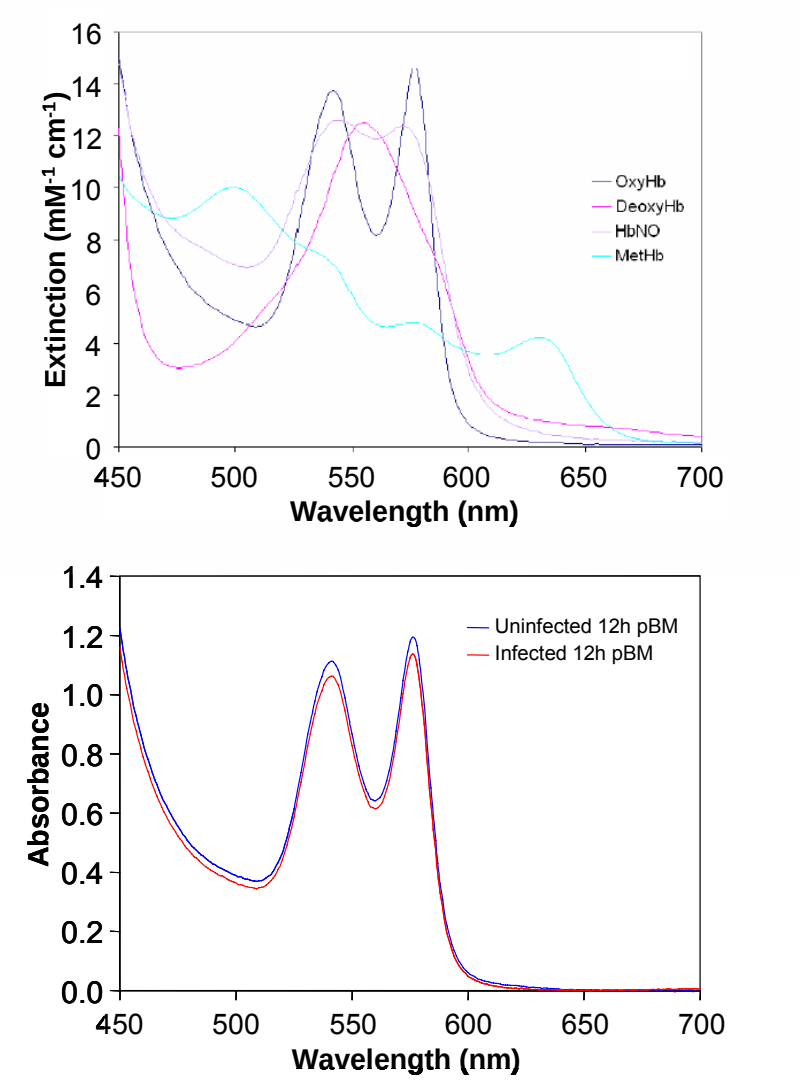

Figure 2-9: Absorbance spectra of hemoglobins (Hb).

OxyHb, deoxyHb, metHb, and HbNO (heme-iron nitrosyl Hb) have characteristic absorption spectra. **(A)** Representative absorption spectra for the four Hb species in the visible region, λ = 450-700 nm (adapted from **[535]**) are shown. **(B)** Spectra of lysates from midguts collected 1-33 h pBM were consistent with spectra for oxyHb. Representative spectra for uninfected and *P. berghei*-infected midguts collected at 12 h pBM are shown.

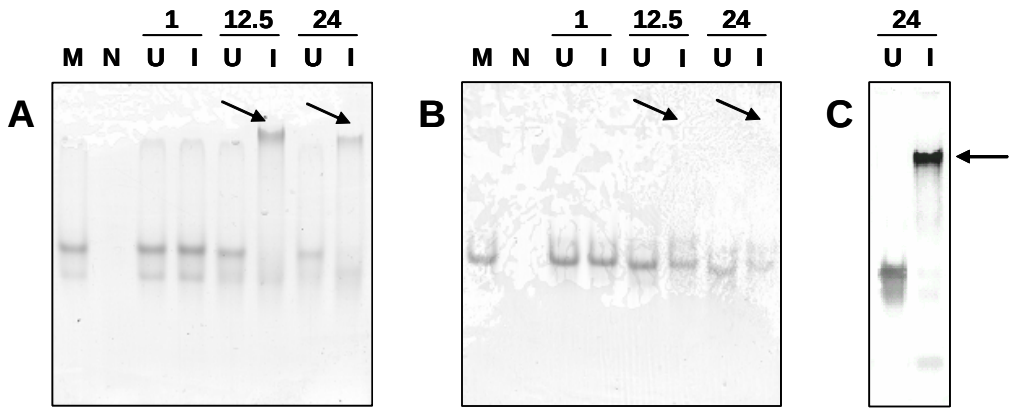

Figure 2-10: Infected midgut lysates contain a disulfide-linked, slow migrating Hb at 12.5 and 24 h pBM.

Proteins from uninfected mouse blood (M) and midgut lysates from non-bloodfed *A. stephensi* (N), and *P. berghei*-infected (I) and uninfected (U) *A. stephensi* collected at 1, 12.5 and 24 h pBM were electrophoretically separated through 7.5% polyacrylamide. The heme-containing Hbs were visible as red-brown bands on unstained gels. **(A)** Under native conditions, a slow migrating Hb was visible in only infected midgut lysates at 12.5 and 24 h pBM (arrows). **(B)** β-Mercaptoethanol treatment eliminated the slow migrating Hb, indicating that altered protein migration was due to disulfide bonds (arrows). **(C)** Western blot analysis using mouse anti-Hb antisera confirmed that the slow migrating protein was Hb (arrow).

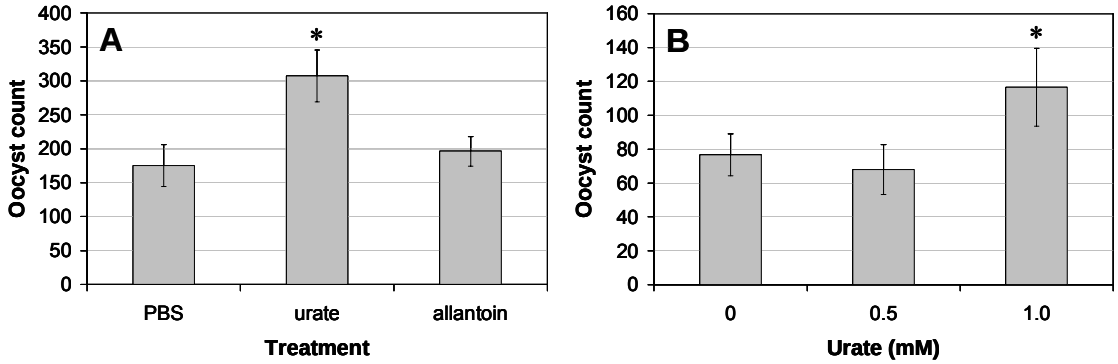

Figure 2-11: Dietary urate increased midgut parasitemia.

Uric acid/urate is a potent scavenger of the peroxynitrite. In insects urate can be oxidized to allantoin by urate oxidase. **(A)** Dietary urate in PBS, but not allantoin in PBS or PBS alone, increased midgut parasitemia as measured by 10-day oocyst count ($p=0.006$ for PBS versus urate, $p=0.296$ for PBS versus allantoin and $p=0.008$ for urate versus allantoin; $n=29$). **(B)** Dietary urate increased parasitemia when provided at 1 mM but not at 0.5 mM relative to control PBS (0 mM) treatment ($p=0.04$ for PBS versus 1 mM, $p=0.33$ for PBS versus 0.5 mM, and $p=0.03$ for 0.5 mM versus 1 mM; $n=20$).

CHAPTER THREE: Mosquito peroxiredoxins as candidate nitrosative stress defense genes

INTRODUCTION

It has long been recognized that reactive oxygen species (ROS) function to defend hosts against pathogens. In addition to the inflammatory process, ROS sources in eukaryotes include the mitochondria (electron transport coupled to oxidative phosphorylation), the peroxisome (H_2O_2 and $O_2^{\bullet-}$ produced during β-oxidation of fatty acids) and oxidation within other subcellular compartments. Oxidative stress is an inevitable result of aerobic metabolism. Thus, a variety of protective mechanisms have evolved to cope with the harmful effects of ROS. The antioxidant defense arsenal consists of: non-enzymatic defenses (*e.g.* vitamins E, C and A, and uric acid), enzymatic defenses (*e.g.* catalase, SOD, glutathione peroxidase) and low molecular weight (MW) reducing agents (*e.g.* glutathione and thioredoxin). Peroxiredoxins (Prx) are a recently discovered family of antioxidant peroxidases that can reduce hydrogen peroxide (H_2O_2) and alkyl hydroperoxides to water and the corresponding alcohols, respectively. In addition to the ROS, reactive nitrogen intermediates (RNIs) can function in defense against invaders (*e.g.* **[52, 92, 530, 536-538]** and reviewed in **[77]**).

Although ROS and RNIs are cytotoxic to pathogens and parasites, they also induce oxidative and nitrosative stresses in the host **[536, 539]** and can damage host tissues. Host protection against oxidative and nitrosative stress, therefore, is vital for homeostasis and survival. Gene products that confer protection against ROS are well known. In contrast, gene products that confer protection against RNIs have been identified, but these are less well studied. Genes involved in protection against nitrosative stress include *noxR1* **[540],** *metL* (homocysteine synthesis;) **[282]**, *Hmp* (bacterial flavohemoglobin; **[78, 274, 541]**), oxyR regulon **[289]** genes including alkyl hydroperoxide reductase (*ahpCF*; **[306, 308-316, 542]**), catalase (*katG*), glutathione reductase (*gorA*), SoxRS regulon **[287]** genes including Mn-SOD (*sodA*) and glucose 6-phosphate dehydrogenase (*zwf*).

AhpC was first identified in 1989 in *Salmonella typhimurium* **[543]** and in *E. coli* **[544]** as part of a two component alkyl hydroperoxidase reductase system. Previous work had predicted the existence of this system in 1963 **[545]**. In 1988, a yeast thiol-specific antioxidant (TSA) was discovered **[546]** that was determined to be similar to glutathione peroxidases (GPx) yet used thioredoxin (Trx) instead of glutathione (GSH) as the reductant **[547]**. Thus, yeast TSA was renamed as a thioredoxin-dependent peroxidase. Because TSA was orthologous to AhpC, which utilizes AhpF rather than Trx for reduction, this emerging family of proteins was renamed the "Peroxiredoxin" (Prx) or occasionally the "Peroxidoxin" family **[548]**. When x-ray analysis and electron microscopy revealed that Prxs could form decameric rings, **[549, 550]** the "torin" protein discovered in the 1960's **[551]** was re-identified as a Prx. Many Prxs discovered prior to 1994 are also referred to by other names **(Table 3-1)**. The Prx decamers are composed of five dimers **[551, 552]** held together predominately by ionic interactions **[553]**. The oligomerization is not well understood, but believed to be dependent on redox environment **[550]**. These higher aggregates are the more active form suggesting a co-operativity between the catalytic sites (reviewed by **[554]**)**.** Today Prxs have been isolated from organisms in all kingdoms, indicating that these proteins have critical conserved physiological roles.

Prxs do not show sequence homology to other known antioxidant enzymes (*e.g.* superoxide dismutase, catalase, and peroxidase) **[555]**. Crystal structures of PrxI, II, V, and VI reveal that Prx are novel members of the Trx fold superfamily **[555-560]**. Other members of this superfamily are GPx, GST (Glutathione *S*-transferase), Trx, Grx (Glutatredoxin), DsbA and protein disulfide isomerases **[559]**. Interestingly, a naturally occurring mutation of a single duplicated codon in the AhpC gene, converts AhpC from a Prx to a disulfide reductase **[561]**. Although similar in sequence and structure to GPx, Prxs contain a Cys whereas GPx contain a selenocysteine. A protein originally identified as a GPx, but lacking selenium, was later re-classified as PrxVI **[562]**. Unlike most peroxidases which contain heme rings at their active sites (*e.g.* cytochrome c peroxidase) or a redox sensitive moiety like selenocysteine (glutathione peroxidase; Gpx), vanadium (algal bromoperoxide) or flavin (bacterial NADH peroxidase), Prxs lack co-factor metal ions, prosthetic groups or cofactors **[546]**. Their activity is dependent upon a conserved

Cys, usually in a Val-Cys-Pro (VCP) motif, near the N-terminus. Unlike other peroxidases, Prxs act as both peroxidase and the co-substrate since they are oxidized upon reaction with peroxide **[563]**. The general catalytic mechanism of Prx depends on this N-terminal redox-active Cys as was demonstrated by site-directed mutagenesis **[564]**. Four general types of Prxs are recognized **(Fig. 3-1)** and are defined according to the number and location of conserved cysteines. These categories are sometimes further subdivided by the identity of the electron donor and localization of the protein (*i.e.* cytosolic, mitochondrial, nuclear, secretable, chloroplastic).

Typical 2-Cys Prx: Mammalian Prx I-IV and bacterial AhpC homologs. Typical 2-Cys Prxs have two highly conserved cysteines and are among the most well studied Prxs. This subfamily includes mammalian PrxI through IV and bacterial AhpC. The 2-Cys Prx initially reacts with the hydroperoxide at the N-terminal Cys (-SH) thus oxidizing it to sulfenic acid (-SOH). This cysteinyl-sulfenic acid is unstable and attacks the C-terminal Cys of a second subunit forming an intermolecular disulfide bridge (-SS-) **[558]**; thus there are two disulfides in a head-to tail dimer.

To regenerate the active 2-Cys Prx, the disulfide must be reduced. The reductant is usually a flavin-dependent enzyme generally containing a dithiol with the Cys-X-X-Cys motif **[565]**. Typically, the Trx system **[547, 566, 567]** functions as the reductant, however reduction can also be completed by the glutaredoxin system **[568, 569]**, by AhpD and AhpF (FAD-dependent disulfide reductases) in certain bacteria **[543, 548, 570]**, and by the tryparedoxin system **[564, 571]**. The Prx/reductant relationship is highly specific. In *D. melanogaster,* 2-Cys DmPrx-4783 uses only one of the two cytosolic Trxs as its substrate **[572]**. In the absence of the physiological electron donors, however, 2-Cys Prxs can be reduced by small thiol molecules such as dithiolthreitol (DTT) and β-mercaptoethanol **[547, 564, 567]**.

Atypical 2-Cys Prx: Mammalian PrxV and Bacterioferritin Co-migratory Protein homologues. The atypical 2-Cys Prxs can be divided into three groups. The first group is generally referred to as the PrxVs. The PrxVs are generally described as containing two conserved cysteines that are approximately 100 amino acids (aa) apart **[573]**, although mammals have three such residues due to an additional conserved cysteine ~25 residues downstream from the peroxidatic cysteine. Unlike the typical 2-Cys

Prxs, the PrxVs are monomeric enzymes in which the N-terminal sulfenic acid reacts with a C-terminal cysteine forming an intramolecular disulfide. Human PrxV contains three conserves cysteines: the proximal conserved Cys (Cys^{48}) as well as two additional Cys (Cys^{73} and Cys^{152}) neither of which corresponds to the C-terminal Cys of typical 2-Cys Prx with respect to distance from the proximal Cys or the surrounding sequence **[574]**. In human PrxV, Cys^{48} and Cys^{152} form an intramolecular disulfide; mutants lacking Cys^{48} or Cys^{152} lack thioredoxin-dependent activity **[574]**. Mutants lacking Cys^{73} are fully active **[574]**. The PrxV disulfide is reduced by thioredoxin but not glutathione or glutaredoxin. When DTT is used as a donor only Cys^{47} is required, mimicking the mechanism described for 1-Cys Prxs.

The atypical 2-Cys Prxs are targeted to a variety of subcellular organelles. For example, a conserved Ser-Gln-Leu sequence dictates the peroxisomal localization of PrxV PMP20 **[575]**. In another example, a transcript derived from alternate initiation of the atypical 2-Cys Prx gene AOEB166, encodes a 52 aa leader sequence with a mitochondrial import signal **[573]**. Since mitochondria and peroxisomes are major sources of H_2O_2, PrxVs contribute to the antioxidant arsenal of these organelles.

A second group of atypical 2-Cys Prxs are referred to as the Type II Prxs. The Type II Prxs are mostly known from plants, but are similar to mammalian PrxVs in that they contain conserved cysteines at positions 51 and 76 but lack the C-terminal Cys at position 152. In poplar Type II Prx, the two conserved Cys form an intramolecular disulfide, which can be reduced by both Trx and Grx **[569]**.

A third group of atypical 2-Cys Prxs are the homologues of bacterioferritin co-migratory protein (BCP). Like the PrxVs, the BCPs form intramolecular disulfides, but the conserved cysteines are separated by only four aa **[576, 577]**.

1-Cys Prx: Mammalian PrxVI. As the name suggests, the 1-Cys Prxs contain a single conserved Cys. Interestingly, mutation of the second conserved cysteine of typical 2-Cys Prxs results in a functionally active enzyme, presumably by allowing the enzyme to adopt a 1-Cys Prx type mechanism **[547, 578]**. Although most researchers concur that 1-Cys Prxs can form dimers **[307, 551, 579-581]**, others insist that, without a resolving Cys, the 1-Cys Prxs cannot dimerize **[582, 583]**. The 1-Cys Prxs are comprised of two domains: the N-terminal domain with a thioredoxin fold and the C-terminal dimerization

domain **[583]**. Although the mechanism by which the sulfenic acid is reduced is not clear **[582]**, it has been proposed that the thiol reductant reacts with the oxidized active site cysteine and, thus, acts as the substrate, becoming disulfide linked to the enzyme. Experimental data confirm that Trx cannot reduce this intermediate **[582, 584]**, but the *in vivo* source of reducing equivalents for 1-Cys Prxs remains controversial. The higher MW thiols cannot access the oxidized cysteine **[582, 584-587]**. Small MW thiols, like DTT, can function as reductants *in vitro* and, as such, GSH is predicted to act as a reductant *in vivo* **[554, 585, 588]**. Despite this prediction, several labs have failed to detect GSH supported peroxidase activity of 1-Cys Prx **[582, 587]**.

The insect Prxs. A family of five Prx genes was identified and characterized in *D. melanogaster* **[589]**. All DmPrxs were shown to have classical peroxidase activity. **[589, 590]**. Neither 1- nor 2-Cys DmPrxs use the GSH system for reduction **[589]**. Rather, the three 2-Cys DmPrxs are Trx peroxidases *i.e.* capable of using Trx to reduce peroxides. In contrast, the two 1-Cys Prxs do not use reducing equivalents from Trx. Although the physiological reducing agent(s) of the 1-Cys Prxs are unknown, these DmPrxs can use DTT as an electron source *in vitro*, thereby classifying them as thiol peroxidases. Inducibility of the DmPrxs suggests that they function in oxidant defense **[589]**. When overexpressed in *D. melanogaster* S2 cells, the DmPrxs confer varying degrees of resistance to H_2O_2 as measured by cell viability **[589]**. Conversely, blocking DmPrx expression with dsRNA-mediated RNAi increased the susceptibility of S2 cells to H_2O_2 treatment **[589, 590]**. These observations and the level of conservation of Prxs among organisms suggest that Prxs may play a protective role in the mosquito.

We have shown that *A. stephensi* possesses a single copy NOS which is induced in response to parasite infection and whose catalytic activity leads to an increase in midgut nitrosative stress **[47, 52, 56]**. The RNIs produced are proposed to limit or inhibit parasite growth. Based on observations that Prxs can protect against RNIs, we sought to determine whether mosquitoes possess Prx(s) and then to determine whether AsPrx(s) could protect against nitrosative stress. Here I describe the identification and characterization of a 2-Cys Prx from *A. stephensi*. The timing of expression in the mosquito midgut suggests that it plays a role in protection during the midgut invasive

stage of *Plasmodium* development. I propose that this 2-Cys AsPrx provides protection to the mosquito cells from self-generated RNIs in response to *Plasmodium* infection.

MATERIALS AND METHODS

Mosquito maintenance and infections. *Anopheles stephensi* (Indian wild type) were reared at 27°C and 75% relative humidity under a 12 h light/dark cycle. The mosquitoes were fed once each life cycle (0 h) on anesthetized Institute of Cancer Research (ICR) mice for egg production. All animal care procedures were performed according to the National Research Council Guide for the Care and Use of Laboratory Animals. Protocols were reviewed by the Institutional Animal Care and Use Committee of Virginia Tech, Blacksburg, VA. For parasite infection, *A. stephensi* were allowed to feed on ICR mice previously inoculated intraperitoneally with thawed aliquots of *Plasmodium berghei* (ANKA). Mouse parasitemia was determined from Giemsa stained tail-vein blood smears. Before and after bloodfeeding, mosquitoes were maintained on cotton pads soaked with 10% sucrose (w/v) in water. *Plasmodium berghei*-infected (INF) mosquitoes were maintained at 21°C and 75% relative humidity. During time-course experiments non-bloodfed (NB) and bloodfed, uninfected (UN) mosquitoes were also maintained at 21°C and 75% relative humidity.

Identification of A. stephensi Prx sequences. To clone the *A. stephensi* 2-Cys Prx gene, degenerate oligonucleotide primers were designed against conserved encoded sequences that appear in most 2-Cys Prx proteins (forward primer, Fb: 5'-GGTGCTKTTCTTCTACCCG, and reverse primer, Rc: 5'-TCGATGATGAACAGGCC; where K = T or G). To obtain genomic and cDNA sequences, PCR was performed on genomic DNA (4^{th} instar larvae) and cDNA prepared from adult female *A. stephensi*. Additional 5' and 3' sequences were obtained using rapid amplification of cDNA ends (RACE) using the Marathon-Ready™ cDNA kit (Clontech) and the gene specific primers (P1: 5'-GGACTTTACCTTCGTCTGCCCGACCG and P2: 5'-CGATGATGAACAGGCCACGGAATGG).

Drosophila melanogaster Prx sequences **[589]** were used as queries to BLAST (Basic Local Alignment Search Tool; **[591]**) search the available *Anopheles gambiae* genome scaffold sequences. Primers were designed to amplify *A. stephensi* 1-Cys Prx based on conserved encoded regions of *D. melanogaster* and *A. gambiae* sequences. A small cDNA fragment, orthologous to *D. melanogaster* Prx-2540, was obtained with the forward primer, 2540F2: 5'-CGCGCCCTGTTCATCATCA, and reverse primer, Deg1: 5'-CAGGATCATGACCTTAGTGC, using the PCR cycling conditions: 1 cycle of 95°C 10 min, 35 cycles of 95°C 1 min, 50°C 45 s, 72°C 30 s, and 1cycle 72°C 10 min. Additional 5' sequence was amplified using a reverse primer designed from the previously obtained sequence, Deg2: 5'-CATCGTAAGACGGACTTTCT, and a new degenerate forward primer, Deg2540: 5'-CAYCCNGCNGAYTTYAC (where Y = T or C, and N = A, T, C, or G) using the PCR cycling conditions: 1 cycle of 95°C 10 min, 35 cycles of 95°C 30 s, 54°C 30 s, 72°C 30 s, and 1 cycle 72°C 10 min.

The PCR amplimers were subcloned into pCR®2.1-TOPO® and transformed into Top10 cells (Invitrogen; **Appendix D**). All cloned PCR amplimers were subjected to double-stranded DNA dideoxy dye terminator sequencing at UC Davis Sequencing to eliminate sequence ambiguities.

RNA extraction. Total RNA was extracted from dissected mosquito midguts using TRIzol (Invitrogen Life Technologies) according to the manufacturer's instructions. For RNA isolation from immortalized *A. stephensi* cells in culture, glycogen (250 μg/mL TRIzol) was added to facilitate precipitation of the RNA. Total RNA was quantified spectrophotometrically. For northern analyses, mRNA was purified from total RNA using the PolyATract® mRNA isolation system (Promega).

Genomic Southern analysis. Genomic DNA was prepared from 4th instar larvae of *A. stephensi* using a protocol adapted from Sambrook *et al.* **[592]**. Briefly, larvae were thoroughly rinsed in tepid water and crushed to a powder in liquid nitrogen. The powder was incubated at 37ºC in extraction buffer (10 mM Tris pH 8, 0.1 M EDTA pH 8, 20 μg/mL pancreatic RNAse, 0.5% SDS) for 1 h. Proteinase K (100 μg/mL) was added to the solution and the mixture was heated at 50ºC for 3 h. Following a phenol/chloroform

extraction, the DNA was ethanol precipitated using ammonium acetate. To eliminate RNAse contamination, the sample was treated with RNAse Cocktail (Ambion; 10 μg/mL). The isolated DNA was digested with EcoRI, KpnI, XhoI or XmnI, electrophoretically separated through 0.8% agarose and transferred to nylon membrane (Boehringer Mannheim) by capillary transfer. Full length *A. stephensi* 2-Cys Prx was amplified from cDNA using PCR (forward primer PWF 5'-CAGCCTCCAAAAACACCATC; reverse primer PWR 5'-GAGGACTCTGGCTGGC; cycling conditions: 1 cycle of 95°C 10 min, 35 cycles of 95°C 30 s, 57°C 30 s, 72°C 30 s, and 1 cycle 72°C 5 min). This PCR product was cloned into pCR®2.1-TOPO® (Stratagene; **Appendix D**); the plasmid is hereafter referred to as "pTLP20". pTLP20 DNA was digested with EcoRI and electrophoretically separated through 0.8% agarose. The insert was purified using the Quantum Prep Freeze and Squeeze kit (BioRad). The insert DNA, consisting of the complete AsPrx open reading frame, was randomly labeled with [α^{32}P] dATP using the Strip-EZ DNA™ synthesis kit (Ambion). Southern hybridization was performed overnight (17 h) at 68°C followed by high stringency washes (two washes for 15 min at room temperature with 2 x SSPE/0.5%, one wash for 1 h at 55°C with 0.1 x SSPE/0.5% SDS and one wash for 20 min at 68°C with 0.1 x SSPE/0.5% SDS). After washing, the filter was exposed to photographic film (X-OMAT LS; Kodak Scientific Imaging Film) at -80°C.

Northern analyses. One carton (~250 female *A. stephensi*) was used for each RNA isolation at 1 h and 7 d post-bloodfeeding for UN and INF groups. RNA was isolated from equal numbers of age-matched, NB individuals as a control. For each sample, 9 μg mRNA was electrophoretically separated through a 1% agarose NorthernMax (Ambion) gel. Separated transcripts were blotted onto Nylon using capillary transfer according to manufacturer's instructions. To visualize transferred mRNA, the blot was washed in 4 x SSC for 10 min then stained using a solution of 0.02% methylene blue and 0.3 M sodium acetate for 3 min. The blot was then rinsed three times with 20% ethanol and the MW standards and ribosomal RNA bands were marked with a pencil. The blot was destained using a solution of 0.2 x SSPE and 1% SDS

twice for 5 min each. The blot was then rinsed in 4 x SSC for 5 min and the wet blot was stored at -20°C until used for hybridization.

pTLP20 DNA was digested using KpnI. The purified insert was used for *in vitro* transcription from the T7 promoter in the presence of ^{32}P α-UTP to create a radio-labeled RNA probe (Ambion, Strip-EZ RNA; Strippable RNA Probe Synthesis & Removal Kit-T7). A NucTrap® Probe Purification Column (Stratagene) was used to remove unincorporated nucleotides. An amplimer encoding the full-length *A. stephensi* S7 ribosomal protein (AsS7) was prepared from *A. stephensi* cDNA using PCR (forward primer S7F 5'-GGCGATCATCATCTACGTGC; reverse primer S7R 5'-GTAGCTGCTGCAAACTTCGG; cycling conditions: 1 cycle of 95°C 10 min, 30 cycles of 95°C 30 s, 53°C 30 s, 72°C 45 s, and 1 cycle 72°C 5 min). The amplimer was concentrated and washed in a 100,000 MW cutoff Microcon centrifugal filter (Millipore) and used to prepare a random-primed, radiolabeled probe in the presence of ^{32}P α-dATP. A NucTrap® Probe Purification Column (Stratagene) was used to remove unincorporated nucleotides.

Northern hybridizations were performed using NorthernMax PreHyb/Hyb solution (Ambion). For *AsPrx* northern analyses, membranes were prehybridized for 2 h at 68°C and hybridized with the *AsPrx* probe for 20 h at 67°C. Blots were stripped twice using the Strip-EZ kit (Ambion) for post-hybridization with the *AsS7* probe. For *AsS7* northern analyses, membranes were prehybridized for 2 h at 68°C and the hybridized with the *AsS7* probe for 21 h at 68°C.

Autoradiographs were made by exposing blots to photographic film (X-OMAT LS, Kodak Scientific Imaging Film). Scanned autoradiographic images were analyzed using Kodak 1D Image Analysis Software (Eastman Kodak). Relative expression of *AsPrx* was calculated by dividing the mean intensity of the *AsPrx* hybridization signal by the mean intensity of the *AsS7* hybridization signal **[52, 593]**.

Cell culture and transfection. *Drosophila melanogaster* Schneider 2 cells (S2; Invitrogen) were propagated in *Drosophila* expression system (DES) medium (Invitrogen), containing 10% fetal calf serum (FCS; Gibco or Cellgro) and antibiotics (Cellgro). Cell cultures were split 1:10 every 5-8 d and were maintained at 27°C. Two *A.*

stephensi cell lines, MSQ43 (provided by the Department of Entomology at Walter Reed Army Institute of Research) and ASE **[594]**, were propagated in Eagle's minimum essential medium with Earl's salts (Cellgro) supplemented with L-glutamine, essential amino acids, glucose, antibiotics, and 5% FCS. Every 5-8 days MSQ43 cells were split 1:10 and ASE cells were split 1:20. Both lines were maintained at 27°C and 5% CO_2. For transfection, cells were plated in either 24-well or 6-well plates and plasmid or dsRNA was transfected into the cells using Effectene (Qiagen) as described by the manufacturer. Cell viability (%) was reported as the ratio of live cells to total cells normalized to the ratio without chemical challenge (to account for variable levels of background death).

Preparation of constructs for AsPrx overexpression. Full-length *AsPrx* was amplified from ASE or MSQ43 cell cDNA by PCR using primers that included the Kozak consensus sequence (underlined; **[595]**) and eliminated the stop codon to permit read-through into plasmid sequence encoding epitope tags: ClonePrxF 5'-ATCATGCCAGTTCCGGAG and ClonePrxR 5'-GTTAACAGCATTGAAGTATTCCTT. This product was cloned into the pMT/V5-His© vector (Invitrogen) for a copper inducible expression in the S2 cell line (pTLP55) and into pcDNA3.1/V5-His© vector (Invitrogen; **Appendix D**) for constitutive expression in the MSQ43 cell line (pTLP58). Hereafter, these clones are referred to as "pTLP55" for S2 cell overexpression and "pTLP58" for MSQ43 cell overexpression. pTLP55 and pTLP58 DNAs were isolated and purified from TOP10 *E. coli* transformants (Qiagen). Correct orientation and sequence was verified for each clone.

Double-stranded RNA production and conditions for RNA interference (RNAi). The complete open reading frame of *AsPrx* (591 bp) was amplified using the primers ClonePrxF1 and ClonePrxR1 and pTLP55 as template. Mouse *cyclophilin* (Cyc) was amplified using primers and template provided by the Lig'nScribe™ kit (Ambion). Both amplimers were purified and T7 adapters added using the Lig'nScribe™ kit. DNA templates for antisense and sense RNA synthesis were amplified using ClonePrxF1/adapter Primer 2 and ClonePrxR1/Adapter primer1 for the adapted *AsPrx* templates and Cyc3'/Adapter Primer 1 and Cyc5'/Adapter Primer1 for the adapted

cyclophilin templates according to manufacturer's cycling protocols. These templates were used to synthesize single-stranded RNA (ssRNA) using the MEGAscript®/T7 *in vitro* transcription kit (Ambion). Template DNA was digested using DNAse; the remaining ssRNA was purified using MEGAclear™ (Ambion) according to manufacturer's instructions. RNA yield was quantified using UV absorbance and integrity was evaluated following electrophoretic separation on a 1.4% MOPS/formaldehyde agarose gel.

To prepare double-stranded RNA (dsRNA), equal quantities of sense and antisense ssRNA were mixed in a 10-20 μL volume, heated in boiling water for 5 min and cooled to room temperature (~2 h). To ensure that dsRNA molecules were formed, dsRNA was resolved in 2% agarose with TBE following treatment with RNAse A under both low (0 M NaCl) and high salt (0.3 M NaCl) conditions (*e.g.* dsRNA is protected from RNAse A digestion under high salt conditions whereas ssRNA is not; **[596]**). MSQ43 cells were transfected with dsRNA following standard Effectene protocols.

Experimentally induced stress and analyses of cell viability. S2 cells were grown to confluency then split 1:2 and allowed to recover overnight. Cell density was assessed using a hemacytometer and protocols followed the Effectene transfection reagent manual (Qiagen). Briefly, 2.29 x 10^5 cells/mL were seeded into 24-well culture plates and were transfected with pTLP55 using Effectene at 18-26 h following seeding. Transfected gene expression was induced by exposure to 500 μM $CuSO_4$. At 18-26 h following induction, transfected cells were exposed to one of the following conditions: 0, 10, or 20 mM H_2O_2 (Fisher) for 0, 3, 6, or 9 h; 0, 1.5, or 3 mM DEA-NO[7] (Cayman Chemical) for 0, 3, 6, or 9 h; 0, 200, or 500 μM peroxynitrite (PN)[8] (Cayman Chemical) for 0, 3, 6, 9 h; or 0, 1, or 2 mM Angeli's salt (AS)[9] (Cayman Chemical) for 0, 2, 4, or 6 h. DEA-NO, AS and PN concentrations were verified by spectroscopy, calculating concentration from the Beer-

[7] DEA-NO is also known by DEA NONOate, DEA/NO, and Diethylamine NONOate. The complete name is Diethylammonium (Z)-1-(N,N-diethylamino)diazen-1-ium-1,2-diolate with a molecular formula of $C_4H_{10}N_3O_2 \bullet C_4H_{12}N$.

[8] Peroxynitrite here refers to the equilibrium mixture of peroxynitrite anion ($ONOO^-$) and peroxynitrous acid (ONOOH). The IUPAC recommended names are oxoperoxinitrate (-1) and hydrogen oxoperoxinitrate respectively.

[9] The formal name for Angeli's salt is sodium α-oxyhyponitrite. The molecular formula is $Na_2(ONNO_2)$.

Lambert law and their respective extinction coefficients (ε_{250} = 9180 $M^{-1}cm^{-1}$, ε_{237} = 6100 $M^{-1}cm^{-1}$, and ε_{302} = 1670 $M^{-1}cm^{-1}$).

MSQ43 cells were grown to confluency and seeded into 24-well plates for overexpression studies or 6-well plates for RNAi studies. Cells were seeded at 2.5 x 10^5 cells/mL and 18-26 h later transfected as described by the manufacturer (Effectene, Qiagen). Cells were transfected with the AsPrx overexpression construct (pTLP58), dsRNA for *AsPrx*, dsRNA for *cyclophilin*, or mock transfected, which followed the Effectene protocol without dsRNA. At 42-50 h following transfection, transfected cells were challenged with: 0, 125, or 250 μM H_2O_2 (Fisher) for 0, 3, 6, or 9 h; 0, 350, or 700 μM DEA-NO for 0, 3, 6, or 9 h; 0, 75, or 150 μM PN for 0, 3, 6, 9 h; or 0, 50, or 100 μM AS for 0, 2, 4, or 6 h. Cell viability following chemical challenge was assessed using Trypan blue exclusion assay (Gibco).

Quantitative Reverse Transcription-Polymerase Chain Reaction (qRT-PCR). The ABI Prism 7700 sequence detection system (PE Applied Biosystems) was used to quantify the expression of *AsPrx*. For quantification of *AsPrx* expression in the midgut of *A. stephensi*, total RNA was isolated at selected time points using TRIzol (Invitrogen) according to the manufacturer's instructions. Expression was normalized against the expression of the *S7* ribosomal protein gene **[52, 593]**. The relative efficiencies of the *AsS7* and *AsPrx* reactions were optimized such that the comparative C_t method of analysis could be used to quantify and normalize gene expression **[597, 598]**. Primers and probes were designed with Primer Express® (version 1; PE Applied Biosystems). The AsS7 primers and probe were designed using the highly homologous *A. gambiae* gene sequence **[599]**. PCR assays were performed using 10 ng of total RNA isolated from pools of 25 mosquito midguts and the following primers and probes for *AsS7* or *AsPrx*: 300 nM s7f2 (5'-GAAGGCCTTCCAGAAGGTACAGA), 350 nM s7r2 (5'-CATCGGTTTGGGCAGAATG), and 200 nM TaqMan probe s7p (5'-VIC-AGAAGTTCTCCGGCAAGCACGTCGT-TAMRA) or 600 nM PrxF2 (5'-CTGCCCGACCGAAATCG), 600 nM PrxR2 (5'-TCGGCGAGCAGTGGAATC), and 200 nM TaqMan probe PrxP (5'-FAM-CTCGCGTGGATCAATGTACCGCG-TAMRA). All reactions, including

controls with no added template, were duplicated and performed as 1-step RT-PCRs as recommended (TaqMan Gold RT-PCR, PE Biosystems). Induction of *AsPrx* was calculated as the ratio of *AsS7*-normalized expression of *AsPrx* from *P. berghei*-infected mosquitoes to the *AsS7*-normalized expression of *AsPrx* from uninfected mosquitoes. Genomic contamination was evaluated by repeating template-containing reactions without the RT step.

For validation of gene silencing by RNAi, 2-step RT-PCR was performed on RNA collected from cultured cells. The RNA was isolated using TRIzol, and cDNA was synthesized by reverse transcribing 200 ng RNA with the TaqMan® Universal PCR Master Mix Kit (Applied Biosystems). Oligo $d(T)_{16}$ primers were used for first-strand cDNA synthesis, thereby selectively amplifying mRNA and excluding any contribution from dsRNA. One μL of cDNA was used as template in the reaction, and reduction in transcript levels was evaluated using the comparative C_t method.

Blood meal-induced AsPrx RNA expression in midgut explants. To determine whether blood alone could induce *AsPrx* expression in the *A. stephensi* midgut, a brief test was performed on midgut explants. Midgut explants were prepared as described by Gubler *et al.* **[600]**. Briefly, midguts were dissected from ethanol-rinsed, non-blood fed female *A. stephensi* and were transferred as groups of three midguts into 200 μL E5 medium in a 48-well culture plate. Following a 1 h incubation at room temperature, pooled midguts were treated with 1, 2.5 or 5 μL mouse blood or equivalent volumes of PBS as a control for 6 h. Blood for these assays was collected from the tail vein of an uninfected ICR mouse into a heparinized tube; an equivalent volume of PBS was added to another heparinized tube to control for sample handling. After treatment, total RNA was isolated from each midgut pool using 800 μL TRIzol supplemented with 250 μg/mL glycogen. Relative expression was determined by 1-step qRT-PCR and the comparative C_t method as described previously.

Experimentally-induced stress and analyses of AsPrx RNA expression in immortalized mosquito cell culture. Treatments used to induce stress in *A. stephensi* cells included H_2O_2, DEA-NO, AS, PN, *S*-nitrosoglutathione (GSNO), and killed microbes.

ASE cells were treated with H_2O_2, DEA-NO, AS, PN, killed microbes and GSNO, while MSQ43 cells were treated with H_2O_2, AS and GSNO.

For all assays, ASE and MSQ43 cells were grown to confluency. MSQ43 cells were collected and resuspended in fresh E5 medium for plating at 1 x 10^6 cells per well in 24-well plates and allowed to recover 22-26 h prior to treatment. For H_2O_2, microbe and GSNO treatments, ASE cells were resuspended in fresh E5 medium prior to plating. For DEA-NO, AS, and PN treatments, ASE cells were resuspended in preconditioned E5 medium collected from ASE cells in log phase growth. Pre-conditioned media was needed to sufficiently buffer the addition of these chemicals in alkaline diluent; insufficient buffering increased the media pH, which adversely affected cell viability and prevented RNI release from the parent compound. ASE cells were then seeded at 1 x 10^6 cells per 6 cm diameter culture dish and allowed to recover for 22-26 h prior to treatment. Following the treatments described below, plated ASE and MSQ43 cells were collected and lysed in TRIzol for RNA isolation. RNA concentration was determined by spectroscopy. Relative expression of *AsPrx* was determined by qRT-PCR and the comparative C_t method as described previously.

A. Hydrogen peroxide, DEA-NO, AS, PN, GSNO: These chemicals were selected to determine whether agents that induce oxidative and/or nitrosative stress could induce AsPrx expression in *A. stephensi* cells.

ASE cells were treated with H_2O_2 (Sigma) at 50, 150, 300 and 500 μM for 10 min or 2 h, or at 300 μM for 10 min or 2, 4, 6, 8, 12, 18 and 24 h. MSQ43 cells were treated with 100 or 200 μM H_2O_2 (Fisher) for 2 or 9 h. For both cell lines, equivalent volumes of diluent (water) were used as control treatments at each timepoint. In other assays, ASE cells were treated with DEA-NO (Cayman Chemical) at 100 μM for 2, 6, 12, 18 or 24 h or at 1,000 μM for 2, 6, 24 or 48 h; equivalent volumes and concentrations of decomposed DEA-NO (see below) were used as controls at each timepoint. ASE cells were treated with AS (Cayman Chemical) at 2, 20, 200 and 2,000 μM for 3 or 6 h. MSQ43 cells were treated with 2, 20, 200 μM AS for 2 or 6 h. For both cell lines, equivalent volumes and concentrations of decomposed AS were used as control treatments at each timepoint. In a final set of assays, ASE cells were treated with PN (Cayman Chemical) at 200 μM for 2, 6, or 12 h, or at 500 μM for 6 or 24 h; equivalent

volumes and concentrations of diluent (0.3 M NaOH) were used as controls. Decomposed DEA-NO and AS control treatments were made by adding the appropriate concentration of chemical to an equivalent volume of pre-conditioned E5 medium (for ASE cells) or fresh medium (for MSQ43 cells) without cells at the time of plate seeding. The chemical solutions were held at 27°C and 5% CO_2 for 22-26 h to permit decomposition. After 22-26 h, plated cells were resuspended in the collected media to which active chemical or decomposed chemical had been added.

GSNO was prepared by combining equal volumes of 0.5 M reduced glutathione (GSH; Sigma) in 1 M HCl and 0.5 M sodium nitrite (Sigma) in water. For control treatments, 0.5 M GSH was added to an equivalent volume of water ("GSH"), 0.5 M sodium nitrite was added to an equivalent volume of 1 M HCl ("Nitrite") or equal combined volumes of 0.5 M HCl and water ("Buffer") were used. ASE cells were treated with 1, 10, 100, or 1,000 μM of GSNO for 3 or 6 h, while MSQ43 cells were treated with 50 μM GSNO for 2 or 6 h. For both cell lines, equivalent volumes of control solutions were applied for each timed treatment.

B. Killed microbes: To determine whether killed microbes could induce AsPrx expression, ASE cells were treated with killed cells of three species: *Escherichia coli* (Gram negative bacteria), *Micrococcus luteus* (Gram positive bacteria), and *Beauveria bassiana* (fungus) **[601]**. *Escherichia coli* was grown for 24 h in 500 mL LB at 37°C and 270 rpm, while *M. luteus* was grown for 48 h in 500 mL at 37°C and 200 rpm. These cultures were autoclaved, centrifuged and the bacteria were resuspended in sterile PBS. Bacterial cell numbers were estimated by spectroscopy. For fungal assays, *B. bassiana* was grown on potato dextrose agar (PDA; Difco) plates. Plates with sporulating fungi were flooded with sterile water to produce a suspension that was cleared using cheese cloth. The cleared suspension was centrifuged and the pelleted spores were washed twice in sterile water then autoclaved. Autoclaved spores were resuspended in sterile PBS. Spore density was determined using a hemocytometer. For these assays, bacteria were added to culture plates at 1,000 per ASE cell, while fungal spores were added at 1,000 spores per culture plate for 6, 12, 30, or 48 h; control plates of ASE cells were treated with equivalent volumes of sterile PBS for identical exposure times.

Experimentally-induced stress and western blot analyses of AsPrx protein expression in ASE cells. To determine whether experimentally-induced stress could alter AsPrx protein levels in *A. stephensi* cells, western analyses were performed on ASE cells after treatment with H_2O_2, DEA-NO or PN.

For these assays, ASE cells were grown to confluency and resuspended in fresh E5 medium (for H_2O_2 treatment) or preconditioned medium (for DEA-NO and PN treatments). Cells were plated at a density of 5 x 10^6 cells per well of 6-well plates and allowed to recover for 22-26 h before treatment. Cells were challenged with: 200 μM H_2O_2 (or an equivalent volume of water), 200 μM DEA-NO (or an equivalent volume and concentration of expired DEA-NO) and 200 μM PN (or an equivalent volume of 0.3 M NaOH) for 2-18 h.

Cultured cells were collected and washed twice in ice cold PBS containing 5 mM EDTA. Washed pellets were resuspended in 50-100 μL lysis buffer (20 mM Tris-HCl pH 8, 1% Triton X-100, 137 mM NaCl, 2 mM EDTA, 1 mM PMSF, 20 μM leupeptin, 0.15 U/mL aprotinin) and placed on ice for 5 min. The lysates were centrifuged at 10,000 x g for 10 min at 4°C then the supernatants were transferred to fresh tubes for use in western analyses. Protein concentrations were determined by Bradford assay (BioRad) using bovine serum albumin (Sigma) as the standard. Laemmli's buffer was added to protein samples to a final concentration of 1X and the solutions were boiled for 5 min. After boiling, 10 or 20 μg aliquots of protein were electrophoretically separated though 10% or 12% Tris-HCl gels (BioRad). For optimal separation of low MW proteins, some samples were separated on 16.5% Tris-Tricine/Peptide gels (BioRad; running buffer: 100 mM Tris, 100 mM Tricine, 0.1% SDS, pH 8.3; loading buffer: 200 mM Tris-HCl pH 6.8, 2% SDS, 40% glycerol, 0.04% Coomassie brilliant Blue G250). When reducing conditions were required, 100 mM DTT was added to the Laemmli buffer. A protein extract of adult *D. melanogaster* was used as a positive control sample for antibody cross-reactivity. Briefly, fruit fly extract was prepared by grinding cold-anesthetized insects in one volume of 1:1 (vol:vol) Laemmli's buffer and PBS supplemented with protease inhibitors (1 mM PMSF, 20 μM leupeptin and 0.15 U/mL aprotinin). The fly extract was was boiled for 5 min, centrifuged at 10,000 x g for 15 min at 4°C and the supernatant supplemented with 0.125 volume glycerol prior to loading. Electrophoretically separated

mosquito and fruit fly proteins were transferred to Immobilon™-P (Millipore) using semi-dry transfer and a three buffer system (cathode buffer: 25 mM Tris, 40 mM glycine, 10% methanol, pH 9.4; anode buffer 1: 0.3 M Tris, 10% methanol, pH 10.4; anode buffer 2: 25 mM Tris, 10% methanol, pH 10.4). Blots were treated with 1 mM levamisole, pH 7.5 (Sigma) for 20 min to block endogenous alkaline phosphatases, then blocked for 1 h in TBS containing 5% non-fat dry milk powder and 0.05% Tween 20. Blots were then incubated with antisera raised against *D. melanogaster* Prx-4783 (DmPrx-4783) protein (generously provided by Dr. William Orr, **[589]**) at 1:2,000 overnight at 4°C followed by an alkaline phosphatase conjugated goat anti-rabbit secondary antibody (Southern Biotechnology Associates, Inc.) at 1:10,000 for 2-4 h at room temperature. Detection for these assays was based on the colorimetric 5-bromo-4-chloro-3-indolyl-phasphate (BCIP)/nitro blue tetrazolium (NBT) substrate (Vector). In select westerns, bands detected with anti-DmPRX-4783 antisera were analyzed using Kodak 1D Image Analysis Software. Mean intensities of cross-reacting *A. stephensi* proteins were calculated according to manufacturer's instructions. .

Western blot analyses for AsPrx overexpression validation: Western blots were completed as described for chemical treatments with the following modifications. ASE cell pellets were resuspended in 35-50 µL lysis buffer (20 mM Tris-HCl pH 6, 1% Triton X-100, 137 mM NaCl) supplemented with 15% (vol:vol) protease inhibitor cocktail (Roche). For detection of the V5 epitope tag, western blots were incubated with mouse anti-V5 primary antibody (Invitrogen) at 1:10,000 overnight at 4°C followed by a horseradish peroxidase-conjugated goat anti-mouse secondary antibody (Pierce) at 1:20,000 for 2 h at room temperature. Detection was based on the colorimetric VIP substrate (Vector) or chemiluminescent Supersignal substrate (Pierce). In other assays, blots were incubated with anti-DmPrx-4783 antisera as previously described except that the primary antibody titer was decreased from 1:2,000 to 1:5,000.

Statistical analysis. Results with repeated measurements are expressed as mean ± standard error of the mean (SEM). Data were analyzed by Student's *t* test.

RESULTS

Anopheles stephensi and A. gambiae Prx genes. Prior to sequencing of the *A. gambiae* genome and publication of the characterization of the *D. melanogaster* Prx family by Radyuk *et al.* **[589]**, two Trx peroxidases designated Jafrac1 and Jafrac2 were identified in *D. melanogaster* wing imaginal disc cells **[602]**. Based on sequence similarities between Jafrac 1 and 2, degenerate primers were designed for PCR amplification of Prx gene fragments from *A. stephensi* cDNA and genomic DNA. Amplimers of equivalent size were produced from cDNA and from genomic DNA, suggesting that the AsPrx gene lacked introns. Upstream and downstream sequences were amplified using 5' and 3' marathon RACE (Rapid Amplification of cDNA Ends), respectively. The composite full length cDNA sequence of AsPrx **(Fig. 3-2)** was 1223 bp and encoded a predicted protein of 196 aa with a calculated molecular mass and isoelectric point of 21.9 kD and 5.95, respectively (**http://scansite.mit.edu**). BLAST analysis predicted that AsPrx encoded a typical 2-Cys Prx. BLAST analyses of a second incomplete AsPrx sequence (455 bp and 151 predicted aa; **(Fig. 3-3)**), predicted that this fragment encoded part of a typical 1-Cys Prx.

In 2001, Radyuk *et al.* **[589]** described a family of five Prxs in *D. melanogaster*: DmPrx-2540-1 (accession no. AF311879), DmPrx-2540-2 (accession no. AF11880), DmPrx-5037 (accession no. AF311747), DmPrx-6005 (accession no. AF311878), DmPrx-4156 or Jafrac2 (accession no. AF321614), DmPrx-4783-1 or Jafrac1 (accession no. AF321615) and DmPrx-2540-2 (accession no. AF321616). Three of the genes (DmPrx-4156, DmPrx-4783, and DmPrx-5037) fall into the 2-Cys subgroup, while the other two (DmPrx-2540 and DmPrx-6005) belong to the 1-Cys subgroup. Unlike most other organisms studied, insect genomes appear to encode two rather than one 1-Cys Prx. Expression patterns of DmPrx-2540 and DmPrx-6005 revealed that these are cytosolic proteins **[589]**. DmPrx-6005 is expressed throughout the lifecycle of the fruit fly, but the DmPrx2540 variants are expressed largely in embryos. DmPrx-6005 is a single copy gene, while there are three copies of DmPrx-2540.

Using the *D. melanogaster* Prx sequences as queries, five orthologous sequences were identified in the *A. gambiae* genome **(Table 3-2)**. In contrast to *D. melanogaster*, the genome of *A. gambiae* appears to encode single rather than multiple copies of each

Prx gene. In addition, a sixth peroxiredoxin was identified in both genomes which was similar to vertebrate PrxV. Although not described by Radyuk *et al.* **[589]**, this predicted protein was previously identified as a *D. melanogaster* PrxV ortholog **[317, 554, 603]**. Orthologs of BCP, which form a discrete group associated with the Prx family **[603]**, were not identified in the *A. gambiae* or *D. melanogaster* genomes.

Alignment of the predicted Prx proteins from *A. stephensi*, *A. gambiae* and *D. melanogaster* **(Fig. 3-4)** revealed that the 2-Cys AsPrx shared 74.5% nucleotide identity and 78.1% aa identity with DmPrx-4783. Hereafter, the *A. stephensi* 2-Cys Prx ortholog is referred to as "AsPrx-4783". PCR amplification from both cDNA and genomic DNA yielded the same amplimer indicating that *AsPrx-4783* is an intronless gene. The orthologous DmPrx-4783 and *A. gambiae* Prx-4783 are also intronless genes. The partial 1-Cys AsPrx sequence is most similar to DmPrx-2540 and is hereafter referred to as "AsPrx-2540." Further BLAST analysis identified several additional putative Prx sequences in the insect genomes corresponding to the 1-Cys, 2-Cys and PrxV families **(Fig. 3-5, 3-6, and 3-7)**. Insect Prxs orthologous to the BCP family could not be identified.

Examination of the predicted amino acid sequences of *A. stephensi* and *A. gambiae* 1-Cys and 2-Cys Prxs revealed that residues associated with catalysis are conserved. The peroxidatic cysteine of 1-Cys, 2-Cys and BCP-like Prx proteins is conserved in the predicted AsPrx-4783 and corresponds to Cys^{49}. Among the three subgroups, however, the consensus sequence around this C differs slightly. Like all 2-Cys Prx proteins, AsPrx-4783 also contains the resolving cysteine (Cys^{170}), located within conserved Val-Cys-Pro sequences. In insect 1-Cys Prxs, the peroxidatic C is located within a conserved VCT sequence. The peroxidatic and resolving cysteines are presumably involved in protein activation and dimerization. Fruit fly and mosquito 2-Cys Prx proteins contain the conserved Gly-Gly-Val/Ile/Leu-Gly-$(X)_n$-Tyr-Phe sequence (GG(V/I/L)G-$(X)_n$-YF), which is a signature of those Prxs that are sensitive to inactivation by hyperoxidation **[604]**. Proteins of the three Prx subgroups also contain conserved residues corresponding to AsPrx-4783 Thr^{46}, Trp^{84}, and Arg^{125}; Trp^{46} and Arg^{125} are required to "activate" the peroxidatic Cys^{49}. The Thr^{46} hydrogen bonds to Cys^{49}, while Arg^{125} interacts with this peroxidatic Cys thereby lowering the pK_a of the

ionized form of thiol **[583, 605]**. In 1-Cys Prxs, the positively charged environment of the peroxidatic Cys is further maintained by the interaction of Cys^{45} with His^{37} (residues with respect to the AgPrx-6005 sequence) **[583]**. This His is not conserved in 2-Cys Prxs or PrxVs and is replaced instead with Tyr/Trp or Val, respectively. Mutagenesis studies have revealed that the highly conserved Trp^{84} is necessary to maintain structural integrity of the active site **[605]**.

Sequence conservation among the PrxV subgroup proteins is also evident, although the PrxVs are less well studied than the 1-Cys and 2-Cys subgroups. The peroxidatic cysteine of *D. melanogaster* PrxV, like the peroxidatic cysteine C^{85} of AgPrxV, lies within a Gly-Cys-Ser (GCS) sequence. In addition to this conserved cysteine, the PrxVs of *D. melanogaster*, *A. gambiae* and *Glossina marsitans* also contain conserved C^{108} and C^{184} residues, which correspond to the two additional conserved cysteines in mammalian PrxVs and the bacterial thioredoxin peroxidases (TPxs). The firefly *Pyrocoelia rufa*, however, contains only C^{108} and lacks C^{184}, similar to the plant type II peroxiredoxins **[606]**. Despite this difference, the remainder of the *P. rufa* sequence most closely resembles PrxVs. The insect PrxVs, including the predicted AgPrxV, lack the C-terminal SQL signature which directs protein transport into the peroxisome **[575]**, which distinguishes the insect proteins from the mammalian PrxVs.

AsPrx-4783 Southern and northern blot analyses. To determine the copy number of *AsPrx-4783* in the *A. stephensi* genome, Southern analysis was carried out using the complete open reading frame as a probe **(Fig. 3-8)**. Genomic DNA was digested with EcoRI, KpnI, XhoI or XmnI. Since *AsPrx-4783* lacks introns and consensus restriction sites for these enzymes, I expected to see single bands. However, EcoRI and XhoI digests revealed two visible bands **(lanes 1 and 3, Fig. 3-8)** despite apparent complete digestion of the DNA and high stringency washes (see Materials and Methods). High sequence identity of the *AsPrx-4783* probe to other members of the Prx family may account for these observations. In the *A. gambiae* genome, the three members of the 2-Cys Prx subgroup, which are more similar to each other than to the PrxV or 1-Cys Prxs, are located on different chromosomes. Therefore, if the *A. stephensi* genome is similarly organized, at least two bands should be visible in all four lanes. In both the *D.*

melanogaster and *A. gambiae* genomes, however, the Prx-4783 genes are present as single copies. Because the DNA used for the analysis was pooled from a large number of *A. stephensi* females, small sites of silent polymorphism within the *AsPrx-4783* sequence could encode consensus restriction sites for XhoI and EcoRI that were not present in the cloned amplimer sequence, thereby altering the digest pattern. Based on gene number in *A. gambiae* and *D. melanogaster*, I believe that *AsPrx-4783* is a single copy gene.

Northern analysis was carried out to determine transcript size and number for *AsPrx-4783*. Blots using full length *AsPrx-4783* as a probe revealed a single prominent transcript **(Fig. 3-9)** of ~1200 bp, which matches the size of the cDNA amplimer obtained with PCR. Northern analysis of DmPrx-4783 also showed a single transcript of similar size **[589]**. Blood feeding-induced expression was observed at 7 d but not at 1 h (relative induction of 4.019 and 1.283, respectively, compared to matched NB samples). However, no infection-induced AsPrx-4783 expression was noted at 1 h or 7 d (relative expression values of 0.894 and 1.179, respectively, compared to matched UN samples). Under low stringency conditions and longer detection times, three additional transcripts, which may represent transcripts from related *AsPrx* genes, were evident (not shown).

Expression of AsPrx-4783 in A. stephensi cells. Infection of *A. stephensi* with *Plasmodium berghei* **[52]** and with *Plasmodium falciparum* **[Lim *et al.*** unpublished data**]** induces NOS expression in the mosquito midgut. The synthesis of NO, in turn, leads to increased nitrosative stress in the midgut **[56]**. Based on data that implicate Prx family members in protection against nitrosative stress **[306-318]** and observations that expression of 1-Cys, 2-Cys and PrxV genes can be induced by a variety of stimuli **[313, 573, 589, 607-614]**, I proposed that *AsPrx-4783* may be induced in response to parasite infection *in vivo.*

Expression of *AsPrx-4783* was evaluated in dissected tissues of *A. stephensi* using qRT-PCR **[58]**. Expression of the S7 ribosomal protein gene was used for normalization **[52]**, with induction of gene expression determined using the comparative critical threshold cycle analysis (comparative C_t; **[597, 598]**). Comparison of C_t values for reactions with and without RT were used to assess levels of genomic contamination:

RNA samples with <1% genomic contamination (*e.g.* those with a difference of greater than 6.7 cycles between RT^+ and RT^- C_t values) were included in data analyses.

Analyses of midgut RNA isolated from one cohort of uninfected and matched non-bloodfed *A. stephensi* 0-48 h pBM revealed that *AsPrx-4783* expression is induced at 2-20 h pBM due to bloodfeeding alone **(Fig. 3-10A)**. Induction of *AsPrx-4783* due to blood feeding was also shown by northern analysis of RNA isolated at 7 d pBM **(Fig. 3-9)**, a timepoint outside of the qRT-PCR timecourse. At 7 d pBM, *AsPrx-4783* transcript levels in bloodfed uninfected mosquitoes (UN) were 4.0-fold higher than transcript levels in non-bloodfed (NB) mosquitoes **(Fig. 3-9)**. Induction of Prx expression in response to bloodfeeding has also been observed in the tick *Haemaphysalis longicornis* **[608]**.

Analyses of midgut RNA isolated from four cohorts of *P. berghei*-infected and matched uninfected *A. stephensi* revealed that infection with *P. berghei* induced *AsPrx-4783* expression >2- to 7-fold at 12.5-48 h pBM **(Fig. 3-10B)**. In contrast, expression in mosquito carcasses (whole mosquito minus midgut) was not induced by parasite infection (not shown). The inference that *AsPrx-4783* expression is limited to the midgut is further supported by the fact that 10-fold greater amounts of RNA from carcasses (100 ng) were examined than were examined from midguts (10 ng). In infected insects, variability in *AsPrx-4783* expression was likely due to differences in parasite infection intensity as was demonstrated for As60A expression **[58]**. We propose that malaria parasite infection in *A. stephensi* induces NO synthesis and the formation of related reactive nitrogen intermediates (RNIs) which, in turn, induce increases in *AsPrx-4783* expression.

AsPrx-4783 gene expression in A. stephensi midgut explants. Midguts dissected from *A. stephensi* and maintained in cell culture medium were to be used to test for induction of *AsPrx-4783* expression. The difficulty of manipulating the midgut environment *in vivo* made this strategy attractive. Midgut explants would have combined the easy manipulation quality of cell culture while maintaing an environment more closely resembling those *in vivo*. In preliminary assays, treatment of dissected midguts with mouse blood induced moderate *AsPrx-4783* expression in some midgut explants **(Fig. 3-11)**. However, further analyses using this strategy were not feasible as the midgut explants often became contaminated with bacterial growth and were rarely viable past 48 h.

AsPrx-4783 gene expression in immortalized A. stephensi cell lines. In preparation for functional analyses of *AsPrx-4783*, gene expression was examined in two *A. stephensi* cell lines, ASE and MSQ43. The ASE cells are non-adherent with hemocyte-like morphology and behavior **[615]**. AsNOS expression in ASE cells is induced by treatment with heat-killed *E. coli* and *M. luteus* **[615]**. Therefore, I hypothesized that elevated NO synthesis following treatment of ASE cells with killed microbes would induce *AsPrx-4783* expression.

ASE cells were treated with heat-killed *E. coli*, *M. luteus*, or *B. bassiana* **(Fig. 3-12)**. *AsPrx-4783* expression in ASE cells was not significantly changed by treatment with these three microbes. Interestingly, however, 6 and 12 h treatments with *B. bassiana* induced *AsPrx-4783* expression **(Fig. 3-12)**, but high variation among replicates precluded statistical significance.

To more directly test whether NO and other known inducers of Prx expression could induce *AsPrx-4783* expression, ASE cells were treated with H_2O_2 and mediators of nitrosative stress including PN, AS, DEA-NO, GSNO, and acidified nitrite. PN is a reaction product of NO and $O_2^{\bullet-}$ and is mutagenic, inflammatory, pro-apoptotic and cytotoxic **[178, 182, 206, 337, 616-618]**. AS is a commonly used nitroxyl (NO^-) donor **[30, 144]**. DEA-NO is an NO donor with a decay rate is similar to that of AS. GSNO is a small *S*-nitrosothiol (SNO). SNOs are proposed to stabilize and transport NO in biological systems **[102, 108, 248, 249]**, are often elevated in diseased states **[233, 234, 388, 619-624]**, and are toxic to bacteria **[261-263]** and *P. falciparum* **[92]**. Acidified nitrite has long been used as an antimicrobial agent in food preservation **[625]**, has been used to create SNOs *in vitro* and is commonly used as an inexpensive generator of nitrosative stress.

ASE cells were treated with H_2O_2 at various concentrations for different lengths of time **(Figs. 3-13 and 3-14)**. Although similar treatments are known to increase Prx expression in other cells **[611-614, 626-628]**, none induced *AsPrx-4783* expression in ASE cells. Identical assays with MSQ43 cells yielded similar results **(Fig. 3-15)**. Further, treatment of ASE and MSQ43 with AS **(Figs. 3-16 and 3-17)**, PN **(Fig. 3-18)**, GSNO and acidified nitrite **(Figs. 3-19 and 3-20)** also failed to significantly induce *AsPrx-4783*

under the conditions tested despite the fact that these RNIs have been shown to induce Prx in a variety of other eukaryotic cells **[306, 308, 309]**.

Treatment of ASE cells with the NO donor DEA-NO resulted in moderate increases in *AsPrx-4783* expression **(Fig. 3-21)**. Specifically, treatment with 1,000 μM DEA-NO (equivalent to ~1.5 mM NO) resulted in a 1.56- and 1.57-fold increase in *AsPrx-4783* expression at 6 and 48 h following addition. The half-life of DEA-NO is 2 min at 37ºC and 16 min at room temperature and pH 7.4. At pH 5, the decompositional release of NO is nearly instantaneous. Cell culture conditions are maintained at 28ºC and pH ~7, thus by the first time point (2 h) >99% of the available NO had been released. *AsPrx-4783* was clearly not induced at 2 h, thus induction of *AsPrx-4783* occurs between 2 and 6 h after exposure to released NO.

In single experiments, ASE cells were treated with recombinant human TGF-β1, a growth hormone ingested in the bloodmeal **[56]**, and a crude lysate of *P. berghei*, which would contain parasite factors involved in signaling NO synthesis in the midgut **[629]**. Neither of these treatments induced *AsPrx-4783* expression in ASE cells (data not shown).

AsPrx-4783 protein expression in the ASE cell line. Based on a lack of transcriptional induction of *AsPrx-4783*, which included no measurable impact of the classical Prx inducer H_2O_2, I hypothesized that AsPrx-4783 activity may be largely regulated post-transcriptionally. To address this hypothesis, I performed western blot analyses of protein lysates prepared from ASE cells treated with H_2O_2, DEA-NO or PN.

Previously published work provides support for translational regulation of AsPrx-4783 activity. Treatment of mammalian cells with peroxides or cytokines (IL1β+IFN-γ, TNF-α) resulted in obvious increases in Prx protein levels as demonstrated by western analysis **[612, 613, 626, 627, 630]**. Promoter-reporter analyses have also shown that expression of yeast Tsa2p is induced in response to peroxides and PN **[316]**. In other eukaryotic cell types, treatment with peroxides does not alter Prx protein levels, but did induce conversion of dimeric to monomeric Prx **[580, 627, 631, 632]**. This change in protein conformation is likely due to the fact that cysteines oxidized during catalysis are incapable of forming recyclable disulfide linkages. Further oxidation of monomeric

human 1-Cys Prx drives the formation of an intramolecular linkage between Cys^{47} and Cys^{91} and thereby increases the compactness and mobility of the protein under nonreducing conditions **[582]**. In contrast to these examples in which Prxs follow a pattern of dimer to monomer to fast-migrating monomer upon oxidation, purified reduced *Salmonella* monomeric AhpC was converted to a dimer upon treatment with PN **[308]**. Despite these differences, the various redox states of Prx, as revealed by protein conformation on non-reducing gels, are considered a convenient assay for reactivity of Prx **[633]**.

For detection of AsPrx-4783 in western blots, I used antisera to DmPrx-4783 provided by Dr. William Orr **[589]**. To confirm that I could reproduce published results, protein lysate from *D. melanogaster* was analyzed by western blot under non-reducing (without DTT) and reducing (with DTT) conditions. As expected, DmPrx-4783 with apparent molecular mass of the dimeric form was detected under non-reducing conditions, while reductive dissociation of the dimer was observed when the protein extract was treated with DTT **(Fig. 3-22)**. Next, the antiserum was tested for cross-reactivity with protein lysate prepared from ASE and MSQ43 cells. A single cross reacting *A. stephensi* protein from each cell line was observed under reducing conditions **(Fig. 3-23)**. Interestingly, the apparent molecular masses of the monomeric forms of DmPrx-4783 and AsPrx-4783 were larger than anticipated. Based on calculated molecular masses, the mosquito and fruit fly proteins should range from 21-22kD, but instead migrated with apparent molecular masses near 28kD. This observed increase in apparent molecular mass of monomeric Prx has been noted in the literature and appears to be a common characteristic of 2-Cys Prxs **[309, 634-636]**.

For western blot analysis, protein lysates were prepared from ASE cells treated with 200 μM H_2O_2, 200 μM DEA-NO or 200 μM PN. Under reducing conditions, a single cross-reacting band, predicted to be monomeric AsPrx-4783, was detected. However, intensities of this cross-reacting band from treated lysates as measured by densitometry ranged from 50% to 150% of the intensities from control lysates, suggesting that protein levels changed little if at all in response to the three treatments **(Fig. 3-24)**.

Although AsPrx-4783 protein levels did not appear to change in response to treatment, I hypothesized that AsPrx-4783 activity might manifest as changes in protein

conformation, induced by redox cycling. As such, I expected to see shifts from monomeric to dimeric AsPrx-4783, or vice versa, in treated compared to control ASE cells. To address this hypothesis, protein lysates from treated and control ASE cells were electrophoretically separated under non-reducing conditions. The cross-reacting protein, predicted to be AsPrx-4783, migrated as four forms with apparent molecular masses consistent with monomeric, dimeric, "fast migrating," and "slow migrating" conformations **(Fig. 3-25)**. The "slow migrating" form was consistent with multimeric AsPrx-4783 or may have resulted from interactions with other proteins such as cyclophilin A **[637]**. The "fast migrating" form migrated at the predicted size for the monomeric AsPrx-4783 and may have been consistent with an alternate folding structure of AsPrx-4783 or an aggregate of cross-reacting proteins with small molecular masses which were lost from reducing gels due to excessive run times.

I first attempted to resolve the nature of these different conformations to address my hypothesis on AsPrx-4783 activity. First, I treated the ASE cell protein lysate with DTT and electrophoretically separated the proteins on a Tris-Tricine peptide gel. No small cross-reacting proteins were observed in subsequent western blots (not shown), indicating that these proteins had not been "lost" from reducing gels. To determine whether the "fast migrating form" was an alternative folding structure of AsPrx-4783, I attempted to alter the redox state and, hence, the conformation of the protein, which would be predicted to increase the apparent molecular mass to ~28kD. As such, the "fast migrating" band was excised from a non-reducing gel, soaked in DTT-containing buffer and resolved through a second gel. Although I could recover the band following treatment in buffer without DTT, treatment of the excised band with DTT resulted in transition to a band with an apparent molecular mass that was much higher than the predicted monomer **(Fig. 3-26)**.

In addition to difficulties associated with identifying the relationship among the four apparent conformations of AsPrx-4783, patterns of change of AsPrx-4783 conformation in response to experimental treatment were not consistent among experiments completed on different days. In sum, treatment with H_2O_2, DEA-NO or PN did not appear to induce changes in AsPrx-4783 protein levels in ASE cells and I was unable to determine whether AsPrx-4783 activity in ASE cells could be correlated with

redox-induced changes in protein conformation **(Fig. 3-25)**. Although positive data could have implicated AsPrx-4783 in protection against stress, direct tests of AsPrx-4783 function were still necessary. As such, I utilized overexpression and knockout assays to determine directly whether AsPrx-4783 functions to protect *A. stephensi* cells from oxidative and nitrosative stresses associated with parasite infection.

Overexpression of AsPrx-4783 in S2 and MSQ43 cells: assessment of protection to chemical challenge. To test the hypothesis that AsPrx-4783 could provide protection against ROS/RNIs generated in response to parasite infection, I tested whether AsPrx-4783-overexpressing *D. melanogaster* S2 cells and *A. stephensi* MSQ43 cells exhibited greater viability following chemical treatment than matched cells lacking overexpressed AsPrx-4783.

In bacterial cells, single-cell eukaryotes, and mammalian cells, overexpression of Prx has been shown to increase survival following challenge with H_2O_2, t-BOOH, hydroxyl radicals, acidified nitrite, NO, and PN **[312, 314, 630, 638]**. In *D. melanogaster*, overexpression of DmPrx-4783 enhanced viability of S2 cells relative to control cells following treatment with H_2O_2 and paraquat **[590]**. Further, based on reports of that overexpressed Prxs can provide stress protection in heterologous host cells **[306]**, I first attempted to determine whether overexpressed AsPrx-4783 could protect *D. melanogaster* S2 cells from oxidative and nitrosative stress.

Recombinant AsPrx-4783 protein was overexpressed in *D. melanogaster* S2 cells from the recombinant pMT/V5-His TOPO expression vector pTLP55 **(Appendix D)** following Effectene transfection. Overexpression was confirmed with anti-V5 western blots using protein lysates prepared 6-72 h following induction with $CuSO_4$ **(Fig. 3-27)**. Dimerization and reduction of dimers were not prevented by the V5 tag **(Fig. 3-27)**, which confirmed that the overexpressed AsPrx-4783 was likely functional.

In order to confirm that the cross-reacting protein(s) in previous ASE western analyses using anti-DmPrx-4783 represented different redox-induced conformations of AsPrx-4783, S2 cell extract from pTLP55- and mock- transfected cells were electrophoretically separated under reducing and non-reducing conditions then examined by western blot using anti-DmPrx-4783 **(Fig. 3-28)**. In the absence of DTT, anti-DmPrx-

4783 detected three bands in transfected cells: a prominent dimer, a slightly faster migrating doublet, and a slower migrating diffuse band **(lane 1, Fig. 3-28)**. Decreased intensity of the main dimeric band together with the additional higher weight diffuse band may be indicative of a mixed dimer formation. A reductive dissociation was observed when S2 cell protein lysate was incubated for 5 min with 100 mM DTT. In DTT-treated lysates from transfected cells, the anti-DmPrx-4783 antisera clearly also cross-reacted with overexpressed AsPrx-4783 **(compare lanes 3 and 4, Fig. 3-28)**. The apparent molecular mass of overexpressed AsPrx-4783 was higher than that of the endogenous DmPrx-4783 due to the epitope tag. These experiments confirmed again that apparent dimeric forms of AsPrx-4783, like those of DmPrx-4783, were reduced by treatment with DTT, indicating that the epitope tag did not appear to interfere with dimer formation and reduction.

To determine whether AsPrx-4783 could protect S2 cells from ROS- and RNI-associated damage, I assessed viability of pTLP55 transfected and mock-transfected S2 cells following exposure to varying concentrations of H_2O_2, DEA-NO, AS and PN **(Fig. 3-29)**. Treatment conditions were based on literature reports of similar assays and on chemical doses that killed ~50-70% of S2 cells in preliminary dose-dependence studies (not shown). At each time point, cell viability was normalized against non-challenged S2 cells to account for variability in background cell death.

Relative to treated, mock-transfected cells, AsPrx-4783 overexpression resulted in enhanced S2 cell viability following treatment with AS and PN **(Fig. 3-29C, D)**. AsPrx-4783 did not protect S2 cells against DEA-NO **(Fig. 3-29B)**, which suggested that AsPrx-4783 provided RNI-specific protection to S2 cells. Unexpectedly, overexpressed AsPrx-4783 did not protect S2 cells against H_2O_2 **(Fig. 3-29A)**. Radyuk *et al.* **[589]** found, in contrast with our results that DmPrx-4783, overexpressed from a plasmid construct identical to that used for AsPrx-4783 overexpression, protected S2 cells from death due to treatment with 20 mM H_2O_2 for up to 4 h. There are several possible explanations for these conflicting results. First, it would be reasonable to assume that DmPrx-4783 and AsPrx-4783 are not identical in catalytic activity; other *A. stephensi* Prxs may function more efficiently to reduce peroxides. By extension, the pool of heterodimeric (fruit fly and mosquito) Prx-4783 in transfected cells may be less efficient at peroxide reduction

than homodimeric DmPrx-4783. Finally, it is possible that AsPrx-4783 is over-oxidized by H_2O_2, a problem that could be compounded if S2 cells cannot provide sufficient reductants to recycle and reactivate the oxidized AsPrx-4783.

In a subsequent series of experiments, I tested the hypothesis that AsPrx-4783 could protect *A. stephensi* cells from ROS- and RNI-associated damage. Two cell lines were available for these assays: ASE and MSQ43. Although the metallothionein promoter can be induced by 100-200 μM $CuSO_4$ in two *Aedes albopictus* cell lines (C6/36 and C7-10), the success of protein induction varied with cell line, and expression in neither mosquito cell line was as robust as expression in *D. melanogaster* cells **[639, 640]**. Copper induction was not feasible in MSQ43 and ASE cell lines since the concentration required to drive transcription caused significant cell death even in the absence of transfection (not shown). Therefore, for overexpression in *A. stephensi* cells, I constructed a plasmid with constitutive expression of AsPrx-4783 under control of a cytomegalovirus (CMV) promoter **(**pcDNA3.1/His-V5 TOPO, pTLP58; **Appendix D)**. Preliminary attempts to transfect ASE cells were not successful; these cells grow in suspension as hollow sphere aggregates and would be expected to have significantly reduced cell surface area for transfection. By contrast MSQ43 cells grow as a monolayer and showed nearly 100% transfection efficiency as detected following transfection and detection of an identical lacZ-expressing control plasmid (pcDNA3.1/lacZ-His TOPO; not shown). Overexpression of AsPrx-4783 in MSQ43 cells was confirmed with anti-V5 western blots using protein lysate collected 6-96 h following transfection **(Fig. 3-30)**. Maximal protein synthesis was observed at 48-96 h following transfection, thus transfected cells were challenged during this time period.

Both pTLP58-transfected and mock-transfected MSQ43 cells were exposed to varying concentrations of H_2O_2, DEA-NO, AS and PN, prior to assessment of cell viability using Trypan blue exclusion. MSQ43 cells were more sensitive to chemical treatment than were the S2 cells (not shown), thus the concentrations used were lower than were used in the S2 cell study. For all chemical treatments, overexpression of AsPrx-4783 under the CMV promoter enhanced the MSQ43 cell viability relative to mock-transfected treated cells **(Fig. 3-31)**. Protection afforded by overexpressed AsPrx-4783 was different in MSQ43 cells and S2 cells. In S2 cells, AsPrx-4783 did not

protect against H_2O_2 or DEA-NO, whereas in MSQ43 cells AsPrx-4783 did protect against these cytotoxic chemicals. These differences may be attributable to differences in the plasmid contructs, the host cell types and/or varying roles of endogenous Prx gene products (see discussion).

RNAi-mediated gene silencing of AsPrx-4783 in MSQ43 cells: assessment of protection to chemical challenge. To provide additional supporting data that AsPrx-4783 can protect *A. stephensi* cells against ROS- and RNI-associated damage, I used a strategy to silence AsPrx-4783 expression in *A. stephensi* cells to complement analyses of AsPrx-4783 overexpression.

Silencing of Prx using RNA interference (RNAi) to elucidate function is supported by the literature. In organisms ranging from bacteria to yeast to human cells, Prx gene silencing has resulted in decreased cell survival when deficient cells are exposed to H_2O_2, t-BOOH, SNP (sodium nitroprusside; NO and NO^+ donor), GSNO (SNO), and PN (both bolus PN addition and a SIN-1(3-morpholinosydnonimine-HCl, generated PN flux) **[310, 311, 590, 626, 630, 641-644]**. RNAi is now commonly used to create a loss-of-function phenotype and, hence, to understand the function of a particular gene. Although the mechanism by which double-stranded RNA (dsRNA) acts is not completely understood, transfection of dsRNAs into insect cells leads to gene silencing. Introduced dsRNAs are first cleaved by Dicer into double stranded 21-23 nt RNA fragments termed siRNA (small interfering RNA) **[645]**. In *D. melanogaster*, Dicer consists of RNAse III, helicase and PAZ (Piwi/Argonaute/Zwille; **[646]**. RNase III mediates the initial, ATP-dependent cleavage event. The trimmed product is then incorporated into a ribonucleoprotein (RNP) complex that mediates further cleavage **[647]** and the small interfering RNAs (siRNA) are presented to RISC (RNA induced silencing complex) which when incorporated can target and degrade homologous RNA **[648]**. In mosquito cells, transfected dsRNAs effectively reduce transcript levels in *A. gambiae* Sua 5.1 and Sua1B cells **[649, 650]**. Gene silencing has also been achieved *in vivo* in *A. gambiae* following injection of dsRNA into adult females (G3) **[16]** and into larvae of *A. stephensi* (Liston) **[651]**.

For dsRNA-mediated gene silencing of *AsPrx-4783*, I modified existing protocols. Although dsRNA is readily taken up by *D. melanogaster* S2, KC and BG2-C6 cells, the presence of serum in the growth medium decreased the efficiency of RNAi **[652]**. Therefore I used the transfection reagent Effectene for *A. stephensi* cells in serum-containing medium. In addition, I modified published protocols for dsRNA transfection of *A. gambiae* cells **[16, 649, 650, 652]** as follows. The efficiency of *AsPrx-4783* silencing was determined using a two-step qRT-PCR. In the first step, oligo $dT_{(16)}$ primer was used for cDNA synthesis. After treatment with RNAse, this cDNA was used for real time PCR analysis. With this strategy, the potential for amplification from cDNA generated from dsRNA is eliminated. Further, reduction in transcript levels could be accurately quantified; in replicated assays, *AsPrx-4783* expression was decreased by >90% at 24-72 h and 81% at 5 d **(Fig. 3-32)**. Specificity of *AsPrx-4783* silencing was demonstrated by transfection of control *A. stephensi* cells with dsRNA for mouse *cyclophilin*. Expression of *AsPrx-4783* was not affected by transfection of this heterologous dsRNA (not shown). Based on these results, subsequent control *A. stephensi* cells were "mock-transfected" in the absence of dsRNAs to control for impact of the transfection procedure on *AsPrx-4783* expression. The efficiency of *AsPrx-4783* silencing was further confirmed using western blot analysis **(Fig. 3-33)**. Despite the efficiency and apparent specificity of our gene silencing protocol, we are uncertain whether *AsPrx-4783* silencing affects other Prx family members in *A. stephensi* cells. For example, transfection of gene-specific dsRNAs has been reported to impact levels of other highly similar gene products **[653, 654]**.

Transfected and mock-transfected MSQ43 cells were exposed to varying concentrations of H_2O_2, DEA-NO, AS and PN, then cell viability was evaluated using the Trypan blue exclusion assay. For each transfection, qRT-PCR analysis was used to verify that *AsPrx-4783* transcript levels were significantly reduced in dsRNA-treated cells (not shown). Based on replicated assays, AsPrx-4783 silencing in MSQ43 cells resulted in higher mortality than was observed for mock-transfected cells for all four chemicals tested **(Fig. 3-34)**. Together, *AsPrx-4783* overexpression and gene silencing data indicate that this gene product protects *A. stephensi* cells against ROS- and RNI-associated cell damage and death.

DISCUSSION

Numerous studies have demonstrated that Prxs can protect cells against a variety of nitrosative stress challenges **[306-319]**. The majority of work has focused on pathogens and parasites, defining roles for Prx in protection against host defenses. However, a few studies have demonstrated that Prxs of eukaryotic hosts can be induced in response to viral, bacterial and fungal infections **[655-659]**. Here I investigated whether the 2-Cys Prx, AsPrx-4783, protects *A. stephensi* cells against ROS- and RNI-associated cell damage and death that are consistent with conditions known to exist during *P. berghei*-infection of *A. stephensi*.

Insect orthologs of Prx-4783: commonalities and contrasts. In *D. melanogaster*, DmPrx-4783 is expressed primarily in eggs and larvae, not in pupae and adults **[589]**. Additionally, expression of DmPrx-4783 is induced within 4 h after pricking larvae with LPS-contaminated needles, increasing hemolymph levels of DmPrx-4783 protein ~11-fold over that in control insects **[659]**. *Bombyx mori* BmPrx-4783 is expressed in the fat body and midgut but not in the hemolymph of the 5th instar larvae **[658]**. BmPrx-4783 was strongly induced in the fat body in response to H_2O_2 injection **[658]**. In addition, both mRNA and protein of BmPrx-4783 were induced ~2-fold in response to viral infection, presumably associated with infection-dependent synthesis of H_2O_2 **[658]**. *AsPrx-4783* is highly expressed in the midgut and non-midgut tissues of female A. *stephensi*, although induction in response to parasite infection is limited to the midgut epithelium. Thus, despite some species-specific differences in expression, insect Prx-4783 orthologs are induced by oxidative stress, which is likely associated with infection by pathogens and parasites. Interestingly, Prx expression appears to decline over time in a pattern associated with aging in some organisms **[660, 661]**. In *D. melanogaster*, levels and activity of enzymes and proteins involved in antioxidant defenses decrease with age, resulting in commonly observed age-related increases in oxidative stress and damage **[662]**. These observations would suggest that aging, antioxidant defense, and innate immunity are linked in *A. stephensi* as well.

Blood meal-induced expression of AsPrx-4783. *AsPrx-4783* expression was upregulated 4-fold in response to blood meal ingestion. Hematophagous insects ingest heme proteins, principally hemoglogin, in volumes several times their body weight. Within 20 min of feeding, erythrocyte hemolysis frees 1 to 10% of the total ingested hemoglobin in the midgut lumen **[63]**. The globins are dissociated from heme and digested, whereas the heme groups are polymerized to insoluble hematin under oxygenated, slightly alkaline conditions **[663]**. Polymerization, however, is not instantaneous, nor does it completely abolish radical chemistry **[664]**. Thus, significant quantities of heme and hematin can react with iron and oxygen in the blood meal to form free radicals in the mosquito midgut **[665-667]**. In a manner consistent with the chemistry of this stress, northern analysis and qRT-PCR showed that blood ingestion or addition of blood to midgut explants induced expression of *AsPrx-4783*.

In addition to providing protection against radical-induced stress derived from heme, Prx proteins can interact directly with heme. One mammalian Prx was previously named heme binding protein 23 (HBP23; PrxI) for its ability to bind to heme with high affinity (K_d=0.055 μM) **[313, 607, 668]** and to bind protoporphyrin IX with moderate affinity (K_d=0.21 μM) **[610]**. The function of heme binding by HBP23 is unclear; perhaps HBP23 is involved in heme catabolism. I have not determined whether AsPrxs can bind to heme, although conditions in the mosquito midgut may facilitate this interaction. The peritrophic matrix (PM) of *Aedes aegypti* can bind ~18 nmol heme which is roughly equivalent to the complete hydrolysis of a 2 μL blood meal (~10 mM heme) **[402]**. The PM lies along the midgut epithelium, thus trapped heme may drive the induction of *AsPrx* expression in the epithelial cells. Induced AsPrx may subsequently bind free heme thereby suppressing the generation of ROS and protecting the mosquito from the stress of feeding. The positioning of AsPrx at the epithelial cell surface would also provide protection at the site of parasite invasion.

The induction of Prx gene expression by heme is well documented in the literature. For example, HBP23 mRNA was induced in rat liver cells in a dose dependent manner by heme to as high as 6-fold relative to controls after 5 h of treatment with 10 μM heme-BSA **[607]**. Yeast mitochondrial PrxIII also showed heme-inducible expression **[669]**. Finally, heme-interacting enzymes appear to share coordinate regulation. Several

studies have demonstrated that induction of Prx expression is co-regulated with that of heme-degrading heme oxygenase-1 (HO-1) suggesting that these genes are regulated by a similar mechanism **[313, 607, 668]**.

In addition to induction of *AsPrx-4783* by blood and products of blood digestion, parasite induction of inflammatory levels of anti-parasite NO and RNIs in the midgut within the first 25 h after feeding (**[56]**, Chapter 2) induce further stress on the host *A. stephensi*. I propose that induction of *AsPrx-4783* in the midgut epithelium to levels as high as 7-fold relative to control insects is evidence of host defense against self-induced damage.

Functional effects of *AsPrx-4783* expression in the mosquito midgut extend beyond protection against oxidative and nitrosative stress associated with bloodfeeding. When blood is withdrawn from mammalian hosts, autooxidation of oxyhemoglobin (oxyHb) results in the formation of significant quantities of methemoglobin (metHb) within minutes to a few hours despite the large concentration of Prxs in red blood cells **[560]**. I predicted that similar autooxidation would occur in blood withdrawn during mosquito feeding. However, spectroscopic analyses of mosquito midgut blood revealed no appreciable metHb from the time of ingestion through the completion of blood digestion at 48 h after feeding **(Fig. 2-9)**. Based on data that demonstrate that both 1-Cys Prx and PrxIII can suppress the oxidation of oxyHb **[587, 670]**, I suggest that AsPrxs may suppress the oxidation of ingested oxyHb. While the functional importance of maintaining high levels of oxyHb to mosquito physiology is not known, this chemistry has important implications for the formation of RNIs that are the likely parasite killing molecules resulting from NO synthesis.

Expression of AsPrx-4783 in A. stephensi cells. Many studies have shown that Prxs, including the insect orthologs of AsPrx-4783, are induced at both the transcriptional and translational levels **[589, 658, 659]**. Although bloodfeeding and parasite infection induced AsPrx transcription *in vivo*, none of the treatments tested *in vitro* significantly altered AsPrx-4783 mRNA or protein levels. Further, I was unable to detect any dimeric to monomeric conversions, a conformational change occasionally correlated to Prx activity **[580, 627, 631, 632]**, in western blot analyses of treated *A. stephensi* cells. The *A.*

stephensi cell lines are derived from mosquito embryos and their tissue of origin is unknown, hence, direct comparison with the midgut epithelium is impossible. Further, Prx expression is tissue specific: some Prx genes are inducible while others appear to be expressed constitutively at high levels to serve housekeeping functions **[316]**. Therefore, perhaps *AsPrx-4783* is inducible in the midgut epithelium, but in our two cell lines, *AsPrx-4783* functions as a housekeeping gene product with high levels of unchanging expression.

Unresolved questions about AsPrx-4783 from western analysis. Although differences in the physiology of *A. stephensi* cells provide a reasonable hypothesis for the lack of perceptible protein changes, it is also possible that the use of 1D SDS-PAGE can obscure some changes in AsPrx-4783 that are important to function, including those related to redox status.

Following separation by 2D SDS-PAGE, a single isoform of Prx can appear as doublet spots. For example, treatment of a variety of mammalian cell types with H_2O_2 or butyl hydroperoxide (BHP) resulted in an increase in the intensity of a spot corresponding to 2-Cys Prx and a shifted spot to the left, corresponding to a more acidic variant **[563, 671, 672]**. The more basic spot corresponded to the form involved in the normal catalytic cycle **[673]**, whereas the more acidic spot corresponded to the hyperoxidized form **[563, 673, 674]**. The identity of the acidic spot is under debate. Mitsumoto *et al.* **[671]** suggested that these more acidic spots corresponded to the Cys-SOH form, however the study by Rabilloud *et al.* **[563]** showed using LC/MS/MS that the acidic variant of PrxII contained three additional oxygen molecules (*i.e.* $-SO_3H$, the sulfonic acid form). On the other hand, the presence of lower oxidation states such as disulfides and sulfenic acid could not be assessed because of the use of reducing conditions. The overoxidization to sulfinic ($-SO_2H$) or sulfonic acid may facilitate peroxide signaling **[604, 674]**, but also represents an inactive state of the protein. The overoxidized state is recycled by retro-reduction or replaced with newly synthesized reduced protein, processes which occur gradually after initial Prx inactivation **[563, 671, 675, 676]**.

Degradation and *de novo* synthesis versus retro-reduction of the overoxidized form would be detectable as changes in Prx protein level by 1D analysis. In Rabilloud's study **[563]**, peroxide stimulation was followed by the expected change from the reduced to the oxidized form of Prx. Subsequently, reduced Prx increased over time, but levels of oxidized Prx remained stable for 3 h. In this case, the total amount of Prx increased overtime, suggesting that *de novo* synthesis rather than retro-reduction was responsible for the appearance of the reduced form.

Retro-reduction would alter redox status and, hence, protein function without concomitant changes in protein levels detected by 1D SDS-PAGE. However, these changes can observed with 1D analysis and western blotting when antisera that differentially detect total protein versus oxidized forms of the protein are utilized. For example, western analyses of H_2O_2-treated HeLa cells using antisera against against the oxidized form containing Cys-SO_3 **[672]** revealed that oxidized Prx in cells treated with H_2O_2 gradually increased and then decreased over time. In contrast, overall Prx levels as detected with redox status-independent anti-Prx antisera did not change in response to treatment.

For AsPrx-4783, we have yet to determine whether the ratio of oxidized and reduced forms change with chemical treatment. Because we do not have antisera that can differentially detect changes in redox status, I performed a preliminary analysis of AsPrx-4783 using 2D SDS-PAGE. Initial 2D analysis of unstimulated ASE cells using anti-DmPrx-4783, showed that the reduced monomer is indeed made up of several forms believed to be the reduced spot (major form), an oxidized spot and two very minor spots with intermediate pI values (not shown). These minor spots may be the result of another from of post-translational modification such as phosphorylation **[551]**. Rabilloud *et al.* **[563]** proposed that in 2D western analysis the reduced spot is representative of the level of antioxidant defense by Prx, whereas the oxidized spot level is more an indicator of the oxidative injury to the cells. Thus, 2D SDS-PAGE analysis may prove useful to follow the activity of AsPrx-4783 via redox status change in response to chemical challenge and inflammatory conditions in mosquito cells.

The paradox of redox and AsPrx-4783. My preliminary 2D SDS-PAGE analyses suggested that different AsPrx-4783 redox forms are present in *A. stephensi* cells. To elucidate the relationship of these forms to cell stress response, I used non-reducing 1D SDS-PAGE and western analyses with anti-DmPrx-4783 antisera.

Under a variety of conditions, multiple redox forms of AsPrx-4783 observed on non-reducing western blots **(Fig. 3-25)**. The forms that I observed included proteins with masses approximately 65, 45.5, 42.5, 27.5, 26, and 21 kD. The ~45.5 and ~42.5 kD proteins are consistent with dimer migration while the ~27.5 and ~26 kD proteins are believed to be monomers. The doublet nature may be the result of changes in migration due to alternative oxidation states or other protein modifications. The identity of the ~65 Kd protein is unknown but may be a trimer, or heterodimer between AsPrx-4783 and an unknown protein. The fast migrating ~21 kD potein may be an alternate folding structure of AsPrx-4783 or an aggregate of small cross-reacting proteins. Unfortunately, however, the pattern of cross-reacting bands, even for a single stress treatment, was not consistent among replicates, but within the same treatment and replicate, the pattern was the same across treatments. Although I attempted to keep conditions as stable as possible between experiments, perhaps some variable was overlooked. Slight variations in osmolarity or pH may result in significant alterations in banding patterns. As such, I cannot draw any conclusions based on these patterns, but can provide some insight into other unusual observations of Prx redox forms as reported in the literature.

Atypical migration of Prx in PAGE has been observed previously, but never fully addressed. In some cell types, resolved protein samples revealed doublet bands migrating at the predicted molecular size of a dimer **[316, 613, 637, 643, 677, 678]**, while in other cases, three dimers, rather than a single dimer, were apparent **[564, 633]**. Various hypotheses have been proposed to explain the anomalous migration of these proteins, including the presence of a single disulfide bond (peroxidatic-peroxidatic, peroxidatic-resolving, or resolving-resolving) or double disulfide bonds (two peroxidatic-resolving). Similarly the appearance of multiple bands, rather than a single protein band, with the apparent molecular mass of the monomer suggest that the reduced monomer and an oxidized monomer with with an intramolecular disulfide or overoxidation of the

peroxidatic Cys to Cys-SOH or Cys-SO_2H can co-occur under some conditions **[566, 569, 580, 582, 637, 678, 679]**.

In a manner similar to AsPrx-4783, other Prx proteins have been described that migrate significantly faster than the monomer under non-reducing conditions. Unfortunately, these occurrences are often ignored or remain unexplained in the literature **[308, 564, 633, 680]**. However, in a few instances, the faster migrating Prx was identified as a Prx with a C-terminal truncation **[631, 681, 682]**. A C-terminally truncated Prx may occur in poplar tree **[569]**, although the data remain inconclusive. In *Schizosaccharomyces pombe*, a 2-Cys Prx lacking the terminal two residues formed dimers regardless of the H_2O_2 concentration **[631]**, thus truncation created a form more resistant to inactivation by H_2O_2 than the non-truncated 2-Cys Prx. The authors concluded that truncation was a novel type of regulation where removal of the terminal His^{192} inactivated Prx and further removal of the penultimate Lys^{191}, (actually any cleavage between Lys^{191} and Lys^{176}), resulted in release of the inactivation.

A different type of fast migrating form of Prx has been described from *P. falciparum* **[681]**. Storage of *P. falciparum* Prx longer than a week at 4ºC in the absence of DTT led to the appearance of a second protein species with smaller apparent molecular mass **[681]**. This form of *P. falciparum* Prx was thought to result from the formation of non-disulfide intramolecular bonds, since 100 mM DTT did not alter the conformation, or from selective degradation. Relative to monomeric *P. falciparum* Prx, the faster migrating form had a 5-fold higher K_m and a shift in the optimal pH for catalysis from 7.2 to 8.0. Hence, the authors concluded that this oxidized conformation may represent regulation of *P. falciparum* Prx function *in vivo*.

In contrast to faster Prx migration due to truncation or non-disulfide bonding, AsPrx-4783 faster migration was eliminated with DTT, suggesting the involvement of disulfide bonding in the conformational change **(Figs. 3-24, 3-25, and 3-26)**. A similar case of intramolecular disulfide bonding has been reported for a human 1-Cys Prx **[582]**. The occurrence of the fast migrating AsPrx form could not be correlated to number of freeze-thaws or passage number of the cell line used. To attempt to clarify that the fast migrating form was indeed AsPrx-4783, the fast migrating protein was excised from the gel, treated with DTT and resolved on a second SDS-PAGE gel. However, instead of re-

formation of the monomer, a protein with significantly higher apparent molecular mass was detected **(Fig. 3-26)**. Although this was unexpected, the shift in apparent molecular mass may be explained by the formation of higher order Prx structures. In addition to dimers, 2-Cys Prxs can form decameric "doughnuts" containing five dimers. The predominate factor in forming the decameric oligomer is the reduction of the redox-active disulfide center **[550, 552, 560, 683].** Other factors that have been noted to promote oligomerization include changes in ionic strength **[553, 560, 684]**, pH, **[560, 685]**, calcium concentration **[686, 687]** and overoxidation of the peroxidatic Cys. Of interest is the observation that *D. melanogaster* Prx-4783 forms decamers, which are the predominant form even in the presence of 5 mM DTT **[572]**. The decameric structure is held together by hydrophobic and ionic interactions **[553, 560, 687, 688]**, thus although occasionally smaller aggregates of dimers have been observed with native PAGE, the dimer-dimer interactions should be prevented by SDS-PAGE. Hence, the high apparent molecular mass protein that resulted from reduction of the fast migrating AsPrx-4783 is not likely to be a Prx decamer. In light of my data and these observations, the nature of the fast migrating form of AsPrx-4783 is both unresolved and unique.

Overexpression of AsPrx-4783: D. melanogaster S2 versus A. stephensi MSQ43 cells. Because analyses of AsPrx-4783 protein levels and conformation failed to provide insight into AsPrx-4783 function, we designed strategies for overexpression and RNAi-mediated gene silencing to directly address function of AsPrx-4783 in *D. melanogaster* S2 and *A. stephensi* MSQ43 cells. Overexpression assays utilized both *D. melanogaster* S2 cells and *A. stephensi* MSQ43 cells. Based on the level of conservation of Prx protein sequences between *D. melanogaster* and *A. stephensi* **(Fig. 3-4)** and studies demonstrating function of Prx in heterologous host cells (*e.g.* **[306, 309, 567, 582, 638, 689]**), I proposed that AsPrx-4783 would function to protect S2 cells from oxidative and nitrosative stresses.

When AsPrx-4783 was overexpressed in *D. melanogaster* S2 cells, these cells exhibited increased viability following treatment with AS (NO^-l) and PN **(Fig. 3-29)**. In contrast, overexpressed AsPrx-4783 protected MSQ43 cells against nitroxyl, DEA-NO,

H_2O_2 and PN **(Fig. 3-31)**. Insights into the structure of 2-Cys Prx may provide an explanation for these differences.

In all organisms studied to date, the minimal functional unit for 2-Cys Prx is a homodimer joined by a disulfide bond **[551]**. Heterodimer formation and cooperativity between heterologous monomers of 2-Cys Prxs has been observed **[564, 677, 685]** and provides additional regulation of activity **[315, 316, 677]**. In addition, inactivation of one Prx can be compensated for by activation of other Prx family members in the cell **[315, 316]**. When AsPrx-4783 was overexpressed in S2 cells, it is likely that the two species-specific homodimers as well as the heterodimer of AsPrx-4783 and DmPrx-4783 were formed. It is possible that the heterodimer is less efficient than either homodimer in protecting S2 cells from damage due to treatment with H_2O_2 and DEA-NO. This would imply that the mechanism for protection against NO and peroxides differs from that for NO^- and PN, a hypothesis which is addressed below.

In addition to potential differences in activity of AsPrx-4783 homo- and heterodimers, differences in physiology of S2 and MSQ43 cells as well as in the overexpression protocols used for these cell lines may account for differences in AsPrx-4783 protection against oxidative and nitrosative stress. For all stresses tested, *A. stephensi* cell lines were more sensitive to oxidative and nitrosative stress than were the *D. melanogaster* S2 cells, suggesting that the roles of Prx in each of these cell types must also differ. In addition, the S2 cells may lack sufficient reductants to recycle oxidized AsPrx-4783 in necessary quantities for protection against all stresses tested, thus effectively sequestering DmPrx-4783 in inactive heterodimers. For overexpression in S2 cells, copper (II) sulfate was used to induce transcription from a metallothionein promoter in the plasmid construct. This induction would also be expected to induce expression of the endogenous metallothionein in S2 cells, which likely protects these cells from some oxidative and nitrosative stresses **[690, 691]** and potentially confounds analyses of AsPrx-4783. Data in support of this hypothesis came from a preliminary experiment in which S2 cells were mock transfected and challenged with H_2O_2 or DEA-NO with or without copper (II) sulfate pre-treatment. In these assays, S2 cells pre-treated with copper (II) sulfate exhibited enhanced viability relative to cells that were not pre-treated (not shown). Western analyses of these cells showed similar levels of DmPrx-

4783 protein in the presence and absence of copper (II) sulfate pre-treatment **(Fig. 3-33)**. Thus, the added protection was not the result of increased endogenous DmPrx-4783 protein expression. The use of copper (II) sulfate for induction was not feasible for *A. stephensi* cells; concentrations used for induction in S2 cells were lethal for *A. stephensi* cells. As such, AsPrx-4783 was overexpressed in *A. stephensi* cells under control of a constitutive promoter.

A potential role for AsPrx-4783 as a PN reductase. My data demonstrate that AsPrx-4783 can provide protection against PN in MSQ43 cells. DNA is a critical physiological target of PN; oxidation reactions cause base modification, mutations and single- and double- strand breaks **[175-180]**. PN can also oxidize sulfhydryls leading to thiyl radical formation **[182]**. The major nitration targets of PN include phenols such as tyrosine residues in proteins; nitrotyrosine formation has been associated with a number of inflammatory conditions **[188, 189]**. As such, both prokaryotic and eukaryotic cells have evolved selective defenses against PN. For example, GPx, a selenium-containing enzyme structurally similar to Prx, has PN reductase activity in bovine erythrocytes **[692]**. This PN reductase activity is more efficient when the pH is alkaline, such as the pH in the midgut of a mosquito. For full activity, GPx requires GSH; glutathione reductase (GR) catalyzes the conversion of glutathione disulfide (GSSG) to GSH. Insects lack GPx **[662]** and GR **[300, 572]** and instead substitute a Thx system for similar chemical reactions **[300, 572]**. High level NO synthesis in insects such as we have observed in *A. stephensi* may have been a strong selective pressure for this trait because NO inactivates GPx in a dose dependent manner **[693]**. Thioredoxin reductase (ThxR) and GR are similar in structure and function, however, ThxR works on a greater variety of substrates. A high GSH/GSSG ratio is maintained in *D. melanogaster* cells and mM levels of reduced GSH have been shown to be important for intracellular redox homeostasis **[572, 662]**. The function of GPx as a PN reductase in insects has not been demonstrated.

The Prxs have received more attention than have the GPx orthologs for their roles as PN reductases. The first Prx-associated PN reductase activity was reported in bacteria **[308, 311]**. Subsequently, Prx orthologs from a variety of species, including the cow

[307], yeast **[316]**, human **[317]** and *Arabidopsis thaliana* **[309]** have demonstrated PN reductase activity. The majority of reductase activity has been attributed to 2-cys Prx orthologs, with the exception of the bovine 1-Cys (PrxVI) **[307]** and human PrxV **[317]**. A related tryparedoxin peroxidase from the protozoan parasite *Trypanosoma cruzi* can also function as a PN reductase **[318]**. It is perhaps not surprising, therefore, that the 2-Cys Prx AsPrx-4783 would protect *A. stephensi* cells from PN-associated cell death. Interestingly, a bacterial Prx reduces PN seven times faster than does the endogenous GPx **[308]**, which if true for the insect Prx orthologs, would have significant implications for protecting *A. stephensi* from its own anti-parasite defenses.

The chemical reduction of PN by Prx differs among species. For *Leishmania* 2-Cys Prx **[314]**, PN reductase activity required only the resolving Cys^{173}, whereas H_2O_2 reduction required the peroxidatic Cys^{52}. In *S. typhimurium* AhpC **[308]**, the peroxidatic Cys^{46} was essential for the PN reductase activity. In human PrxV **[317]** both peroxidatic and resolving cysteines (Cys^{47} and Cys^{151}) but not Cys^{72} were required for PN reductase activity. To determine whether AsPrx-4783 is a PN reductase, future efforts will focus on the synthesis of recombinant protein for *in vitro* assays and on the use of site-directed mutagenesis to identify the key cysteines involved in reduction.

Overexpression of AsPrx-4783 in MSQ43 cells protected these cells against nitroxyl-associated cell damage and death. Nitroxyl (NO^-) is cytotoxic causing double and single strand DNA breaks and base oxidation **[129, 130, 142, 146, 147]**. It is widely accepted that NO^- and singlet oxygen can react to form PN **[129, 132]**. Thus the ability of AsPrx-4783 to protect against NO^- may be due in part to PN reductase activity of AsPrx-4783. However, the chemistries of NO^- and PN differ and some studies have noted that toxicities of these compounds derive from different reactive intermediates **[145]**. For example, NO^- has a high affinity for GSH **[117]**; exposure of cells to millimolar concentrations of AS can dramatically reduce intracellular GSH through the production of GSNHOH **[129, 130]**. Prxs may reduce GSNHOH (D.A. Wink, personal communication), suggesting that Prxs may also be required to protect cells against nitroxyl-associated damage and to recycle oxidized thiols for cellular homeostasis.

AsPrx-4783 overoxidation: a potential role for Srx in reactivation. In the process of providing protection against oxidative and nitrosative stresses, AsPrx-4783 would be expected to undergo "bystander" oxidation or, specifically, oxidation of the peroxidatic Cys to Cys-SOH which would form a disulfide with the resolving cysteine of a second subunit. This process would be expected to proceed slowly, based on structural analyses of Prx that show that the disulfide-forming Cys residues in 2-Cys Prx may be separated by as much as ~13Å **[558, 560]**. Under high oxidizing conditions the peroxidatic Cys can become further oxidized to sulfinic acid **[560]**. The sulfinic acid cannot be reduced by Thx, thus overoxidation results in inactivation of the Prx **[547, 563, 604, 674]**. Generally proteins that have been oxidized are not repaired; rather they are removed by proteolysis **[694, 695]**. Like most eukaryotic 2-Cys Prx, insect 2-Cys Prxs contain a GG(V/I/L)G…YF motif, which is characteristic of those Prxs that are sensitive to inactivation by hyperoxidation **[604]**. From sequence inspection, *P. falciparum* Prx contains the GG(V/I/L)G motif but has YL instead of YF (not shown). All three 2-Cys Prx from *Schistosoma mansoni* contain a GGLG motif but one lacks the YF motif **[696]**. This *S. mansoni* Prx variant can tolerate high concentrations of peroxides without overoxidation **[696]**. Taken together, these observations suggest that *P. falciparum* Prx is resistant to inactivation by hyperoxidation, whereas AsPrx-4783 is not.

The selective pressure to reverse Prx inactivation has likely resulted in the evolution of unique physiological strategies for reactivation. For example, sulfiredoxin (Srx) has been identified as responsible for the reversal of inactivation of 2-Cys Prx by hyperoxidation in yeast **[697]**. Srx orthologs are found only in eukaryotes, consistent with the fact that prokaryotic Prx orthologs are insensitive to oxidative inactivation **[697]**. Analysis of the human, rat and mouse orthologs revealed that Srx can use Thx or GSH as electron donors **[698]**. Purified Srx reduced the sulfinic acid forms of all four mammalian 2-Cys Prsx (I → IV) but did not reduce PrxV or PrxVI, suggesting that reduction was specific to 2-Cys Prxs, although the mechanism for Srx reversal of Prx overoxidation inactivation has yet to be determined **[699]**. BLAST analysis using the known yeast Srx sequence resulted in the identification of several arthropod Srx sequences **(Fig. 3-35)**. Although an *A. gambiae* sequence could not be identified from the genomic database, an orthologous sequence was identified from the mosquito *Armigeres subalbatus*.

Interestingly, the *A. subalbatus* Srx cDNA sequence was identified among cDNAs from an immune response-activated hemocyte library **[700]**. This cDNA (ASAP ID: 44015) shows high deduced amino acid identity (45.7%) to *D. melanogaster* Srx. The strong similarity between the arthropod Srx suggests that other mosquito genomes likely encode orthologous genes.

In addition to the ATP-dependent Srx, sestrins can increase the rate of recovery of the overoxidized Prxs **[701]**. Sestrins share sequence similarity to AhpD (an enzyme which catalyzes the reduction of AhpC in bacteria **[306, 319, 702]**). Unlike AhpD which is a disulfide reductase, sestrins are cysteine sulfinyl reductases **[701]** which have a single proximal Cys of the essential cysteine dyad of AhpD **[702]**. This Cys is necessary for function. Using small interfering RNAs, expression of the sestrin Hi95 was reduced >50-fold, compromising the ability of cells to detoxify RNIs produced following treatment with 250 mM GSNO or SNAP for 6 h **[701]**. Because Prxs catalyze the decomposition of RNIs **[306, 308, 314, 316]**, it appears that participation of sestrins in the regeneration of the active form of 2-Cys Prx may be important for optimal RNS decomposition. BLAST analysis using human Hi95 as query identified several potential sestrins encoded in the genomes of various insects, including *A. gambiae* **(Fig. 3-36)**. Interestingly, not only does *P. falciparum* 2-Cys Prx lack the signature motif for overoxidation, neither a Srx nor sestrin sequence could be identified in the *P. falciparum* genome. Thus malaria parasite and mosquito Prxs may be regulated differently, with the parasite Prx more similar to prokaryotic than to eukaryotic Prxs. Given that Prxs protect both the host mosquito and the parasite from nitrosative stress **[310]**, this difference may be a suitable target for the future development of antiparasitic Prx inhibitors to control mosquito-stage malaria parasite infection.

AsPrx-4783 and potential roles in apoptosis. Apoptosis is a form of programmed cell death **[703]**, which can result from a variety of stresses including oxidative and nitrosative damage **[704, 705]**. Both PN and Fe nitrosylHb, which can form oxygen radicals and NO^-, are inducers of apoptosis **[147, 467, 616]**. Nitric oxide may stimulate apoptosis by increasing cellular p53 levels **[706]**. In *A. stephensi*, NO and RNIs are present at inflammatory levels in the anopheline midgut and are involved in killing

Plasmodium **[52, 56]**. These blood meal RNIs provide conditions conducive to initiating parasite apoptotic pathways. Several NO-induced intracellular mechanisms result in apoptosis via activation of caspases **[707]**; caspase-like activity has been detected in the cytoplasm of *P. berghei* ookinetes at an early stage of apoptosis **[329]**. When a caspase inhibitor was added to the blood meal the number of oocysts developing *in A. stephensi* doubled demonstrating that ookinetes remain viable if apoptosis is inhibited **[329]**. In addition, when the NOS inhibitor L-NAME was added to an infective blood meal, the percentage of *P. berghei* ookinetes undergoing apoptosis in the midgut lumen significantly decreased whereas D-NAME had no effect **[329]**. Thus, mosquito midgut RNIs are likely inducers of parasite apoptosis. If the mosquito could be genetically engineered to overexpress signals that induce the apoptotic pathway in the parasite without causing harm to the mosquito, novel control measures to reduce the likelihood of transmission could be devised. Protecting the mosquito from harm would be essential: NO production has also been shown to induce apoptosis in insect cells **[708]**. Thus although NO-related innate immunity can adversely affect parasite proliferation in the mosquito, it may also harm host mosquito tissues. I propose that mosquito Prxs provide protection against the nitrosative stresses encountered during parasite infection.

Based on the literature, a strategy of overexpression of AsPrx-4783 may succeed in protecting mosquito cells from an enhanced immune response to *P. falciparum*. Overexpression of cytoplasmic 2-Cys Prx can counteract several proapoptotic signals **[567, 612, 709-711]**. Mitochondrial 2-Cys Prx, 1-Cys Prx and PrxV also provide protection against H_2O_2 induced apoptosis **[712-714]**. The nature of the response of Prxs to pro-apoptotic signals is not understood, but these enzymes are clearly capable of modulating the apoptotic pathways activated by p53 **[715-717]** and tumor necrosis factor (TNF) **[567, 574, 718]**. It appears that PrxI prevents apoptosis by competing with p73 (a p53 tumor suppressor homolog) for the SH3 domain of c-Abl thereby preventing complex formation and propagation of the apoptotic signal (**Review [719]**). PrxII can regulate at least three signal transduction pathways that directly relate to apoptotic cell death: AP-1(activator protein) **[720]**, caspases **[709, 720]**, and NF-κB **[677]**. Analyses of PrxII by 2D electrophoresis suggest that the redox balance may play a role in TNF-related apoptosis **[563]**. The situation is complicated by the fact that sestrin protein

expression is modulated by p53, but overexpression of sestrins protects against H_2O_2-induced apoptosis **[721]**, which may partially be due to their ability to regenerate hyperoxidized Prx to its active form **[701]**.

In contrast to these anti-apoptotic roles, some Prxs can activate apoptotic pathways. The c-Myc transcription factor is implicated in apoptosis **[722]** and can activate expression of human mitochondrial PrxIII. Overexpression of PrxIII in human breast cancer epithelial cells increased apoptosis while cells with diminished PrxIII were resistant to apoptosis **[723]**. Similarly, under certain conditions *D. melanogaster* Jafrac2 (DmPrx-4156) was shown to promote apoptosis **[724]**. Normally DmPrx-4156 resides in the endoplasmic reticulum, but following induction of apoptosis it is released to interact with *Drosophila* inhibitor of apoptosis (DIAP1), thereby displacing the fly caspase Dronc and promoting cell death **[724]**.

NF-κB can mediate the inhibition of apoptosis by transcriptionally regulating genes involved in inflammation, including numerous cytokines, cytokine receptors, and adhesion molecules **[725-727]**. This transcription factor is also involved in the regulation of iNOS **[728]**. Nitrosative stress has been shown to induce apoptosis through inhibition of NF-κB activity **[729]**. Overexpression of PrxII suppressed TNF-activation of NF-κB **[567, 677]**, and overexpression of AOE372 (PrxIV) blocked the activation of NF-κB that was induced by TNF and phorbol ester **[677]**. Yet another Prx IV (TRANK) dose-dependently activated NF-κB **[730]** and stimulated iNOS expression **[730]**, thereby classifying TRANK as an inflammatory cytokine. This dichotomy of Prx activity in promoting or inhibiting apoptosis is further exemplified by the fact that overexpression of PrxII can either enhance or suppress ROS generation depending on cell type **[731]**. Further, Prx orthologs appear to function as peroxidases when the protein is not aggregated, but function shifts to chaperone roles when dimers aggregate to form high MW structures **[732]**. Overall Prxs appear to play an integral part in the redox status and potential apoptosis of a cell by playing dual roles in induction and inhibition of inflammation and apoptosis.

Anopheles stephensi 2-Cys Prx-4783 provides protection against nitrosative stress in cultured mosquito cells: overexpression and gene silencing data reveal that AsPrx-4783 protects mosquito cells from H_2O_2, NO, PN, and NO^-. The timing of elevated

expression of AsPrx-4783 in the midgut epithelium is correlated with increased RNI levels that form when mobile malarial ookinetes develop and subsequently invade this tissue. Thus under direct insult from parasite invasion and alteration of host redox status, AsPrx-4783 may provide protection to mosquito tissues through reduction of hostile RNIs, through chaperone-like function to repair damaged proteins and/or modulation of immune gene expression. Yet it is also possible that AsPrx-4783 may induce apoptosis to kill parasites by eliminating infected cells. As such, AsPrx-4783 likely influences multiple aspects of the parasite-host relationship. Further study of AsPrx-4783 and other mosquito Prx orthologs is necessary to determine how these gene products might be manipulated to enhance protection of insect cells, while facilitating parasite apoptosis.

FUTURE DIRECTIONS

Identifying other members of the AsPrx family. Because Prxs have overlapping functions and, as shown in yeast, they can function cooperatively, it may be useful to identify the full complement of Prx orthologs in *A. stephensi*. With several insect genomes now completed (*D. melanogaster*, *A. gambiae* and *Apis mellifera*), designing primers to amplify desired homologs should be relatively straightforward. Tissue localization, developmental expression and, of course, parasite-regulated expression should be investigated. It may be of special interest to determine whether two 1-Cys Prxs are functionally important in mosquitoes, in light of the fact that most genomes encode only a single 1-Cys Prx.

Additional insights into AsPrx-4783 function. Investigating differences in the regulation and function of *A. stephensi* versus *P. falciparum* Prxs will help to reveal how the mosquito and parasite differ in their response to hostile midgut ROS and RNS. Such differences may provide novel avenues for blocking parasite transmission and thus interrupting the spread of the disease agent.

For example, the predicted amino acid sequence of AsPrx-4783 provides insight into additional levels of regulation that could be manipulated to enhance activity at the

cost of the parasite. The predicted sequence of AsPrx-4783 is similar to encoded sequences of the mammalian 2-Cys Prxs. Mammalian PrxI through IV all contain Ser/Thr-Pro-(X)-Lys/Arg consensus sequences for cdc2 phosphorylation. Phosphorylation of Thr^{90} by cdc2 resulted in an 80% decrease in Prx activity **[733]**, thus cdc2 is involved in the regulation of these 2-Cys Prx orthologs. Like the mammalian proteins, all known malaria parasite 2-Cys Prx orthologs encode the identical consensus sequence (not shown). However AsPrx-4783 encodes a predicted Val instead of Ser/Thr suggesting that it is not regulated by cdc2 phosphorylation. This may be an interesting difference in parasite and mosquito Prx regulation worth further investigation.

Western analysis. My 1D western analysis data suggested that unoxidized and oxidized monomers of AsPrx-4783 were indistinguishable. I propose that 2D SDS-PAGE and native gels should be performed to resolve potential redox changes in AsPrx-4783. The 2D gels may reveal overoxidation of AsPrx-4783 resulting from different stresses. If patterns suggest an association with a particular stress, it may be worthwhile to investigate mosquito sestrins and sulfiredoxins as potential regenerators of the hyperoxidized AsPrx-4783. In addition to 2D SDS-PAGE, native westerns would reveal whether higher weight oligomerization is associated with AsPrx-4783 activity **[732]**. To further understand the pattern of AsPrx-4783 reduction on native westerns, I suggest that a range of concentrations of DTT be added to the buffer as was done by Kawazu *et al.* **[734]**. This will effect a gradual change in AsPrx-4783 conformation which can provide important insights into the nature of redox status of the protein. The fast migrating band should be analyzed by Edman degradation and mass spectroscopy to confirm that it is AsPrx-4783. For native analyses, it is advisable that leupeptin be excluded from protein lysate preparation since this proteinase inhibitor artifactually increases the formation of the higher MW forms **[687]**.

Biochemical assays with purified AsPrx-4783. His/V5-tagged AsPrx-4783 can be used to generate specific antisera for analysis of AsPrx-4783 localization in the mosquito. Localization will provide further support for the hypothesis that this enzyme plays a critical role in the mosquito midgut during infection. Purified recombinant protein

can also be used for *in vitro* assays. For example, it may be interesting to determine whether Thx and/or GSH can facilitate reduction of AsPrx-4783 and to determine whether AsPrx-4783 can function as a PN reductase. Koo *et al.* **[631]** provided critical advice for maintaining the integrity and activity of recombinant Prx. For example, proteolytic truncation of C-terminal residues critical for activity can be prevented by heating protein lysates quickly after collection. Further, extraction in buffer containing 25 mM NEM prevented Prx re-oxidation when analyzing extracts following H_2O_2 addition **[631]**.

In vivo analysis. Blandin *et al.* **[16]** have successfully used dsRNA-mediated gene silencing to disrupt defensin gene function in *A. gambiae* during malaria parasite development. I propose that a similar strategy could be used to examine function of AsPrx-4783 in apoptosis and parasite development in *A. stephensi*.

Redox status. Genetic mutations like glucose-6-phosphate dehydrogenase deficiency or sickle cell anemia alter erythocyte GSH levels, thus weakening host susceptibility to malaria parasite infection **[565]**. Cellular redox status also affects gene expression, including that of NF-κB **[677]**. As summarized above, NOS activity and redox status are interrelated **[735-739]** as are redox status, GSH/GSSG levels and Prx function. Thus, to understand fully how mosquito Prxs are involved in protection, I suggest that it is necessary to define the redox status (GSH/GSSG) in mosquito following normal bloodfeeding and during parasite infection. It is likely that changes in the GSH/GSSG ratio would affect malaria parasite development within the mosquito.

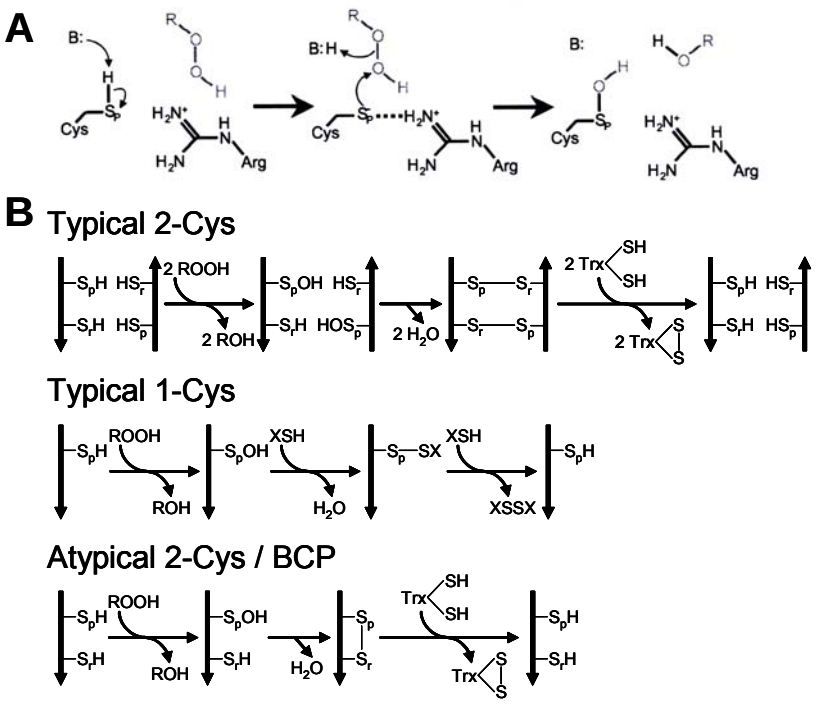

Figure 3-1: Mechanism for the different classes of Prxs. (adapted from **[547, 551, 554, 567, 574, 606, 687, 740]**)

(A) All classes of Prx contain the peroxidatic Cys (S_p) and share the first step of peroxide reduction in common. Nucleophilic attack of the peroxide by the S_p (-SH) reduces the peroxide to the corresponding water or alcohol while oxidizing S_p to a sulfenic acid intermediate (-SOH). The guanidino group of the conserved Arg stabilizes the ionized S_p. The catalytic base that deprotonates the S_p and the catalytic acid that protonates the RO^- leaving group are both labeled "B" although they may not be the same entity. **(B)** The second step of the mechanism where the reduced S_p is regenerated differs between Prx types. Hyperoxidation to sufinic ($-SO_2H$) or sulfonic ($-SO_3H$) acid inactivates the enzyme (not depicted). Except for 1-Cys Prxs, all Prxs contain a second conserved Cys referred to as the resolving Cys (S_r). Attack of the sulfenic acid by the S_r results in an inter- and intra- molecular disulfide bonds in typical 2-Cys Prxs and atypical Prx/BCP orthologs, respectively. The disulfide bond is then reduced by an external thiol, usually thioredoxin (Trx). In typical 2-Cys Prxs the resolving Cys (S_r) is ~125 aa downstream from S_p. The general mechanism for BCP and atypical Prxs is the same; however the spacing between the S_p and S_r differs. In BCP S_p and S_r are always four amino acids apart. In atypical 2-Cys Prx the spacing falls into two main categories: in PrxV types the S_r is ~125 aa downstream from S_p while the Type II variants have the S_r ~25 aa down stream from S_p. The biological electron donor for 1-Cys Prxs is yet unidentified.

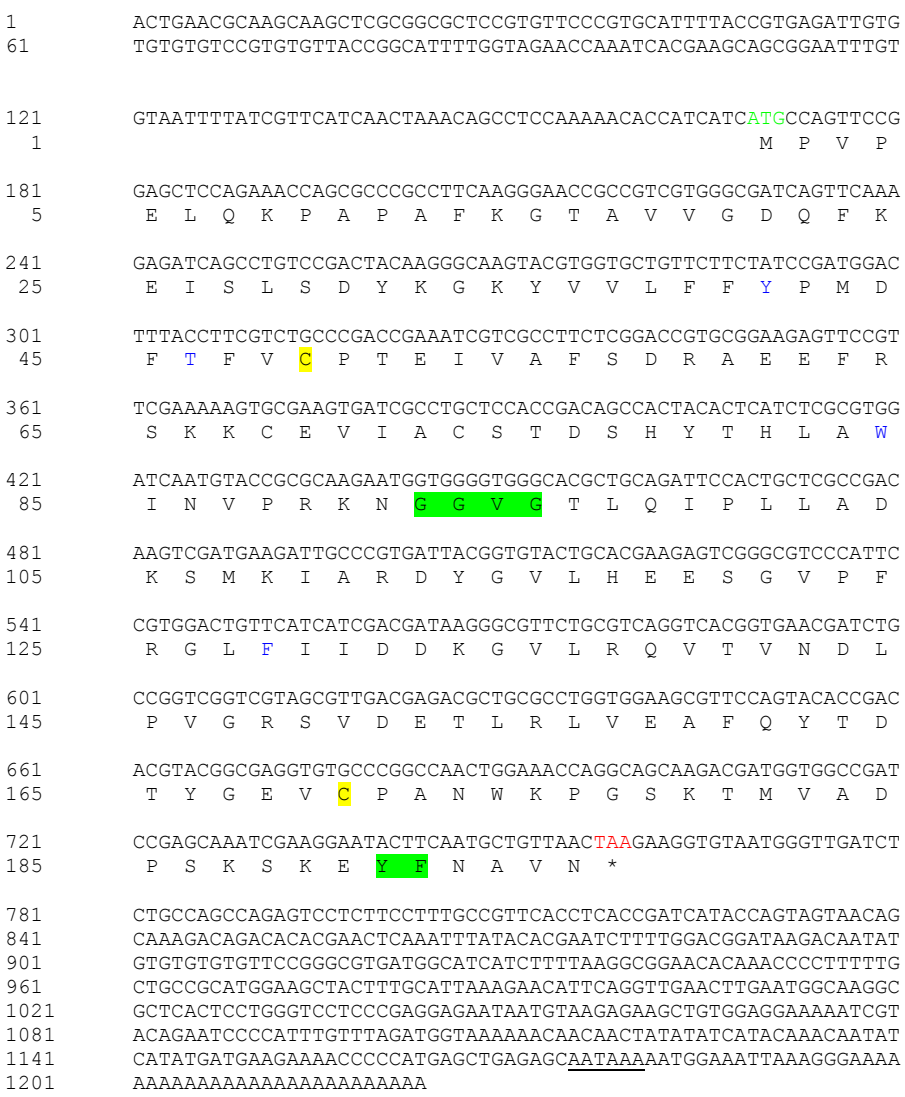

Figure 3-2: Deduced amino acid sequence of AsPrx-4783.

The predicted start codon **ATG** of the AsPrx ortholog to *D. melanogaster* DmPrx-4783 is indicated in green while the predicted stop codon **TAA** is in red. A likely polyadenylation sequence is underlined. A total of 1223 bp of the cDNA have been identified. Based on genomic DNA sequence, AsPrx-4783 lacks introns and encodes a single open reading frame of 591 bp. The deduced protein sequence is 196 aa in length and predicted to have a molecular weight of 21,897.9 daltons and an isoelectric point of 5.95 (Scansite; http://scansite.mit.edu). The peroxidatic cysteine, C^{50}, and resolving cysteine, C^{171}, which are highlighted in yellow constitute the conserved cysteines defining this Prx as a 2-Cys type. The ^{93}GGVG^{96} and ^{192}YF^{193} motif, highlighted in green, identifies AsPrx-4783 as a Prx sensitive to inactivation by hyperoxidation of the peroxidatic cysteine. Residues conserved in Prxs and proposed to aid in stabilizing the peroxidatic cysteine or maintaining structure, Y^{42}, T^{47}, W^{85}, and R^{126}, are shown in blue.

```
1          ATCCAGCCGATTTTACGCCAGTTTGCACAACGGAACTTGGAAGGATCGCAGTGCACCAGC
1             P  A  D  F  T  P  V  C  T  T  E  L  G  R  I  A  V  H  Q

61         CTCATTTTGAGAAGCGCAATGTGAAGGTCCTTGCTCATTCGGTCGATGATCTCAAGTGTC
20         P  H  F  E  K  R  N  V  K  V  L  A  H  S  V  D  D  L  K  C

121        ACGTGGATTGGGTGAATGACATCAAGTCGTACTGTCCGGATATTATCGGTAACTTTCCCT
40         H  V  D  W  V  N  D  I  K  S  Y  C  P  D  I  I  G  N  F  P

181        ACCCCATCATCGCCGACCCAAGCCGTGATTTGGCCGTCCGATTCGGTATGCTGGACGAGA
60         Y  P  I  I  A  D  P  S  R  D  L  A  V  R  F  G  M  L  D  E

241        AGGATAAGGACAACGTGGAGCTAGCGCAAACGGTGCGCGCCCTGTTCATYATYAGCCCCG
80         K  D  K  D  N  V  E  L  A  Q  T  V  R  A  L  F  I  I  S  P

301        ATAAGAAAGTCCGTCTTACGATGCACTATCCAACGTCCACGGGCCGTAATGTAGATGAAA
100        D  K  K  V  R  L  T  M  H  Y  P  T  S  T  G  R  N  V  D  E

361        TTCTGCGCGTCATCGACTCACTGCAGCTGACCGACCGCTTGAAGGTGATTGCGACGCCCG
120        I  L  R  V  I  D  S  L  Q  L  T  D  R  L  K  V  I  A  T  P

421        CCAACTGGACGCCCGGCACTAAGGTCATGATCCTG
140        A  N  W  T  P  G  T  K  V  M  I  L
```

Figure 3-3: Partial deduced amino acid sequence of an *Anopheles stephensi* 1-Cys Prx.

A partial sequence (455 bp) of the *A. stephensi* Prx ortholog to *D. melanogaster* Prx variant 2540 was obtained through PCR. The 151 aa deduced sequence is most similar to a 1-Cys type Prx. The defining peroxidatic cysteine, C^{8}, is highlighted in yellow. Residues conserved in Prx and proposed to aid in stabilizing the peroxidatic cysteine or maintaining protein structure, T^{5}, W^{43} and R^{92} are shown in blue.

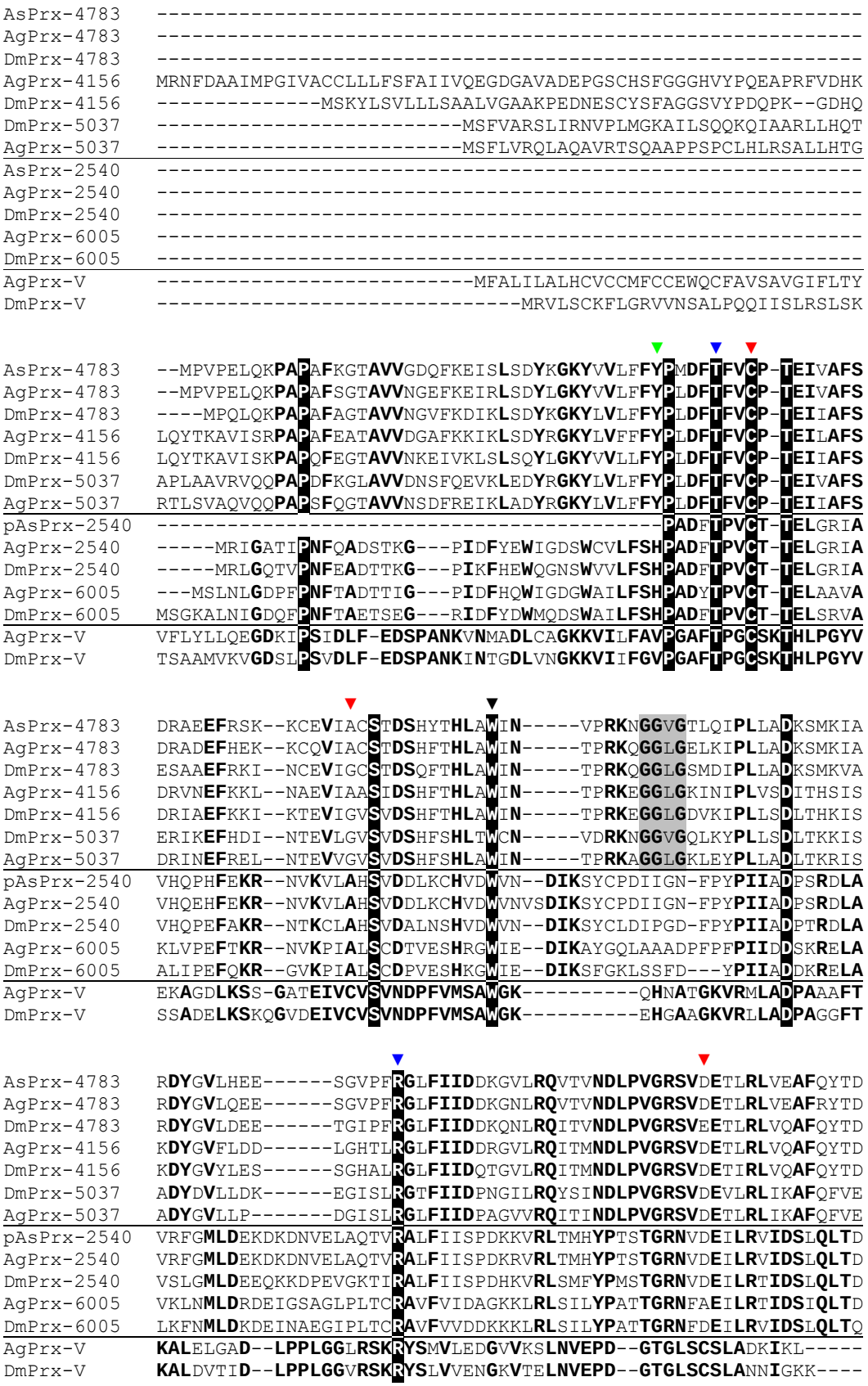
AsPrx-4783
AgPrx-4783
DmPrx-4783
AgPrx-4156
DmPrx-4156
DmPrx-5037
AgPrx-5037
AsPrx-2540
AgPrx-2540
DmPrx-2540
AgPrx-6005
DmPrx-6005
AgPrx-V
DmPrx-V
pAsPrx-2540

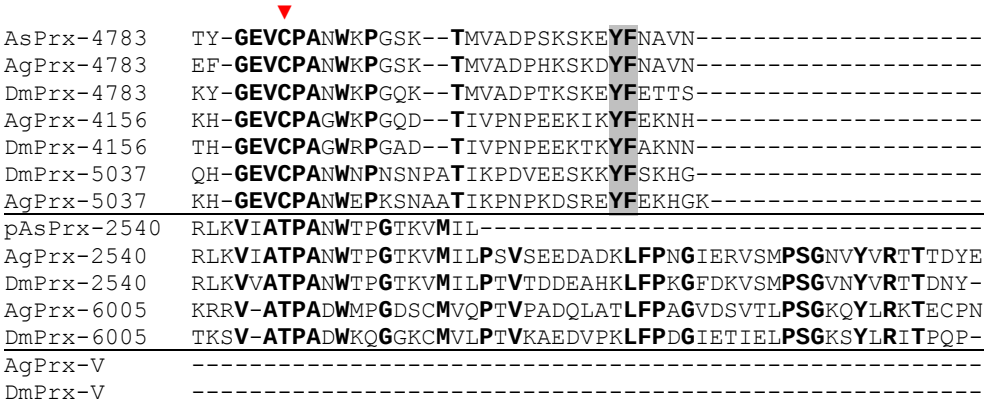

Figure 3-4: Alignment of *Anopheles* and *Drosophila* peroxiredoxins.

Three of the four major Prx clades are represented: typical 2-Cys, 1-Cys and atypical 2-Cys (PrxV). Not shown are the BCP proteins since they were not identified in these insect genomes. Using the ClustalW method in conjunction with data from **[554]**, the sequences were aligned and residues conserved on all three types were shaded in black. Residues conserved in each clade are in bold. Redox-active cysteines are indicated with a red arrow (▼); residues purposed to be involved in the activation of the peroxidatic cysteine are identified with a blue arrow (▼); residues believed to be involved in maintaining the structure if Prx are marked with a black arrow (▼) **[605]**; and residues highlighted in gray make up the signature sequence for 2-Cys Prx that are sensitive to hyperoxidation **[604]**. In addition the conserved H marked with a green arrow (▼) is believed to assist in the activation of the peroxidatic cysteine only in the 1-Cys Prxs **[583]**. Abbreviations are, Ag=*Anopheles gambiae*, As=*Anopheles stephensi*, and Dm=*Drosophila melanogaster*. The prefix "p" indicates that only a partial sequence was obtained.

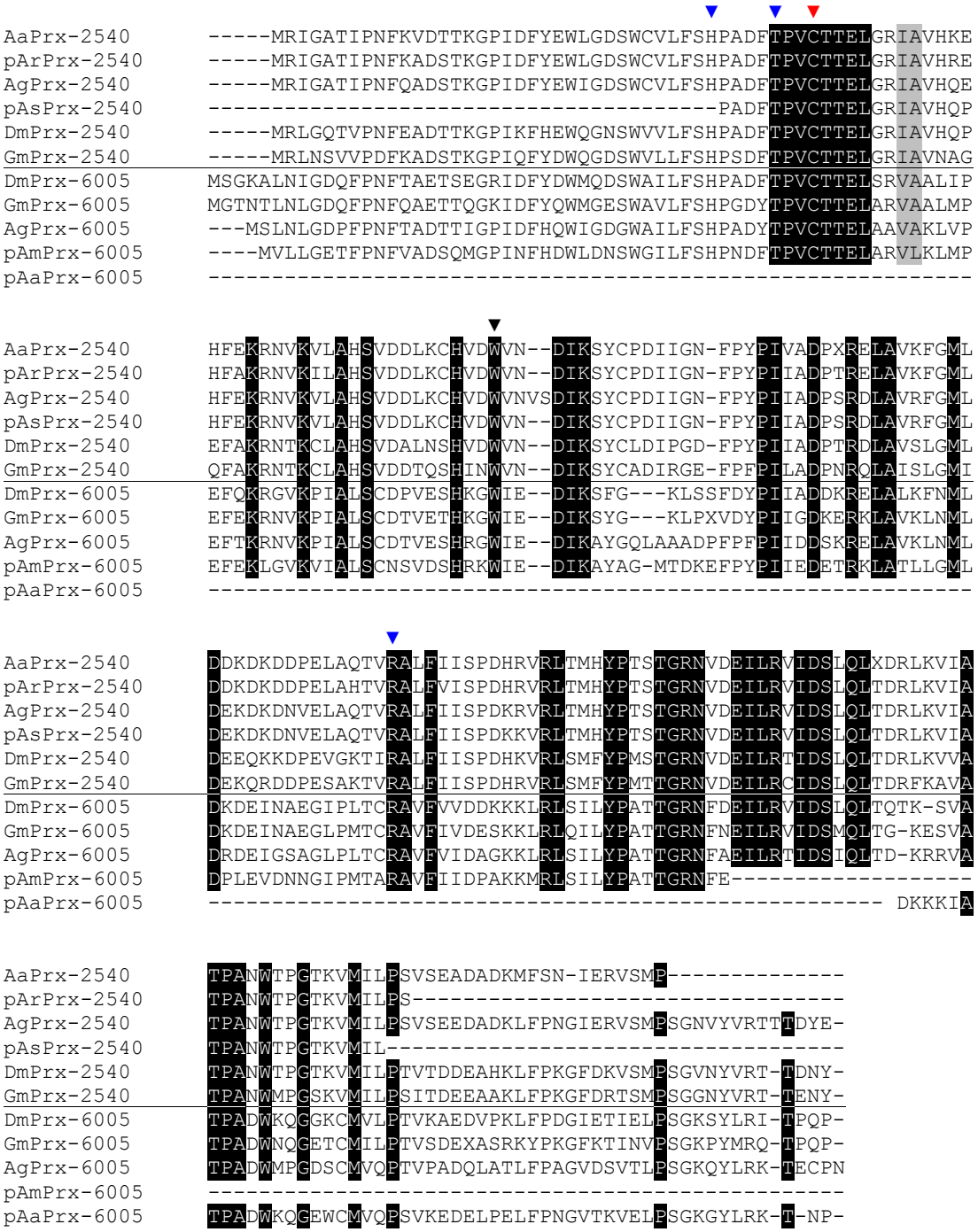
AaPrx-2540
pArPrx-2540
AgPrx-2540
pAsPrx-2540
DmPrx-2540
GmPrx-2540
DmPrx-6005
GmPrx-6005
AgPrx-6005
pAmPrx-6005
pAaPrx-6005

(Previous page)

Figure 3-5: Alignment of predicted insect 1-Cys Prx sequences by the ClustalW method.

Amino acids conserved in the aligned sequences are shaded black for identity and grey for similarity based on side chain chemistry. Similar amino acids are grouped by presence of nonpolar side chains (G, A, V, L, I, P, F, M, W, C), uncharged polar side chains (N, Q, S, T, Y), acidic side chains (D, E), and basic side chains (K, R, H). Dashes indicate gaps introduced during the alignment process. Redox-active cysteines are indicated with a red arrow (▼). C^{45} (with respect to the *A. gambiae* Prx-6005 sequence) is the strictly conserved peroxidatic cysteine. Residues proposed to be involved in the activation of the peroxidatic cysteine are identified with a blue arrow (▼). Residues believed to be involved in maintaining the structure of the active site pocket surrounding the peroxidatic Cys are marked with a black arrow (▼). Abbreviations are Aa=*Aedes aegypti*, Ag=*Anopheles gambiae*, Am=*Apis mellifera*, Ar=*Armigeres subalbatus*, As=*Anopheles stephensi*, Dm=*Drosophila melanogaster*, and Gm=*Glossina morsitans*. Genbank accession numbers are AaPrx-2540 (AY432974), pArPrx-2540 (AY441216), DmPrx-2540 (AF311880), GmPrx-2540 (AY625505), DmPrx-6005 (AF311878), GmPrx-6005 (AY625503), pAmPrx-6005 (XM_395319), and pAaPrx-6005 (AY432202). The Ag sequences obtained from scaffold sequences (scaffold; positions), AgPrx-2540 (AAAB01008986; 8101720→8102725) and AgPrx-6005 (AAAB01008807; 8364093→8364766). The prefix "p" indicates that only a partial sequence was obtained.

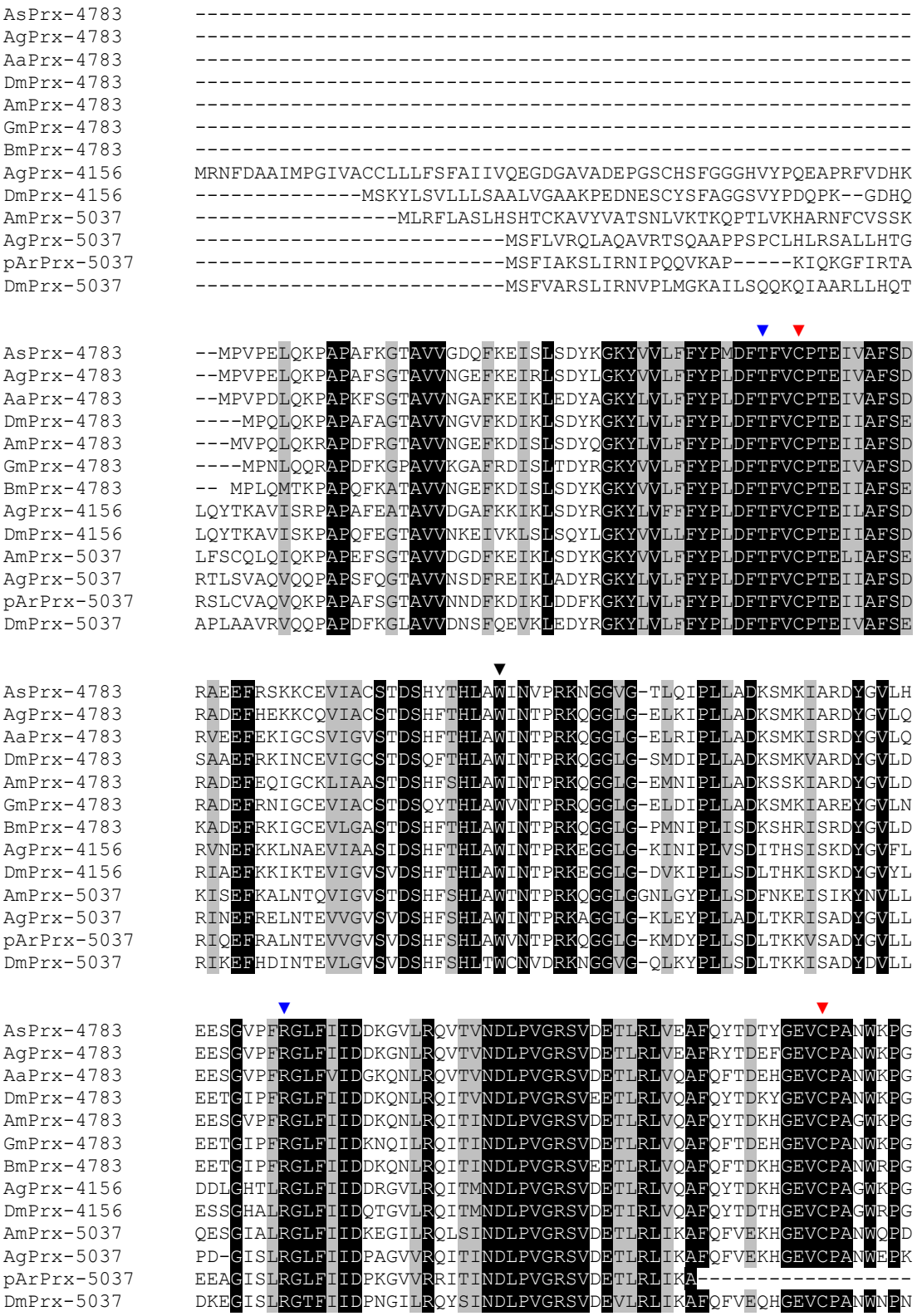
AsPrx-4783
AgPrx-4783
AaPrx-4783
DmPrx-4783
AmPrx-4783
GmPrx-4783
BmPrx-4783
AgPrx-4156
DmPrx-4156
AmPrx-5037
AgPrx-5037
pArPrx-5037
DmPrx-5037

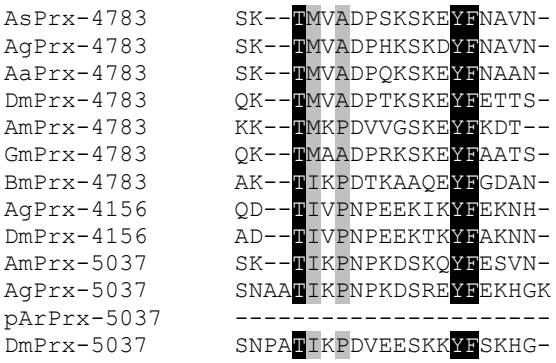

Figure 3-6: Alignment of predicted insect 2-Cys Prx sequences by the ClustalW method.

Amino acids conserved in the aligned sequences are shaded black for identity and grey for similarity based on side chain chemistry. Similar amino acids are grouped by presence of nonpolar side chains (G, A, V, L, I, P, F, M, W, C), uncharged polar side chains (N, Q, S, T, Y), acidic side chains (D, E), and basic side chains (K, R, H). Dashes indicate gaps introduced during the alignment process. Redox-active cysteines are indicated with a red arrow (▼). C^{49} (with respect to the *A. stephensi* sequence) is the strictly conserved peroxidatic cysteine and C^{170} is the resolving cysteine. Residues proposed to be involved in the activation of the peroxidatic cysteine, T^{46} and R^{125}, are identified with a blue arrow (▼). Residues believed to be involved in maintaining the structure the active site pocket surrounding the peroxidatic Cys of Prx, W^{84}, are marked with a black arrow (▼). Abbreviations are Aa=*Aedes aegypti*, Ag=*Anopheles gambiae*, Am=*Apis mellifera*, Ar=*Armigeres subalbatus*, As=*Anopheles stephensi*, Bm=*Bombyx mori*, Dm=*Drosophila melanogaster*, Gm=*Glossina morsitans*. Genbank accession numbers are AaPrx-4783 (AAL37254), DmPrx-4783 (AF321615), AmPrx-4783Gm (XM_393445), BmPrx-4783 (AY438331), GmPrx-4783 (AY625507), DmPrx-4156 (AF321614), AmPrx-5037 (XM_392086), pArPrx-5037 (AY441290), and DmPrx-5037 (AF311747). The Ag sequences obtained from scaffold sequences (scaffold; positions), AgPrx-4783 (AAAB01008804; 84651←84061), AgPrx-4156 (AAAB01008807; 1925781←1924853), and AgPrx-5037 (AAAB01008846; 4068809←4067923). The prefix "p" indicates that only a partial sequence was obtained.

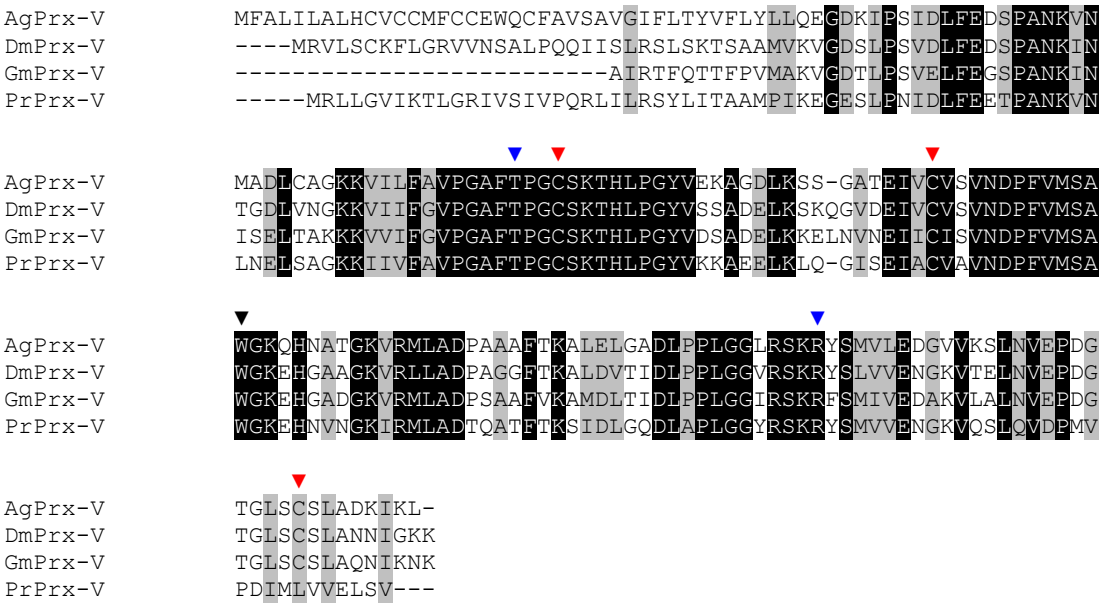

Figure 3-7: Alignment of predicted insect PrxV sequences by the ClustalW method.

Amino acids conserved in the aligned sequences are shaded black for identity and grey for similarity based on side chain chemistry. Similar amino acids are grouped by presence of nonpolar side chains (G, A, V, L, I, P, F, M, W, C), uncharged polar side chains (N, Q, S, T, Y), acidic side chains (D, E), and basic side chains (K, R, H). Dashes indicate gaps introduced during the alignment process. Redox-active cysteines are indicated with a red arrow (▼). C^{85} (with respect to the *A. gambiae* sequence) is the strictly conserved peroxidatic cysteine. C^{108} and C^{184} are variably conserved in PrxV sequences, although C^{108} is conserved among the represented sequences. Residues proposed to be involved in the activation of the peroxidatic cysteine are identified with a blue arrow (▼).Residues believed to be involved in maintaining the structure of the active site pocket surrounding the peroxidatic Cys are marked with a black arrow (▼). Abbreviations are as follows: Dm indicates (*Drosophila melanogaster* with a Genbank accession number of (NM_176512.1), Pr (*Pyrocoelia rufa*; AF516693) and Gm (*Glossina morsitans*; AY625504). The Ag (*Anopheles gambiae*) sequence was obtained from scaffold AAAB01008987, positions 13214667←13214089. The prefix "p" indicates that only a partial sequence was obtained.

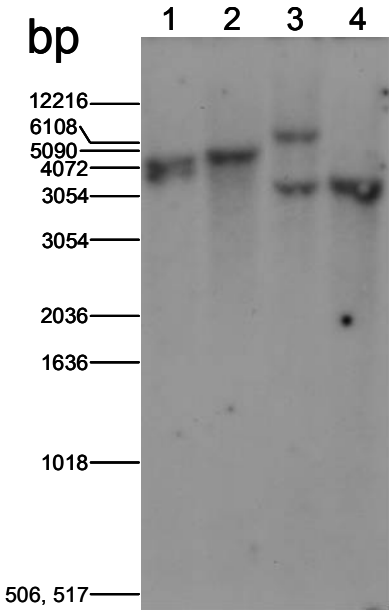

Figure 3-8: Southern blot analysis of the *AsPrx-4783* gene.

Genomic DNA was isolated from adult *A. stephensi* and 12 µg of purified genomic DNA was digested with EcoRI (lane 1), KpnI (lane 2), XhoI (lane 3) or XmnI (lane 4), electrophoretically separated through 0.8% agarose and transferred onto nylon membrane. The filter was hybridized with the ^{32}P-labelled *AsPrx* coding region probe as described in the Materials and Methods. Molecular size markers (bp) are indicated at the left side of the gel.

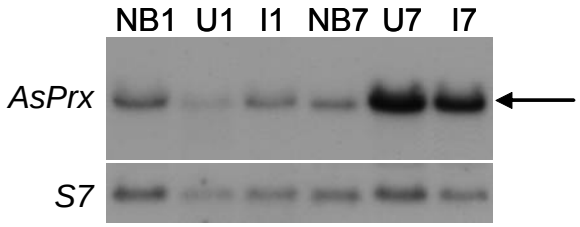

Figure 3-9: A single *AsPrx-4783* transcript was observed from northern analysis.

Messenger RNA (mRNA) was collected from non-bloodfed (NB), *P. berghei*-infected (I) and uninfected (U) *A. stephensi* at 1 h and 7 d following blood feeding. Aliquots of 9 μg mRNA were separated on a 1% agarose NorthernMax (Ambion) gel and transferred to a nylon membrane. RNA probe was made from cloned template containing full length coding sequence of AsPrx. The cross-hybridizing band (arrow) has a calculated molecular weight of 1194 bp which closely corresponded to the predicted *As*Prx transcript size (1223 bp) based on sequence analysis. Densitometry was used to quantitate transcript abundance. AsPrx-4783 transcript levels were normalized against S7 ribosomal protein gene transcript levels to correct for loading differences **[58]**. Blood feeding-induced expression was observed at 7 d but not at 1 h. No infection-induced AsPrx-4783 expression was noted at 1 h or 7 d.

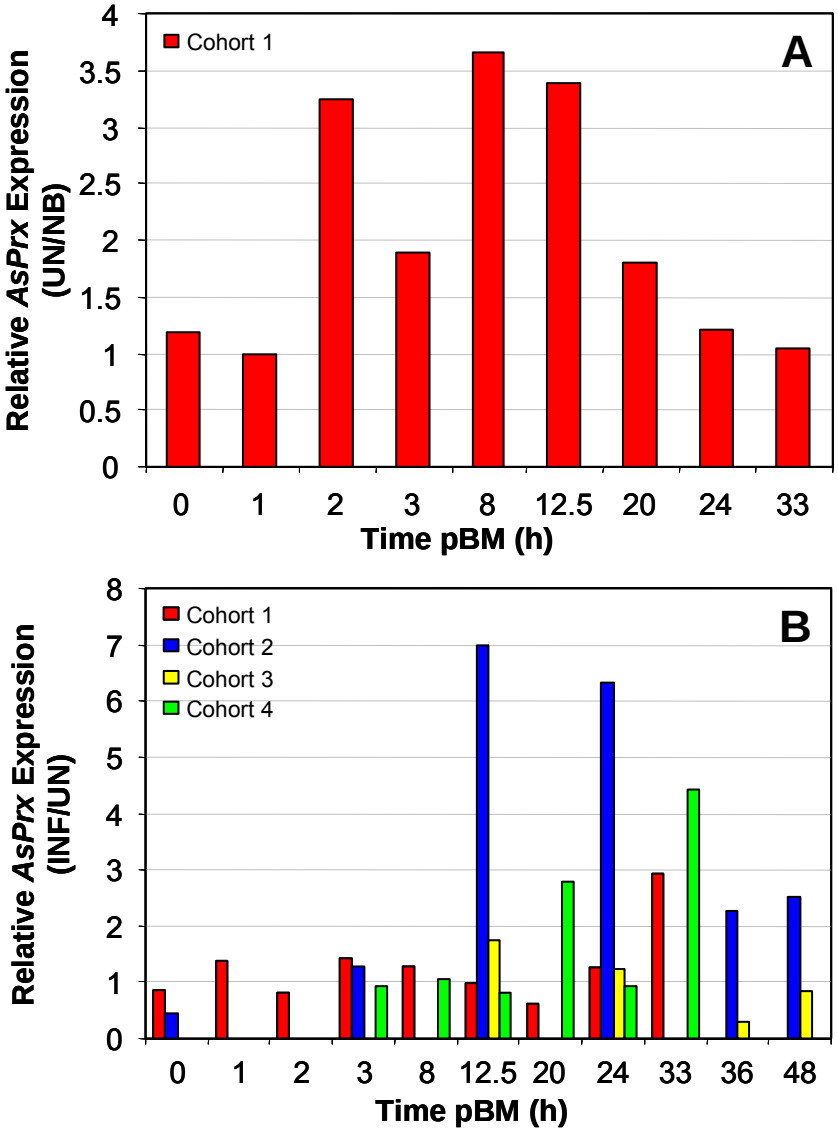

Figure 3-10: Induction of *AsPrx-4783* mRNA in the *A. stephensi* midgut following bloodfeeding.

Quantitative RT-PCR was performed on RNA collected from midguts, carcasses and whole bodies of non-bloodfed (NB) mosquitoes and from the same tissues of mosquitoes following ingestion of an uninfected (UN) or *P. berghei*-infected (INF) blood meal. A single cohort of mosquitoes was used to determine the effects of bloodfeeding alone **(A)**, while four cohorts of mosquitoes with overlapping time points were used to determine the effects of parasite infection on *AsPrx-4783* expression **(B)**. No induction of *AsPrx-4783* was apparent in the carcass or whole body following bloodfeeding or infection (not shown). **(A)** Ingestion of blood induced *AsPrx-4783* expression 1.8-3.7-fold relative to NB midguts at 2-20 h pBM. **(B)** *AsPrx-4783* expression was induced >2-7 fold in *P. berghei*-infected midguts relative to UN midguts at 12.5-48 h pBM.

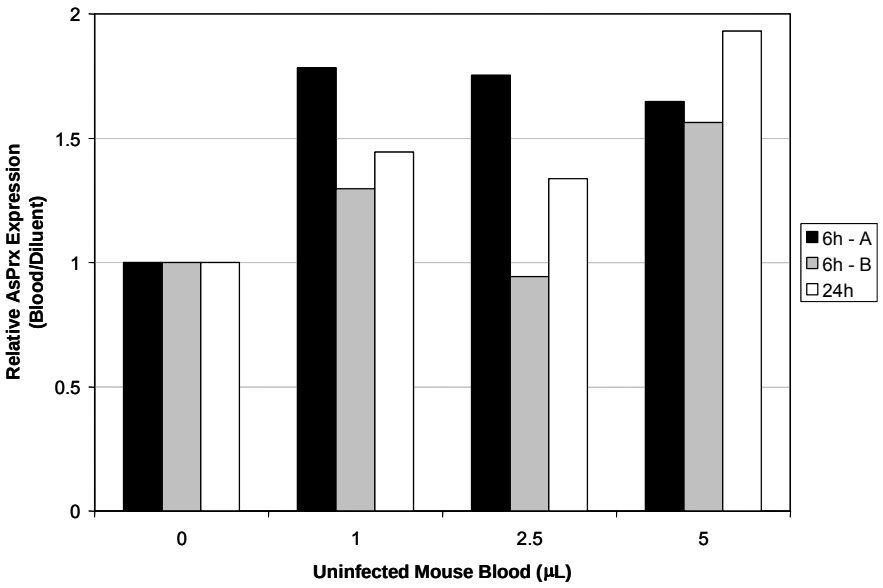

Figure 3-11: Treatment of *A. stephensi* midguts *in vitro* with mouse blood induced expression of *AsPrx-4783* in the dissected tissue.

Midguts were dissected from female *A. stephensi* and maintained in E5 medium at 27°C, 5% CO_2 during all assays. Dissected midguts were treated with 1, 2.5 or 5 µL uninfected mouse blood or equivalent volumes of diluent (PBS, 0 µL mouse blood) for 6 or 24 h. *AsPrx-4783* expression levels for treatments and PBS control samples were normalized to PBS controls; hence, PBS controls are shown here as "1". Inductions of >1.5-fold were observed for all blood treatments, but additional replicates were not completed due to technical problems with the assay.

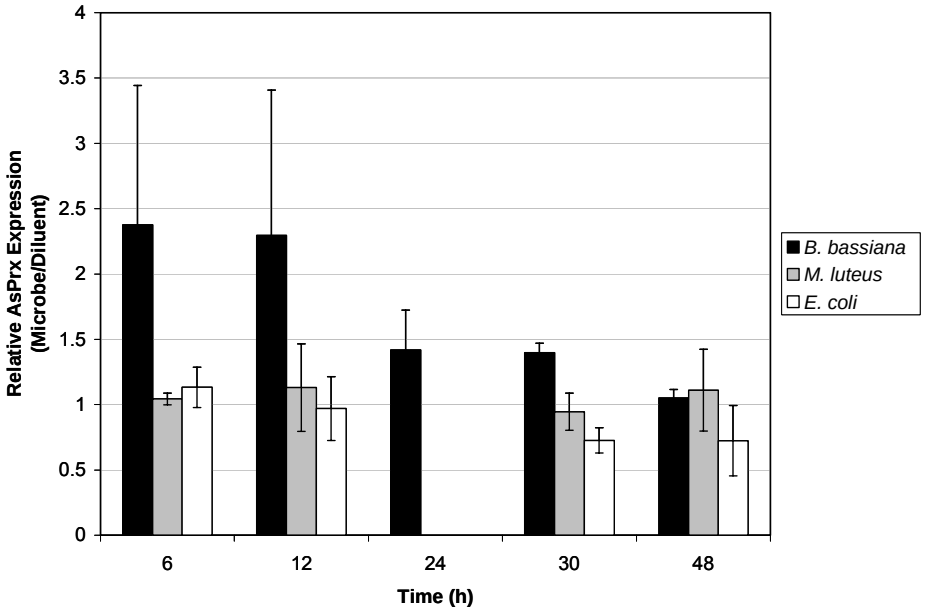

Student's *t* test within a time point (*p* values are shown)

Micrococcus luteus				
	Buffer	**6**	**12**	**30**
6	0.199			
12	0.358	0.405		
30	0.361	0.274	0.319	
48	0.371	0.422	0.483	0.329

Escherichia coli				
	Buffer	**6**	**12**	**30**
6	0.221			
12	0.454	0.303		
30	0.023	0.045	0.203	
48	0.182	0.130	0.268	0.497

Beauveria bassiana					
	Buffer	**6**	**12**	**24**	**30**
6	0.122				
12	0.182	0.482			
24	0.151	0.292	0.263		
30	0.016	0.287	0.252	0.474	
48	0.215	0.131	0.072	0.077	0.015

Figure 3-12: AsPrx-4783 expression in ASE cells treated with heat-killed microbes.

ASE cells (1 x 10^6) were stimulated with heat-killed *M. luteus*, *E. coli*, or *B. bassiana* and *AsPrx-4783* induction was evaluated using quantitative RT-PCR and the comparative C_t method. Values >1.5 are considered to represent induction while values <0.5 are considered to represent repression. Treatment with *B. bassiana* induced AsPrx expression at 6 and 12 h, but high variation in expression levels in the samples precluded statistical significance relative to the buffer controls (p=0.122 and 0.182, respectively). At 30 h, *AsPrx-4783* expression in *B. bassiana*-treated ASE cells was significantly different (p=0.016) from the buffer control, but induction was less than 1.5-fold. Neither induction nor repression of *AsPrx-4783* expression was observed following treatment with *M. luteus*. In response to *E. coli* treatment, *AsPrx-4783* expression was significantly different from the buffer control (p=0.023), but repression was moderate at approximately 0.7-fold.

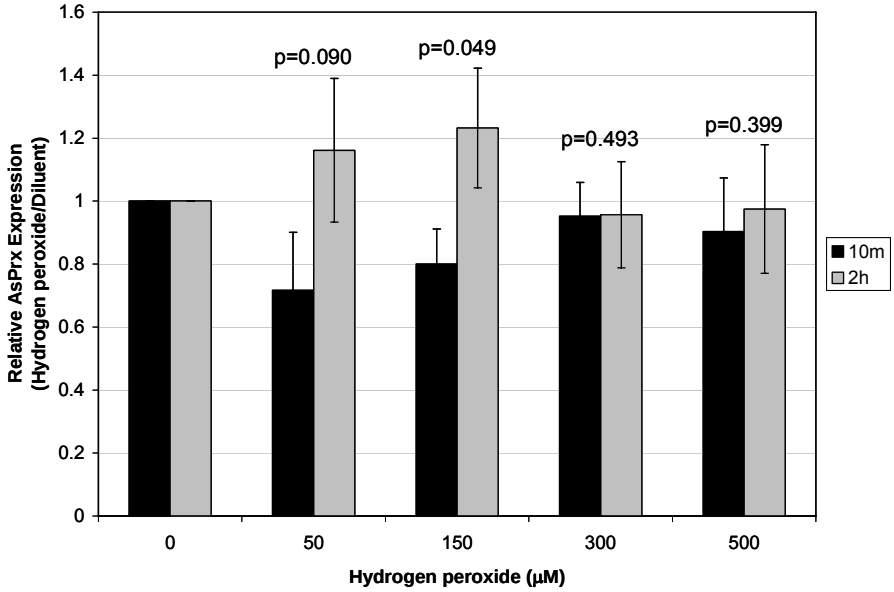

Student's *t* test within a time point (*p* values are shown)

10m stimulations				
	0	**50**	**150**	**300**
50	0.087			
150	0.061	0.355		
300	0.336	0.155	0.180	
500	0.296	0.242	0.314	0.408

2h stimulations				
	0	**50**	**150**	**300**
50	0.253			
150	0.134	0.410		
300	0.402	0.248	0.160	
500	0.453	0.282	0.196	0.473

Figure 3-13: *AsPrx-4783* expression is not induced in ASE cells exposed to H_2O_2 for 10 min or 2 h.

Quantitative RT-PCR was performed on ASE cell RNA collected 10 min and 2 h following exposure of cells to 0, 50, 150, 300 and 500 μM H_2O_2 (n=4). *AsPrx-4783* expression levels were measured relative to expression of the controls (0 μM) which is set at 1 to show relative induction. Values represent means ± standard errors. Neither induction (>1.5) nor repression (<0.5) was observed under these conditions. Data were analyzed using the Student's *t* test. Expression levels relative to controls and between exposure times for each dose were not significantly different from each other with the exception of treatment at 150 μM at 10 min versus 2 h (p=0.049). This difference, however, indicates only a slight induction at the longer treatment time, which is not significantly different from the matched control at 2 h (p=0.134). In addition to the comparisons indicated in the tables, results at 10 m and 2 h after stimulation were compared at each concentration of H_2O_2. These p values are shown above the bars in the figure. Although some significant differences were apparent, expression levels, as already noted did not implicate repression or induction.

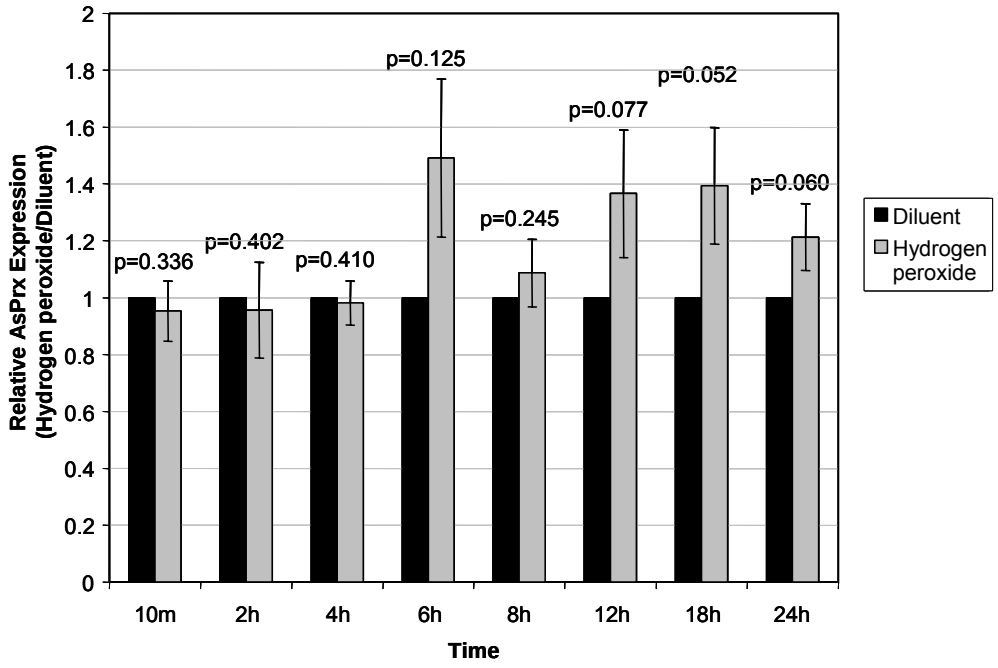

Student's *t* test within a time point (*p* values are shown)

300 µM							
	1/6	**2**	**4**	**6**	**8**	**12**	**18**
2	0.493						
4	0.417	0.448					
6	0.108	0.114	0.118				
8	0.216	0.275	0.242	0.173			
12	0.073	0.097	0.078	0.388	0.156		
18	0.052	0.075	0.055	0.411	0.121	0.465	
24	0.075	0.129	0.075	0.256	0.236	0.284	0.237

Figure 3-14: *AsPrx-4783* expression is not induced in ASE cells exposed to 300 µM H_2O_2 0-24 h.

Quantitative RT-PCR was performed on ASE cell RNA collected from 10 min through 24 h following exposure of the cells 300 µM H_2O_2 or diluent as control (n=4, except 6 h where n=8). *AsPrx-4783* expression levels were measured relative to the expression levels of the controls which are set at 1 to show relative induction. Values represent means ± standard errors. Neither induction (>1.5) nor repression (<0.5) was observed under these conditions. Data were analyzed using the Student's *t* test. There were no significant differences in *AsPrx-4783* expression between treatments and controls (p values indicated above bars) and among treatments at the various time points examined (table).

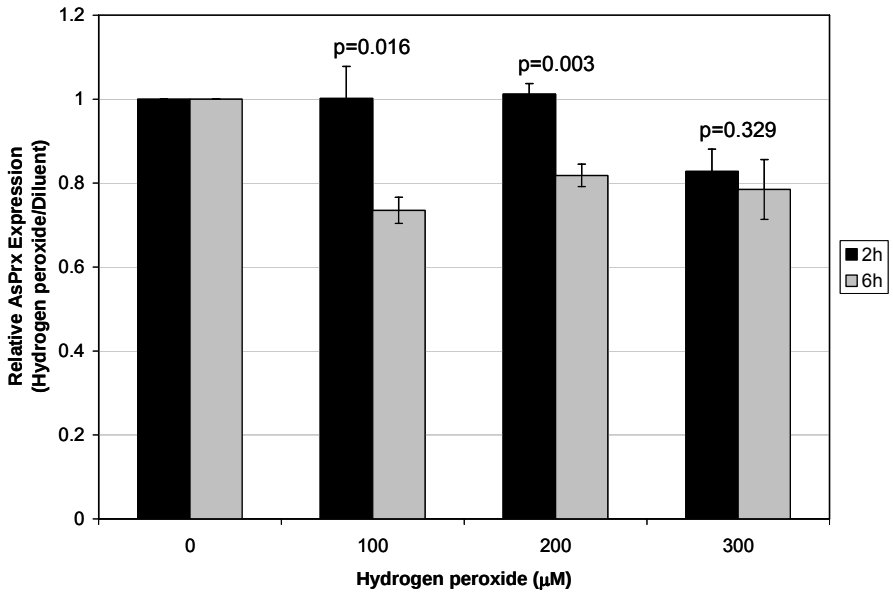

Student's *t* test within a time point (*p* values are shown)

2h stimulations			
	0	**100**	**200**
100	0.491		
200	0.330	0.453	
300	0.016	0.067	0.018

6h stimulations			
	0	**100**	**200**
100	0.001		
200	0.001	0.056	
300	0.020	0.277	0.341

Figure 3-15: Hydrogen peroxide fails to induce *AsPrx-4783* expression in MSQ43 cells.

MSQ43 cells were stimulated with 0, 100, 200, or 300 μM H_2O_2 for 2 or 6 h (n=3). *AsPrx-4783* expression levels were measured relative to controls (0 μM) which are set at 1 to show relative induction. Values represent means ± standard errors. Data were analyzed using the Student's *t* test. Although some significant differences were noted between treatments and matched controls and between exposure times for a single dose, none of the expression levels were >1.5 or <0.5, indicating that AsPrx-4783 is neither induced nor repressed under these conditions. In addition to the comparisons indicated in the tables, results at 2 and 6 h after stimulation were compared at each concentration of H_2O_2. These p values are shown above the bars in the figure. Although some significant differences were apparent, expression levels, as already noted did not implicate repression or induction.

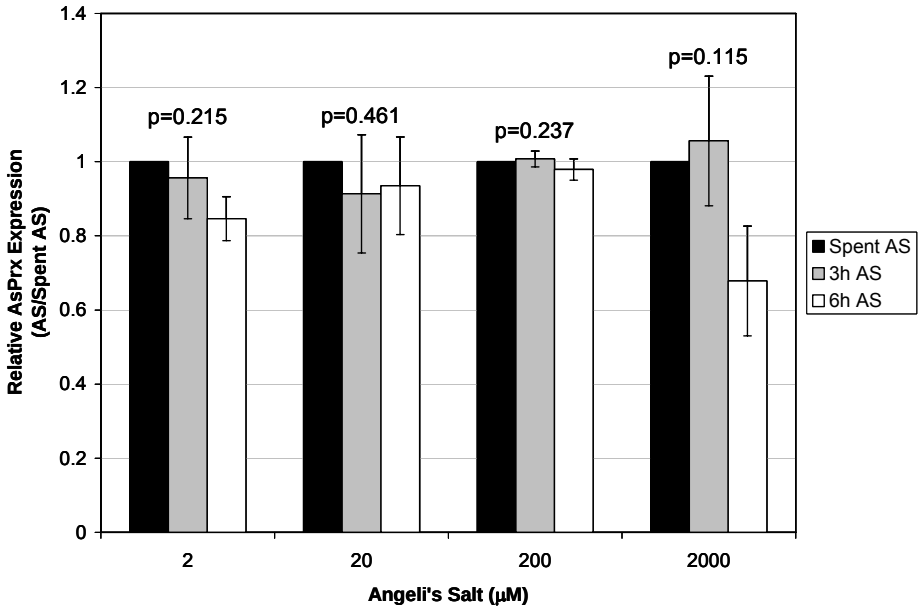

Student's *t* test within a time point (*p* values are shown)

3h stimulations				
	Spent	**2**	**20**	**200**
2	0.355			
20	0.309	0.419		
200	0.373	0.335	0.296	
2000	0.382	0.326	0.290	0.398

6h stimulations				
	Spent	**2**	**20**	**200**
2	0.031			
20	0.325	0.286		
200	0.255	0.058	0.381	
2000	0.031	0.150	0.147	0.041

Figure 3-16: Angeli's salt (AS) fails to induce *AsPrx-4783* expression in ASE cells.

ASE cells were stimulated with 2, 20, 200 or 2,000 μM AS for 3 or 6 h (n=3). *AsPrx-4783* expression levels were measured relative to the expression levels of controls (spent AS) which are set at 1 to show relative induction. Values represent means ± standard errors. Data were analyzed using the Student's *t* test. Although significant differences were noted between some treatments and matched controls, none of the treatment expression levels were >1.5 or <0.5, indicating that *AsPrx-4783* is neither induced nor repressed under these conditions. In addition to the comparisons indicated in the tables, results at 3 and 6 h after stimulation were compared at each concentration of AS. These p values are shown above the bars in the figure. No significant differences were apparent.

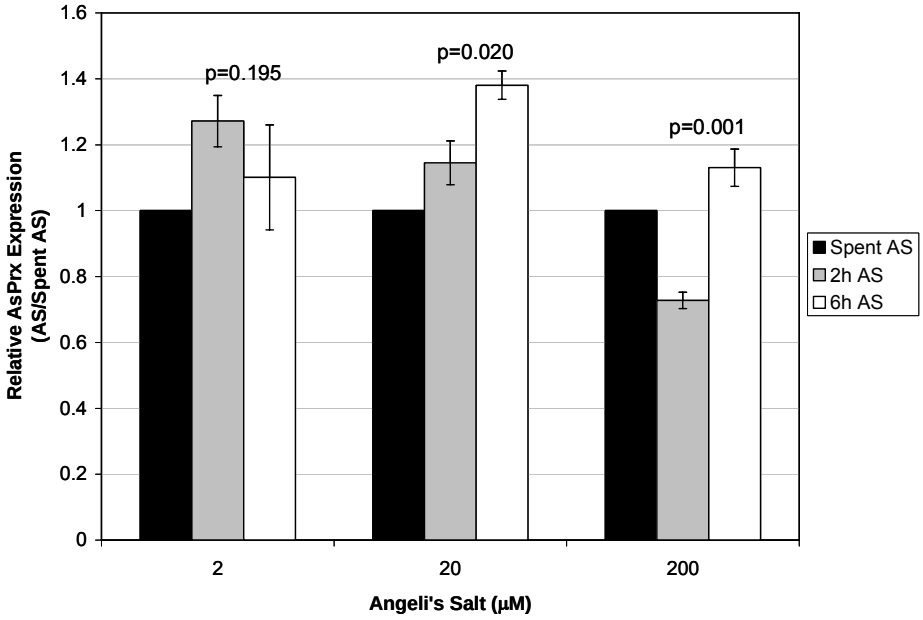

Student's *t* test within a time point (*p* values are shown)

2h stimulations			
	Spent	**2**	**20**
2	0.0126		
20	0.0469	0.1416	
200	0.0002	0.0013	0.0021

6h stimulations			
	Spent	**2**	**20**
2	0.2802		
20	0.0004	0.0826	
200	0.0415	0.4354	0.0122

Figure 3-17: Angeli's salt (AS) fails to induce *AsPrx-4783* expression in MSQ43 cells.

MSQ43 cells were stimulated with 2, 20, or 200 μM AS for 2 or 6 h (n=3). *AsPrx-4783* expression levels were measured relative to the expression levels of controls (spent AS) which are set at 1 to show relative induction. Values represent means ± standard errors. Data were analyzed using the Student's *t* test. Although some significant differences were noted between treatments and matched controls and between exposure times for a single dose, none of the treatment expression levels were >1.5 or <0.5, indicating that *AsPrx-4783* is neither induced nor repressed under these conditions. In addition to the comparisons indicated in the tables, results at 2 and 6 h after stimulation were compared at each concentration of AS. These p values are shown above the bars in the figure. Although some significant differences were apparent, expression levels, as already noted did not implicate repression or induction.

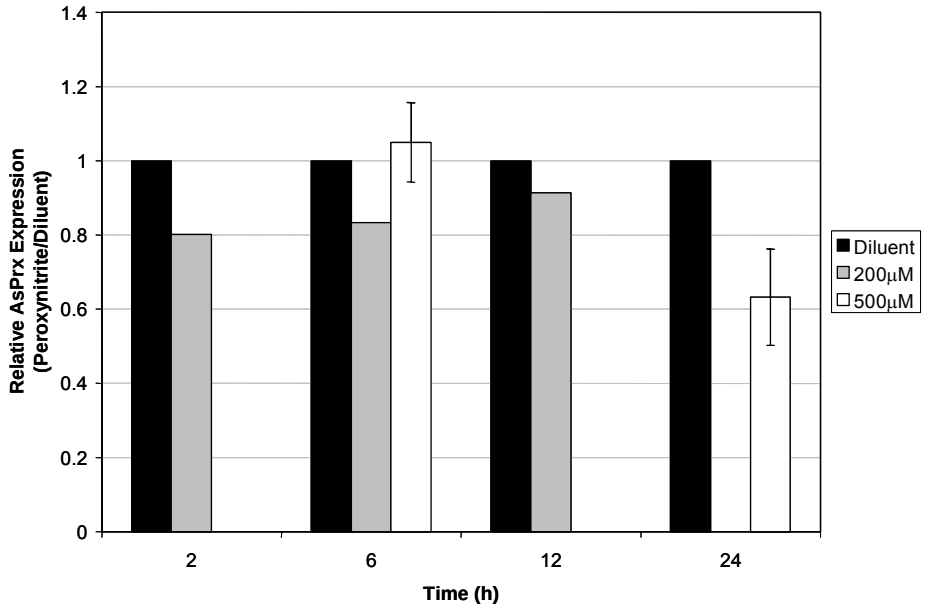

Figure 3-18: *AsPrx-4783* expression is not induced in ASE cells exposed to peroxynitrite (PN).

ASE cell were stimulated with PN at 200 μM (n=1) for 2, 6 or 12 h, and 500 μM (n=2) for 6 or 24 h. *AsPrx-4783* expression was evaluated using qRT-PCR and the comparative C_t method. *AsPrx-4783* expression levels were measured relative to the expression levels of controls (diluent) which are set at 1 to show relative induction. Values represent means; standard errors are provided for replicated assays. Data were analyzed using the Student's *t* test. No significant differences were noted between replicated treatments and controls. Further, expression levels in the treatments were neither induced (values >1.5) nor repressed (values <0.5) relative to the diluent controls.

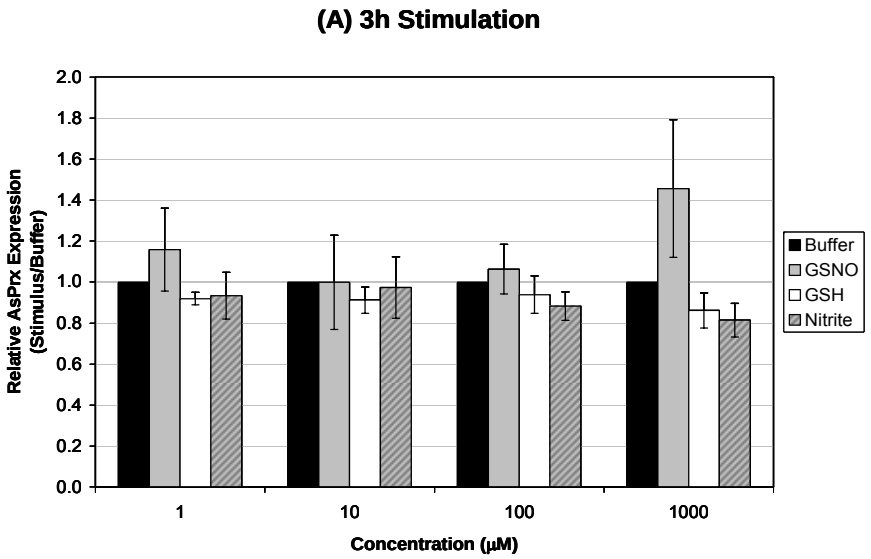

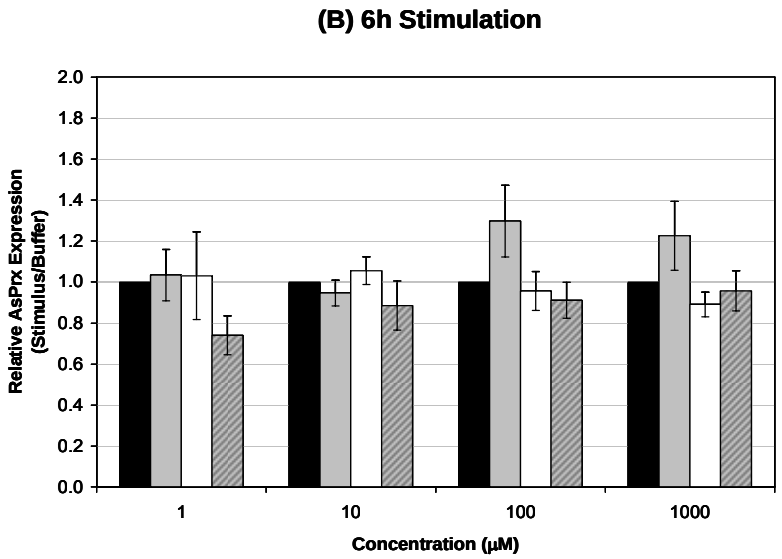

Student's *t* test (*p* values are shown)

3h / 1μM		
	Buffer	**GSNO**
GSNO	0.239	
GSH	0.028	0.154
Nitrite	0.295	0.194

3h / 10μM		
	Buffer	**GSNO**
GSNO	0.498	
GSH	0.121	0.368
Nitrite	0.434	0.465

3h / 100μM		
	Buffer	**GSNO**
GSNO	0.314	
GSH	0.272	0.230
Nitrite	0.084	0.133

3h / 1000μM		
	Buffer	**GSNO**
GSNO	0.123	
GSH	0.091	0.081
Nitrite	0.043	0.068

6h / 1μM		
	Buffer	**GSNO**
GSNO	0.399	
GSH	0.446	0.495
Nitrite	0.026	0.067

6h / 10μM		
	Buffer	**GSNO**
GSNO	0.223	
GSH	0.230	0.153
Nitrite	0.195	0.336

6h / 100μM		
	Buffer	**GSNO**
GSNO	0.082	
GSH	0.334	0.080
Nitrite	0.186	0.060

6h / 1000μM		
	Buffer	**GSNO**
GSNO	0.125	
GSH	0.072	0.067
Nitrite	0.340	0.119

3 vs. 6h				
	1	**10**	**100**	**1000**
GSNO	0.315	0.419	0.166	0.286
GSH	0.317	0.100	0.100	0.396
Nitrite	0.131	0.335	0.335	0.164

(Previous page)

Figure 3-19: *S*-Nitrosoglutathione (GSNO) stimulation for 3 h fails to induce *AsPrx-4783* expression in ASE cells.

ASE cells were stimulated with 1, 10, 100 or 1,000 μM GSNO, GSH or $NaNO_2$ for 3 or 6 h (n=3). *AsPrx-4783* expression levels were measured relative to the controls (an equivalent volume of buffer) which are set at 1 to show relative induction. Values represent means ± standard errors. Data were analyzed using the Student's *t* test. Although some significant differences were noted between treatments and matched controls, none of the treatment expression levels were >1.5 or <0.5, indicating that *AsPrx-4783* is neither induced nor repressed under these conditions.

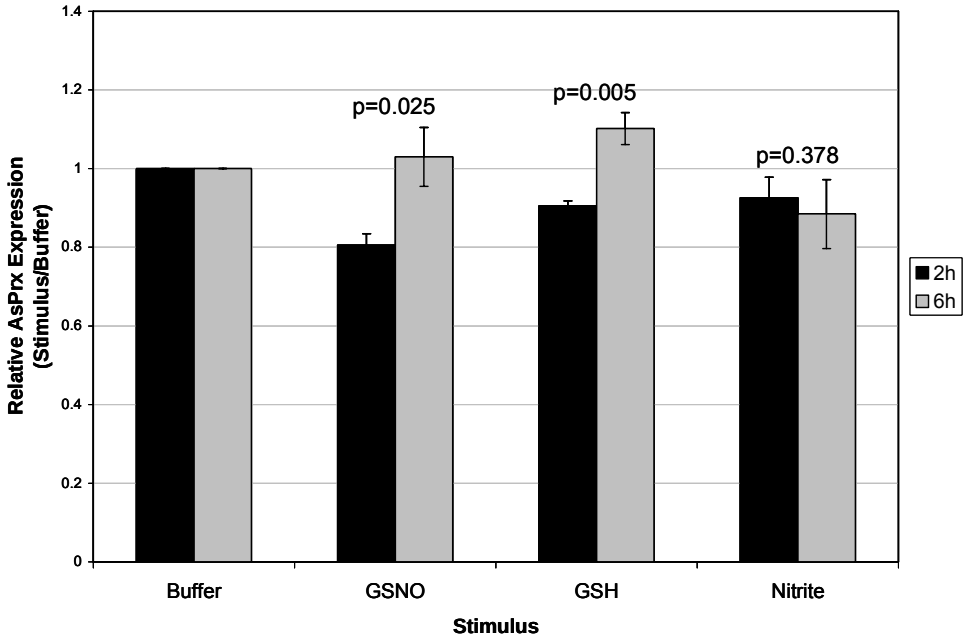

Student's *t* test within a time point (*p* values are shown)

2h stimulations		
	Buffer	**GSNO**
GSNO	0.001	
GSH	0.001	0.017
Nitrite	0.077	0.057

6h stimulations		
	Buffer	**GSNO**
GSNO	0.356	
GSH	0.034	0.223
Nitrite	0.130	0.138

Figure 3-20: *S*-Nitrosoglutathione (GSNO) fails to induce *AsPrx-4783* expression in MSQ43 cells.

MSQ43 cells were stimulated with 50 μM GSNO, GSH or $NaNO_2$ for 2 or 6 h (n=3). *AsPrx-4783* expression levels were measured relative to controls (an equivalent volume of buffer) which are set at 1 to show relative induction. Values represent means ± standard errors. Data were analyzed using the Student's *t* test. Although some significant differences were noted between treatments and matched controls and between exposure times for some treatments, none of the treatment expression levels were >1.5 or <0.5, indicating that *AsPrx-4783* is neither induced nor repressed under these conditions. In addition to the comparisons indicated in the tables, results at 2 and 6 h after stimulation were compared at each concentration of GSNO, GSH, and nitrite. These p values are shown above the bars in the figure. Although some significant differences were apparent, expression levels, as already noted did not implicate repression or induction.

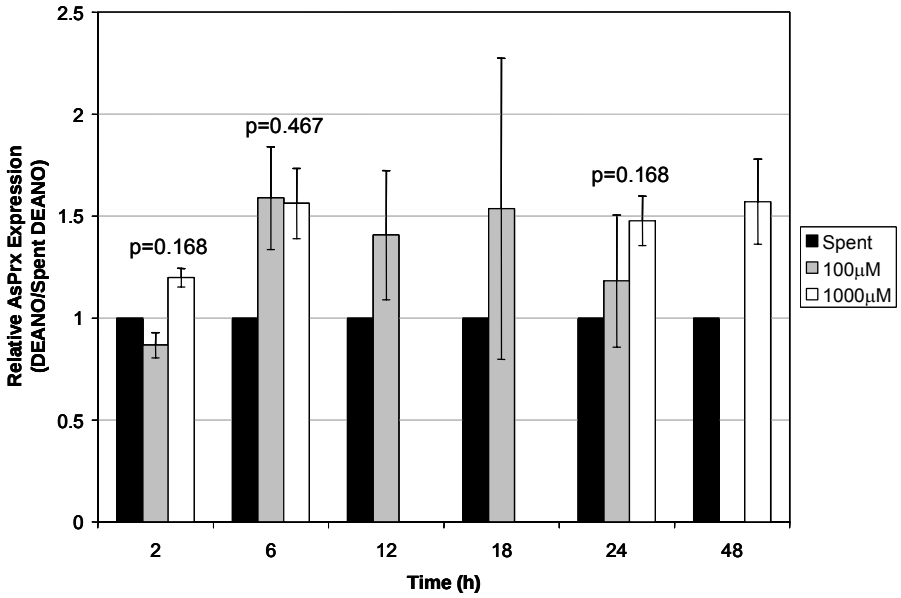

Student's *t* test (*p* values are shown)

100μM stimulations					
	Spent	**2**	**6**	**12**	**18**
2	0.082				
6	0.072	0.054			
12	0.164	0.118	0.348		
18	0.271	0.231	0.476	0.443	
24	0.315	0.220	0.213	0.334	0.352

1000μM stimulations				
	Spent	**2**	**6**	**24**
2	0.024			
6	0.009	0.117		
24	0.004	0.103	0.350	
48	0.010	0.194	0.488	0.372

Figure 3-21: The NO donor DEA-NO may induce *AsPrx-4783* induce in ASE cells.

ASE cells were stimulated with 100 μM (n=2) or 1,000 μM (2 h, n=2; 6 and 24 h, n=4; 48 h, n=6) of the NO donor DEA-NO for 2-48 h. AsPrx-4783 expression levels were measured relative to the controls (spent DEA-NO) which are set at 1 to show relative induction. Values represent means ± standard errors. Data were analyzed using the Student's *t* test. Because of high sample variation, *AsPrx-4783* expression was not significantly induced by treatment with 100 μM DEA-NO. In contrast, treatment with 1,000 μM DEA-NO significantly increased *AsPrx-4783* expression compared to controls at 2, 6, 24 and 48 h, although these expression levels were not significantly different from each other. Based on a >1.5-fold cut-off for induction, treatment with DEA-NO may induce *AsPrx-4783* expression. In addition to the comparisons indicated in the tables, results at 2, 6, and 24 h after stimulation were compared at each concentration of DEA-NO. These p values are shown above the bars in the figure. No significant differences were apparent.

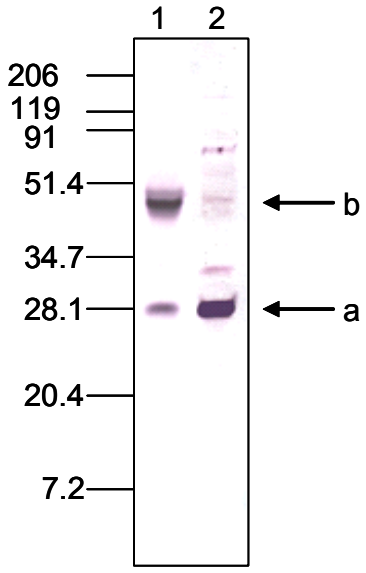

Figure 3-22: Anti-DmPrx-4783 antiserum recognizes proteins of the expected size in lysates of *D. melanogaster*.

Antisera to DmPrx-4783 was kindly provided by Dr. William Orr. To test the antiserum and confirm that 2-Cys Prx forms disulfide-bonded dimers, 20 μg of *D. melanogaster* extract was electrophoretically separated on a 12% Tris-HCl acrylamide gel under non-reducing (lane 1; without DTT) and reducing (lane 2; with DTT) conditions. As expected, DmPrx-4783 was visible predominantly as a dimer (b) with molecular weight ~45kD under non-reducing conditions and as a monomer (a) after treatment with 100 mM DTT. The apparent molecular weight of 28 kD for the monomer is larger than predicted size of ~22 kD. Molecular weight markers (kD) are indicated on the left.

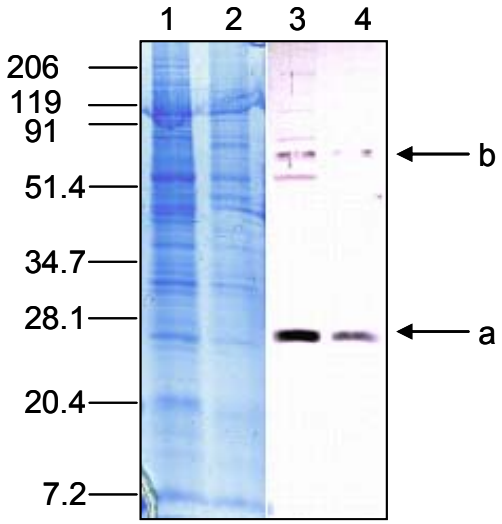

Figure 3-23: Anti-DmPrx-4783 antiserum recognizes proteins of the expected size in lysates of *A. stephensi* cells.

Protein lysates from ASE and MSQ43 cells were boiled in Laemmli's buffer containing DTT. Proteins (15 µL) from ~250,000 ASE cells (lanes 1, 3) or 100,000 MSQ43 (lanes 2, 4) cells were electrophoretically separated on a 12% Tris-HCl acrylamide gel and transferred to membrane with semi-dry blotting. Lanes 1 and 2 are from a Coomassie-stained gel and lanes 3 and 4 are western blot results. A strong cross-reacting band believed to represent the monomer (a) of a single AsPrx isoform had an apparent molecular weight of ~27.5 kD. A second faint band (b) of ~70 kD was also detected. Molecular weight markers (kD) are shown on the left.

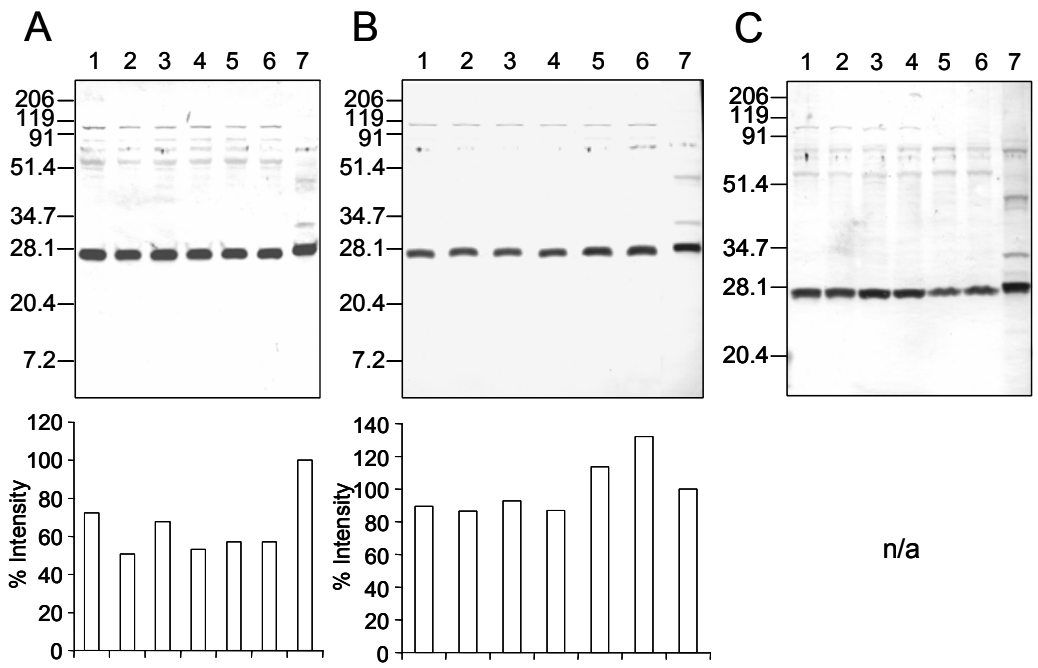

Figure 3-24: AsPrx-4783 protein levels do not appear to change in response to chemical treatment.

Protein lysates were prepared from replicates of 5 x 10^6 ASE cells treated with 200 µM DEA-NO, 200 µM H_2O_2 or 200 µM peroxynitrite. For each treatment, 20 µg proteins were electrophoretically separated on a 12% SDS-PAGE gel and transferred to membrane by semi-dry blotting. Western blots were probed with DmPrx-4783 antisera and detected using the NBT/BCIP colorimetric substrate. Open bars represent relative signal intensities of the most intensely cross-reacting bands (AsPrx-4783) as determined by densitometric analysis. **(A)** ASE cells exposed to DEA-NO (lanes 1, 3, 5) or spent DEA-NO (lanes 2, 4, 6) for 3 h (lanes 1, 2), 6 h (lanes 3, 4) or 18 h (lanes 5, 6). Relative intensities of AsPrx-4783 in the active DEA-NO-treated compared to the spent DEA-NO-treated cells were 1.43 at 3 h, 1.27 at 6 h and 1.00 at 18 h. **(B)** ASE cells were exposed to H_2O_2 (lanes 1, 3, 5) or diluent (lanes 2, 4, 6) for 2 h (lanes 1, 2), 6 h (lanes 3, 4) or 12 h (lanes 5, 6). Relative intensities of AsPrx-4783 in the H_2O_2-treated compared to the diluent-treated cells were 1.03 at 2 h, 1.06 at 6 h and 0.86 at 12 h. **(C)** ASE cells were exposed to peroxynitrite (lanes 1, 3, 5) or diluent (lanes 2, 4, 6) for 2 h (lanes 1, 2), 6 h (lanes 3, 4) or 12 h (lanes 5, 6). Densitometry analysis was not performed. In all blots lane 7 contained 20 µg *D. melanogaster* proteins as a control. Molecular weight markers (kD) are shown on the left of each blot.

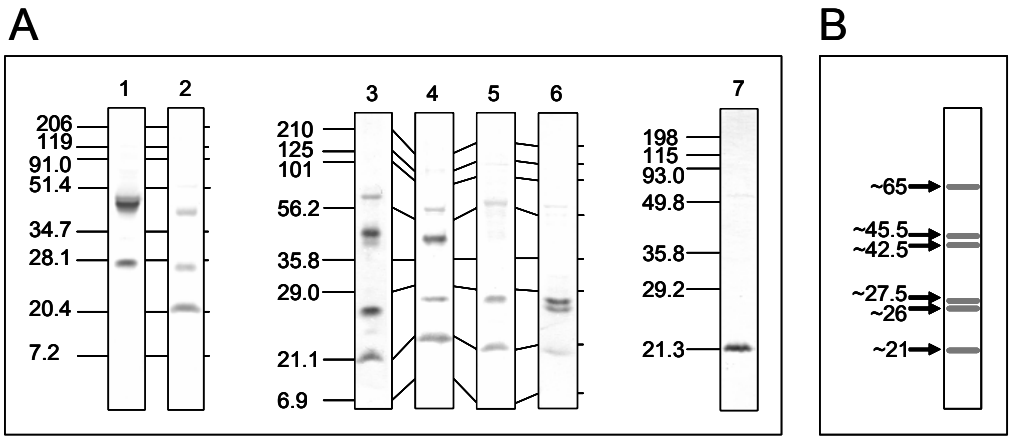

Figure 3-25: Examples of AsPrx-4783 western blots under non-reducing conditions.

Replicates of 5 x 10^6 ASE cells were stimulated with 200 μM H_2O_2, DEA-NO or peroxynitrite. For each treatment, 20 μg protein was electrophoretically separated on 12% Tris-HCl acrylamide gels under non-reducing conditions. Proteins were transferred to membrane by semi-dry blotting. Western blotting was performed using anti-DmPrx-4783 antiserum and BCIP/NBT as the detection substrate. The banding pattern was inconsistent between independent experiments using the same chemical stimulation conditions; examples are shown here to illustrate the cross-reacting protein forms. Panel **(A),** lane 1 *D. melanogaster* fly extract, lane 2 ASE cells treated with DEA-NO for 3 h, lane 3 ASE cells treated with DEA-NO for 6 h, lane 4 ASE cells treated with H_2O_2 for 3 h, lane 5 ASE cells treated with H_2O_2 for 6 h, lane 6 ASE cells treated with peroxynitrite for 3 h, and lane 7 ASE cells treated with peroxynitrite for 6 h. The cross-reacting *D. melanogaster* proteins in lane 1 show the expected monomer and dimer for a 2-Cys Prx. Molecular weight markers (kD) are shown on the left. Panel **(B)** is a cartoon summary of the four cross-reacting *A. stephensi* proteins: ~21 kD "fast migrating", ~27.5 kD monomer with a ~26 kD doublet, ~45 kD dimer with a ~42 kD doublet, and ~65kD "slow migrating."

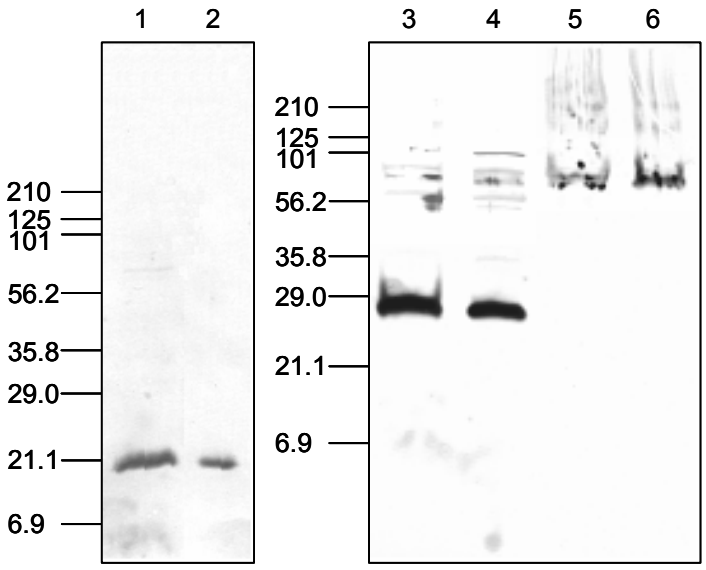

Figure 3-26: Analysis of "fast migrating" AsPrx-4783.

Proteins (20 μg) from ASE cells treated with 200 μM H_2O_2 for 2 h were electrophoretically separated on a 12% Tris-HCl acrylamide gel under non-reducing conditions. Protein samples incubated in Laemmli buffer (lane 1) or Laemmli buffer supplemented with 100 mM DTT (lane 3) or 10% β-mercaptoethanol (lane 4) revealed the expected fast migrating form (lane 1) and the monomer (lanes 3, 4) following anti-DmPrx-4783 western bloting. To resolve the nature of the fast migrating protein, the corresponding band was excised from a duplicate gel and incubated in Laemmli buffer (lane 2) or Laemmli buffer supplemented with 100 mM DTT (lane 5) or 10% β-mercaptoethanol (lane 6) for 30 min. The treated gel samples were loaded into wells of a second 12% Tris-HCl acrylamide gel and immobilized with a thin layer of melted agarose. Following electrophoresis, proteins were transferred from the gel to membrane by semi-dry blotting. Antiserum against DmPrx-4783 was used to probe the blot and detection used the BCIP/NBT substrate. Although the fast migrating band (lane 1) was successfully excised and resolved on a second gel (lane 2), this band was not reduced to the monomer form similar to that of lanes 3 and 4. Instead, the reduced fast migrating band appeared as a doublet of higher molecular weight bands, ~70 and ~80 kD (lanes 5 and 6), which have been observed as weakly cross-reacting bands in the reduced protein lysate. Molecular weight markers (kD) are shown on the left.

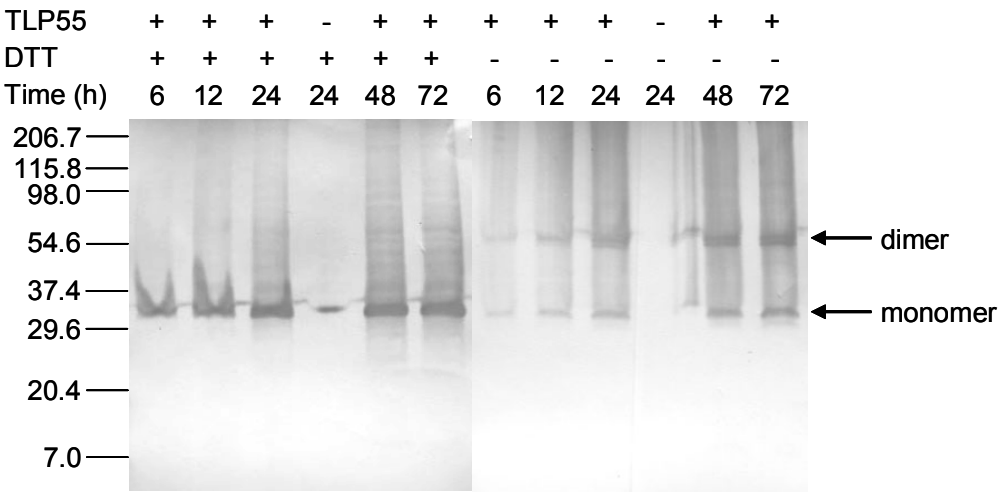

Figure 3-27: Anti-V5 western analysis of AsPrx-4783 overexpression in *D. melanogaster* S2 cells.

S2 cells were collected at various times following mock transfection or transfection with plasmid pTLP55 (TLP55), which encodes AsPrx-4783 under the inducible metallothionein promoter. Crude protein lysates (20 µg per lane) were boiled for 5 min in Laemmli buffer and electrophoretically separated on a 12% SDS-PAGE gel under reducing (with DTT) or non-reducing (without DTT) conditions. The separated proteins were blotted onto Immobilon™-P and probed with antisera to the V5 tag. Proteins with the expected masses of monomer and dimer are indicated. Appreciable protein synthesis occurs at 6 h following $CuSO_4$ induction and continues through at least 72 h following induction. The anti-V5 antibody did not cross-react with proteins in cell extracts prepared from mock-transfected cells (not shown). Molecular weight markers (kD) are shown on the left.

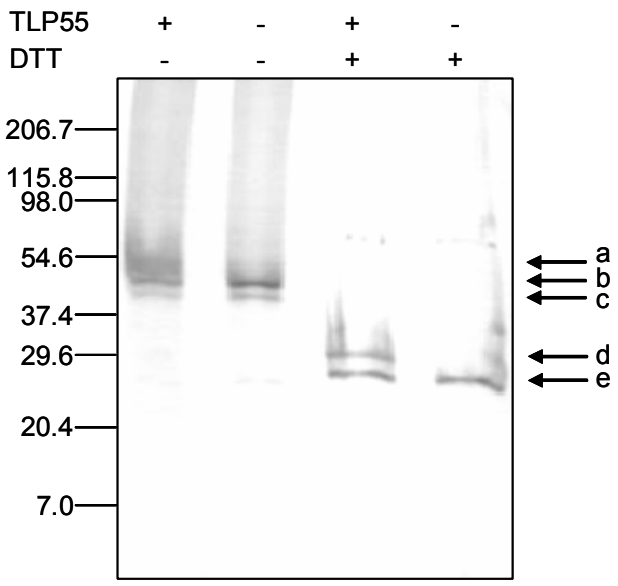

Figure 3-28: Anti-DmPrx-4783 western analysis of AsPrx-4783 overexpression in *D. melanogaster* S2 cells.

Protein was isolated 24 h following $CuSO_4$ treatment of S2 cells that were mock-transfected or transfected with plasmid pTLP55 (TLP55). Crude protein lysates (20 µg per lane) were boiled for 5 min in Laemmli buffer and electrophoretically separated on 12% SDS-PAGE gels under reducing (with DTT) or non-reducing (without DTT) conditions. The separated proteins were transferred to membrane and probed with anti-DmPrx-4783 antisera. The blot shows the presence of possible AsPrx dimers and mixed AsPrx/DmPrx dimers **(a)**, endogenous dimeric DmPrx **(b)**, minor dimeric DmPrx doublet, recombinant monomeric AsPrx **(d)** and endogenous monomeric DmPrx **(e)**. Molecular weight markers (kD) are shown on the left.

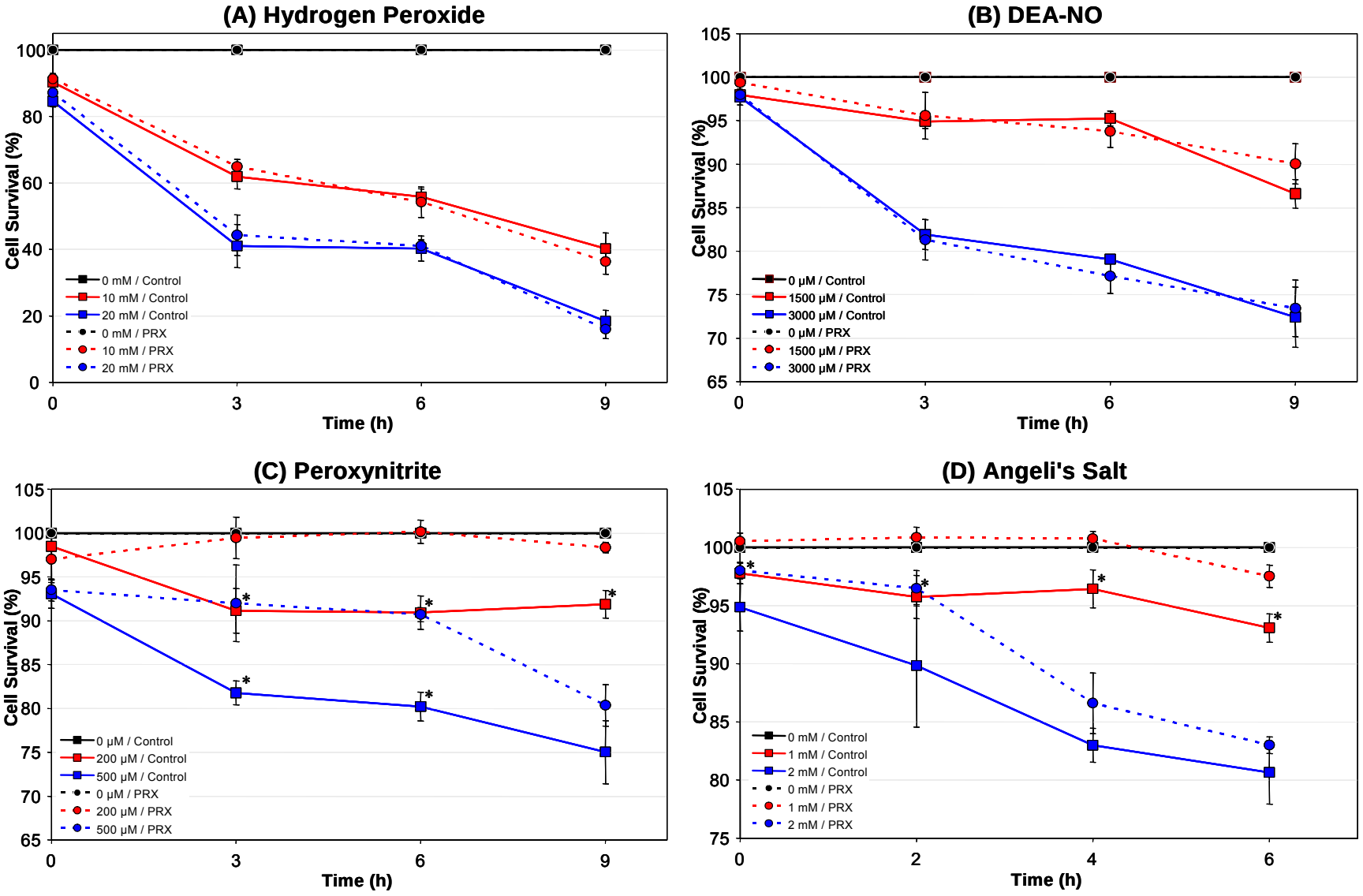
(A) Hydrogen Peroxide
Cell Survival (%)
Time (h)
0 mM / Control
10 mM / Control
20 mM / Control
0 mM / PRX
10 mM / PRX
20 mM / PRX
(B) DEA-NO
Cell Survival (%)
Time (h)
0 µM / Control
1500 µM / Control
3000 µM / Control
0 µM / PRX
1500 µM / PRX
3000 µM / PRX
(C) Peroxynitrite
Cell Survival (%)
Time (h)
0 µM / Control
200 µM / Control
500 µM / Control
0 µM / PRX
200 µM / PRX
500 µM / PRX
(D) Angeli's Salt
Cell Survival (%)
Time (h)
0 mM / Control
1 mM / Control
2 mM / Control
0 mM / PRX
1 mM / PRX
2 mM / PRX

(Previous page)

Figure 3-29: AsPrx-4783 protected transfected *D. melanogaster* S2 cells from RNI-specific cytotoxicity.

Drosophila melanogaster S2 cells were mock transfected (control cells; squares) or transfected with the pTLP55 plasmid containing copper-inducible AsPrx-4783 (PRX cells; circles). Protection due to overexpression of AsPrx-4783 was assessed by the Trypan blue exclusion assay. Cells were challenged with 0, 10, or 20 mM hydrogen peroxide **(A)**, 0, 1500, or 3000 μM DEA-NO **(B)**, 0, 200, or 500 μM peroxynitrite **(C)**, and 0, 1, or 2 mM Angeli's salt **(D)** as described in the materials and methods. Values represent means ± SEM of three independent replicates. Significance versus control is designated as * ($p<0.05$; Student's *t* test). AsPrx-4783 protected S2 cells against treatment with peroxynitrite and Angeli's salt (nitroxyl).

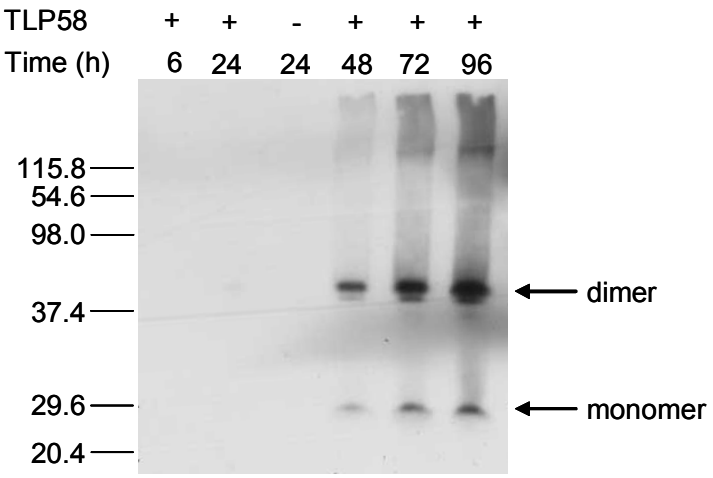

Figure 3-30: Anti-V5 western analysis of AsPrx-4783 overexpression in *A. stephensi* MSQ43 cells.

MSQ43 cells were collected at various times following mock transfection or transfection with plasmid pTLP58 (TLP58) encoding AsPrx-4783 under the constitutive CMV promoter. Crude protein lysates (20 µg per lane) were boiled for 5 min in Laemmli's buffer and electrophoretically separated on a 10% SDS-PAGE gel under non-reducing conditions. The separated proteins were blotted onto membrane and probe with anti-V5 antibody. Proteins with the expected masses of monomer and dimer are indicated. Appreciable protein synthesis occurred 48 h following plasmid transfection. Molecular weight markers (kD) are shown on the left.

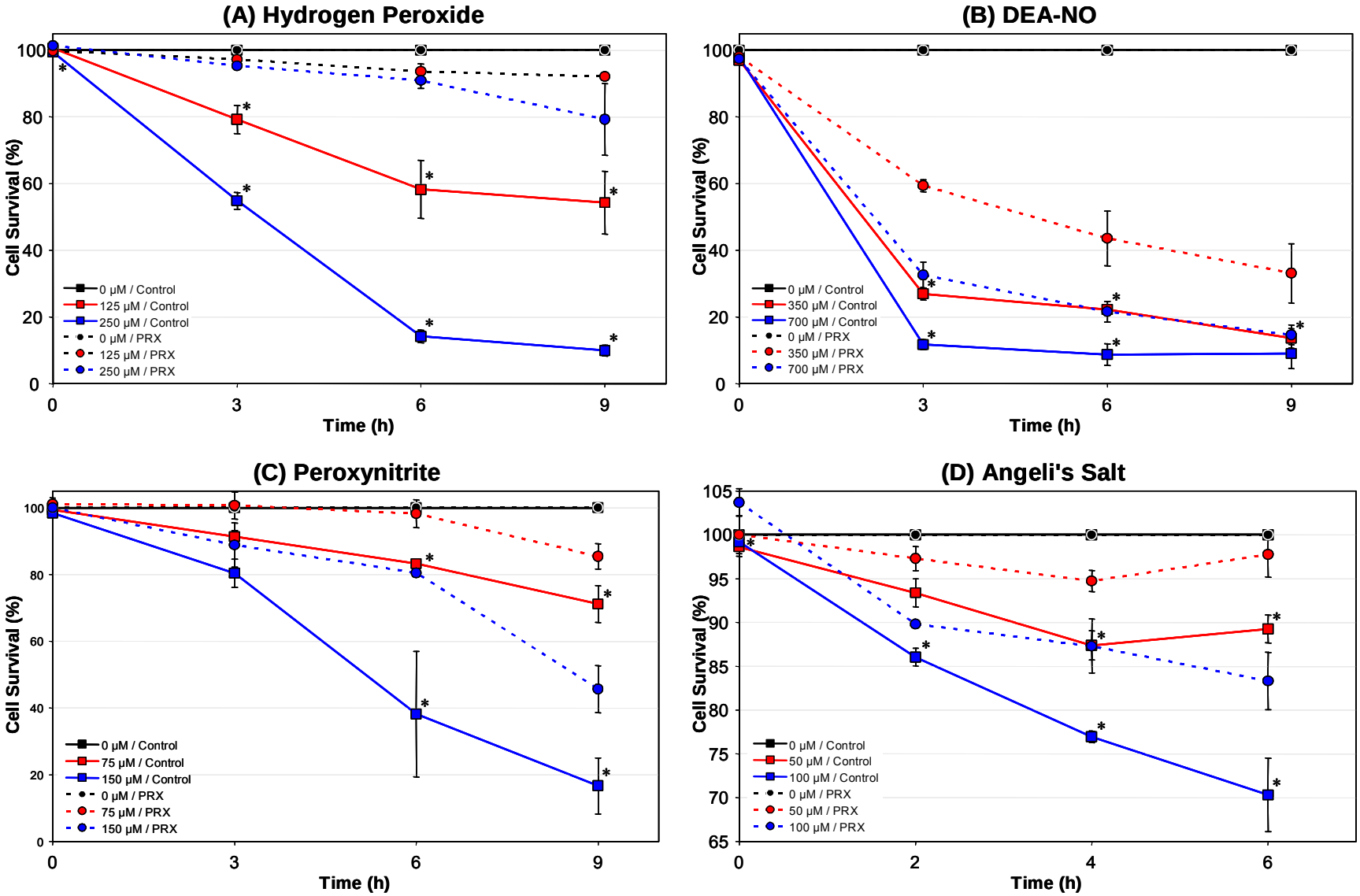
(A) Hydrogen Peroxide
Cell Survival (%)
Time (h)
0 μM / Control
125 μM / Control
250 μM / Control
0 μM / PRX
125 μM / PRX
250 μM / PRX
(B) DEA-NO
Cell Survival (%)
Time (h)
0 μM / Control
350 μM / Control
700 μM / Control
0 μM / PRX
350 μM / PRX
700 μM / PRX
(C) Peroxynitrite
Cell Survival (%)
Time (h)
0 μM / Control
75 μM / Control
150 μM / Control
0 μM / PRX
75 μM / PRX
150 μM / PRX
(D) Angeli's Salt
Cell Survival (%)
Time (h)
0 μM / Control
50 μM / Control
100 μM / Control
0 μM / PRX
50 μM / PRX
100 μM / PRX

(Previous page)

Figure 3-31: Cytotoxicity induced by reactive oxygen and nitrogen species in MSQ43 cells overexpressing AsPrx-4783.

Anopheles stephensi MSQ43 cells were mock transfected without plasmid (control cells; squares) or transfected with the pTLP58 plasmid containing AsPrx-4783 under the constitutive CMV promoter (PRX cells; circles). Protection due to overexpression of AsPrx-4783 was assessed by the Trypan blue exclusion assay. Cells were challenged with 0, 125, or 250 μM hydrogen peroxide **(A)**, 0, 300, or 700 μM DEA-NO **(B)**, 0, 75, or 150 μM peroxynitrite **(C)**, and 0, 50, or 100 μM Angeli's salt **(D)** as described in the materials and methods. Values are the mean ± SEM of the results from three independent replicates. Significance versus control is designated as * ($p<0.05$; Student's *t* test). In MSQ43 cells, AsPrx-4783 overexpression provided a certain degree of protection against all four chemicals.

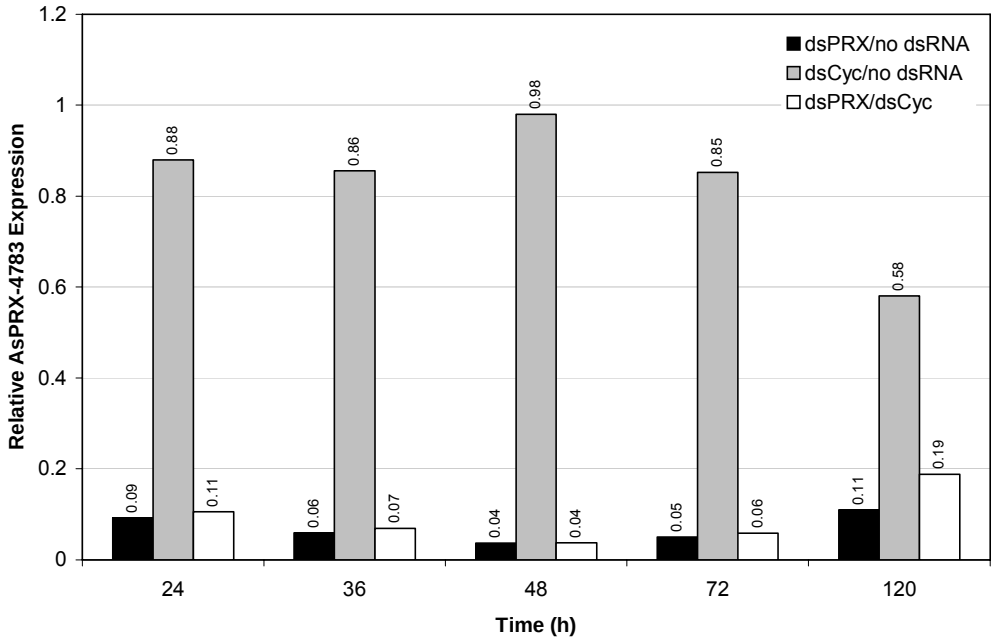

Figure 3-32: Quantitative RT-PCR analysis of the dsRNA-mediated impact on *AsPrx-4783* transcription in MSQ43 cells.

MSQ43 cell cultures were collected 24-120 h following mock transfection (no dsRNA) or transfection with double stranded AsPrx-4783 (dsPRX) or murine cyclophilin (dsCyc). Total RNA was isolated (TRIzol™) and cDNA was synthesized using oligo dT_{16} (Applied Biosystems) for use in 2-step RT-PCR. The relative transcript levels of AsPrx were normalized to AsS7. Relative levels of *AsPrx-4783* shown as normalized ratios in cells transfected with dsPrx or dsCyc; no impact of transfection on AsPrx-4783 would be equivalent to a relative expression level of 1.0. Addition of 400 ng dsPRX resulted in an 81-96% decrease in *AsPrx-4783* transcript levels relative to both dsCyc and no dsRNA controls.

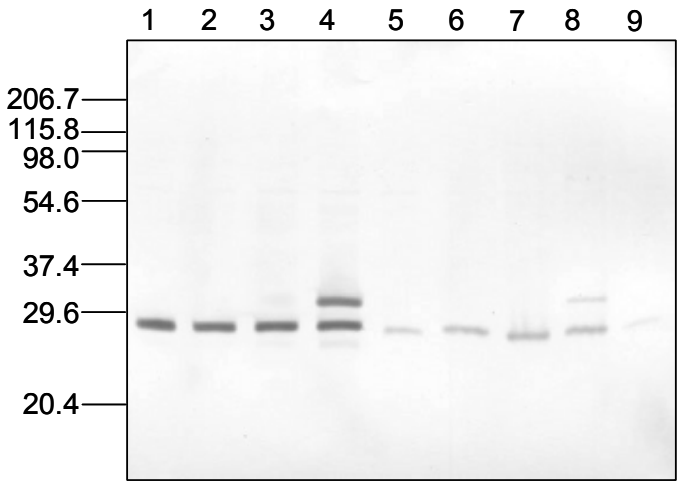

Figure 3-33: Western analysis of AsPrx-4783 expression.

Treatment conditions: (1) untreated S2 cells, (2) S2 cells stimulated with $CuSO_4$ for 24 h, (3) S2 cells mock transfected 48 h and $CuSO_4$ stimulated for 24 h, (4) S2 cells transfected with pTLP55 for 48 h and $CuSO_4$ stimulated for 24 h, (5) untreated ASE cells, (6) untreated MSQ43 cells, (7) MSQ43 cells mock transfected for 48 h, (8) MSQ43 cells transfected with pTLP58 for 48 h, and (9) MSQ43 cells transfected with dsPRX for 48 h. Crude protein lysate (10 μg) was boiled for 5 min in Laemmli buffer and subjected to 12% SDS-PAGE under reducing conditions (DTT). The separated proteins were blotted onto Immobilon™-P and incubated with rabbit DmPrx-4783 antisera. Molecular weight markers in kD are shown on the left.

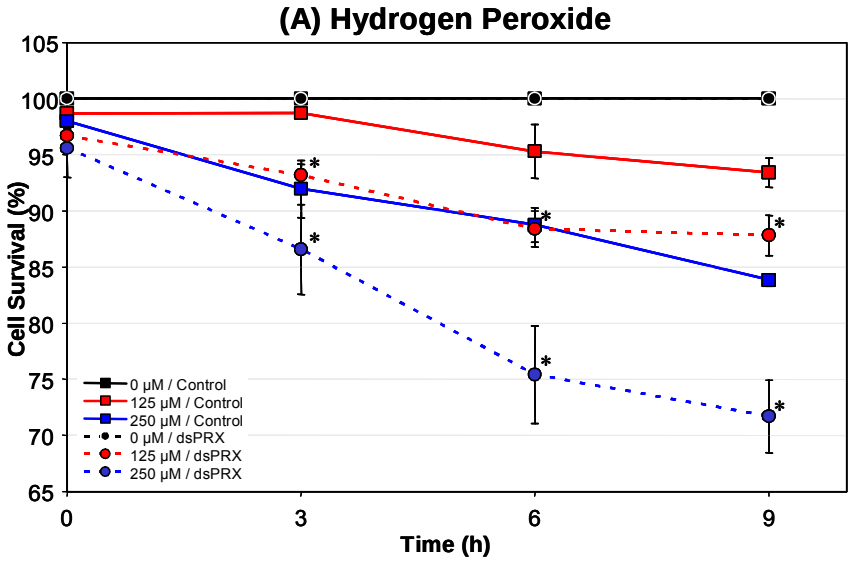
(A) Hydrogen Peroxide
Cell Survival (%)
Time (h)
0 μM / Control
125 μM / Control
250 μM / Control
0 μM / dsPRX
125 μM / dsPRX
250 μM / dsPRX

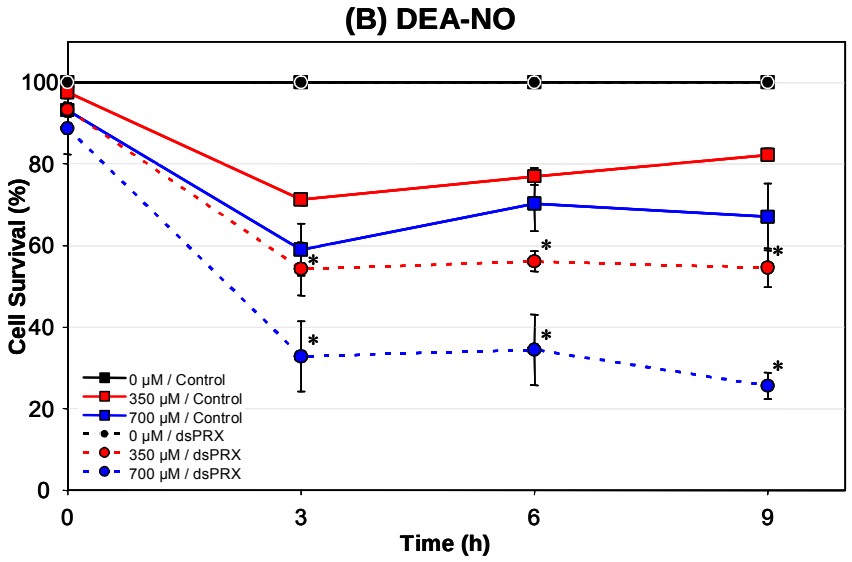
(B) DEA-NO
Cell Survival (%)
Time (h)
0 μM / Control
350 μM / Control
700 μM / Control
0 μM / dsPRX
350 μM / dsPRX
700 μM / dsPRX

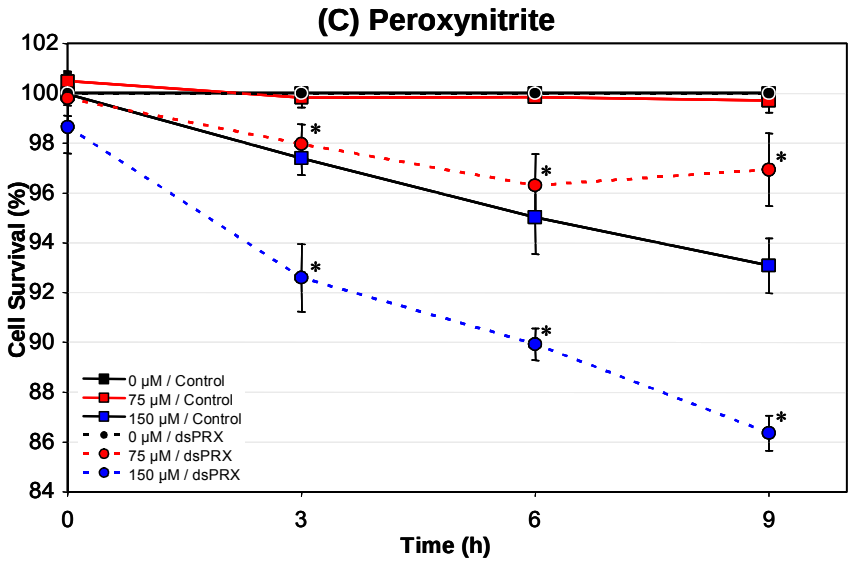
(C) Peroxynitrite
Cell Survival (%)
Time (h)
0 μM / Control
75 μM / Control
150 μM / Control
0 μM / dsPRX
75 μM / dsPRX
150 μM / dsPRX

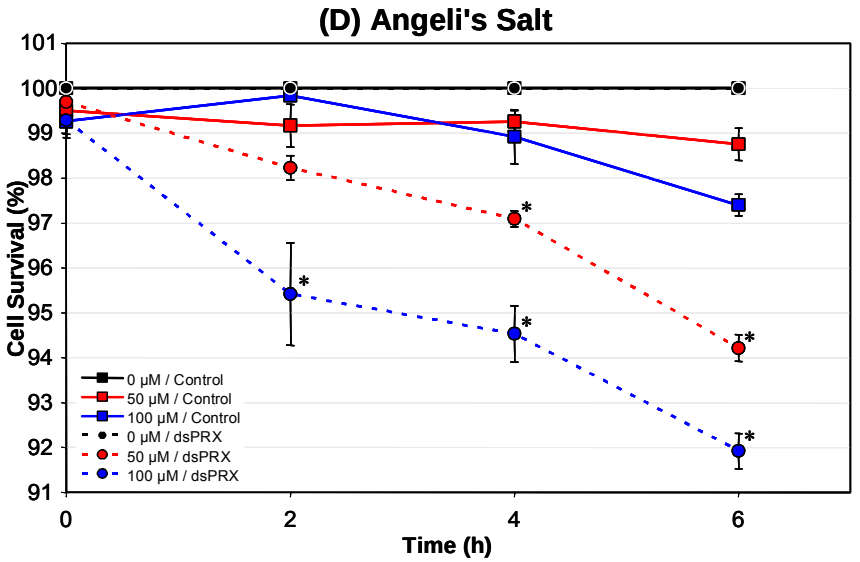
(D) Angeli's Salt
Cell Survival (%)
Time (h)
0 μM / Control
50 μM / Control
100 μM / Control
0 μM / dsPRX
50 μM / dsPRX
100 μM / dsPRX

(Previous page)

Figure 3-34: Viability of MSQ43 cells following RNAi and exposure to reactive oxygen and nitrogen species.

Anopheles stephensi MSQ43 were mock transfected (control) or transfected with double stranded AsPrx-4783 RNA (dsPRX). Following transfection, cells were challenged with 0, 125, or 250 μM hydrogen peroxide **(A)**, 0, 300, or 700 μM DEA-NO **(B)**, 0, 75, or 150 μM peroxynitrite **(C)**, and 0, 50, or 100 μM Angeli's salt **(D)** as described in the Materials and Methods. Cell viability was assessed by the Trypan blue exclusion assay. Values represent means ± SEM from three independent replicates. Significance versus control is designated as * ($p<0.05$; Student's *t* test). In MSQ43 cells, AsPrx-4783 RNAi increased cell mortality in response to all reactive oxygen and nitrogen species tested relative to the controls.

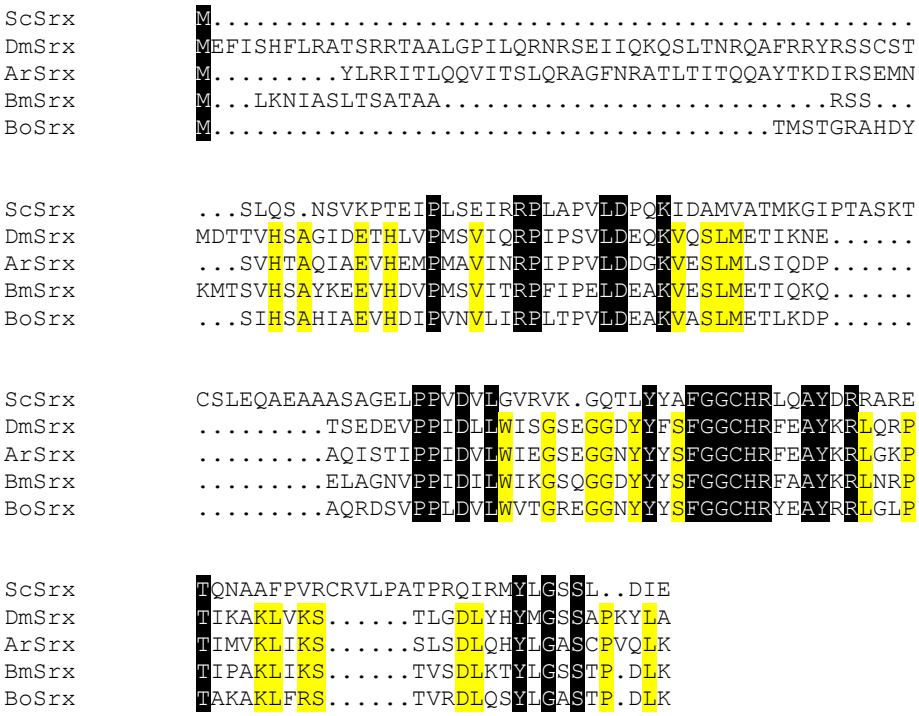

Figure 3-35: Alignment of predicted arthropod sulfiredoxins with the yeast orthologs.

Yeast sulfiredoxin (Srx) can reverse cysteine hyperoxidation and, hence, inactivation of 2-Cys Prx **[697]**. BLAST analysis identified homologs of yeast Srx in several arthropods. Those amino acids which are conserved in arthropods are highlighted in yellow, while those conserved between arthropods and yeast are highlighted in black. Abbreviations are as follows, Sc (*Saccharomyces cerevisiae*, yeast; NC_001143), Dm (*Drosophila melanogaster*, fruit fly; NM_133022), Ar (*Armigeres subalbatus*, culicine mosquito; AY439474), Bm (*Bombyx mori*, silkworm moth; CK524466), and Bo (*Boophilus microplus*, southern cattle tick; CK190551).

First region of similar sequence:

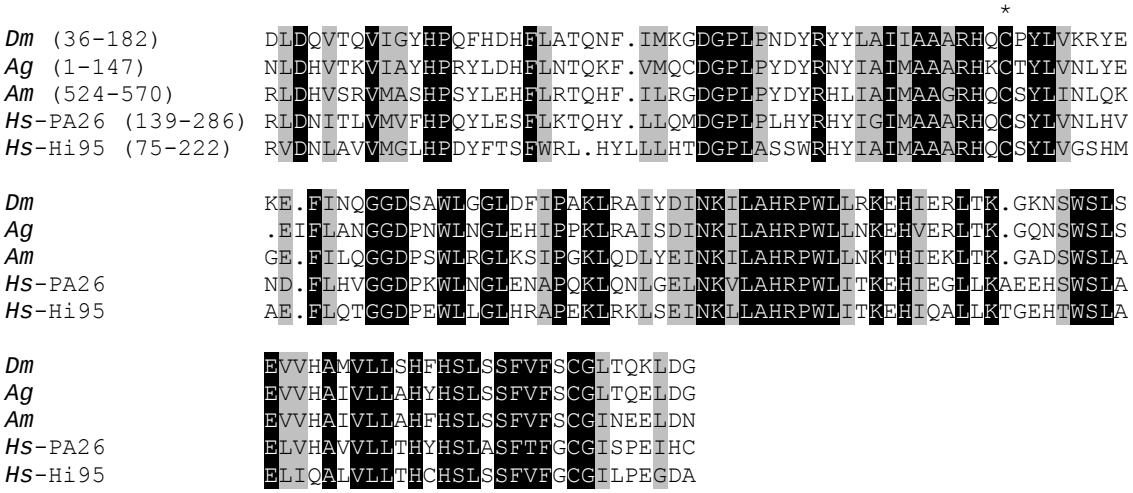

Second region of similar sequence:

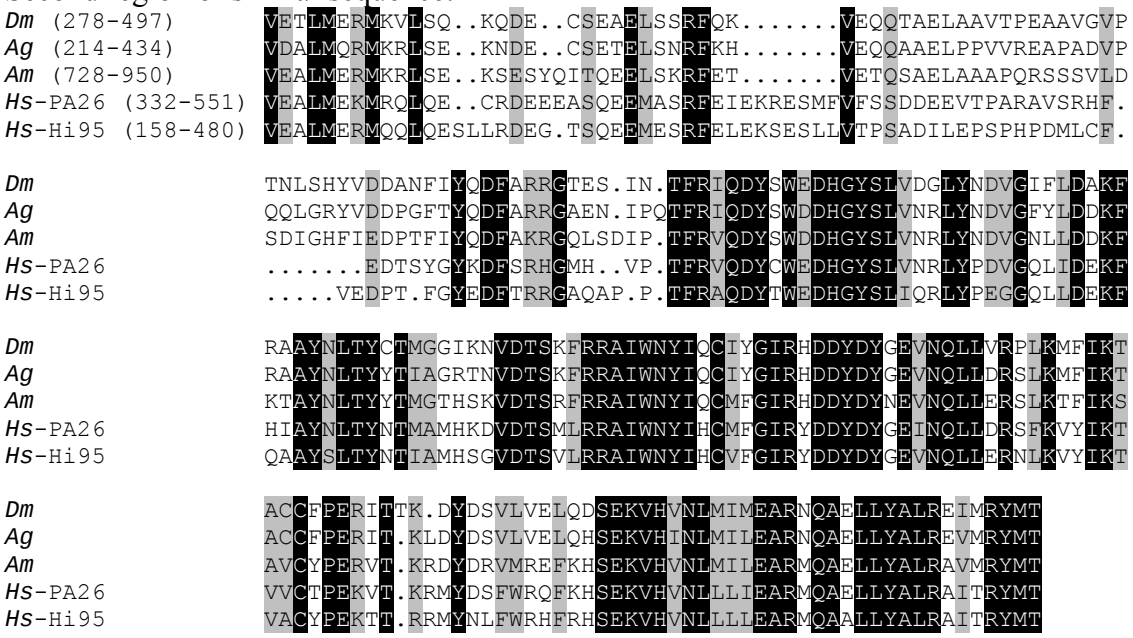

(Previous page)
Figure 3-36: Multiple alignment of sestrins.

Sestrins share sequence similarity to AhpD, an enzyme which catalyzes the reduction of AhpC in bacteria **[306, 319, 702]**. The sestrins increase the rate of recovery of the inactivated, hyperoxidized Prxs **[701].** This alignment was constructed using DNAMAN. Amino acid residues conserved in the aligned sequences are shaded black for identity and grey for similarity). Similar amino acids are grouped by presence of nonpolar side chains (G, A, V, L, I, P, F, M, W, C), uncharged polar side chains (N, Q, S, T, Y), acidic side chains (D, E), and basic side chains (K, R, H). The Cys conserved in sestrin and AhpD sequences is denoted by an asterisk. Values in parentheses indicate amino acid locations of the aligned proteins. The alignment was split into two sections since the middle regions of the proteins are highly divergent. *Dm* (*Drosophila melanogaster*; Q9W1K5), *Ag* (*Anopheles gambiae*; XM_308599), *Am* (*Apis mellifera*; XM_394521), *Hs*-PA26 (*Homo sapiens*; NP_055269), *Hs*-Hi95 (*Homo sapiens*; NP_113647).

Table 3-1: Alternate names for peroxiredoxins.

Typical 2-Cys Prx

Bacterial 2-Cys peroxiredoxin
- alkyl hydroperoxidase C (AhpC)
- alkyl hydroperoxide peroxidase C (AhpC)
- alkyl hydroperoxide reductase C (AhpC)
- c22 component of alkyl hydroperoxide reductase (c22) **[570]**

basiplast 1 (BAS) **[634]**

Prx1/PrxI/PrdxI:
- heme-binding protein 23 (HBP23) **[610]**
- macrophage stress protein 23 kD (MSP23) **[741]**
- natural killer enhancing factor (NKEFA) **[742]**
- osteoblast-specific factor 3 (OSF-3) **[743]**
- proliferation-associated gene product (PAG) **[744]**
- thioredoxin peroxidase 2 (TPx II) **[671]**

Prx2/PrxII/PrdxII:
- band 8 protein **[560]**
- calpromotin **[685]**
- natural killer enhancing factor B (NKEFB) **[742]**
- protector protein (PRP) **[745]**
- thiol specific antioxidant (TSA) **[746]**
- thioredoxin peroxidase 1 (TPxI) **[671]**
- thioredoxin peroxidase B (TPx-B) **[747]**
- torin **[549]**

Prx3/PrxIII/PrdxIII:
- antioxidant protein 1 (AOP1) **[748]**
- *Drosophila* Prx-5037 (Dpx-5037) **[589]**
- mitochondrial thioredoxin dependent peroxide reductase precursor
- mouse erythroleukemic gene 5 protein (MER5) **[749]**
- substrate protein 22kD (SP22) **[750]**

Prx4/PrxIV/PrdxIV:
- antioxidant enzyme 37-2 (AOE372) **[677]**
- thioredoxin peroxidase-related activator of NF-kappa B and c-Jun N-terminal kinase (TRANK) **[730]**

Atypical 2-Cys Prx*

Bacterial thiol peroxidase (TPx) **[751]**
- 20 kD protein (p20) **[752]**
- scavengase **[753]**

Prx5/PrxV
- Alu co-suppressor protein 1 (ACR1) **[754]**
- antioxidant enzyme AOEB166 (AOEB166) **[573]**
- peroxisomal membrane protein 20 (PMP20) **[575]**

Type II Prx **[606]**

yeast alkyl hydroperoxidase 1 (yeast Ahp1) **[678, 755, 756]**

1-Cys Prx:

Drosophila Prx-2540 (Dpx-2540) **[589]**

Drosophila Prx-6005 (Dpx-6005) **[589]**

Prx6/PrxVI:
- acidic calcium-independent phospholipase A2 (aiPLA2) **[757]**
- antioxidant protein 2 (AOP2) **[758]**
- Clara cell 26-kDA protein (CC26) **[759]**
- keratinocyte growth factor-regulated gene 1 (KRG-1) **[760]**
- liver 20,000-30,000 molecular weight protein 4 (LTW4) **[761]**
- non-selenium glutathione peroxidase (NSGPx) **[585]**
- open reading frame 06 protein (ORF06) **[583]**

peroxiredoxin 1 (PER1) **[762]**

Arabidopsis 1-Cys Prx (1CP-prx) **[633]**

Bacterioferritin Co-migratory Protein (BCP)

Peroxiredoxin Q (Prx-Q) **[577]**

disrupter of telomeric silencing (DOT5) **[755]**

* In some older literature these atypical 2-Cys were mislabeled as 1-Cys Prx.

Table 3-2: Comparison between *Anopheles gambiae* and *Drosophila melanogaster Prx* sequences.

	Prx Name					
	4783	**5037**	**4156**	**2540**	**6005**	**V**
D. melanogaster sequence characteristics	2-Cys cystolic 0 introns 22.0 kD pI = 5.52	2-Cys mitochondrial 3 introns 26.3 kD pI = 7.01	2-Cys secretable 3 introns 26.7 kD pI = 6.31	1-Cys cytosolic 3 introns 24.8 kD pI = 5.96	1-Cys cytosolic 2 introns 24.8 kD pI =5.19	Atypical 2-Cys n/a 2 introns 19.9 kD pI = 8.88
A. gambiae sequence	AAAB01008804 (84651-84061)	AAAB01008846 (4068809-4067923)	AAAB01008807 (1925781-1924853)	AAAB01008986 (8101720-8102725)	AAAB01008807 (8364093-8364766)	AAAB01008987 (13214667-13214089)
A. gambiae sequence characteristics	0 introns Chromosome 3 22.0 kD pI = 5.61	2 introns Chromosome X 26.1 kD pI = 8.75	2 introns Chromosome 2 28.8 kD pI = 5.98	4 introns Chromosome 3 25.2 kD pI = 5.25	0 introns Chromosome 2 24.4 kD pI = 5.21	0 introns Chromosome 2 20.5 kD pI = 5.90
A. gambiae % identity (amino acid / nucleotide)	79.1 / 78.0	66.8 / 68.0	68.4 / 65.3	74.9 / 68.9	67.3 / 65.1	79.1 / 64.4

Sequences and characteristics for *D. melanogaster* DmPrx-4783, -5037, -4157, -2540, and -6005 were provided by Dr. Orr's lab **[589]**. The sequence for DmPrxV was first identified by Verdoucq *et al.* **[603]**. *Anopheles gambiae* Prx sequences were identified from BLAST searches of the available scaffold sequences using the DmPrx sequences as queries. Sequences are listed by scaffold number with the ORF on the scaffold, in bp, in parentheses. Sequences include stop codons. Molecular weights and pIs of the deduced amino acid sequences of the AgPrx and DmPrxV nucleotide sequences were determined using the calculator at http://scansite.mit.edu.

CHAPTER FOUR: Summary and conclusions

From the data presented herein, I conclude that *P. berghei* infection in *A. stephensi* induces the synthesis of RNIs in the midgut above that observed in control mosquitoes provided with an uninfected blood meal. These RNIs include nitrates, higher oxides of nitrogen (predicted to be PN and NO^-) and a photolyzable $^{\bullet}NO$ adduct (inferred to be iron nitrosyl derived from Hb). Tyrosine nitration at 24 h pBM is greater in tissues of infected mosquitoes compared to tissues of uninfected mosquitoes presumably as the result of elevated PN levels.

Previous studies showed that inhibition of AsNOS through dietary supplementation of the enzyme inhibitor L-NAME increased the number of parasites developing to the oocyst stage. Based on this observation, I hypothesized that RNIs derived from $^{\bullet}NO$ are directly toxic to the parasite and, therefore, limit development in the mosquito. Low concentrations of $^{\bullet}NO$ are typically associated with direct effects on protein targets, including those associated with signaling **[120]**. At higher concentrations, $^{\bullet}NO$ reacts with $O_2^{\bullet-}$ or O_2 to yield redox species which induce oxidative and nitrosative stress **[120]**. In the mosquito midgut, $^{\bullet}NO$ could function to signal the synthesis of secondary compounds that might be toxic to the parasite, but the high concentrations of RNIs in the midgut suggest that $^{\bullet}NO$ synthesis is predominantly associated with indirect cytotoxic effects that are characteristic of inflammation **[83-85, 334]**. Thus. I have concluded that the RNIs generated are directly toxic to the parasite.

PN and NO^- and PN are strongly reactive and can oxidize lipids and proteins, nitrosylate metals, induce DNA strand breaks and base oxidation **[129, 130, 142, 144-148, 465]**, deaminate DNA, oxidize sugars, and significantly alter protein activity through nitration (reviewed in **[153, 159, 162, 177, 341, 466-469]**). Both NO^- and PN can induce apoptosis **[147, 177, 467, 616, 763]**, a process that appears to limit the number of developing zygotes and ookinetes of *P. berghei* in *A. stephensi* **[329]**. Further, parasite apoptosis has been linked to $^{\bullet}NO$ synthesis. Specifically, provision of L-NAME to an infective blood meal significantly decreased the number of *P. berghei* ookinetes undergoing apoptosis **[329]**. Thus PN and NO^- may promote parasite reduction through induction of apoptosis.

Alternatively, •NO/RNIs may affect parasite development by inhibiting the function of critical enzyme(s). The catalytic activity of proteolytic enzymes can be altered by modification of reactive residues (*e.g.* Cys → SNO, Tyr → NTYR) or by binding of •NO to metal centers (metal nitrosyl) **[764]**. Although •NO/RNIs can kill *Plasmodium* spp., the toxic mechanism(s) are largely unknown. To date, most studies have focused on the modification of cysteine proteases, such as falcipain. Chemical NO donors (GSNO, NOR-3, SIN-1, SNP, SNAP and SNO-102) dose-dependently inactivate *P. falciparum* falcipain activity through *S*-nitrosation of Cys^{25}, although additional chemical modifications of Tyr were not ruled out **[264, 765, 766]**. In addition, the aspartic protease of *P. vivax*, plasmepsin, was also inhibited by NO donors (GNSO, NOR-3, SIN-1 and SNP) **[524]**. Falcipain, plasmepsin and other proteases are important for Hb digestion, development and host cell invasion **[767-769]**. In addition to protease modifications, *Plasmodium falciparum* GR is inactivated by PN by nitration of Tyr^{106} and Tyr^{114} **[770]**. Inactivation of parasite GR slows GSSG reduction and lowers GSH levels and, therefore, could reduce protection against redox-altering ROS and RNIs (*e.g.* PN). The disruption of proteins needed for ookinete adhesion and invasion of the mosquito midgut epithelium/basal lamina could also prevent oocyst formation. The timing of *AsNOS* induction suggests that •NO/RNIs act on the mobile ookinete and oocyst. Potential targets of •NO/RNI inactivation could include Pbs21 (*P. berghei* surface protein 21kD; **[771]**), CTRP (circumsporozoite thromobospondin-related adhesion protein; **[772]**), and SOAP (secreted oocyst adhesion protein; **[773]**). Pbs21 and SOAP are Cys-rich, therefore nitrosation may inhibit their action. Alternatively, tyrosine nitration could hinder phosphorylation by protein tyrosine kinases and inhibit parasite maturation **[774, 775]**.

The toxic effects of RNIs may be potentiated by nitrosyls. Although nitrosyls can inhibit protein activity through inactivation of heme and Fe-S centers, nitrosyls also preserve the bioactivity of •NO by protecting it from decomposition in aqueous solution, preventing reaction with oxygen and other radicals, and transporting •NO away from the site of synthesis. As such, I predict that nitrosyls increase the persistence of •NO in the midgut and allow for the continued synthesis of RNIs at later times following bloodfeeding. For example, PN can release •NO from DNICs, which can then react with

other targets to form damaging redox species **[776]**. The biphasic nature of *AsNOS* transcription would support an initial formation of nitrosyls at early times following bloodfeeding that could store $^{\bullet}$NO for later release by RNIs (*e.g.* PN) resulting from the second induction of *AsNOS* activity. This release would be predicted to significantly increase the levels of RNIs formed in the midgut.

The damaging effects of $^{\bullet}$NO/RNIs can extend to host tissues as perhaps indicated by elevated levels of NTYR formed in infected *A. stephensi*, suggesting that self protection may be critical to the success of mosquito immunity. Numerous studies have indicated that Prxs protect against oxidative and nitrosative stresses. However, many Prxs were originally identified without reference to antioxidant function **(Table 3-1)**, their catalytic efficiency is ~3 orders of magnitude lower than other peroxidases **[604]** and they can be inactivated by high quantities of H_2O_2 **[563, 604, 671, 674-676]**. These observations highlighted the fact that Prxs catalyze reactions beyond those associated with peroxidase activity. For example, 1- and 2-Cys Prxs can suppress the oxidation of oxyHb **[587, 670]**, thus induction of *AsPrx-4783* by blood feeding may suppress the oxidation of ingested oxyHb. Overexpression of cytoplasmic 2-Cys Prx can counteract several pro-apoptotic signals **[567, 612, 709-711]**, hence AsPrx-4783 may protect *A. stephensi* cells from parasite-induced nitrosative stress. Specifically, overexpression of AsPrx-4783 protected MSQ43 cells from the cytotoxic effects of DEA-NO ($^{\bullet}$NO donor), AS (NO^- donor) PN, and H_2O_2. In addition to the expected protection afforded against H_2O_2-mediated cell death, AsPrx-4783 may have functioned as a PN reductase. Since NO^- can form from PN, AsPrx-4783 may prevent the formation of damaging NO^- through PN reductase activity. Further, because NO^- can react with oxygen to yield H_2O_2 **[142, 148]**, AsPrx-4783 may provide protection from AS by preventing the formation of downstream oxidants. The activity would be especially important in the midgut since the presence of transition metal ions enhances H_2O_2/AS mediated DNA damage **[148]**. Both SIN-1 (PN donor) and AS significantly potentiate the toxicity of H_2O_2 **[148, 777, 778]**. As such, AsPrx-4783 may also protect cells by scavenging H_2O_2. However $^{\bullet}$NO released from DEA-NO can reduce the toxicity of H_2O_2 **[777, 778]**, so the converse should also be true. Yet AsPrx-4783 also protected against DEA-NO. This activity has not been reported

in the literature, suggesting that AsPrx-4783 may provide novel insights into the range of biological functions of Prxs.

The functions of Prxs can be organized into three categories: prevention of damage, interception of damaging redox species, and repair of redox-related damage. *Anopheles stephensi* AsPrx-4783 may provide protection on all three levels. As previously stated, I believe that the toxic pro-oxidant PN is formed in the *Plasmodium*-infected *A. stephensi* midgut. AsPrx-4783 could limit PN formation by regulating NF-κB activity critical to *AsNOS* induction (**[567, 677, 730]**; Luckhart *et al.* unpublished) and $^{\bullet}$NO synthesis for PN formation. In some situations, PN formation can be protective **[779, 780]**. For example, PN can neutralize $^{\bullet}$NO and $O_2^{\bullet-}$ and PN can be rapidly detoxified by enzymatic (*e.g.* Prx) and non-enzymatic reactions **[160, 182, 308, 781]**. Lastly, AsPrx-4783 could function in repair of damaged cellular targets since Prxs appear to possess chaperone-like functions in the decameric state **[732]**.

The formation of RNIs in the *A. stephensi* midguts is dependent on in the inflammatory generation of ROS ($O_2^{\bullet-}$, H_2O_2, hydroxyl radical). Thus, in addition to the toxic effects of $^{\bullet}$NO/RNIs, parasite killing may be attributable to the direct toxic affects of ROS **[407, 448, 480]**. The abundance of heme Fe would predict that Fenton chemistry, which would impact $^{\bullet}$NO chemistry, occurs in the mosquito midgut during the first ~48 pBM. ROS and RNIs can synergize in killing of microorganisms with maximal killing depending on the timing of exposure to H_2O_2, $O_2^{\bullet-}$ and $^{\bullet}$NO **[778, 782]**. RNIs can enhance or hinder the toxic effects of ROS **[777, 778]**. Thus AsPrx-4783 may modulate $^{\bullet}$NO/RNI cytotoxicity by detoxifying H_2O_2 and altering the profile of RNIs formed in the mosquito midgut.

We have suggested that parasite invasion and development may be attenuated if the timing and/or level of *AsNOS* induction could be modified to yield higher levels of $^{\bullet}$NO/RNIs for longer periods of time **[328]**. In general, $^{\bullet}$NO alone is not harmful to cells; rather, secondary RNIs are responsible for the toxicity of $^{\bullet}$NO **[168, 283]**. The generation of RNIs might serve to (a) facilitate transport, (b) preserve $^{\bullet}$NO, (c) target $^{\bullet}$NO delivery to specific effectors, and/or (d) mitigate the cytotoxicity of other redox species **[131]**. However, the chemistry of RNI formation predicts that care must be taken to preserve the balance of $^{\bullet}$NO and ROS to maintain levels of toxic RNIs. If the levels of toxic RNIs can

be increased, the success of anti-parasite activity could depend on the activity of host defenses against increased oxidative and nitrosative stresses. In this light, manipulation of AsPrx-4783 to enhance host protection could give the advantage to the mosquito thereby limiting parasite survival and transmission.

APPENDICES

APPENDIX A: Schematic of equipment used in the photolysis-chemiluminescence based RNI detection.

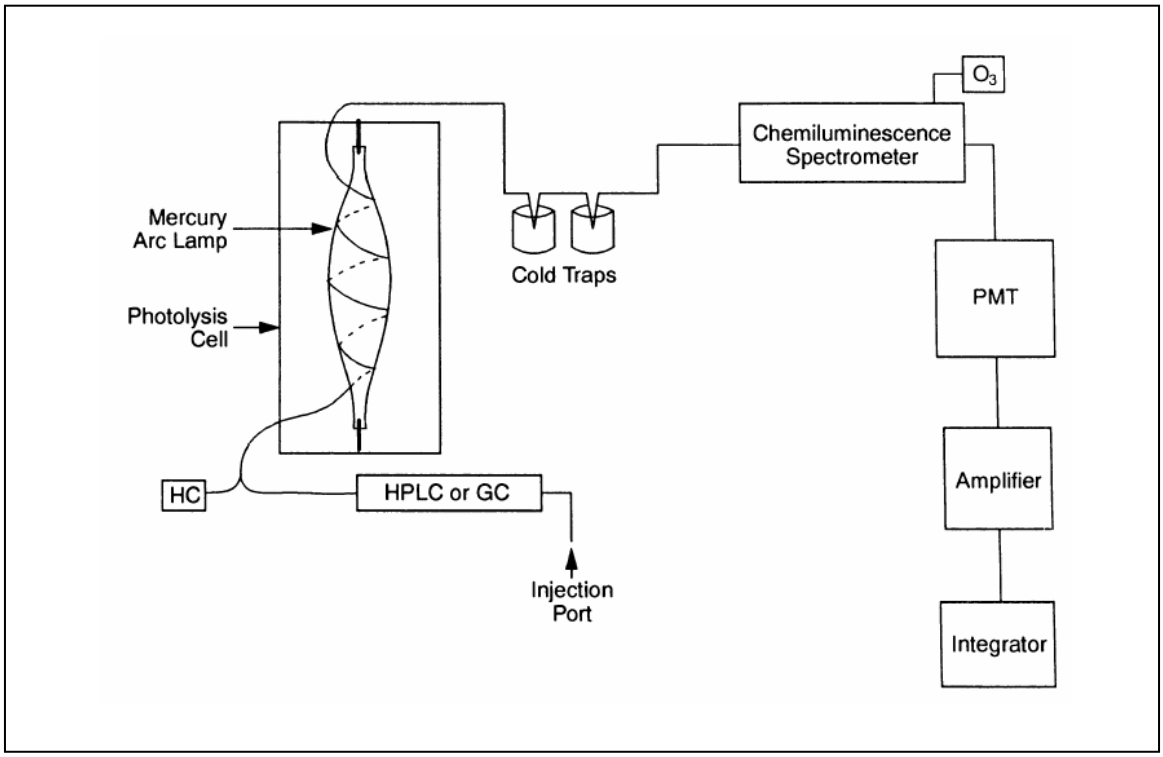

Schematic of the Nitrolyte/TEA system (Thermedics, Inc.) for the detection of "photolyzed-NO" **[102]**. PMT (photomultiplier tube), HC (Helium canister or other inert gas source).

<u>APPENDIX B</u>: Schematic of equipment used in the chemical reduction-chemiluminescence based RNI detection.

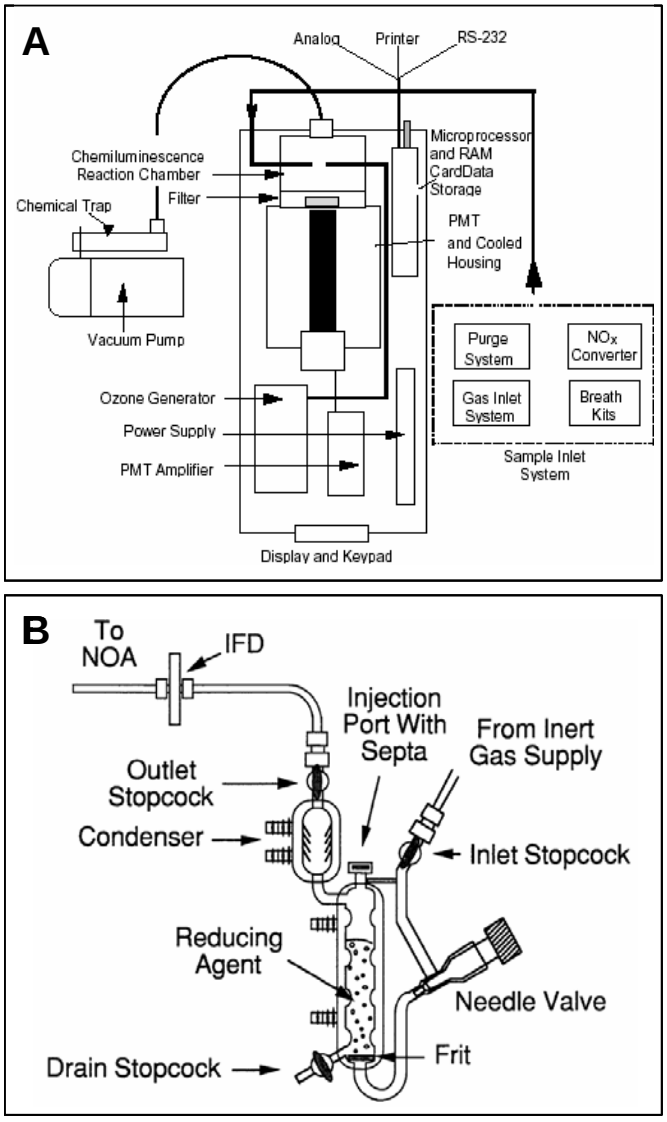

(A) Schematic of the Sievers Model 280 Nitric Oxide Analyzer (adapted from manual). **(B)** Radical purger attachment for chemical reduction of liquid samples (adapted from manual).

APPENDIX C: NOA analyses of midgut samples.

Using different chemical treatments, $^{\bullet}NO$ can be displaced from various biological components and measured in the Sievers NOA. Thusly the midgut lysates could be analyzed for a variety of RNIs.

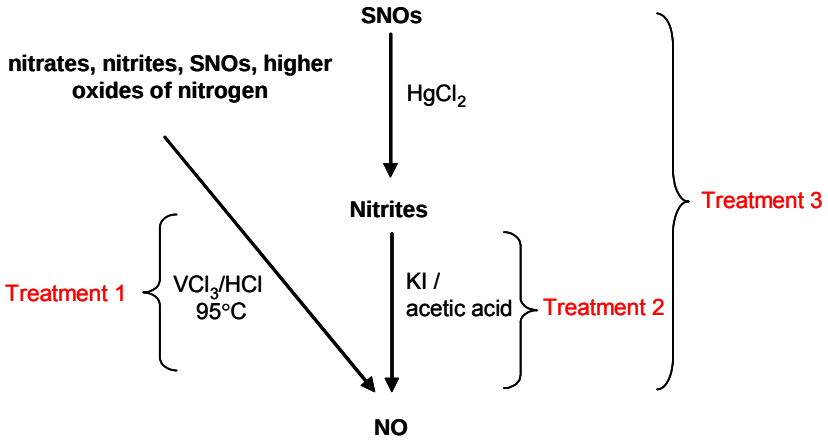

Treatment	RNIs Measured
1	nitrates, nitrites, SNOs, higher oxides of nitrogen
2	nitrites
1 minus 2	nitrates, SNOs, higher oxides of nitrogen
3 minus 2	SNOs
1 minus 3	nitrates, higher oxides of nitrogen

<u>APPENDIX D</u>: Plasmid vectors.

All plasmids were chemically transformed into TOP10 [*E. coli* strain genotype: F$^-$ *mcr*A Δ(*mrr-hsd*RMS-*mcr*BC) Φ80*lac*ZΔM15 Δ*lac*X74 *rec*A1 *ara*D139 Δ(*ara-leu*)7697 *gal*U *gal*K *rps*L (Str^R) *end*A1 *nup*G]. Purified plasmid DNA was sent to UC Davis Sequencing for verification of the insert sequence. Those plasmids containing relevant sequence were maintained as 80% glycerol bacteria stocks at -80ºC.

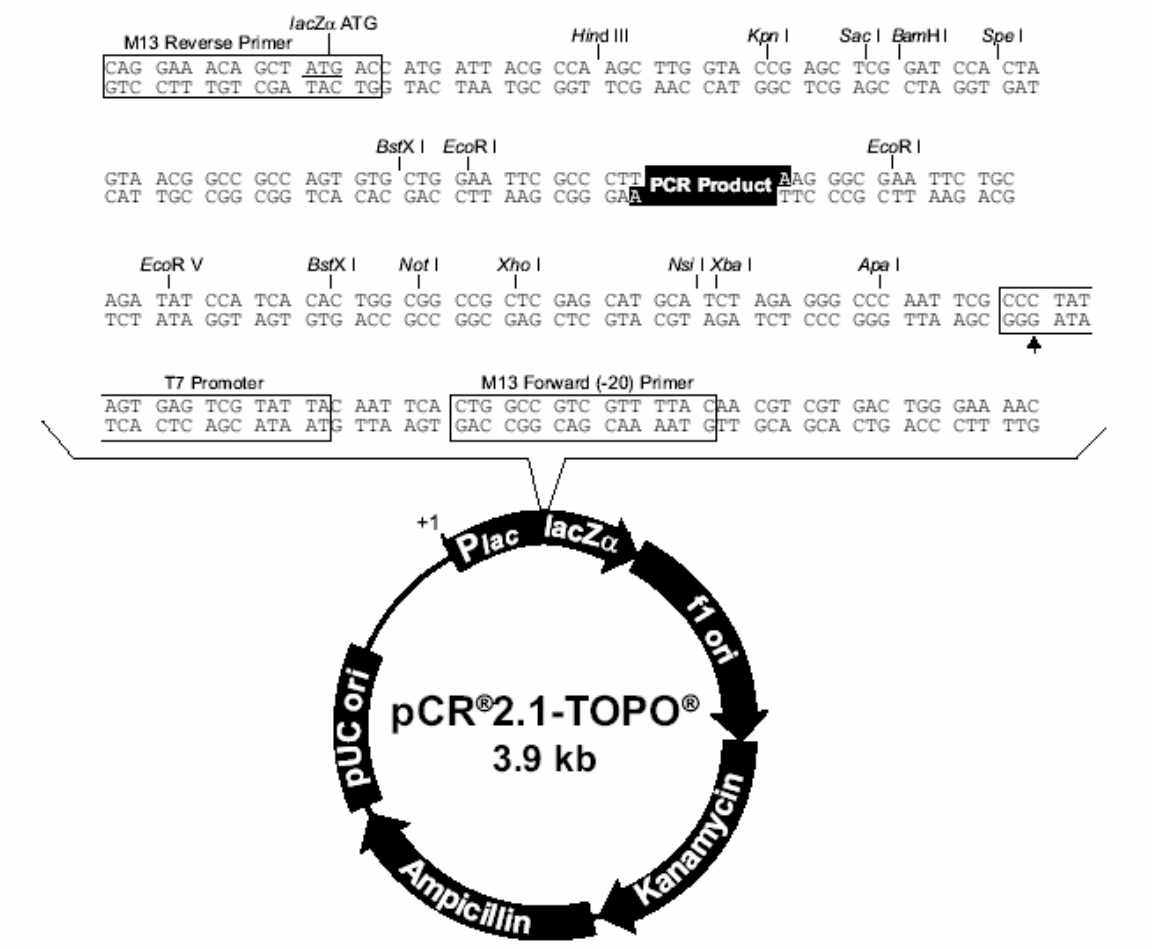

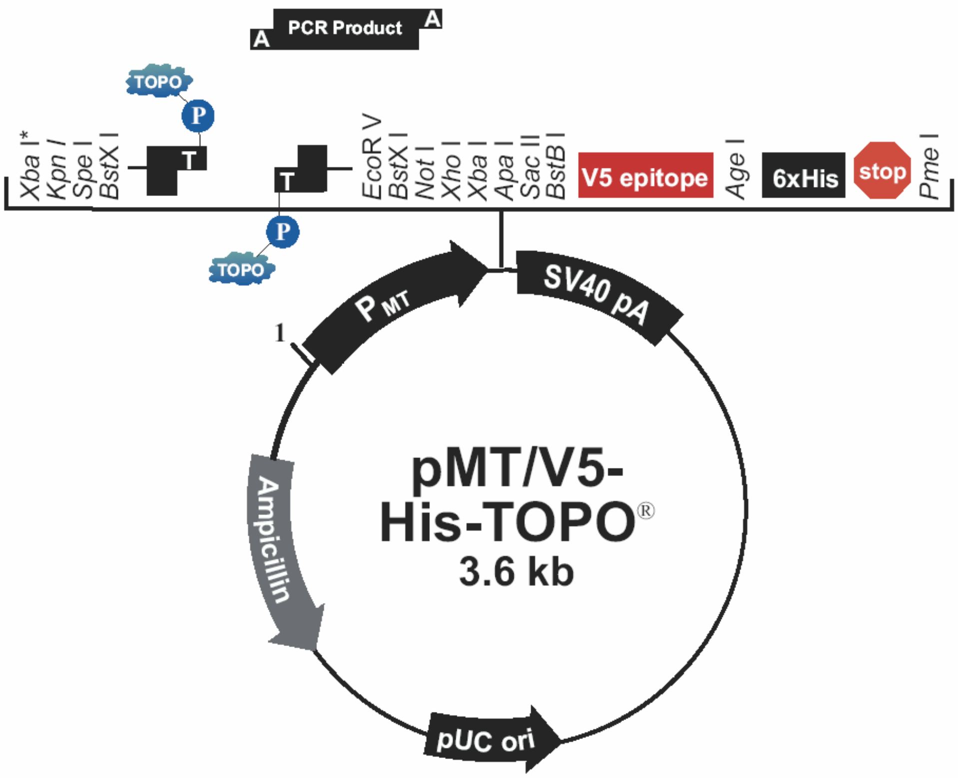


```
                                                                        TATA                         Start of transcription
701  AGAGGTGAAT CGAACGAAAG ACCCGTGTGT AAAGCCGCGT TTCCAAAATG TATAAAACCG AGAGCATCTG GCCAATGTGC
                    Metal Regulatory regions

                                   MT Forward priming site                 Xba I*#               Kpn I  Spe I
781  ATCAGTTGTG GTCAGCAGCA AAATCAAGTG AATCATCTCA GTGCAACTAA AGGGGGGATC TAGATCGGGG TACCTACTAG

            BstX I*                                                   EcoR V           BstX I*   Not I      Xho I
861  TCCAGTGTGG TGGAATTGCC CTT  PCR Product  AAG GGC AAT TCT GCA GAT ATC CAG CAC AGT GGC GGC CGC
                           GAA               TTC CCG TTA...
                                             Lys Gly Asn Ser Ala Asp Ile Gln His Ser Gly Gly Arg

          Xba I*           Apa I  Sac II  BstB I               V5 epitope
923  TCG AGT CTA GAG GGC CCG CGG TTC GAA GGT AAG CCT ATC CCT AAC CCT CTC CTC GGT CTC GAT TCT
     Ser Ser Leu Glu Gly Pro Arg Phe Glu Gly Lys Pro Ile Pro Asn Pro Leu Leu Gly Leu Asp Ser

             Age I         Polyhistidine region                Pme I                 BGH Reverse priming site
989  ACG CGT ACC GGT CAT CAT CAC CAT CAC CAT TGA GTTTAAACC CGCTGATCAG CCTCGACTGT GCCTTCTAAG
     Thr Arg Thr Gly His His His His His His ***

1061 ATCCAGACAT GATAAGATAC ATTGATGAGT TTGGACAAAC CACAACTAGA ATGCAGTGAA AAAAATGCTT TATTTGTGAA

                                                   SV40 late polyadenylation signal
1141 ATTTGTGATG CTATTGCTTT ATTTGTAACC ATTATAAGCT GCAATAAACA AGTTAACAAC AACAATTGCA TTCATTTTAT
```

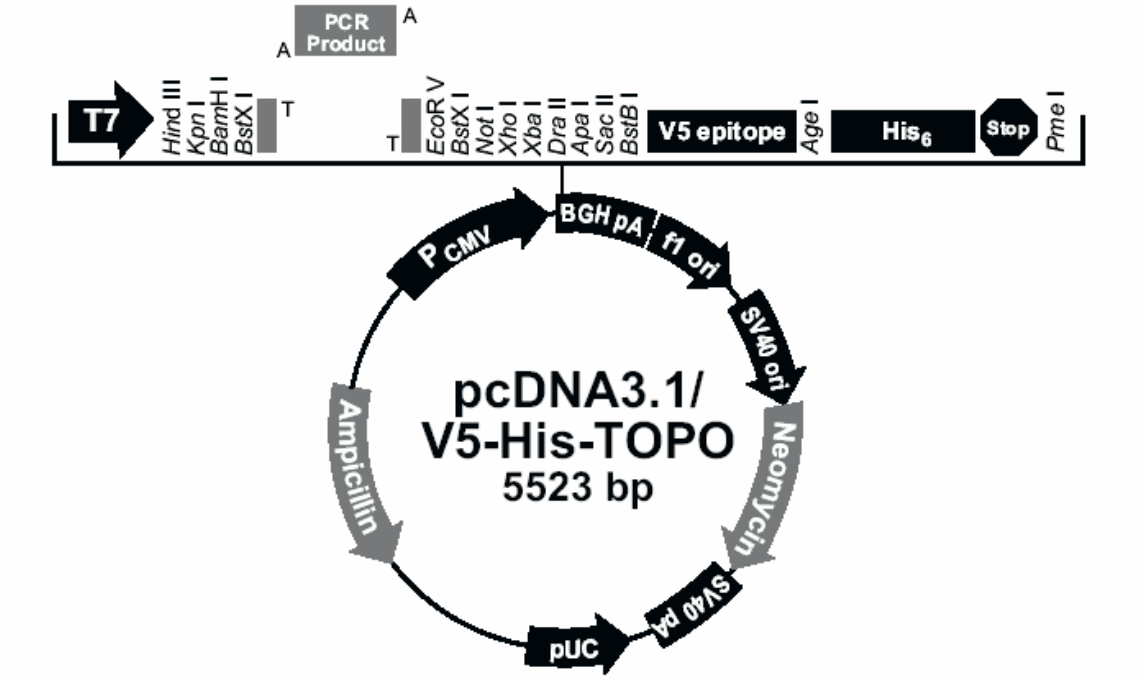


```
                CAAT                                    TATA                3´end of CMV promoter   Putative transcriptional start
761  CCCATTGACG CAAATGGGCG GTAGGCGTGT ACGGTGGGAG GTCTATATAA GCAGAGCTCT CTGGCTAACT AGAGAACCCA

                      T7 promoter/priming site                                  Hind III    Kpn I       BamH I
841  CTGCTTACTG GCTTATCGAA ATTAATACGA CTCACTATAG GGAGACCCAA GCTGGCTAGT TAAGCTTGGT ACCGAGCTCG

                BstX I                                                          EcoR V      BstX I  Not I
921  GATCCACTAG TCCAGTGTGG TGGAATTGCC CTT[PCR Product]AAG GGC AAT TCT GCA GAT ATC CAG CAC AGT GGC
                         ACCTTAACGG GAA[PCR Product]TTC CCG TTA AGT
                                                    Lys Gly Asn Ser Ala Asp Ile Gln His Ser Gly
       Xho I     Xba I     Dra II  Apa I  Sac II  BstB I                    V5 epitope
987  GGC CGC TCG AGT CTA GAG GGC CCG CGG TTC GAA GGT AAG CCT ATC CCT AAC CCT CTC CTC GGT CTC
     Gly Arg Ser Ser Leu Glu Gly Pro Arg Phe Glu Gly Lys Pro Ile Pro Asn Pro Leu Leu Gly Leu

                Age I                Polyhistidine region                Pme I                BGH Reverse
1053 GAT TCT ACG CGT ACC GGT CAT CAT CAC CAT CAC CAT TGA GTTTAAACCC GCTGATCAGC CTCGACTGTG
     Asp Ser Thr Arg Thr Gly His His His His His His ***

priming site
1122 CCTTCTAGTT GCCAGCCATC TGTTGTTTGC CCCTCCCCCG TGCCTTCCTT GACCCTGGAA GGTGCCACTC CCACTGTCCT

     BGH polyadenylation signal
1202 TTCCTAATAA AATGAGGAAA TTGCATCGCA TTGTCTGAGT AGGTGTCATT CTATTCTGGG GGGTGGGGTG GGGCAGGAC
```

REFERENCES

1. www.cdc.gov/malaria.
2. www.who.int/tdr/diseases/malaria.
3. Desowitz RS. The Malaria Capers: Tales of Parasites and People. New York: W. W. Norton & Company, Inc.; 1993.
4. www.malaria.org.
5. Sinden RE. Chapter 3: Cell biology. In: Killick-Kendrick R, Peters W (eds.), Rodent Malaria. London: Academic Press; 1978: 85-168.
6. Nussenzweig V, Nussenzweig RS. Progress toward a malaria vaccine. Hosp Pract (Off Ed) 1990; 25: 45-52, 55-47.
7. Richman AM, Dimopoulos G, Seeley D, Kafatos FC. *Plasmodium* activates the innate immune response of *Anopheles gambiae* mosquitoes. Embo J 1997; 16: 6114-6119.
8. Dimopoulos G. Insect immunity and its implication in mosquito-malaria interactions. Cell Microbiol 2003; 5: 3-14.
9. Meister S, Koutsos AC, Christophides GK. The *Plasmodium* parasite--a 'new' challenge for insect innate immunity. Int J Parasitol 2004; 34: 1473-1482.
10. Hoffmann JA. The immune response of *Drosophila*. Nature 2003; 426: 33-38.
11. Dimopoulos G, Richman A, Muller HM, Kafatos FC. Molecular immune responses of the mosquito *Anopheles gambiae* to bacteria and malaria parasites. Proc Natl Acad Sci U S A 1997; 94: 11508-11513.
12. Vizioli J, Bulet P, Charlet M, Lowenberger C, Blass C, Muller HM, Dimopoulos G, Hoffmann J, Kafatos FC, Richman A. Cloning and analysis of a cecropin gene from the malaria vector mosquito, *Anopheles gambiae*. Insect Mol Biol 2000; 9: 75-84.
13. Vizioli J, Bulet P, Hoffmann JA, Kafatos FC, Muller HM, Dimopoulos G. Gambicin: a novel immune responsive antimicrobial peptide from the malaria vector *Anopheles gambiae*. Proc Natl Acad Sci U S A 2001; 98: 12630-12635.
14. Christophides GK, Zdobnov E, Barillas-Mury C, Birney E, Blandin S, Blass C, Brey PT, Collins FH, Danielli A, Dimopoulos G, Hetru C, Hoa NT, Hoffmann JA, Kanzok SM, Letunic I, Levashina EA, Loukeris TG, Lycett G, Meister S, Michel K, Moita LF, Muller HM, Osta MA, Paskewitz SM, Reichhart JM, Rzhetsky A, Troxler L, Vernick KD, Vlachou D, Volz J, von Mering C, Xu J, Zheng L, Bork P, Kafatos FC. Immunity-related genes and gene families in *Anopheles gambiae*. Science 2002; 298: 159-165.
15. Kim W, Koo H, Richman AM, Seeley D, Vizioli J, Klocko AD, O'Brochta DA. Ectopic expression of a cecropin transgene in the human malaria vector mosquito *Anopheles gambiae* (Diptera: Culicidae): effects on susceptibility to *Plasmodium*. J Med Entomol 2004; 41: 447-455.
16. Blandin S, Moita LF, Kocher T, Wilm M, Kafatos FC, Levashina EA. Reverse genetics in the mosquito *Anopheles gambiae*: targeted disruption of the Defensin gene. EMBO Rep 2002; 3: 852-856.
17. Sinden RE. Molecular interactions between *Plasmodium* and its insect vectors. Cell Microbiol 2002; 4: 713-724.
18. Stuehr DJ. Purification and properties of nitric oxide synthases. Methods Enzymol 1996; 268: 324-333.
19. Nathan CF, Hibbs JB, Jr. Role of nitric oxide synthesis in macrophage antimicrobial activity. Curr Opin Immunol 1991; 3: 65-70.
20. Karupiah G, Xie QW, Buller RM, Nathan C, Duarte C, MacMicking JD. Inhibition of viral replication by interferon-gamma-induced nitric oxide synthase. Science 1993; 261: 1445-1448.
21. Stuehr DJ. Structure-function aspects in the nitric oxide synthases. Annu Rev Pharmacol Toxicol 1997; 37: 339-359.
22. Marletta MA. Mammalian synthesis of nitrite, nitrate, nitric oxide, and *N*-nitrosating agents. Chem Res Toxicol 1988; 1: 249-257.
23. Knowles RG, Moncada S. Nitric oxide synthases in mammals. Biochem J 1994; 298 (Pt 2): 249-258.
24. Marletta MA. Nitric oxide synthase: function and mechanism. Adv Exp Med Biol 1993; 338: 281-284.

25. Masters BS. Nitric oxide synthases: why so complex? Annu Rev Nutr 1994; 14: 131-145.
26. Palmer RM, Ashton DS, Moncada S. Vascular endothelial cells synthesize nitric oxide from L-arginine. Nature 1988; 333: 664-666.
27. Sakuma I, Stuehr DJ, Gross SS, Nathan C, Levi R. Identification of arginine as a precursor of endothelium-derived relaxing factor. Proc Natl Acad Sci U S A 1988; 85: 8664-8667.
28. Kwon NS, Nathan CF, Gilker C, Griffith OW, Matthews DE, Stuehr DJ. L-citrulline production from L-arginine by macrophage nitric oxide synthase. The ureido oxygen derives from dioxygen. J Biol Chem 1990; 265: 13442-13445.
29. Leone AM, Palmer RM, Knowles RG, Francis PL, Ashton DS, Moncada S. Constitutive and inducible nitric oxide synthases incorporate molecular oxygen into both nitric oxide and citrulline. J Biol Chem 1991; 266: 23790-23795.
30. Schmidt HH, Hofmann H, Schindler U, Shutenko ZS, Cunningham DD, Feelisch M. No *NO from NO synthase. Proc Natl Acad Sci U S A 1996; 93: 14492-14497.
31. Xia Y, Zweier JL. Direct measurement of nitric oxide generation from nitric oxide synthase. Proc Natl Acad Sci U S A 1997; 94: 12705-12710.
32. Hobbs AJ, Fukuto JM, Ignarro LJ. Formation of free nitric oxide from L-arginine by nitric oxide synthase: direct enhancement of generation by superoxide dismutase. Proc Natl Acad Sci U S A 1994; 91: 10992-10996.
33. Pufahl RA, Wishnok JS, Marletta MA. Hydrogen peroxide-supported oxidation of N^{G}-hydroxy-L-arginine by nitric oxide synthase. Biochemistry 1995; 34: 1930-1941.
34. Rusche KM, Spiering MM, Marletta MA. Reactions catalyzed by tetrahydrobiopterin-free nitric oxide synthase. Biochemistry 1998; 37: 15503-15512.
35. Adak S, Wang Q, Stuehr DJ. Arginine conversion to nitroxide by tetrahydrobiopterin-free neuronal nitric-oxide synthase. Implications for mechanism. J Biol Chem 2000; 275: 33554-33561.
36. Buga GM, Singh R, Pervin S, Rogers NE, Schmitz DA, Jenkinson CP, Cederbaum SD, Ignarro LJ. Arginase activity in endothelial cells: inhibition by N^{G}-hydroxy-L-arginine during high-output NO production. Am J Physiol 1996; 271: H1988-1998.
37. Mayer B, John M, Heinzel B, Werner ER, Wachter H, Schultz G, Bohme E. Brain nitric oxide synthase is a biopterin- and flavin-containing multi-functional oxido-reductase. FEBS Lett 1991; 288: 187-191.
38. Heinzel B, John M, Klatt P, Bohme E, Mayer B. Ca^{2+}/calmodulin-dependent formation of hydrogen peroxide by brain nitric oxide synthase. Biochem J 1992; 281 (Pt 3): 627-630.
39. Klatt P, Schmidt K, Uray G, Mayer B. Multiple catalytic functions of brain nitric oxide synthase. Biochemical characterization, cofactor-requirement, and the role of *N* omega-hydroxy-L-arginine as an intermediate. J Biol Chem 1993; 268: 14781-14787.
40. Pou S, Pou WS, Bredt DS, Snyder SH, Rosen GM. Generation of superoxide by purified brain nitric oxide synthase. J Biol Chem 1992; 267: 24173-24176.
41. Xia Y, Zweier JL. Superoxide and peroxynitrite generation from inducible nitric oxide synthase in macrophages. Proc Natl Acad Sci U S A 1997; 94: 6954-6958.
42. Xia Y, Roman LJ, Masters BS, Zweier JL. Inducible nitric-oxide synthase generates superoxide from the reductase domain. J Biol Chem 1998; 273: 22635-22639.
43. Xia Y, Tsai AL, Berka V, Zweier JL. Superoxide generation from endothelial nitric-oxide synthase. A Ca^{2+}/calmodulin-dependent and tetrahydrobiopterin regulatory process. J Biol Chem 1998; 273: 25804-25808.
44. Culcasi M, Lafon-Cazal M, Pietri S, Bockaert J. Glutamate receptors induce a burst of superoxide via activation of nitric oxide synthase in arginine-depleted neurons. J Biol Chem 1994; 269: 12589-12593.
45. Miller RT, Martasek P, Roman LJ, Nishimura JS, Masters BS. Involvement of the reductase domain of neuronal nitric oxide synthase in superoxide anion production. Biochemistry 1997; 36: 15277-15284.
46. Cirino G, Santagada V, Caliendo G. The nitric oxide related therapeutic phenomenon: a challenging task. Curr Pharm Des 2002; 8: 233-239.
47. Luckhart S, Rosenberg R. Gene structure and polymorphism of an invertabrate nitric oxide synthase gene. Gene 1999; 232: 25-34.

48. Luckhart S, Li K. Transcriptional complexity of the *Anopheles stephensi* nitric oxide synthase gene. Insect Biochem Mol Biol 2001; 31: 249-256.
49. Regulski M, Tully T. Molecular and biochemical characterization of dNOS: a *Drosophila* Ca^{2+}/calmodulin-dependent nitric oxide synthase. Proc Natl Acad Sci U S A 1995; 92: 9072-9076.
50. Yuda M, Hirai M, Miura K, Matsumura H, Ando K, Chinzei Y. cDNA cloning, expression and characterization of nitric-oxide synthase from the salivary glands of the blood-sucking insect *Rhodnius prolixus*. Eur J Biochem 1996; 242: 807-812.
51. Nighorn A, Gibson NJ, Rivers DM, Hildebrand JG, Morton DB. The nitric oxide-cGMP pathway may mediate communication between sensory afferents and projection neurons in the antennal lobe of *Manduca sexta*. J Neurosci 1998; 18: 7244-7255.
52. Luckhart S, Vodovotz Y, Cui L, Rosenberg R. The mosquito *Anopheles stephensi* limits malaria parasite development with inducible synthesis of nitric oxide. Proc Natl Acad Sci U S A 1998; 95: 5700-5705.
53. Hall AV, Antoniou H, Wang Y, Cheung AH, Arbus AM, Olson SL, Lu WC, Kau CL, Marsden PA. Structural organization of the human neuronal nitric oxide synthase gene (NOS1). J Biol Chem 1994; 269: 33082-33090.
54. Stasiv Y, Regulski M, Kuzin B, Tully T, Enikolopov G. The *Drosophila* nitric-oxide synthase gene (dNOS) encodes a family of proteins that can modulate NOS activity by acting as dominant negative regulators. J Biol Chem 2001; 276: 42241-42251.
55. Eissa NT, Strauss AJ, Haggerty CM, Choo EK, Chu SC, Moss J. Alternative splicing of human inducible nitric-oxide synthase mRNA. tissue-specific regulation and induction by cytokines. J Biol Chem 1996; 271: 27184-27187.
56. Luckhart S, Crampton AL, Zamora R, Lieber MJ, Dos Santos PC, **Peterson TML**, Emmith N, Lim J, Wink DA, Vodovotz Y. Mammalian transforming growth factor-β1, activated after ingestion by *Anopheles stephensi*, modulates mosquito immunity. Infect Immun 2003; 71: 3000-3009.
57. Dimopoulos G, Seeley D, Wolf A, Kafatos FC. Malaria infection of the mosquito *Anopheles gambiae* activates immune-responsive genes during critical transition stages of the parasite life cycle. Embo J 1998; 17: 6115-6123.
58. Crampton A, Luckhart S. The role of As60A, a TGF-beta homolog, in *Anopheles stephensi* innate immunity and defense against *Plasmodium* infection. Infection, Genetics and Evolution 2001; 1: 131-141.
59. Robinson AS, Franz G, Atkinson PW. Insect transgenesis and its potential role in agriculture and human health. Insect Biochem Mol Biol 2004; 34: 113-120.
60. Ramasamy MS, Kulasekera R, Wanniarachchi IC, Srikrishnaraj KA, Ramasamy R. Interactions of human malaria parasites, *Plasmodium vivax* and *P. falciparum*, with the midgut of *Anopheles* mosquitoes. Med Vet Entomol 1997; 11: 290-296.
61. Vodovotz Y. Modified microassay for serum nitrite and nitrate. Biotechniques 1996; 20: 390-392, 394.
62. Jacobs-Lorena M, Oo MM. Chapter 19: The Peritrophic Matrix of Insects. In: Beaty BJ, Marquardt WC (eds.), The Biology of Disease Vectors. Colorado: University Press of Colorado; 1996: 318-332.
63. Chege GM, Beier JC. Blood acquisition and processing by three *Anopheles* (Diptera: *Culicidae*) species with different innate susceptibilities to *Plasmodium falciparum*. J Med Entomol 1998; 35: 319-323.
64. Billker O, Miller AJ, Sinden RE. Determination of mosquito bloodmeal pH in situ by ion-selective microelectrode measurement: implications for the regulation of malarial gametogenesis. Parasitology 2000; 120: 547-551.
65. Vaughan JA, Noden BH, Beier JC. Concentration of human erythrocytes by anopheline mosquitoes (*Diptera*: *Culicidae*) during feeding. J Med Entomol 1991; 28: 780-786.
66. Briegel H, Rezzonico L. Concentration of host blood protein during feeding by anopheline mosquitoes (*Diptera*: *Culicidae*). J Med Entomol 1985; 22: 612-618.
67. Gakhar SK, Shandilya H. Heat shock response during development of the malaria vector *Anopheles stephensi* (*Culicidae*: *Diptera*). Cytobios 1999; 99: 173-182.

68. Billingsley PF, Hecker H. Blood digestion in the mosquito, *Anopheles stephensi* Liston (Diptera: *Culicidae*): activity and distribution of trypsin, aminopeptidase, and alpha-glucosidase in the midgut. J Med Entomol 1991; 28: 865-871.
69. Clements AN. Chapter 14: Adult digestion. In: Development, Nutrition and Reproduction, vol. 1. London: Chapman & Hall; 1992: 272-291.
70. Romoster WS. Chapter 18: The vector alimentary system. In: Beaty BJ, Marquardt WC (eds.), The Biology of Disease Vectors. Colorado: University Press of Colorado; 1996: 298-317.
71. Chen Z, Zhang J, Stamler JS. From the cover: Identification of the enzymatic mechanism of nitroglycerin bioactivation. Proc Natl Acad Sci U S A 2002; 99: 8306-8311.
72. Moreland RB, Goldstein I, Traish A. Sildenafil, a novel inhibitor of phosphodiesterase type 5 in human corpus cavernosum smooth muscle cells. Life Sci 1998; 62: PL 309-318.
73. Palmer RM, Ferrige AG, Moncada S. Nitric oxide release accounts for the biological activity of endothelium-derived relaxing factor. Nature 1987; 327: 524-526.
74. Zafiriou OC, McFarland M. Determination of trace levels of nitric oxide in aqueous solution. Anal Chem 1980; 52.
75. Culotta E, Koshland DE, Jr. NO news is good news. Science 1992; 258: 1862-1865.
76. Girard P, Potier P. NO, thiols and disulfides. FEBS Lett 1993; 320: 7-8.
77. Fang FC (ed.). Nitric Oxide and Infection. New York: Kluwer Academic/Plenum Publishers; 1999.
78. Poole RK. Nitric oxide and nitrosative stress tolerance in bacteria. Biochem Soc Trans 2005; 33: 176-180.
79. Kelm M. Nitric oxide metabolism and breakdown. Biochim Biophys Acta 1999; 1411: 273-289.
80. Wink DA, Hanbauer I, Krishna MC, DeGraff W, Gamson J, Mitchell JB. Nitric oxide protects against cellular damage and cytotoxicity from reactive oxygen species. Proc Natl Acad Sci U S A 1993; 90: 9813-9817.
81. Hughes MN. Relationships between nitric oxide, nitroxyl ion, nitrosonium cation and peroxynitrite. Biochim Biophys Acta 1999; 1411: 263-272.
82. Ignarro LJ (ed.). Nitric Oxide: Biology and Pathobiology. San Diego, CA: Academic Press; 2000.
83. Gow AJ, Luchsinger BP, Pawloski JR, Singel DJ, Stamler JS. The oxyhemoglobin reaction of nitric oxide. Proc Natl Acad Sci U S A 1999; 96: 9027-9032.
84. Wink DA, Grisham MB, Mitchell JB, Ford PC. Direct and indirect effects of nitric oxide in chemical reactions relevant to biology. Methods Enzymol 1996; 268: 12-31.
85. Wink DA, Mitchell JB. Chemical biology of nitric oxide: Insights into regulatory, cytotoxic, and cytoprotective mechanisms of nitric oxide. Free Radic Biol Med 1998; 25: 434-456.
86. Ignarro LJ, Fukuto JM, Griscavage JM, Rogers NE, Byrns RE. Oxidation of nitric oxide in aqueous solution to nitrite but not nitrate: comparison with enzymatically formed nitric oxide from L-arginine. Proc Natl Acad Sci U S A 1993; 90: 8103-8107.
87. Miranda K, Espey MG, Jourd'heuil D, Grisham MB, Fukuto J, Feelisch M, Wink DA. Chapter 3: The chemical biology of nitric oxide. In: Ignarro LJ (ed.) Nitric Oxide: Biology and Pathobiology. San Diego, CA: Academic Press; 2000: 41-55.
88. Zhang Y, Hogg N. Mixing artifacts from the bolus addition of nitric oxide to oxymyoglobin: implications for *S*-nitrosothiol formation. Free Radic Biol Med 2002; 32: 1212-1219.
89. Radi R, Cosgrove TP, Beckman JS, Freeman BA. Peroxynitrite-induced luminol chemiluminescence. Biochem J 1993; 290 (Pt 1): 51-57.
90. Henry Y, Ducrocq C, Drapier JC, Servent D, Pellat C, Guissani A. Nitric oxide, a biological effector. Electron paramagnetic resonance detection of nitrosyl-iron-protein complexes in whole cells. Eur Biophys J 1991; 20: 1-15.
91. Gow AJ, Foust III R, Malcolm S, Gole M, Ischiropoulos H. Chapter 8: Biochemistry regulation of nitric oxide cytotoxicity. In: Fang FC (ed.) Nitric Oxide and Infection. New York: Kluwer Academic/Plenum Publishers; 1999: 175-187.
92. Rockett KA, Awburn MM, Cowden WB, Clark IA. Killing of *Plasmodium falciparum in vitro* by nitric oxide derivatives. Infect Immun 1991; 59: 3280-3283.
93. Richter-Addo GB, Legzdins P. Metal Nitrosyls. New York, NY: Oxford University Press, Inc.; 1992.

94. Thomas DD, Miranda KM, Colton CA, Citrin D, Espey MG, Wink DA. Heme proteins and nitric oxide (NO): the neglected, eloquent chemistry in NO redox signaling and regulation. Antioxid Redox Signal 2003; 5: 307-317.
95. Henry YA, Guissani A, Ducastel B. Nitric Oxide Research from Chemistry to Biology: EPR Spectroscopy of Nitrosylated Compounds. Austin, Texas: R. G. Landes Company; 1997.
96. Reynolds MF, Burstyn JN. Chapter 25: Mechansims of activation of soluable guanylyl cyclase by NO. In: Ignarro LJ (ed.) Nitric Oxide: Biology and Pathobiology. San Diego, CA: Academic Press; 2000: 381-399.
97. Drapier JC, Hirling H, Wietzerbin J, Kaldy P, Kuhn LC. Biosynthesis of nitric oxide activates iron regulatory factor in macrophages. Embo J 1993; 12: 3643-3649.
98. Westenberger U, Thanner S, Ruf HH, Gersonde K, Sutter G, Trentz O. Formation of free radicals and nitric oxide derivative of hemoglobin in rats during shock syndrome. Free Radic Res Commun 1990; 11: 167-178.
99. Lancaster JR, Jr., Langrehr JM, Bergonia HA, Murase N, Simmons RL, Hoffman RA. EPR detection of heme and nonheme iron-containing protein nitrosylation by nitric oxide during rejection of rat heart allograft. J Biol Chem 1992; 267: 10994-10998.
100. Drapier JC, Pellat C, Henry Y. Generation of EPR-detectable nitrosyl-iron complexes in tumor target cells cocultured with activated macrophages. J Biol Chem 1991; 266: 10162-10167.
101. Stamler JS, Simon DI, Osborne JA, Mullins ME, Jaraki O, Michel T, Singel DJ, Loscalzo J. *S*-nitrosylation of proteins with nitric oxide: synthesis and characterization of biologically active compounds. Proc Natl Acad Sci U S A 1992; 89: 444-448.
102. Stamler JS, Jaraki O, Osborne J, Simon DI, Keaney J, Vita J, Singel D, Valeri CR, Loscalzo J. Nitric oxide circulates in mammalian plasma primarily as an *S*-nitroso adduct of serum albumin. Proc Natl Acad Sci U S A 1992; 89: 7674-7677.
103. Vanin AF, Stukan RA, Manukhina EB. Physical properties of dinitrosyl iron complexes with thiol-containing ligands in relation with their vasodilator activity. Biochim Biophys Acta 1996; 1295: 5-12.
104. Fukuto JM. Chemistry of nitric oxide: biologically relevant aspects. Adv Pharmacol 1995; 34: 1-15.
105. Gow AJ, Stamler JS. Reactions between nitric oxide and haemoglobin under physiological conditions. Nature 1998; 391: 169-173.
106. Turk T, Hollocher TC. Oxidation of dithiothreitol during turnover of nitric oxide reductase: evidence for generation of nitroxyl with the enzyme from *Paracoccus denitrificans*. Biochem Biophys Res Commun 1992; 183: 983-988.
107. Sharpe MA, Cooper CE. Reactions of nitric oxide with mitochondrial cytochrome c: a novel mechanism for the formation of nitroxyl anion and peroxynitrite. Biochem J 1998; 332 (Pt 1): 9-19.
108. Vanin AF. Dinitrosyl iron complexes and *S*-nitrosothiols are two possible forms for stabilization and transport of nitric oxide in biological systems. Biochemistry (Mosc) 1998; 63: 782-793.
109. Fukuto JM, Cho JY, Switzer CH. Chapter 2: The chemical properties of nitric oxide and related nitrogen oxides. In: Ignarro LJ (ed.) Nitric Oxide: Biology and Pathobiology. San Diego, CA.: Academic Press; 2000: 23-40.
110. Fukuto JM, Wallace GC, Hszieh R, Chaudhuri G. Chemical oxidation of *N*-hydroxyguanidine compounds. Release of nitric oxide, nitroxyl and possible relationship to the mechanism of biological nitric oxide generation. Biochem Pharmacol 1992; 43: 607-613.
111. Vanin AF, Papina AA, Serezhenkov VA, Koppenol WH. The mechanisms of *S*-nitrosothiol decomposition catalyzed by iron. Nitric Oxide 2004; 10: 60-73.
112. Bonner FT, Pearsall KA. Aqueous nitrosyliron(II) chemistry. 1. Reduction of nitrite and nitric oxide by iron(II) and (trioxodinitrato)iron(II) in acetate buffer. Intermediacy of nitrosyl hydride. Inorg Chem 1982; 21: 1973-1978.
113. Vanin AF, Malenkova IV, Serezhenkov VA. Iron catalyzes both decomposition and synthesis of *S*-nitrosothiols: optical and electron paramagnetic resonance studies. Nitric Oxide 1997; 1: 191-203.
114. Stojanovic S, Stanic D, Nikolic M, Spasic M, Niketic V. Iron catalyzed conversion of NO into nitrosonium (NO^+) and nitroxyl (HNO/NO^-) species. Nitric Oxide 2004; 11: 256-262.

115. Arnelle DR, Stamler JS. NO^+, NO, and NO^- donation by *S*-nitrosothiols: implications for regulation of physiological functions by *S*-nitrosylation and acceleration of disulfide formation. Arch Biochem Biophys 1995; 318: 279-285.
116. Pino RZ, Feelisch M. Bioassay discrimination between nitric oxide (NO) and nitroxyl (NO^-) using L-cysteine. Biochem Biophys Res Commun 1994; 201: 54-62.
117. Wong PS, Hyun J, Fukuto JM, Shirota FN, DeMaster EG, Shoeman DW, Nagasawa HT. Reaction between *S*-nitrosothiols and thiols: generation of nitroxyl (HNO) and subsequent chemistry. Biochemistry 1998; 37: 5362-5371.
118. Hogg N, Singh RJ, Kalyanaraman B. The role of glutathione in the transport and catabolism of nitric oxide. FEBS Lett 1996; 382: 223-228.
119. Park JW. Reaction of *S*-nitrosoglutathione with sulfhydryl groups in protein. Biochem Biophys Res Commun 1988; 152: 916-920.
120. Mancardi D, Ridnour LA, Thomas DD, Katori T, Tocchetti CG, Espey MG, Miranda KM, Paolocci N, Wink DA. The chemical dynamics of NO and reactive nitrogen oxides: a practical guide. Curr Mol Med 2004; 4: 723-740.
121. Singh SP, Wishnok JS, Keshive M, Deen WM, Tannenbaum SR. The chemistry of the *S*-nitrosoglutathione/glutathione system. Proc Natl Acad Sci U S A 1996; 93: 14428-14433.
122. Murphy ME, Sies H. Reversible conversion of nitroxyl anion to nitric oxide by superoxide dismutase. Proc Natl Acad Sci U S A 1991; 88: 10860-10864.
123. Niketic V, Stojanovic S, Nikolic A, Spasic M, Michelson AM. Exposure of Mn and FeSODs, but not Cu/ZnSOD, to NO leads to nitrosonium and nitroxyl ions generation which cause enzyme modification and inactivation: an *in vitro* study. Free Radic Biol Med 1999; 27: 992-996.
124. Reif A, Zecca L, Riederer P, Feelisch M, Schmidt HH. Nitroxyl oxidizes NADPH in a superoxide dismutase inhibitable manner. Free Radic Biol Med 2001; 30: 803-808.
125. Liochev SI, Fridovich I. Copper, zinc superoxide dismutase as a univalent NO^- oxidoreductase and as a dichlorofluorescin peroxidase. J Biol Chem 2001; 276: 35253-35257.
126. Liochev SI, Fridovich I. The mode of decomposition of Angeli's salt ($Na_2N_2O_3$) and the effects thereon of oxygen, nitrite, superoxide dismutase, and glutathione. Free Radic Biol Med 2003; 34: 1399-1404.
127. Khan AU, Kovacic D, Kolbanovskiy A, Desai M, Frenkel K, Geacintov NE. The decomposition of peroxynitrite to nitroxyl anion (NO^-) and singlet oxygen in aqueous solution. Proc Natl Acad Sci U S A 2000; 97: 2984-2989.
128. Bartberger MD, Fukuto JM, Houk KN. On the acidity and reactivity of HNO in aqueous solution and biological systems. Proc Natl Acad Sci U S A 2001; 98: 2194-2198.
129. Miranda KM, Espey MG, Yamada K, Krishna M, Ludwick N, Kim S, Jourd'heuil D, Grisham MB, Feelisch M, Fukuto JM, Wink DA. Unique oxidative mechanisms for the reactive nitrogen oxide species, nitroxyl anion. J Biol Chem 2001; 276: 1720-1727.
130. Wink DA, Feelisch M, Fukuto J, Chistodoulou D, Jourd'heuil D, Grisham MB, Vodovotz Y, Cook JA, Krishna M, DeGraff WG, Kim S, Gamson J, Mitchell JB. The cytotoxicity of nitroxyl: possible implications for the pathophysiological role of NO. Arch Biochem Biophys 1998; 351: 66-74.
131. Stamler JS, Singel DJ, Loscalzo J. Biochemistry of nitric oxide and its redox-activated forms. Science 1992; 258: 1898-1902.
132. Kirsch M, de Groot H. Formation of peroxynitrite from reaction of nitroxyl anion with molecular oxygen. J Biol Chem 2002; 277: 13379-13388.
133. Ma XL, Gao F, Liu GL, Lopez BL, Christopher TA, Fukuto JM, Wink DA, Feelisch M. Opposite effects of nitric oxide and nitroxyl on postischemic myocardial injury. Proc Natl Acad Sci U S A 1999; 96: 14617-14622.
134. Fukuto JM, Hobbs AJ, Ignarro LJ. Conversion of nitroxyl (HNO) to nitric oxide (NO) in biological systems: the role of physiological oxidants and relevance to the biological activity of HNO. Biochem Biophys Res Commun 1993; 196: 707-713.
135. Shafirovich V, Lymar SV. Nitroxyl and its anion in aqueous solutions: Spin states, protic equilibria, and reactivities toward oxygen and nitric oxide. Proc Natl Acad Sci U S A 2002; 99: 7340-7345.
136. Espey MG, Miranda KM, Thomas DD, Wink DA. Ingress and reactive chemistry of nitroxyl-derived species within human cells. Free Radic Biol Med 2002; 33: 827-834.

137. Donald CE, Hughes MN, Thompson JM. Photolysis of the N=N bond in trioxodinitrate: reaction between triplet NO^- and O_2 to form peroxynitrite. Inorg Chem 1986; 25: 2676-2677.
138. Doyle MP, Mahapatro SN, Broene RD, Guy JK. Oxidation and reduction of hemoproteins by trioxodinitrate(II) - the role of nitrosyl hydride and nitrite. J Am Chem Soc 1988; 110: 593-599.
139. Cooper CE. Nitric oxide and iron proteins. Biochim Biophys Acta 1999; 1411: 290-309.
140. Bazylinski DA, Hollocher TC. Metmyoglobin and methemoglobin as efficient traps for nitrosyl hydride (nitroxyl) in neutral aqueous solution. J Am Chem Soc 1985; 107: 7982-7986.
141. Bazylinski DA, Goretski J, Hollocher TC. On the reaction of trioxodinitrate(II) with hemoglobin and myoglobin. J Am Chem Soc 1985; 107: 7986-7989.
142. Ohshima H, Gilibert I, Bianchini F. Induction of DNA strand breakage and base oxidation by nitroxyl anion through hydroxyl radical production. Free Radic Biol Med 1999; 26: 1305-1313.
143. Stoyanovsky DA, Clancy R, Cederbaum AI. Decomposition of sodium trioxodinitrate (Angeli's salt) to hydroxyl radical: an ESR spin-trapping study. J Am Chem Soc 1999; 121: 5093-5094.
144. Ohshima H, Yoshie Y, Auriol S, Gilibert I. Antioxidant and pro-oxidant actions of flavonoids: Effects on DNA damage induced by nitric oxide, peroxynitrite and nitroxyl anion. Free Radic Biol Med 1998; 25: 1057-1065.
145. Miranda KM, Yamada K, Espey MG, Thomas DD, DeGraff W, Mitchell JB, Krishna MC, Colton CA, Wink DA. Further evidence for distinct reactive intermediates from nitroxyl and peroxynitrite: effects of buffer composition on the chemistry of Angeli's salt and synthetic peroxynitrite. Arch Biochem Biophys 2002; 401: 134-144.
146. Hughes MN, Cammack R. Synthesis, chemistry, and applications of nitroxyl ion releasers sodium trioxodinitrate or Angeli's salt and Piloty's acid. Methods Enzymol 1999; 301: 279-287.
147. Bai P, Bakondi E, Szabo E, Gergely P, Szabo C, Virag L. Partial protection by poly(ADP-ribose) polymerase inhibitors from nitroxyl-induced cytotoxity in thymocytes. Free Radic Biol Med 2001; 31: 1616-1623.
148. Chazotte-Aubert L, Oikawa S, Gilibert I, Bianchini F, Kawanishi S, Ohshima H. Cytotoxicity and site-specific DNA damage induced by nitroxyl anion (NO^-) in the presence of hydrogen peroxide. Implications for various pathophysiological conditions. J Biol Chem 1999; 274: 20909-20915.
149. Ohshima H, Celan I, Chazotte L, Pignatelli B, Mower HF. Analysis of 3-nitrotyrosine in biological fluids and protein hydrolyzates by high-performance liquid chromatography using a postseparation, on-line reduction column and electrochemical detection: results with various nitrating agents. Nitric Oxide 1999; 3: 132-141.
150. Giorgio S, Linares E, Capurro M, de Bianchi AG, Augusto O. Formation of nitrosyl hemoglobin and nitrotyrosine during murine leishmaniasis. Photochem Photobiol 1996; 63: 750-754.
151. Beckman JS, Chen J, Ischiropoulos H, Crow JP. Oxidative chemistry of peroxynitrite. Methods Enzymol 1994; 233: 229-240.
152. Blough NV, Zafiriou OC. Reaction of superoxide with nitric oxide to form peroxynitrite in alkaline aqueous solution. Inorganic chemistry 1985; 24: 3502 - 3504.
153. Radi R, Denicola A, Alvarez B, Ferrer-Suerta G, Rubbo H. Chapter 4: The biological chemistry of peroxynitrite. In: Ignarro LJ (ed.) Nitric Oxide: Biology and Pathobiology. San Diego: Academic Press; 2000: 57-82.
154. Kissner R, Nauser T, Bugnon P, Lye PG, Koppenol WH. Formation and properties of peroxynitrite as studied by laser flash photolysis, high-pressure stopped-flow technique, and pulse radiolysis. Chem Res Toxicol 1997; 10: 1285-1292.
155. Pfeiffer S, Gorren AC, Schmidt K, Werner ER, Hansert B, Bohle DS, Mayer B. Metabolic fate of peroxynitrite in aqueous solution. Reaction with nitric oxide and pH-dependent decomposition to nitrite and oxygen in a 2:1 stoichiometry. J Biol Chem 1997; 272: 3465-3470.
156. Huie RE, Padmaja S. The reaction of NO with superoxide. Free Radic Res Commun 1993; 18: 195-199.
157. Wink DA, Feelisch M. Chapter 28: Formation and detection of nitroxyl and nitrous oxide. In: Feelisch M, Stamler JS (eds.), Methods in Nitric Oxide Research. Chichester: John Wiley & Sons Ltd.; 1996: 403-412.
158. Nathan C, Xie QW. Regulation of biosynthesis of nitric oxide. J Biol Chem 1994; 269: 13725-13728.
159. Beckman JS, Koppenol WH. Nitric oxide, superoxide, and peroxynitrite: the good, the bad, and ugly. Am J Physiol 1996; 271: C1424-1437.

160. Arteel GE, Briviba K, Sies H. Protection against peroxynitrite. FEBS Lett 1999; 445: 226-230.
161. Beckman JS, Beckman TW, Chen J, Marshall PA, Freeman BA. Apparent hydroxyl radical production by peroxynitrite: implications for endothelial injury from nitric oxide and superoxide. Proc Natl Acad Sci U S A 1990; 87: 1620-1624.
162. Pryor WA, Squadrito GL. The chemistry of peroxynitrite: a product from the reaction of nitric oxide with superoxide. Am J Physiol 1995; 268: L699-722.
163. Symons MC. *Cis*- and *trans*-conformations for peroxynitrite anions. J Inorg Biochem 2000; 78: 299-301.
164. Merenyi G, Lind J, Goldstein S, Czapski G. Peroxynitrous acid homolyzes into *OH and *NO_2 radicals. Chem Res Toxicol 1998; 11: 712-713.
165. Pfeiffer S, Mayer B. Lack of tyrosine nitration by peroxynitrite generated at physiological pH. J Biol Chem 1998; 273: 27280-27285.
166. Tsai J-HM, Harrison JG, Martin JC, Hamilton TP, van der Woerd M, Jablonsky MJ, Beckman JS. Role of conformation of peroxynitrite anion ($ONOO^-$) in its stability and toxicity. J Am Chem Soc 1994; 116: 4115-4116.
167. Tsai H-H, Hamilton TP, Tsai J-H, van der Woerd M, Harrison JG, Jablonsky MJ, Beckman JS, Koppenol WH. An *ab iInitio* study of peroxynitrite and peroxynitrous acid: important biological oxidants. J Phys Chem 1996; 100: 15087–15095.
168. Reiter CD, Teng RJ, Beckman JS. Superoxide reacts with nitric oxide to nitrate tyrosine at physiological pH via peroxynitrite. J Biol Chem 2000; 275: 32460-32466.
169. Sawa T, Akaike T, Maeda H. Tyrosine nitration by peroxynitrite formed from nitric oxide and superoxide generated by xanthine oxidase. J Biol Chem 2000; 275: 32467-32474.
170. Brunelli L, Crow JP, Beckman JS. The comparative toxicity of nitric oxide and peroxynitrite to *Escherichia coli*. Arch Biochem Biophys 1995; 316: 327-334.
171. Shin JT, Barbeito L, MacMillan-Crow LA, Beckman JS, Thompson JA. Acidic fibroblast growth factor enhances peroxynitrite-induced apoptosis in primary murine fibroblasts. Arch Biochem Biophys 1996; 335: 32-41.
172. Koppenol WH, Moreno JJ, Pryor WA, Ischiropoulos H, Beckman JS. Peroxynitrite, a cloaked oxidant formed by nitric oxide and superoxide. Chem Res Toxicol 1992; 5: 834-842.
173. Koppenol WH. Thermodynamics of reactions involving nitrogen-oxygen compounds. Methods Enzymol 1996; 268: 7-12.
174. Fritsche G, Larcher C, Schennach H, Weiss G. Regulatory interactions between iron and nitric oxide metabolism for immune defense against *Plasmodium falciparum* infection. J Infect Dis 2001; 183: 1388-1394.
175. Douki T, Cadet J. Peroxynitrite mediated oxidation of purine bases of nucleosides and isolated DNA. Free Radic Res 1996; 24: 369-380.
176. Salgo MG, Stone K, Squadrito GL, Battista JR, Pryor WA. Peroxynitrite causes DNA nicks in plasmid pBR322. Biochem Biophys Res Commun 1995; 210: 1025-1030.
177. Szabo C, Ohshima H. DNA damage induced by peroxynitrite: subsequent biological effects. Nitric Oxide 1997; 1: 373-385.
178. Szabo C. DNA strand breakage and activation of poly-ADP ribosyltransferase: a cytotoxic pathway triggered by peroxynitrite. Free Radic Biol Med 1996; 21: 855-869.
179. Zingarelli B, O'Connor M, Wong H, Salzman AL, Szabo C. Peroxynitrite-mediated DNA strand breakage activates poly-adenosine diphosphate ribosyl synthetase and causes cellular energy depletion in macrophages stimulated with bacterial lipopolysaccharide. J Immunol 1996; 156: 350-358.
180. Yermilov V, Rubio J, Ohshima H. Formation of 8-nitroguanine in DNA treated with peroxynitrite *in vitro* and its rapid removal from DNA by depurination. FEBS Lett 1995; 376: 207-210.
181. Van der Vliet A, Smith D, O'Neill CA, Kaur H, Darley-Usmar V, Cross CE, Halliwell B. Interactions of peroxynitrite with human plasma and its constituents: oxidative damage and antioxidant depletion. Biochem J 1994; 303 (Pt 1): 295-301.
182. Radi R, Beckman JS, Bush KM, Freeman BA. Peroxynitrite oxidation of sulfhydryls. The cytotoxic potential of superoxide and nitric oxide. J Biol Chem 1991; 266: 4244-4250.
183. Quijano C, Alvarez B, Gatti RM, Augusto O, Radi R. Pathways of peroxynitrite oxidation of thiol groups. Biochem J 1997; 322 (Pt 1): 167-173.

184. Radi R, Beckman JS, Bush KM, Freeman BA. Peroxynitrite-induced membrane lipid peroxidation: the cytotoxic potential of superoxide and nitric oxide. Arch Biochem Biophys 1991; 288: 481-487.
185. Beckman JS, Ischiropoulos H, Zhu L, van der Woerd M, Smith C, Chen J, Harrison J, Martin JC, Tsai M. Kinetics of superoxide dismutase- and iron-catalyzed nitration of phenolics by peroxynitrite. Arch Biochem Biophys 1992; 298: 438-445.
186. Alvarez B, Rubbo H, Kirk M, Barnes S, Freeman BA, Radi R. Peroxynitrite-dependent tryptophan nitration. Chem Res Toxicol 1996; 9: 390-396.
187. van der Vliet A, O'Neill CA, Halliwell B, Cross CE, Kaur H. Aromatic hydroxylation and nitration of phenylalanine and tyrosine by peroxynitrite. Evidence for hydroxyl radical production from peroxynitrite. FEBS Lett 1994; 339: 89-92.
188. Ischiropoulos H. Biological tyrosine nitration: a pathophysiological function of nitric oxide and reactive oxygen species. Arch Biochem Biophys 1998; 356: 1-11.
189. Shigenaga MK, Lee HH, Blount BC, Christen S, Shigeno ET, Yip H, Ames BN. Inflammation and $NO_{(X)}$-induced nitration: assay for 3-nitrotyrosine by HPLC with electrochemical detection. Proc Natl Acad Sci U S A 1997; 94: 3211-3216.
190. Minetti M, Pietraforte D, Carbone V, Salzano AM, Scorza G, Marino G. Scavenging of peroxynitrite by oxyhemoglobin and identification of modified globin residues. Biochemistry 2000; 39: 6689-6697.
191. Moro MA, Darley-Usmar VM, Goodwin DA, Read NG, Zamora-Pino R, Feelisch M, Radomski MW, Moncada S. Paradoxical fate and biological action of peroxynitrite on human platelets. Proc Natl Acad Sci U S A 1994; 91: 6702-6706.
192. van der Vliet A, Hoen PA, Wong PS, Bast A, Cross CE. Formation of *S*-nitrosothiols via direct nucleophilic nitrosation of thiols by peroxynitrite with elimination of hydrogen peroxide. J Biol Chem 1998; 273: 30255-30262.
193. Kharitonov VG, Sundquist AR, Sharma VS. Kinetics of nitrosation of thiols by nitric oxide in the presence of oxygen. J Biol Chem 1995; 270: 28158-28164.
194. Marley R, Patel RP, Orie N, Ceaser E, Darley-Usmar V, Moore K. Formation of nanomolar concentrations of *S*-nitroso-albumin in human plasma by nitric oxide. Free Radic Biol Med 2001; 31: 688-696.
195. Wink DA, Cook JA, Kim SY, Vodovotz Y, Pacelli R, Krishna MC, Russo A, Mitchell JB, Jourd'heuil D, Miles AM, Grisham MB. Superoxide modulates the oxidation and nitrosation of thiols by nitric oxide-derived reactive intermediates. Chemical aspects involved in the balance between oxidative and nitrosative stress. J Biol Chem 1997; 272: 11147-11151.
196. Scorza G, Minetti M. One-electron oxidation pathway of thiols by peroxynitrite in biological fluids: bicarbonate and ascorbate promote the formation of albumin disulphide dimers in human blood plasma. Biochem J 1998; 329 (Pt 2): 405-413.
197. Moro MA, Darley-Usmar VM, Lizasoain I, Su Y, Knowles RG, Radomski MW, Moncada S. The formation of nitric oxide donors from peroxynitrite. Br J Pharmacol 1995; 116: 1999-2004.
198. Wu M, Pritchard KA, Jr., Kaminski PM, Fayngersh RP, Hintze TH, Wolin MS. Involvement of nitric oxide and nitrosothiols in relaxation of pulmonary arteries to peroxynitrite. Am J Physiol 1994; 266: H2108-2113.
199. Miles AM, Bohle DS, Glassbrenner PA, Hansert B, Wink DA, Grisham MB. Modulation of superoxide-dependent oxidation and hydroxylation reactions by nitric oxide. J Biol Chem 1996; 271: 40-47.
200. Wink DA, Grisham MB, Miles AM, Nims RW, Krishna MC, Pacelli R, Teague D, Poore CM, Cook JA, Ford PC. Determination of selectivity of reactive nitrogen oxide species for various substrates. Methods Enzymol 1996; 268: 120-130.
201. Wink DA, Nims RW, Darbyshire JF, Christodoulou D, Hanbauer I, Cox GW, Laval F, Laval J, Cook JA, Krishna MC, DeGraff W, Mitchell JB. Reaction kinetics for nitrosation of cysteine and glutathione in aerobic nitric oxide solutions at neutral pH. Insights into the fate and physiological effects of intermediates generated in the NO/O_2 reaction. Chem Res Toxicol 1994; 7: 519-525.
202. Beckman JS. Oxidative damage and tyrosine nitration from peroxynitrite. Chem Res Toxicol 1996; 9: 836-844.

203. Eiserich JP, Cross CE, Jones AD, Halliwell B, van der Vliet A. Formation of nitrating and chlorinating species by reaction of nitrite with hypochlorous acid. A novel mechanism for nitric oxide-mediated protein modification. J Biol Chem 1996; 271: 19199-19208.
204. Eiserich JP, Hristova M, Cross CE, Jones AD, Freeman BA, Halliwell B, van der Vliet A. Formation of nitric oxide-derived inflammatory oxidants by myeloperoxidase in neutrophils. Nature 1998; 391: 393-397.
205. Gunther MR, Hsi LC, Curtis JF, Gierse JK, Marnett LJ, Eling TE, Mason RP. Nitric oxide trapping of the tyrosyl radical of prostaglandin H synthase-2 leads to tyrosine iminoxyl radical and nitrotyrosine formation. J Biol Chem 1997; 272: 17086-17090.
206. van der Vliet A, Eiserich JP, O'Neill CA, Halliwell B, Cross CE. Tyrosine modification by reactive nitrogen species: a closer look. Arch Biochem Biophys 1995; 319: 341-349.
207. Ischiropoulos H, Zhu L, Chen J, Tsai M, Martin JC, Smith CD, Beckman JS. Peroxynitrite-mediated tyrosine nitration catalyzed by superoxide dismutase. Arch Biochem Biophys 1992; 298: 431-437.
208. Prutz WA, Monig H, Butler J, Land EJ. Reactions of nitrogen dioxide in aqueous model systems: oxidation of tyrosine units in peptides and proteins. Arch Biochem Biophys 1985; 243: 125-134.
209. Kikugawa K, Kato T, Okamoto Y. Damage of amino acids and proteins induced by nitrogen dioxide, a free radical toxin, in air. Free Radic Biol Med 1994; 16: 373-382.
210. Davis KL, Martin E, Turko IV, Murad F. Novel effects of nitric oxide. Annu Rev Pharmacol Toxicol 2001; 41: 203-236.
211. Turko IV, Murad F. Protein nitration in cardiovascular diseases. Pharmacol Rev 2002; 54: 619-634.
212. Ischiropoulos H, al-Mehdi AB. Peroxynitrite-mediated oxidative protein modifications. FEBS Lett 1995; 364: 279-282.
213. Gow A, Duran D, Thom SR, Ischiropoulos H. Carbon dioxide enhancement of peroxynitrite-mediated protein tyrosine nitration. Arch Biochem Biophys 1996; 333: 42-48.
214. Gow AJ, Duran D, Malcolm S, Ischiropoulos H. Effects of peroxynitrite-induced protein modifications on tyrosine phosphorylation and degradation. FEBS Lett 1996; 385: 63-66.
215. Zhu L, Gunn C, Beckman JS. Bactericidal activity of peroxynitrite. Arch Biochem Biophys 1992; 298: 452-457.
216. Sampson JB, Rosen H, Beckman JS. Peroxynitrite-dependent tyrosine nitration catalyzed by superoxide dismutase, myeloperoxidase, and horseradish peroxidase. Methods Enzymol 1996; 269: 210-218.
217. Bonini MG, Radi R, Ferrer-Sueta G, Ferreira AM, Augusto O. Direct EPR detection of the carbonate radical anion produced from peroxynitrite and carbon dioxide. J Biol Chem 1999; 274: 10802-10806.
218. Lehnig M. Radical mechanisms of the decomposition of peroxynitrite and the peroxynitrite-CO_2 adduct and of reactions with L-tyrosine and related compounds as studied by ^{15}N chemically induced dynamic nuclear polarization. Arch Biochem Biophys 1999; 368: 303-318.
219. Augusto O, Bonini MG, Amanso AM, Linares E, Santos CC, De Menezes SL. Nitrogen dioxide and carbonate radical anion: two emerging radicals in biology. Free Radic Biol Med 2002; 32: 841-859.
220. Ischiropoulos H, Nelson J, Duran D, Al-Mehdi A. Reactions of nitric oxide and peroxynitrite with organic molecules and ferrihorseradish peroxidase: interference with the determination of hydrogen peroxide. Free Radic Biol Med 1996; 20: 373-381.
221. O'Donnell VB, Chumley PH, Hogg N, Bloodsworth A, Darley-Usmar VM, Freeman BA. Nitric oxide inhibition of lipid peroxidation: kinetics of reaction with lipid peroxyl radicals and comparison with α-tocopherol. Biochemistry 1997; 36: 15216-15223.
222. van der Vliet A, Eiserich JP, Kaur H, Cross CE, Halliwell B. Nitrotyrosine as biomarker for reactive nitrogen species. Methods Enzymol 1996; 269: 175-184.
223. Halliwell B, Gutteridge JM. Role of free radicals and catalytic metal ions in human disease: an overview. Methods Enzymol 1990; 186: 1-85.
224. Bian K, Gao Z, Weisbrodt N, Murad F. The nature of heme/iron-induced protein tyrosine nitration. Proc Natl Acad Sci U S A 2003.

225. van der Vliet A, Eiserich JP, Halliwell B, Cross CE. Formation of reactive nitrogen species during peroxidase-catalyzed oxidation of nitrite. A potential additional mechanism of nitric oxide-dependent toxicity. J Biol Chem 1997; 272: 7617-7625.
226. Kettle AJ, van Dalen CJ, Winterbourn CC. Peroxynitrite and myeloperoxidase leave the same footprint in protein nitration. Redox Rep 1997; 3: 257-258.
227. Cohen G, Martinez M, Hochstein P. Generation of hydrogen peroxide during the reaction of nitrate with oxyhemoglobin. Biochemistry 1964; 155: 901-903.
228. Grzelak A, Balcerczyk A, Mateja A, Bartosz G. Hemoglobin can nitrate itself and other proteins. Biochim Biophys Acta 2001; 1528: 97-100.
229. Knowles ME, McWeeny DJ, Couchman L, Thorogood M. Interaction of nitrite with proteins at gastric pH. Nature 1974; 247: 288-289.
230. Natake M, Ueda M. Changes in food proteins reacted with nitrite at gastric pH. Nutr Cancer 1986; 8: 41-45.
231. Panasenko OM, Briviba K, Klotz LO, Sies H. Oxidative modification and nitration of human low-density lipoproteins by the reaction of hypochlorous acid with nitrite. Arch Biochem Biophys 1997; 343: 254-259.
232. Viera L, Ye YZ, Estevez AG, Beckman JS. Immunohistochemical methods to detect nitrotyrosine. Methods Enzymol 1999; 301: 373-381.
233. Gaston B, Reilly J, Drazen JM, Fackler J, Ramdev P, Arnelle D, Mullins ME, Sugarbaker DJ, Chee C, Singel DJ, Loscalzo J, Stamler J. Endogenous nitrogen oxides and bronchodilator *S*-nitrosothiols in human airways. Proc Natl Acad Sci U S A 1993; 90: 10957-10961.
234. Ottesen LH, Harry D, Frost M, Davies S, Khan K, Halliwell B, Moore K. Increased formation of S-nitrothiols and nitrotyrosine in cirrhotic rats during endotoxemia. Free Radic Biol Med 2001; 31: 790-798.
235. Pryor WA, Church DF, Govindan CK, Crank G. Oxidation of thiols by nitric oxide and nitrogen dioxide: synthetic utility and toxicological implications. J Org Chem 1982; 47: 156-159.
236. Walker MW, Kinter MT, Roberts RJ, Spitz DR. Nitric oxide-induced cytotoxicity: involvement of cellular resistance to oxidative stress and the role of glutathione in protection. Pediatr Res 1995; 37: 41-49.
237. DeMaster EG, Quast BJ, Redfern B, Nagasawa HT. Reaction of nitric oxide with the free sulfhydryl group of human serum albumin yields a sulfenic acid and nitrous oxide. Biochemistry 1995; 34: 11494-11499.
238. Foster MW, McMahon TJ, Stamler JS. *S*-nitrosylation in health and disease. Trends Mol Med 2003; 9: 160-168.
239. Hogg N. The biochemistry and physiology of *S*-nitrosothiols. Annu Rev Pharmacol Toxicol 2002; 42: 585-600.
240. Upchurch GR, Jr., Welch GN, Loscalzo J. *S*-nitrosothiols: chemistry, biochemistry, and biological actions. Adv Pharmacol 1995; 34: 343-349.
241. Espey MG, Thomas DD, Miranda KM, Wink DA. Focusing of nitric oxide mediated nitrosation and oxidative nitrosylation as a consequence of reaction with superoxide. Proc Natl Acad Sci U S A 2002; 99: 11127-11132.
242. Hogg N. Biological chemistry and clinical potential of *S*-nitrosothiols. Free Radic Biol Med 2000; 28: 1478-1486.
243. Boese M, Mordvintcev PI, Vanin AF, Busse R, Mulsch A. *S*-nitrosation of serum albumin by dinitrosyl-iron complex. J Biol Chem 1995; 270: 29244-29249.
244. Stamler JS, Toone EJ, Lipton SA, Sucher NJ. (S)NO signals: translocation, regulation, and a consensus motif. Neuron 1997; 18: 691-696.
245. Ignarro LJ, Lippton H, Edwards JC, Baricos WH, Hyman AL, Kadowitz PJ, Gruetter CA. Mechanism of vascular smooth muscle relaxation by organic nitrates, nitrites, nitroprusside and nitric oxide: evidence for the involvement of *S*-nitrosothiols as active intermediates. J Pharmacol Exp Ther 1981; 218: 739-749.
246. Minamiyama Y, Takemura S, Inoue M. Albumin is an important vascular tonus regulator as a reservoir of nitric oxide. Biochem Biophys Res Commun 1996; 225: 112-115.
247. Jia L, Bonaventura C, Bonaventura J, Stamler JS. *S*-nitrosohaemoglobin: a dynamic activity of blood involved in vascular control. Nature 1996; 380: 221-226.

248. Cooke JP, Stamler J, Andon N, Davies PF, McKinley G, Loscalzo J. Flow stimulates endothelial cells to release a nitrovasodilator that is potentiated by reduced thiol. Am J Physiol 1990; 259: H804-812.
249. Kowaluk EA, Fung HL. Spontaneous liberation of nitric oxide cannot account for in vitro vascular relaxation by *S*-nitrosothiols. J Pharmacol Exp Ther 1990; 255: 1256-1264.
250. Singh RJ, Hogg N, Joseph J, Kalyanaraman B. Mechanism of nitric oxide release from *S*-nitrosothiols. J Biol Chem 1996; 271: 18596-18603.
251. Nikitovic D, Holmgren A. *S*-nitrosoglutathione is cleaved by the thioredoxin system with liberation of glutathione and redox regulating nitric oxide. J Biol Chem 1996; 271: 19180-19185.
252. Barnett DJ, McAninly J, Williams DLH. Transnitrosation between nitrosothiols and thiols. J Chem Soc Perkin Trans 1994; 2: 1131-1133.
253. Barnett DJ, Rios A, Williams DLH. NO-group transfer (transnitrosation) between *S*-nitrosothiols and thiols. Part 2. J Chem Soc Perkin Trans 1994; 2: 1279-1282.
254. Wang K, Wen Z, Zhang W, Xian M, Cheng JP, Wang PG. Equilibrium and kinetics studies of transnitrosation between *S*-nitrosothiols and thiols. Bioorg Med Chem Lett 2001; 11: 433-436.
255. Stamler JS. *S*-nitrosothiols and the bioregulatory actions of nitrogen oxides through reactions with thiol groups. Curr Top Microbiol Immunol 1995; 196: 19-36.
256. Xian M, Wang K, Chen X, Hou Y, McGill A, Zhou B, Zhang ZY, Cheng JP, Wang PG. Inhibition of protein tyrosine phosphatases by low-molecular-weight *S*-nitrosothiols and *S*-nitrosylated human serum albumin. Biochem Biophys Res Commun 2000; 268: 310-314.
257. Hogg N. The kinetics of *S*-transnitrosation--a reversible second-order reaction. Anal Biochem 1999; 272: 257-262.
258. Williams DL. *S*-nitrosothiols and role of metal ions in decomposition to nitric oxide. Methods Enzymol 1996; 268: 299-308.
259. Scorza G, Pietraforte D, Minetti M. Role of ascorbate and protein thiols in the release of nitric oxide from *S*-nitroso-albumin and *S*-nitroso-glutathione in human plasma. Free Radic Biol Med 1997; 22: 633-642.
260. Kashiba-Iwatsuki M, Yamaguchi M, Inoue M. Role of ascorbic acid in the metabolism of *S*-nitroso-glutathione. FEBS Lett 1996; 389: 149-152.
261. DeGroote MA, Granger D, Xu Y, Campbell G, Prince R, Fang FC. Genetic and redox determinants of nitric oxide cytotoxicity in a *Salmonella typhimurium* model. Proc Natl Acad Sci U S A 1995; 92: 6399-6403.
262. Morris SL, Walsh RC, Hansen JN. Identification and characterization of some bacterial membrane sulfhydryl groups which are targets of bacteriostatic and antibiotic action. J Biol Chem 1984; 259: 13590-13594.
263. Roy B, Lepoivre M, Henry Y, Fontecave M. Inhibition of ribonucleotide reductase by nitric oxide derived from thionitrites: reversible modifications of both subunits. Biochemistry 1995; 34: 5411-5418.
264. Venturini G, Colasanti M, Salvati L, Gradoni L, Ascenzi P. Nitric oxide inhibits falcipain, the *Plasmodium falciparum* trophozoite cysteine protease. Biochem Biophys Res Commun 2000; 267: 190-193.
265. Gamboa de Dominguez ND, Rosenthal PJ. Cysteine proteinase inhibitors block early steps in hemoglobin degradation by cultured malaria parasites. Blood 1996; 87: 4448-4454.
266. Olson JE, Lee GK, Semenov A, Rosenthal PJ. Antimalarial effects in mice of orally administered peptidyl cysteine protease inhibitors. Bioorg Med Chem 1999; 7: 633-638.
267. Aleryani S, Milo E, Rose Y, Kostka P. Superoxide-mediated decomposition of biological *S*-nitrosothiols. J Biol Chem 1998; 273: 6041-6045.
268. Jourd'heuil D, Mai CT, Laroux FS, Wink DA, Grisham MB. The reaction of *S*-nitrosoglutathione with superoxide. Biochem Biophys Res Commun 1998; 244: 525-530.
269. Trujillo M, Alvarez MN, Peluffo G, Freeman BA, Radi R. Xanthine oxidase-mediated decomposition of *S*-nitrosothiols. J Biol Chem 1998; 273: 7828-7834.
270. Hess DT, Matsumoto A, Nudelman R, Stamler JS. *S*-nitrosylation: spectrum and specificity. Nat Cell Biol 2001; 3: E46-49.
271. Stamler JS, Lamas S, Fang FC. Nitrosylation. the prototypic redox-based signaling mechanism. Cell 2001; 106: 675-683.

272. Gow AJ, Farkouh CR, Munson DA, Posencheg MA, Ischiropoulos H. Biological significance of nitric oxide-mediated protein modifications. Am J Physiol Lung Cell Mol Physiol 2004; 287: L262-268.
273. Gardner PR, Gardner AM, Martin LA, Salzman AL. Nitric oxide dioxygenase: an enzymic function for flavohemoglobin. Proc Natl Acad Sci U S A 1998; 95: 10378-10383.
274. Hausladen A, Gow A, Stamler JS. Flavohemoglobin denitrosylase catalyzes the reaction of a nitroxyl equivalent with molecular oxygen. Proc Natl Acad Sci U S A 2001; 98: 10108-10112.
275. Durner J, Gow AJ, Stamler JS, Glazebrook J. Ancient origins of nitric oxide signaling in biological systems. Proc Natl Acad Sci U S A 1999; 96: 14206-14207.
276. Minning DM, Gow AJ, Bonaventura J, Braun R, Dewhirst M, Goldberg DE, Stamler JS. *Ascaris* haemoglobin is a nitric oxide-activated 'deoxygenase'. Nature 1999; 401: 497-502.
277. Liu L, Zeng M, Hausladen A, Heitman J, Stamler JS. Protection from nitrosative stress by yeast flavohemoglobin. Proc Natl Acad Sci U S A 2000.
278. Wennmalm A, Benthin G, Petersson AS. Dependence of the metabolism of nitric oxide (NO) in healthy human whole blood on the oxygenation of its red cell haemoglobin. Br J Pharmacol 1992; 106: 507-508.
279. Doyle MP, Hoekstra JW. Oxidation of nitrogen oxides by bound dioxygen in hemoproteins. J Inorg Biochem 1981; 14: 351-358.
280. Taylor-Robinson AW, Looker M. Sensitivity of malaria parasites to nitric oxide at low oxygen tensions. Lancet 1998; 351: 1630.
281. Jourd'heuil D, Hallen K, Feelisch M, Grisham MB. Dynamic state of *S*-nitrosothiols in human plasma and whole blood. Free Radic Biol Med 2000; 28: 409-417.
282. DeGroote MA, Testerman T, Xu Y, Stauffer G, Fang FC. Homocysteine antagonism of nitric oxide-related cytostasis in *Salmonella typhimurium*. Science 1996; 272: 414-417.
283. DeGroote MA, Fang FC. Chapter 12: Antimicrobial properties of nitric oxide. In: Fang FC (ed.) Nitric Oxide and Infection. New York: Kluwer Academic/Plenum Publishers; 1999: 231-261.
284. Tsaneva IR, Weiss B. *soxR*, a locus governing a superoxide response regulon in *Escherichia coli* K-12. J Bacteriol 1990; 172: 4197-4205.
285. Nunoshiba T, deRojas-Walker T, Wishnok JS, Tannenbaum SR, Demple B. Activation by nitric oxide of an oxidative-stress response that defends *Escherichia coli* against activated macrophages. Proc Natl Acad Sci U S A 1993; 90: 9993-9997.
286. Vasil'eva SV, Stupakova MV, Lobysheva, II, Mikoyan VD, Vanin AF. Activation of the *Escherichia coli* SoxRS-regulon by nitric oxide and its physiological donors. Biochemistry (Mosc) 2001; 66: 984-988.
287. Nunoshiba T, DeRojas-Walker T, Tannenbaum SR, Demple B. Roles of nitric oxide in inducible resistance of *Escherichia coli* to activated murine macrophages. Infect Immun 1995; 63: 794-798.
288. Christman MF, Morgan RW, Jacobson FS, Ames BN. Positive control of a regulon for defenses against oxidative stress and some heat-shock proteins in *Salmonella typhimurium*. Cell 1985; 41: 753-762.
289. Hausladen A, Privalle CT, Keng T, DeAngelo J, Stamler JS. Nitrosative stress: activation of the transcription factor OxyR. Cell 1996; 86: 719-729.
290. Hand CE, Honek JF. Biological chemistry of naturally occurring thiols of microbial and marine origin. J Nat Prod 2005; 68: 293-308.
291. Vogt RN, Steenkamp DJ. The metabolism of *S*-nitrosothiols in the trypanosomatids: the role of ovothiol A and trypanothione. Biochem J 2003; 371: 49-59.
292. Buchmeier NA, Newton GL, Koledin T, Fahey RC. Association of mycothiol with protection of *Mycobacterium tuberculosis* from toxic oxidants and antibiotics. Mol Microbiol 2003; 47: 1723-1732.
293. Rawat M, Newton GL, Ko M, Martinez GJ, Fahey RC, Av-Gay Y. Mycothiol-deficient *Mycobacterium smegmatis* mutants are hypersensitive to alkylating agents, free radicals, and antibiotics. Antimicrob Agents Chemother 2002; 46: 3348-3355.
294. Vogt RN, Steenkamp DJ, Zheng R, Blanchard JS. The metabolism of nitrosothiols in the *Mycobacteria*: identification and characterization of *S*-nitrosomycothiol reductase. Biochem J 2003; 374: 657-666.

295. Thomson L, Denicola A, Radi R. The trypanothione-thiol system in *Trypanosoma cruzi* as a key antioxidant mechanism against peroxynitrite-mediated cytotoxicity. Arch Biochem Biophys 2003; 412: 55-64.
296. Luperchio S, Tamir S, Tannenbaum SR. NO-induced oxidative stress and glutathione metabolism in rodent and human cells. Free Radic Biol Med 1996; 21: 513-519.
297. Tian L, Shi MM, Forman HJ. Increased transcription of the regulatory subunit of γ-glutamylcysteine synthetase in rat lung epithelial L2 cells exposed to oxidative stress or glutathione depletion. Arch Biochem Biophys 1997; 342: 126-133.
298. Kim SJ, Kim HG, Kim BC, Kim K, Park EH, Lim CJ. Transcriptional regulation of the gene encoding γ-glutamylcysteine synthetase from the fission yeast *Schizosaccharomyces pombe*. J Microbiol 2004; 42: 233-238.
299. Moellering D, Mc Andrew J, Patel RP, Forman HJ, Mulcahy RT, Jo H, Darley-Usmar VM. The induction of GSH synthesis by nanomolar concentrations of NO in endothelial cells: a role for γ-glutamylcysteine synthetase and γ-glutamyl transpeptidase. FEBS Lett 1999; 448: 292-296.
300. Kanzok SM, Fechner A, Bauer H, Ulschmid JK, Muller HM, Botella-Munoz J, Schneuwly S, Schirmer RH, Becker K. Substitution of the thioredoxin system for glutathione reductase in *Drosophila melanogaster*. Science 2001; 291: 643-646.
301. Bauer H, Gromer S, Urbani A, Schnolzer M, Schirmer RH, Muller HM. Thioredoxin reductase from the malaria mosquito *Anopheles gambiae*. Eur J Biochem 2003; 270: 4272-4281.
302. Kanzok SM, Schirmer RH, Turbachova I, Iozef R, Becker K. The thioredoxin system of the malaria parasite *Plasmodium falciparum*. Glutathione reduction revisited. J Biol Chem 2000; 275: 40180-40186.
303. Ferret PJ, Soum E, Negre O, Wollman EE, Fradelizi D. Protective effect of thioredoxin upon NO-mediated cell injury in THP1 monocytic human cells. Biochem J 2000; 346 Pt 3: 759-765.
304. Haqqani AS, Do SK, Birnboim HC. The role of a formaldehyde dehydrogenase-glutathione pathway in protein *S*-nitrosation in mammalian cells. Nitric Oxide 2003; 9: 172-181.
305. Liu L, Hausladen A, Zeng M, Que L, Heitman J, Stamler JS. A metabolic enzyme for *S*-nitrosothiol conserved from bacteria to humans. Nature 2001; 410: 490-494.
306. Chen L, Xie QW, Nathan C. Alkyl hydroperoxide reductase subunit C (AhpC) protects bacterial and human cells against reactive nitrogen intermediates. Mol Cell 1998; 1: 795-805.
307. Peshenko IV, Shichi H. Oxidation of active center cysteine of bovine 1-Cys peroxiredoxin to the cysteine sulfenic acid form by peroxide and peroxynitrite. Free Radic Biol Med 2001; 31: 292-303.
308. Bryk R, Griffin P, Nathan C. Peroxynitrite reductase activity of bacterial peroxiredoxins. Nature 2000; 407: 211-215.
309. Sakamoto A, Tsukamoto S, Yamamoto H, Ueda-Hashimoto M, Takahashi M, Suzuki H, Morikawa H. Functional complementation in yeast reveals a protective role of chloroplast 2-Cys peroxiredoxin against reactive nitrogen species. Plant J 2003; 33: 841-851.
310. Komaki-Yasuda K, Kawazu S, Kano S. Disruption of the *Plasmodium falciparum* 2-Cys peroxiredoxin gene renders parasites hypersensitive to reactive oxygen and nitrogen species. FEBS Lett 2003; 547: 140-144.
311. Master SS, Springer B, Sander P, Boettger EC, Deretic V, Timmins GS. Oxidative stress response genes in *Mycobacterium tuberculosis*: role of AhpC in resistance to peroxynitrite and stage-specific survival in macrophages. Microbiology 2002; 148: 3139-3144.
312. Loprasert S, Sallabhan R, Whangsuk W, Mongkolsuk S. Compensatory increase in ahpC gene expression and its role in protecting *Burkholderia pseudomallei* against reactive nitrogen intermediates. Arch Microbiol 2003; 180: 498-502.
313. Immenschuh S, Stritzke J, Iwahara S, Ramadori G. Up-regulation of heme-binding protein 23 (HBP23) gene expression by lipopolysaccharide is mediated via a nitric oxide-dependent signaling pathway in rat Kupffer cells. Hepatology 1999; 30: 118-127.
314. Barr SD, Gedamu L. Role of peroxidoxins in *Leishmania chagasi* survival: Evidence of an enzymatic defense against nitrosative stress. J Biol Chem 2003: 10816-10823.
315. Wong CM, Siu KL, Jin DY. Peroxiredoxin-null yeast cells are hypersensitive to oxidative stress and are genomically unstable. J Biol Chem 2004; 279: 23207-23213.

316. Wong CM, Zhou Y, Ng RW, Kung Hf HF, Jin DY. Cooperation of yeast peroxiredoxins Tsa1p and Tsa2p in the cellular defense against oxidative and nitrosative stress. J Biol Chem 2002; 277: 5385-5394.
317. Dubuisson M, Vander Stricht D, Clippe A, Etienne F, Nauser T, Kissner R, Koppenol WH, Rees JF, Knoops B. Human peroxiredoxin 5 is a peroxynitrite reductase. FEBS Lett 2004; 571: 161-165.
318. Trujillo M, Budde H, Pineyro MD, Stehr M, Robello C, Flohe L, Radi R. *Trypanosoma brucei* and *Trypanosoma cruzi* tryparedoxin peroxidases catalytically detoxify peroxynitrite via oxidation of fast reacting thiols. J Biol Chem 2004.
319. Bryk R, Lima CD, Erdjument-Bromage H, Tempst P, Nathan C. Metabolic enzymes of mycobacteria linked to antioxidant defense by a thioredoxin-like protein. Science 2002; 295: 1073-1077.
320. Hausladen A, Gow AJ, Stamler JS. Nitrosative stress: metabolic pathway involving the flavohemoglobin. Proc Natl Acad Sci U S A 1998; 95: 14100-14105.
321. Poole RK, Anjum MF, Membrillo-Hernandez J, Kim SO, Hughes MN, Stewart V. Nitric oxide, nitrite, and Fnr regulation of *hmp* (flavohemoglobin) gene expression in *Escherichia coli* K-12. J Bacteriol 1996; 178: 5487-5492.
322. Membrillo-Hernandez J, Coopamah MD, Anjum MF, Stevanin TM, Kelly A, Hughes MN, Poole RK. The flavohemoglobin of *Escherichia coli* confers resistance to a nitrosating agent, a "nitric oxide releaser" and paraquat and is essential for transcriptional responses to oxidative stress. J Biol Chem 1999; 274: 748-754.
323. Hu Y, Butcher PD, Mangan JA, Rajandream MA, Coates AR. Regulation of *hmp* gene transcription in *Mycobacterium tuberculosis*: effects of oxygen limitation and nitrosative and oxidative stress. J Bacteriol 1999; 181: 3486-3493.
324. Crawford MJ, Goldberg DE. Role for the *Salmonella* flavohemoglobin in protection from nitric oxide. J Biol Chem 1998; 273: 12543-12547.
325. Elvers KT, Wu G, Gilberthorpe NJ, Poole RK, Park SF. Role of an inducible single-domain hemoglobin in mediating resistance to nitric oxide and nitrosative stress in *Campylobacter jejuni* and *Campylobacter coli*. J Bacteriol 2004; 186: 5332-5341.
326. Ouellet H, Ouellet Y, Richard C, Labarre M, Wittenberg B, Wittenberg J, Guertin M. Truncated hemoglobin HbN protects *Mycobacterium bovis* from nitric oxide. Proc Natl Acad Sci U S A 2002; 99: 5902-5907.
327. Liu L, Zeng M, Stamler JS. Hemoglobin induction in mouse macrophages. Proc Natl Acad Sci U S A 1999; 96: 6643-6647.
328. Han YS, Thompson J, Kafatos FC, Barillas-Mury C. Molecular interactions between *Anopheles stephensi* midgut cells and *Plasmodium berghei*: the time bomb theory of ookinete invasion of mosquitoes. EMBO J 2000; 19: 6030-6040.
329. Al-Olayan EM, Williams GT, Hurd H. Apoptosis in the malaria protozoan, *Plasmodium berghei*: a possible mechanism for limiting intensity of infection in the mosquito. Int J Parasitol 2002; 32: 1133-1143.
330. Ghosh A, Edwards MJ, Jacobs-Lorena M. The journey of the malaria parasite in the mosquito: hopes for the new century. Parasitol Today 2000; 16: 196-201.
331. Bredt DS, Snyder SH. Nitric oxide mediates glutamate-linked enhancement of cGMP levels in the cerebellum. Proc Natl Acad Sci U S A 1989; 86: 9030-9033.
332. Kolb H, Kolb-Bachofen V. Nitric oxide: a pathogenetic factor in autoimmunity. Immunol Today 1992; 13: 157-160.
333. Moncada S, Palmer RM, Higgs EA. Nitric oxide: physiology, pathophysiology, and pharmacology. Pharmacol Rev 1991; 43: 109-142.
334. Miranda KM, Espey MG, Wink DA. A discussion of the chemistry of oxidative and nitrosative stress in cytotoxicity. J Inorg Biochem 2000; 79: 237-240.
335. Eiserich JP, Patel RP, O'Donnell VB. Pathophysiology of nitric oxide and related species: free radical reactions and modification of biomolecules. Mol Aspects Med 1998; 19: 221-357.
336. Denicola A, Rubbo H, Rodriguez D, Radi R. Peroxynitrite-mediated cytotoxicity to *Trypanosoma cruzi*. Arch Biochem Biophys 1993; 304: 279-286.

337. Linares E, Giorgio S, Mortara RA, Santos CX, Yamada AT, Augusto O. Role of peroxynitrite in macrophage microbicidal mechanisms *in vivo* revealed by protein nitration and hydroxylation. Free Radic Biol Med 2001; 30: 1234-1242.
338. Vazquez-Torres A, Jones-Carson J, Balish E. Peroxynitrite contributes to the candidacidal activity of nitric oxide-producing macrophages. Infect Immun 1996; 64: 3127-3133.
339. Denicola A, Souza JM, Radi R. Diffusion of peroxynitrite across erythrocyte membranes. Proc Natl Acad Sci U S A 1998; 95: 3566-3571.
340. Ignarro LJ. Biosynthesis and metabolism of endothelium-derived nitric oxide. Annu Rev Pharmacol Toxicol 1990; 30: 535-560.
341. Radi R, Peluffo G, Alvarez MN, Naviliat M, Cayota A. Unraveling peroxynitrite formation in biological systems. Free Radic Biol Med 2001; 30: 463-488.
342. Ohshima H, Friesen M, Brouet I, Bartsch H. Nitrotyrosine as a new marker for endogenous nitrosation and nitration of proteins. Food Chem Toxicol 1990; 28: 647-652.
343. Radi R. Nitric oxide, oxidants, and protein tyrosine nitration. Proc Natl Acad Sci U S A 2004.
344. Monzani E, Roncone R, Galliano M, Koppenol WH, Casella L. Mechanistic insight into the peroxidase catalyzed nitration of tyrosine derivatives by nitrite and hydrogen peroxide. Eur J Biochem 2004; 271: 895-906.
345. Minamiyama Y, Takemura S, Inoue M. Effect of thiol status on nitric oxide metabolism in the circulation. Arch Biochem Biophys 1997; 341: 186-192.
346. Taylor-Robinson AW. Antimalarial activity of nitric oxide: cytostasis and cytotoxicity towards *Plasmodium falciparum*. Biochem Soc Trans 1997; 25: 262S.
347. Taylor-Robinson AW. Nitric oxide can be released as well as scavenged by haemoglobin: relevance to its antimalarial activity [letter; comment]. Parasite Immunol 1998; 20: 49-50.
348. Balmer P, Phillips HM, Maestre AE, McMonagle FA, Phillips RS. The effect of nitric oxide on the growth of *Plasmodium falciparum*, *P. chabaudi* and *P. berghei in vitro*. Parasite Immunol 2000; 22: 97-106.
349. Antonini E, Brunori M. Hemoglobin and myoglobin in their reactions with ligands. Elsevier Press, NewYork; 1971.
350. Griess JP. Ber Deutsch Chem Ger 1879; 12: 426.
351. Green LC, Wagner DA, Glogowski J, Skipper PL, Wishnok JS, Tannenbaum SR. Analysis of nitrate, nitrite, and [^{15}N]nitrate in biological fluids. Anal Biochem 1982; 126: 131-138.
352. Davison W, Woof C. Comparison of different forms of cadmium as reducing agents for the batch determination of nitrate. Analyst 1978; 103: 403-406.
353. Gutman SI, Hollywood CA. Simple, rapid method for determining nitrates and nitrites in biological fluids. Clin Chem 1992; 38: 2152.
354. Fontijn A, Sabadell AJ, Ronco RJ. Homogeneous chemiluminescent measurement of nitric oxide with ozone. Implications for continuous selective monitoring of gaseous air pollutants. Anal Chem 1970; 42: 575–579.
355. Beckman JS, Conger KA. Direct measurement of dilute nitric oxide in solution with an ozone chemiluminescent detector. Methods: A companion to methods in enzymology 1995; 7: 35–39.
356. Yang F, Troncy E, Francoeur M, Vinet B, Vinay P, Czaika G, Blaise G. Effects of reducing reagents and temperature on conversion of nitrite and nitrate to nitric oxide and detection of NO by chemiluminescence. Clin Chem 1997; 43: 657-662.
357. McMurtry MS, Kim DH, Dinh-Xuan T, Archer SL. Nitric oxide and superoxide in biological systems -- Measurement of nitric oxide, nitrite and nitrate using chemiluminescence assay: an update for the year 2000. Analusis 2000; 28: 455-465.
358. Nitric oxide analyzer: operations and service manual (version D). In. Boulder, CO, USA: Sievers Instruments, Inc.; October 1999.
359. Gladwin MT, Wang X, Reiter CD, Yang BK, Vivas EX, Bonaventura C, Schechter AN. *S*-Nitrosohemoglobin is unstable in the reductive erythrocyte environment and lacks O_2/NO-linked allosteric function. J Biol Chem 2002; 277: 27818-27828.
360. Alpert C, Ramdev N, George D, Loscalzo J. Detection of *S*-nitrosothiols and other nitric oxide derivatives by photolysis-chemiluminescence spectrometry. Anal Biochem 1997; 245: 1-7.
361. Feelisch M, Rassaf T, Mnaimneh S, Singh N, Bryan NS, Jourd'Heuil D, Kelm M. Concomitant *S*-, *N*-, and heme-nitros(yl)ation in biological tissues and fluids: implications for the fate of NO in vivo. Faseb J 2002; 16: 1775-1785.

362. Miranda KM, Espey MG, Wink DA. A rapid, simple spectrophotometric method for simultaneous detection of nitrate and nitrite. Nitric Oxide 2001; 5: 62-71.
363. Archer SL, Shultz PJ, Warren JB, Hampl V, DeMaster EG. Preparation of standards and measurement of nitric oxide, nitroxyl, and related oxidation products. Methods: A companion to methods in enzymology 1995; 7: 21-34.
364. Hendrix SA, Braman RS. Determination of nitrite and nitrate by vanadium(III) reduction with chemiluminescence detection. Methods: A companion to methods in enzymology 1995: 91-97.
365. Fang K, Ragsdale NV, Carey RM, MacDonald T, Gaston B. Reductive assays for *S*-nitrosothiols: implications for measurements in biological systems. Biochem Biophys Res Commun 1998; 252: 535-540.
366. Ewing JF, Janero DR. Specific *S*-nitrosothiol (thionitrite) quantification as solution nitrite after vanadium(III) reduction and ozone-chemiluminescent detection. Free Radic Biol Med 1998; 25: 621-628.
367. Saville BA. A scheme for colorimetric determination of microgram amounts of thiols. Analyst 1958; 83: 670–672.
368. Conboy JJ, Hotchkiss JH. Photolytic interface for high-performance liquid chromatography--chemiluminescence detection of non-volatile *N*-nitroso compounds. Analyst 1989; 114: 155-159.
369. Jaffrey SR, Snyder SH. The biotin switch method for the detection of *S*-nitrosylated proteins. Sci STKE 2001; 2001: PL1.
370. Ischiropoulos H, Oshima H, Chen W, Hertkorn C, Lorch S, Weisse M, Lightfoot R, Souza J, Yermilov V, Pignatelli B, Masuda M, Szabo C. Chapter 9: Detection of Certain Peroxynitrite-Induced DNA Modifications. In: Armstrong D (ed.) Oxidative Stress Biomarkers and Antioxidant Protocols: Humana Press; 2000: 77-88.
371. Hsu SM, Raine L. Protein A, avidin, and biotin in immunohistochemistry. J Histochem Cytochem 1981; 29: 1349-1353.
372. Hsu SM, Raine L, Fanger H. Use of avidin-biotin-peroxidase complex (ABC) in immunoperoxidase techniques: a comparison between ABC and unlabeled antibody (PAP) procedures. J Histochem Cytochem 1981; 29: 577-580.
373. Myers TA, Nickoloff JA. Modification of enzyme-conjugated streptavidin-biotin western blot technique to avoid detection of endogenous biotin-containing proteins. BioTechniques 1999; 26: 854-857.
374. Wood GS, Warnke R. Suppression of endogenous avidin-binding activity in tissues and its relevance to biotin-avidin detection systems. J Histochem Cytochem 1981; 29: 1196-1204.
375. Steel RGD, Torrie JH. Chapter 5: Comparisons involving two sample means. In: Principles and procedures of statistics: a biometrical approach, 2nd ed. New York, USA: McGraw-Hill Book Co.; 1980: 86-121.
376. Liu X, Miller MJ, Joshi MS, Sadowska-Krowicka H, Clark DA, Lancaster JR, Jr. Diffusion-limited reaction of free nitric oxide with erythrocytes. J Biol Chem 1998; 273: 18709-18713.
377. Awad HH, Stanbury DM. Autoxidation of NO in aqueous solution. Int J Chem Kinet 1993; 25: 375–381.
378. Lancaster JR, Jr. Simulation of the diffusion and reaction of endogenously produced nitric oxide. Proc Natl Acad Sci U S A 1994; 91: 8137-8141.
379. Doyle MP, Herman JG, Dykstra RL. Autocatalytic oxidation of hemoglobin induced by nitrite: activation and chemical inhibition. J Free Radic Biol Med 1985; 1: 145-153.
380. Titheradge MA. Chapter 9: The enzymatic measurement of nitrate and nitrite. In: Titheradge MA (ed.) Nitric oxide protocols, vol. 100. Totowa, NJ, USA: Humana Press Inc.; 1998: 83-91.
381. Moshage H, Kok B, Huizenga JR, Jansen PL. Nitrite and nitrate determinations in plasma: a critical evaluation. Clin Chem 1995; 41: 892-896.
382. Verdon CP, Burton BA, Prior RL. Sample pretreatment with nitrate reductase and glucose-6-phosphate dehydrogenase quantitatively reduces nitrate while avoiding interference by $NADP^+$ when the Griess reaction is used to assay for nitrite. Anal Biochem 1995; 224: 502-508.
383. Granger DL, Taintor RR, Boockvar KS, Hibbs JB, Jr. Determination of nitrate and nitrite in biological samples using bacterial nitrate reductase coupled with the Griess reaction. Methods: A companion to methods in enzymology 1995; 7: 78-83.
384. Gilliam MB, Sherman MP, Griscavage JM, Ignarro LJ. A spectrophotometric assay for nitrate using NADPH oxidation by *Aspergillus* nitrate reductase. Anal Biochem 1993; 212: 359-365.

385. Senn DR, Carr PW, Klatt LN. Determinatlon of nitrate ion at the part per billion level in environmental samples with a continuous flow immobilized enzyme reaction. Anal Chem 1976; 48: 954-958.
386. Nussler AK, Eling W, Kremsher PG. Patients with *Plasmodium falciparum* malaria and *Plasmodium vivax* malaria show increased nitrite and nitrate plasma levels. J Infect Dis 1994; 169: 1418-1419.
387. Cot S, Ringwald P, Mulder B, Miailhes P, Yap-Yap J, Nussler AK, Eling WM. Nitric oxide in cerebral malaria. J Infect Dis 1994; 169: 1417-1418.
388. Jourd'heuil D, Gray L, Grisham MB. *S*-nitrosothiol formation in blood of lipopolysaccharide-treated rats. Biochem Biophys Res Commun 2000; 273: 22-26.
389. Gaston B, Stamler JS. Chapter 3: Biochemistry of Nitric Oxide. In: C. FF (ed.) Nitric Oxide and Infection. New York: Kluwer Academic/Plenum Publishers; 1999: 37-55.
390. Stamler JS, Jia L, Eu JP, McMahon TJ, Demchenko IT, Bonaventura J, Gernert K, Piantadosi CA. Blood flow regulation by *S*-nitrosohemoglobin in the physiological oxygen gradient. Science 1997; 276: 2034-2037.
391. Spack L, Havens PL, Griffith OW. Measurements of total plasma nitrite and nitrate in pediatric patients with the systemic inflammatory response syndrome. Crit Care Med 1997; 25: 1071-1078.
392. Wong HR, Carcillo JA, Burckart G, Shah N, Janosky JE. Increased serum nitrite and nitrate concentrations in children with the sepsis syndrome. Crit Care Med 1995; 23: 835-842.
393. Sonoda M, Kobayashi J, Takezawa M, Miyazaki T, Nakajima T, Shimomura H, Koike K, Satomi A, Ogino H, Omoto R, Komoda T. An assay method for nitric oxide-related compounds in whole blood. Anal Biochem 1997; 247: 417-427.
394. Chamulitrat W, Jordan SJ, Mason RP. Nitric oxide production during endotoxic shock in carbon tetrachloride-treated rats. Mol Pharmacol 1994; 46: 391-397.
395. Glover RE, Germolec DR, Patterson R, Walker NJ, Lucier GW, Mason RP. Endotoxin (lipopolysaccharide)-induced nitric oxide production in 2,3,7,8-tetrachlorodibenzo-p-dioxin-treated Fischer rats: detection of nitrosyl hemoproteins by EPR spectroscopy. Chem Res Toxicol 2000; 13: 1051-1055.
396. Ghigo D, Todde R, Ginsburg H, Costamagna C, Gautret P, Bussolino F, Ulliers D, Giribaldi G, Deharo E, Gabrielli G, Pescarmona G, Bosia A. Erythrocyte stages of *Plasmodium falciparum* exhibit a high nitric oxide synthase (NOS) activity and release an NOS-inducing soluble factor. J Exp Med 1995; 182: 677-688.
397. Murata K, Takano F, Fushiya S, Oshima Y. Potentiation by febrifugine of host defense in mice against *Plasmodium berghei* NK65. Biochem Pharmacol 1999; 58: 1593-1601.
398. Greenberg SS, Xie J, Spitzer JJ, Wang JF, Lancaster J, Grisham MB, Powers DR, Giles TD. Nitro containing L-arginine analogs interfere with assays for nitrate and nitrite. Life Sci 1995; 57: 1949-1961.
399. Tsikas D, Fuchs I, Gutzki FM, Frolich JC. Measurement of nitrite and nitrate in plasma, serum and urine of humans by high-performance liquid chromatography, the Griess assay, chemiluminescence and gas chromatography-mass spectrometry: interferences by biogenic amines and N^G-nitro-L-arginine analogs. J Chromatogr B Biomed Sci Appl 1998; 715: 441-444; discussion 445-448.
400. Rassaf T, Bryan NS, Kelm M, Feelisch M. Concomitant presence of *N*-nitroso and *S*-nitroso proteins in human plasma. Free Radic Biol Med 2002; 33: 1590-1596.
401. Han TH, Hyduke DR, Vaughn MW, Fukuto JM, Liao JC. Nitric oxide reaction with red blood cells and hemoglobin under heterogeneous conditions. Proc Natl Acad Sci U S A 2002; 21: 21.
402. Pascoa V, Oliveira PL, Dansa-Petretski M, Silva JR, Alvarenga PH, Jacobs-Lorena M, Lemos FJ. *Aedes aegypti* peritrophic matrix and its interaction with heme during blood digestion. Insect Biochem Mol Biol 2002; 32: 517-523.
403. Gow AJ, McClelland M, Garner SE, Malcolm S, Ischiropoulos H. The determination of nitrotyrosine residues in proteins. In: Titheradge M (ed.) Nitric Oxide Protocols. Totowa, NJ, USA: Humana Press Inc.; 1998: 291-299.
404. Vaananen AJ, Liebkind R, Kankuri E, Liesi P, Rauhala P. Angeli's salt and spinal motor neuron injury. Free Radic Res 2004; 38: 271-282.

405. Grune T, Blasig IE, Sitte N, Roloff B, Haseloff R, Davies KJ. Peroxynitrite increases the degradation of aconitase and other cellular proteins by proteasome. J Biol Chem 1998; 273: 10857-10862.
406. Souza JM, Choi I, Chen Q, Weisse M, Daikhin E, Yudkoff M, Obin M, Ara J, Horwitz J, Ischiropoulos H. Proteolytic degradation of tyrosine nitrated proteins. Arch Biochem Biophys 2000; 380: 360-366.
407. Kumar S, Gupta L, Han YS, Barillas-Mury C. Inducible peroxidases mediate nitration of *Anopheles* midgut cells undergoing apoptosis in response to *Plasmodium* invasion. J Biol Chem 2004; 279: 53475-53482.
408. Smith RP. Chemicals reacting with various forms of hemoglobin: biological significance, mechanisms, and determination. J Forensic Sci 1991; 36: 662-672.
409. Yonetani T, Tsuneshige A, Zhou Y, Chen X. Electron paramagnetic resonance and oxygen binding studies of alpha-Nitrosyl hemoglobin. A novel oxygen carrier having no-assisted allosteric functions. J Biol Chem 1998; 273: 20323-20333.
410. Takeoka S, Sakai H, Kose T, Mano Y, Seino Y, Nishide H, Tsuchida E. Methemoglobin formation in hemoglobin vesicles and reduction by encapsulated thiols. Bioconjug Chem 1997; 8: 539-544.
411. Zerez CR, Lachant NA, Tanaka KR. Impaired erythrocyte methemoglobin reduction in sickle cell disease: dependence of methemoglobin reduction on reduced nicotinamide adenine dinucleotide content. Blood 1990; 76: 1008-1014.
412. Milani M, Pesce A, Ouellet H, Guertin M, Bolognesi M. Truncated hemoglobins and nitric oxide action. IUBMB Life 2003; 55: 623-627.
413. de Jesus-Berrios M, Liu L, Nussbaum JC, Cox GM, Stamler JS, Heitman J. Enzymes that counteract nitrosative stress promote fungal virulence. Curr Biol 2003; 13: 1963-1968.
414. Barrett J, Brophy PM. *Ascaris* haemoglobin: new tricks for an old protein. Parasitol Today 2000; 16: 90-91.
415. Trager W, Jensen JB. Human malaria parasites in continuous culture. Science 1976; 193: 673-675.
416. Mak P, Wojcik K, Silberring J, Dubin A. Antimicrobial peptides derived from heme-containing proteins: hemocidins. Antonie Van Leeuwenhoek 2000; 77: 197-207.
417. Mak P, Wojcik K, Wicherek L, Suder P, Dubin A. Antibacterial hemoglobin peptides in human menstrual blood. Peptides 2004; 25: 1839-1847.
418. Parish CA, Jiang H, Tokiwa Y, Berova N, Nakanishi K, McCabe D, Zuckerman W, Xia MM, Gabay JE. Broad-spectrum antimicrobial activity of hemoglobin. Bioorg Med Chem 2001; 9: 377-382.
419. Froidevaux R, Krier F, Nedjar-Arroume N, Vercaigne-Marko D, Kosciarz E, Ruckebusch C, Dhulster P, Guillochon D. Antibacterial activity of a pepsin-derived bovine hemoglobin fragment. FEBS Lett 2001; 491: 159-163.
420. Fogaca AC, da Silva PI, Miranda MT, Bianchi AG, Miranda A, Ribolla PE, Daffre S. Antimicrobial activity of a bovine hemoglobin fragment in the tick *Boophilus microplus*. J Biol Chem 1999; 274: 25330-25334.
421. Nakajima Y, Ogihara K, Taylor D, Yamakawa M. Antibacterial hemoglobin fragments from the midgut of the soft tick, *Ornithodoros moubata* (*Acari: Argasidae*). J Med Entomol 2003; 40: 78-81.
422. Liepke C, Baxmann S, Heine C, Breithaupt N, Standker L, Forssmann WG. Human hemoglobin-derived peptides exhibit antimicrobial activity: a class of host defense peptides. J Chromatogr B Analyt Technol Biomed Life Sci 2003; 791: 345-356.
423. Robinson KM, Morre JT, Beckman JS. Triuret: a novel product of peroxynitrite-mediated oxidation of urate. Arch Biochem Biophys 2004; 423: 213-217.
424. Hooper DC, Scott GS, Zborek A, Mikheeva T, Kean RB, Koprowski H, Spitsin SV. Uric acid, a peroxynitrite scavenger, inhibits CNS inflammation, blood-CNS barrier permeability changes, and tissue damage in a mouse model of multiple sclerosis. Faseb J 2000; 14: 691-698.
425. Varela-Echavarria A, Montes de Oca-Luna R, Barrera-Saldana HA. Uricase protein sequences: conserved during vertebrate evolution but absent in humans. Faseb J 1988; 2: 3092-3096.
426. Ames BN, Cathcart R, Schwiers E, Hochstein P. Uric acid provides an antioxidant defense in humans against oxidant- and radical-caused aging and cancer: a hypothesis. Proc Natl Acad Sci U S A 1981; 78: 6858-6862.

427. Wu XW, Lee CC, Muzny DM, Caskey CT. Urate oxidase: primary structure and evolutionary implications. Proc Natl Acad Sci U S A 1989; 86: 9412-9416.
428. Wallrath LL, Burnett JB, Friedman TB. Molecular characterization of the *Drosophila melanogaster* urate oxidase gene, an ecdysone-repressible gene expressed only in the malpighian tubules. Mol Cell Biol 1990; 10: 5114-5127.
429. Linares E, Nakao LS, Augusto O, Kadiiska MB. EPR studies of *in vivo* radical production by lipopolysaccharide: potential role of iron mobilized from iron-nitrosyl complexes. Free Radic Biol Med 2003; 34: 766-773.
430. Keese MA, Bose M, Mulsch A, Schirmer RH, Becker K. Dinitrosyl-dithiol-iron complexes, nitric oxide (NO) carriers *in vivo*, as potent inhibitors of human glutathione reductase and glutathione-*S*-transferase. Biochem Pharmacol 1997; 54: 1307-1313.
431. Herold S. Kinetic and spectroscopic characterization of an intermediate peroxynitrite complex in the nitrogen monoxide induced oxidation of oxyhemoglobin. FEBS Lett 1999; 443: 81-84.
432. Eich RF, Li T, Lemon DD, Doherty DH, Curry SR, Aitken JF, Mathews AJ, Johnson KA, Smith RD, Phillips GN, Jr., Olson JS. Mechanism of NO-induced oxidation of myoglobin and hemoglobin. Biochemistry 1996; 35: 6976-6983.
433. Gibson WH, Roughton FJ. The kinetics and equilibria of the reactions of nitric oxide with sheep haemoglobin. J Physiol 1957; 136: 507-524.
434. Miller MJ, Sandoval M. Nitric Oxide. III. A molecular prelude to intestinal inflammation. Am J Physiol 1999; 276: G795-799.
435. Ignarro LJ, Byrns RE, Buga GM, Wood KS. Endothelium-derived relaxing factor from pulmonary artery and vein possesses pharmacologic and chemical properties identical to those of nitric oxide radical. Circ Res 1987; 61: 866-879.
436. McMahon TJ, Moon RE, Luschinger BP, Carraway MS, Stone AE, Stolp BW, Gow AJ, Pawloski JR, Watke P, Singel DJ, Piantadosi CA, Stamler JS. Nitric oxide in the human respiratory cycle. Nat Med 2002; 8: 711-717.
437. Kosaka H, Sawai Y, Sakaguchi H, Kumura E, Harada N, Watanabe M, Shiga T. ESR spectral transition by arteriovenous cycle in nitric oxide hemoglobin of cytokine-treated rats. Am J Physiol 1994; 266: C1400-1405.
438. Kagan VE, Day BW, Elsayed NM, Gorbunov NV. Dynamics of haemoglobin. Nature 1996; 383: 30-31.
439. Liu X, Miller MJ, Joshi MS, Thomas DD, Lancaster JR, Jr. Accelerated reaction of nitric oxide with O_2 within the hydrophobic interior of biological membranes. Proc Natl Acad Sci U S A 1998; 95: 2175-2179.
440. Patel RP. Biochemical aspects of the reaction of hemoglobin and NO: implications for Hb-based blood substitutes. Free Radic Biol Med 2000; 28: 1518-1525.
441. Reiter CD, Wang X, Tanus-Santos JE, Hogg N, Cannon RO, 3rd, Schechter AN, Gladwin MT. Cell-free hemoglobin limits nitric oxide bioavailability in sickle-cell disease. Nat Med 2002; 8: 1383-1389.
442. Cassoly R, Gibson Q. Conformation, co-operativity and ligand binding in human hemoglobin. J Mol Biol 1975; 91: 301-313.
443. Herold S, Exner M, Nauser T. Kinetic and mechanistic studies of the NO*-mediated oxidation of oxymyoglobin and oxyhemoglobin. Biochemistry 2001; 40: 3385-3395.
444. Catteruccia F, Nolan T, Blass C, Muller HM, Crisanti A, Kafatos FC, Loukeris TG. Toward *Anopheles* transformation: Minos element activity in anopheline cells and embryos. Proc Natl Acad Sci U S A 2000; 97: 2157-2162.
445. Tahar R, Boudin C, Thiery I, Bourgouin C. Immune response of *Anopheles gambiae* to the early sporogonic stages of the human malaria parasite *Plasmodium falciparum*. Embo J 2002; 21: 6673-6680.
446. Edens WA, Sharling L, Cheng G, Shapira R, Kinkade JM, Lee T, Edens HA, Tang X, Sullards C, Flaherty DB, Benian GM, Lambeth JD. Tyrosine cross-linking of extracellular matrix is catalyzed by Duox, a multidomain oxidase/peroxidase with homology to the phagocyte oxidase subunit gp91phox. J Cell Biol 2001; 154: 879-891.
447. Al-Olayan EM, Beetsma AL, Butcher GA, Sinden RE, Hurd H. Complete development of mosquito phases of the malaria parasite in vitro. Science 2002; 295: 677-679.

448. Lanz-Mendoza H, Hernandez-Martinez S, Ku-Lopez M, Rodriguez Mdel C, Herrera-Ortiz A, Rodriguez MH. Superoxide anion in *Anopheles albimanus* hemolymph and midgut is toxic to *Plasmodium berghei* ookinetes. J Parasitol 2002; 88: 702-706.
449. Xia Y, Dawson VL, Dawson TM, Snyder SH, Zweier JL. Nitric oxide synthase generates superoxide and nitric oxide in arginine-depleted cells leading to peroxynitrite-mediated cellular injury. Proc Natl Acad Sci U S A 1996; 93: 6770-6774.
450. Vasquez-Vivar J, Kalyanaraman B, Martasek P, Hogg N, Masters BS, Karoui H, Tordo P, Pritchard KA, Jr. Superoxide generation by endothelial nitric oxide synthase: the influence of cofactors. Proc Natl Acad Sci U S A 1998; 95: 9220-9225.
451. Lanz-Mendoza H, Hernández-Martínez S, Herrera-Ortiz A, Martínez-Bartneche J, Escobar-Urrutia D, Gil-Acevedo A, Rodríguez-López M. Mosquito immunity: Generation of free radicals in *Anopheles albimanus* and *Ae. aegypti* infected with *Plasmodium berghei.* Kolymbari, Greece: Orthodox Academy of Crete at Kolymbari; August 13-19, 2003.
452. Lymar SV, Hurst JK. Rapid reaction between peroxynitrite ion and carbon dioxide: Implications for biological activity. J Am Chem Soc 1995; 117: 8867-8868.
453. Scott GS, Hooper DC. The role of uric acid in protection against peroxynitrite-mediated pathology. Med Hypotheses 2001; 56: 95-100.
454. Becker BF. Towards the physiological function of uric acid. Free Radic Biol Med 1993; 14: 615-631.
455. Kaur H, Halliwell B. Action of biologically-relevant oxidizing species upon uric acid. Identification of uric acid oxidation products. Chem Biol Interact 1990; 73: 235-247.
456. Pfeiffer S, Lass A, Schmidt K, Mayer B. Protein tyrosine nitration in cytokine-activated murine macrophages. Involvement of a peroxidase/nitrite pathway rather than peroxynitrite. J Biol Chem 2001; 276: 34051-34058.
457. Naughton P, Foresti R, Bains SK, Hoque M, Green CJ, Motterlini R. Induction of heme oxygenase 1 by nitrosative stress. A role for nitroxyl anion. J Biol Chem 2002; 277: 40666-40674.
458. Pagliaro P, Mancardi D, Rastaldo R, Penna C, Gattullo D, Miranda KM, Feelisch M, Wink DA, Kass DA, Paolocci N. Nitroxyl affords thiol-sensitive myocardial protective effects akin to early preconditioning. Free Radic Biol Med 2003; 34: 33-43.
459. Cook NM, Shinyashiki M, Jackson MI, Leal FA, Fukuto JM. Nitroxyl-mediated disruption of thiol proteins: inhibition of the yeast transcription factor Ace1. Arch Biochem Biophys 2003; 410: 89-95.
460. Davies KJ, Delsignore ME. Protein damage and degradation by oxygen radicals. III. Modification of secondary and tertiary structure. J Biol Chem 1987; 262: 9908-9913.
461. Pacifici RE, Kono Y, Davies KJ. Hydrophobicity as the signal for selective degradation of hydroxyl radical-modified hemoglobin by the multicatalytic proteinase complex, proteasome. J Biol Chem 1993; 268: 15405-15411.
462. Giulivi C, Pacifici RE, Davies KJ. Exposure of hydrophobic moieties promotes the selective degradation of hydrogen peroxide-modified hemoglobin by the multicatalytic proteinase complex, proteasome. Arch Biochem Biophys 1994; 311: 329-341.
463. Grossman SJ, Simson J, Jollow DJ. Dapsone-induced hemolytic anemia: effect of *N*-hydroxy dapsone on the sulfhydryl status and membrane proteins of rat erythrocytes. Toxicol Appl Pharmacol 1992; 117: 208-217.
464. Giorgio S, Linares E, Ischiropoulos H, Von Zuben FJ, Yamada A, Augusto O. *In vivo* formation of electron paramagnetic resonance-detectable nitric oxide and of nitrotyrosine is not impaired during murine leishmaniasis. Infect Immun 1998; 66: 807-814.
465. Fukuto JM, Switzer CH, Miranda KM, Wink DA. NITROXYL (HNO): Chemistry, Biochemistry, and Pharmacology. Annu Rev Pharmacol Toxicol 2005; 45: 335-355.
466. Burney S, Caulfield JL, Niles JC, Wishnok JS, Tannenbaum SR. The chemistry of DNA damage from nitric oxide and peroxynitrite. Mutat Res 1999; 424: 37-49.
467. Szabo C. Multiple pathways of peroxynitrite cytotoxicity. Toxicol Lett 2003; 140-141: 105-112.
468. Hogg N, Kalyanaraman B. Nitric oxide and lipid peroxidation. Biochim Biophys Acta 1999; 1411: 378-384.
469. Squadrito GL, Pryor WA. Oxidative chemistry of nitric oxide: the roles of superoxide, peroxynitrite, and carbon dioxide. Free Radic Biol Med 1998; 25: 392-403.

470. Berka V, Wu G, Yeh HC, Palmer G, Tsai AL. Three different oxygen-induced radical species in endothelial nitric-oxide synthase oxygenase domain under regulation by L-arginine and tetrahydrobiopterin. J Biol Chem 2004; 279: 32243-32251.
471. Huisman A, Vos I, van Faassen EE, Joles JA, Grone HJ, Martasek P, van Zonneveld AJ, Vanin AF, Rabelink TJ. Anti-inflammatory effects of tetrahydrobiopterin on early rejection in renal allografts: modulation of inducible nitric oxide synthase. Faseb J 2002; 16: 1135-1137.
472. Hemmens B, Mayer B. Chapter 1: Enzymology of nitric oxide synthases. In: Titheradge MA (ed.) Nitric Oxide Protocols, vol. 100. Totowa, NJ: Humana Press, Inc.; 1998: 1-32.
473. Hatakeyama K. Chapter 24: Measurement of biopterin and the use of inhibitors of biopterin biosynthesis. In: Titheradge MA (ed.) Nitric Oxide Protocols, vol. 100. Totowa, NJ: Humana Press, Inc.; 1998: 251-264.
474. Whitten MM, Mello CB, Gomes SA, Nigam Y, Azambuja P, Garcia ES, Ratcliffe NA. Role of superoxide and reactive nitrogen intermediates in *Rhodnius prolixus* (*Reduviidae*)/*Trypanosoma rangeli* interactions. Exp Parasitol 2001; 98: 44-57.
475. Whitten MM, Ratcliffe NA. *In vitro* superoxide activity in the haemolymph of the West Indian leaf cockroach, *Blaberus discoidalis*. J Insect Physiol 1999; 45: 667-675.
476. Nappi AJ, Vass E, Frey F, Carton Y. Superoxide anion generation in *Drosophila* during melanotic encapsulation of parasites. Eur J Cell Biol 1995; 68: 450-456.
477. Ribeiro JM. NAD(P)H-dependent production of oxygen reactive species by the salivary glands of the mosquito *Anopheles albimanus*. Insect Biochem Mol Biol 1996; 26: 715-720.
478. Chien CT, Lee PH, Chen CF, Ma MC, Lai MK, Hsu SM. *De novo* demonstration and co-localization of free-radical production and apoptosis formation in rat kidney subjected to ischemia/reperfusion. J Am Soc Nephrol 2001; 12: 973-982.
479. Chen CF, Tsai SY, Ma MC, Wu MS. Hypoxic preconditioning enhances renal superoxide dismutase levels in rats. J Physiol 2003; 552: 561-569.
480. Kumar S, Christophides GK, Cantera R, Charles B, Han YS, Meister S, Dimopoulos G, Kafatos FC, Barillas-Mury C. The role of reactive oxygen species on *Plasmodium* melanotic encapsulation in *Anopheles gambiae*. Proc Natl Acad Sci U S A 2003; 100: 14139-14144.
481. Ribeiro JM, Nussenzveig RH. The salivary catechol oxidase/peroxidase activities of the mosquito *Anopheles albimanus*. J Exp Biol 1993; 179: 273-287.
482. Yang T, Olsen KW. Enzymatic protection from autoxidation for crosslinked hemoglobins. Artif Cells Blood Substit Immobil Biotechnol 1994; 22: 709-717.
483. Keilin D, Hartree EF. Catalase, peroxidase and metmyoglobin as catalysts of coupled peroxidatic reactions. Biochem J 1955; 60: 310-325.
484. Nagasawa HT, DeMaster EG, Redfern B, Shirota FN, Goon DJ. Evidence for nitroxyl in the catalase-mediated bioactivation of the alcohol deterrent agent cyanamide. J Med Chem 1990; 33: 3120-3122.
485. Levine RL, Garland D, Oliver CN, Amici A, Climent I, Lenz AG, Ahn BW, Shaltiel S, Stadtman ER. Determination of carbonyl content in oxidatively modified proteins. Methods Enzymol 1990; 186: 464-478.
486. Quinlan GJ, Gutteridge JMC. Chapter 73: Carbonyl assay for oxidative damage to proteins. In: Taniguchi N, Gutteridge JMC (eds.), Experimental Protocols for Reactive Oxygen and Nitrogen Species. Oxford: Oxford University Press; 2000: 257-258.
487. Leski ML, Bao F, Wu L, Qian H, Sun D, Liu D. Protein and DNA oxidation in spinal injury: neurofilaments--an oxidation target. Free Radic Biol Med 2001; 30: 613-624.
488. Adams S, Green P, Claxton R, Simcox S, Williams MV, Walsh K, Leeuwenburgh C. Reactive carbonyl formation by oxidative and non-oxidative pathways. Front Biosci 2001; 6: A17-24.
489. Luxford C, Morin B, Dean RT, Davies MJ. Histone H1- and other protein- and amino acid-hydroperoxides can give rise to free radicals which oxidize DNA. Biochem J 1999; 344 Pt 1: 125-134.
490. Asami S, Kasai H. Chapter 65: 8-OH-dG: extraction/enzyme treatment/measurement of 8-OH-dG. In: Taniguchi N, Gutteridge JMC (eds.), Experimental Protocols for Reactive Oxygen and Nitrogen Species. Oxford: Oxford University Press; 2000: 224-228.
491. Crow JP, Ye YZ, Strong M, Kirk M, Barnes S, Beckman JS. Superoxide dismutase catalyzes nitration of tyrosines by peroxynitrite in the rod and head domains of neurofilament-L. J Neurochem 1997; 69: 1945-1953.

492. Berlett BS, Friguet B, Yim MB, Chock PB, Stadtman ER. Peroxynitrite-mediated nitration of tyrosine residues in *Escherichia coli* glutamine synthetase mimics adenylylation: relevance to signal transduction. Proc Natl Acad Sci U S A 1996; 93: 1776-1780.
493. Ischiropoulos H, Gow A. Pathophysiological functions of nitric oxide-mediated protein modifications. Toxicology 2005; 208: 299-303.
494. Kong SK, Yim MB, Stadtman ER, Chock PB. Peroxynitrite disables the tyrosine phosphorylation regulatory mechanism: Lymphocyte-specific tyrosine kinase fails to phosphorylate nitrated cdc2(6-20)NH2 peptide. Proc Natl Acad Sci U S A 1996; 93: 3377-3382.
495. Monteiro HP. Signal transduction by protein tyrosine nitration: competition or cooperation with tyrosine phosphorylation-dependent signaling events? Free Radic Biol Med 2002; 33: 765-773.
496. Gole MD, Souza JM, Choi I, Hertkorn C, Malcolm S, Foust RF, 3rd, Finkel B, Lanken PN, Ischiropoulos H. Plasma proteins modified by tyrosine nitration in acute respiratory distress syndrome. Am J Physiol Lung Cell Mol Physiol 2000; 278: L961-967.
497. Shahabuddin M, Toyoshima T, Aikawa M, Kaslow DC. Transmission-blocking activity of a chitinase inhibitor and activation of malarial parasite chitinase by mosquito protease. Proc Natl Acad Sci U S A 1993; 90: 4266-4270.
498. Langer RC, Li F, Popov V, Kurosky A, Vinetz JM. Monoclonal antibody against the *Plasmodium falciparum* chitinase, PfCHT1, recognizes a malaria transmission-blocking epitope in *Plasmodium gallinaceum* ookinetes unrelated to the chitinase PgCHT1. Infect Immun 2002; 70: 1581-1590.
499. Rubbo H, Radi R, Trujillo M, Telleri R, Kalyanaraman B, Barnes S, Kirk M, Freeman BA. Nitric oxide regulation of superoxide and peroxynitrite-dependent lipid peroxidation. Formation of novel nitrogen-containing oxidized lipid derivatives. J Biol Chem 1994; 269: 26066-26075.
500. Goldstein S, Czapski G, Lind J, Merenyi G. Tyrosine nitration by simultaneous generation of NO and O_2^- under physiological conditions. How the radicals do the job. J Biol Chem 2000; 275: 3031-3036.
501. Henry YA, Singel DJ. Chapter 24: Metal-nitrosyl interactions in nitric oxide biology probed by electron paramagnetic resonance spectroscopy. In: Stamler MFaJS (ed.) Methods in NItric Oxide Research: John Wiley & Sons Ltd; 1996: 357-372.
502. Henry Y, Lepoivre M, Drapier JC, Ducrocq C, Boucher JL, Guissani A. EPR characterization of molecular targets for NO in mammalian cells and organelles. FASEB J 1993; 7: 1124-1134.
503. Chamulitrat W, Jordan SJ, Mason RP, Litton AL, Wilson JG, Wood ER, Wolberg G, Vedia LM. Targets of nitric oxide in a mouse model of liver inflammation by *Corynebacterium parvum*. Arch Biochem Biophys 1995; 316: 30-37.
504. Michejda CJ, Rydstrom T. Photochemistry of *N*-nitrosamines in neutral media. IARC Sci Publ 1984: 365-369.
505. Ohshima H, Bartsch H. Chronic infections and inflammatory processes as cancer risk factors: possible role of nitric oxide in carcinogenesis. Mutat Res 1994; 305: 253-264.
506. Nagasawa HT, Fraser PS, Yuzon DL. A new method for nitrosation of proline and related sec-α-amino acids to *N*-nitrosamino acids with possible oncogenic activity. J Med Chem 1973; 16: 583-585.
507. Demaio J, Pumpuni CB, Kent M, Beier JC. The midgut bacterial flora of wild *Aedes triseriatus*, *Culex pipiens*, and *Psorophora columbiae* mosquitoes. Am J Trop Med Hyg 1996; 54: 219-223.
508. Pumpuni CB, Demaio J, Kent M, Davis JR, Beier JC. Bacterial population dynamics in three anopheline species: the impact on *Plasmodium* sporogonic development. Am J Trop Med Hyg 1996; 54: 214-218.
509. Zayed ME, Bream AS. Biodiversity of the microbial flora associated with two strains of *Culex pipiens* (*Diptera: Culicidae*). Commun Agric Appl Biol Sci 2004; 69: 229-234.
510. Pumpuni CB, Beier MS, Nataro JP, Guers LD, Davis JR. *Plasmodium falciparum*: inhibition of sporogonic development in *Anopheles stephensi* by gram-negative bacteria. Exp Parasitol 1993; 77: 195-199.
511. Gonzalez-Ceron L, Santillan F, Rodriguez MH, Mendez D, Hernandez-Avila JE. Bacteria in midguts of field-collected *Anopheles albimanus* block *Plasmodium vivax* sporogonic development. J Med Entomol 2003; 40: 371-374.
512. Straif SC, Mbogo CN, Toure AM, Walker ED, Kaufman M, Toure YT, Beier JC. Midgut bacteria in *Anopheles gambiae* and *An. funestus* (*Diptera: Culicidae*) from Kenya and Mali. J Med Entomol 1998; 35: 222-226.

513. Gardner PR, Gardner AM, Martin LA, Dou Y, Li T, Olson JS, Zhu H, Riggs AF. Nitric-oxide dioxygenase activity and function of flavohemoglobins. sensitivity to nitric oxide and carbon monoxide inhibition. J Biol Chem 2000; 275: 31581-31587.
514. Watmough NJ, Butland G, Cheesman MR, Moir JW, Richardson DJ, Spiro S. Nitric oxide in bacteria: synthesis and consumption. Biochim Biophys Acta 1999; 1411: 456-474.
515. Berks BC, Ferguson SJ, Moir JW, Richardson DJ. Enzymes and associated electron transport systems that catalyse the respiratory reduction of nitrogen oxides and oxyanions. Biochim Biophys Acta 1995; 1232: 97-173.
516. Ayanaba A, Alexander M. Microbial formation of nitrosamines *in vitro*. Appl Microbiol 1973; 25: 862-868.
517. Calmels S, Ohshima H, Henry Y, Bartsch H. Characterization of bacterial cytochrome cd(1)-nitrite reductase as one enzyme responsible for catalysis of nitrosation of secondary amines. Carcinogenesis 1996; 17: 533-536.
518. Membrillo-Hernandez J, Poole RK. Bacterial flavohaemoglobins: a consensus sequence and identification of a discrete enterobacterial group and of further bacterial globins. FEMS Microbiol Lett 1997; 155: 179-184.
519. Hardison RC. A brief history of hemoglobins: plant, animal, protist, and bacteria. Proc Natl Acad Sci U S A 1996; 93: 5675-5679.
520. Wittenberg JB, Wittenberg BA. Mechanisms of cytoplasmic hemoglobin and myoglobin function. Annu Rev Biophys Biophys Chem 1990; 19: 217-241.
521. Zhu H, Riggs AF. Yeast flavohemoglobin is an ancient protein related to globins and a reductase family. Proc Natl Acad Sci U S A 1992; 89: 5015-5019.
522. Gyan B, Troye-Blomberg M, Perlmann P, Bjorkman A. Human monocytes cultured with and without interferon-gamma inhibit *Plasmodium falciparum* parasite growth *in vitro* via secretion of reactive nitrogen intermediates. Parasite Immunol 1994; 16: 371-375.
523. Siu PM. Antimalarial activity of 1-methyl-3-nitro-1-nitrosoguanidine. Proc Soc Exp Biol Med 1968; 129: 753-756.
524. Sharma A, Eapen A, Subbarao SK. Parasite killing in *Plasmodium vivax* malaria by nitric oxide: implication of aspartic protease inhibition. J Biochem (Tokyo) 2004; 136: 329-334.
525. Herrera-Ortiz A, Lanz-Mendoza H, Martinez-Barnetche J, Hernandez-Martinez S, Villarreal-Trevino C, Aguilar-Marcelino L, Rodriguez MH. *Plasmodium berghei* ookinetes induce nitric oxide production in *Anopheles pseudopunctipennis* midguts cultured *in vitro*. Insect Biochem Mol Biol 2004; 34: 893-901.
526. Alavi Y, Arai M, Mendoza J, Tufet-Bayona M, Sinha R, Fowler K, Billker O, Franke-Fayard B, Janse CJ, Waters A, Sinden RE. The dynamics of interactions between *Plasmodium* and the mosquito: a study of the infectivity of *Plasmodium berghei* and *Plasmodium gallinaceum*, and their transmission by *Anopheles stephensi*, *Anopheles gambiae* and *Aedes aegypti*. Int J Parasitol 2003; 33: 933-943.
527. Gupta L, Kumar S, Han YS, Pimenta PF, Barillas-Mury C. Midgut epithelial responses of different mosquito-*Plasmodium* combinations: the actin cone zipper repair mechanism in *Aedes aegypti*. Proc Natl Acad Sci U S A 2005; 102: 4010-4015.
528. Lim J, Gowda DC, Krishnegowda G, Luckhart S. Induction of nitric oxide synthase in *Anopheles stephensi* by *Plasmodium falciparum*: Mechanism of signaling and the role of parasite glycosylphosphatidylinositols. Infect Immun 2005; 73: 2778-2789.
529. Meis JF, Pool G, van Gemert GJ, Lensen AH, Ponnudurai T, Meuwissen JH. *Plasmodium falciparum* ookinetes migrate intercellularly through *Anopheles stephensi* midgut epithelium. Parasitol Res 1989; 76: 13-19.
530. Nahrevanian H, Dascombe MJ. Nitric oxide and reactive nitrogen intermediates during lethal and nonlethal strains of murine malaria. Parasite Immunol 2001; 23: 491-501.
531. Anastasi J. Hemoglobin S-mediated membrane oxidant injury: protection from malaria and pathology in sickle cell disease. Med Hypotheses 1984; 14: 311-320.
532. Grinberg LN, Rachmilewitz EA, Kitrossky N, Chevion M. Hydroxyl radical generation in β-thalassemic red blood cells. Free Radic Biol Med 1995; 18: 611-615.
533. Sorensen S, Rubin E, Polster H, Mohandas N, Schrier S. The role of membrane skeletal-associated α-globin in the pathophysiology of β-thalassemia. Blood 1990; 75: 1333-1336.

534. Clark IA, Chaudhri G, Cowden WB. Some roles of free radicals in malaria. Free Radic Biol Med 1989; 6: 315-321.
535. Lockamy VL. The search for the mechanism of nitric oxide release in hydroxyurea therapy. Winston-Salem, NC: Wake Forest University; May 2004. Dissertation.
536. Nathan C, Shiloh MU. Reactive oxygen and nitrogen intermediates in the relationship between mammalian hosts and microbial pathogens. Proc Natl Acad Sci U S A 2000; 97: 8841-8848.
537. Liew FY. The role of nitric oxide in parasitic diseases. Ann Trop Med Parasitol 1993; 87: 637-642.
538. Colasanti M, Gradoni L, Mattu M, Persichini T, Salvati L, Venturini G, Ascenzi P. Molecular bases for the anti-parasitic effect of NO (Review). Int J Mol Med 2002; 9: 131-134.
539. Marshall HE, Merchant K, Stamler JS. Nitrosation and oxidation in the regulation of gene expression. Faseb J 2000; 14: 1889-1900.
540. Ehrt S, Shiloh MU, Ruan J, Choi M, Gunzburg S, Nathan C, Xie Q, Riley LW. A novel antioxidant gene from *Mycobacterium tuberculosis*. J Exp Med 1997; 186: 1885-1896.
541. Bonamore A, Gentili P, Ilari A, Schinina ME, Boffi A. *Escherichia coli* flavohemoglobin is an efficient alkylhydroperoxide reductase. J Biol Chem 2003; 278: 22272-22277.
542. Peng Y, Yang PH, Guo Y, Ng SS, Liu J, Fung PC, Tay D, Ge J, He ML, Kung HF, Lin MC. Catalase and peroxiredoxin 5 protect *Xenopus* embryos against alcohol-induced ocular anomalies. Invest Ophthalmol Vis Sci 2004; 45: 23-29.
543. Jacobson FS, Morgan RW, Christman MF, Ames BN. An alkyl hydroperoxide reductase from *Salmonella typhimurium* involved in the defense of DNA against oxidative damage. Purification and properties. J Biol Chem 1989; 264: 1488-1496.
544. Storz G, Jacobson FS, Tartaglia LA, Morgan RW, Silveira LA, Ames BN. An alkyl hydroperoxide reductase induced by oxidative stress in *Salmonella typhimurium* and *Escherichia coli*: genetic characterization and cloning of ahp. J Bacteriol 1989; 171: 2049-2055.
545. Paul KG. Peroxidases. In: Boyer PD, Lardy H, Myrback K (eds.), The Enzymes, 2nd ed. New York: Academic Press; 1963: 227-274.
546. Kim K, Kim IH, Lee KY, Rhee SG, Stadtman ER. The isolation and purification of a specific "protector" protein which inhibits enzyme inactivation by a thiol/Fe(III)/O_2 mixed-function oxidation system. J Biol Chem 1988; 263: 4704-4711.
547. Chae HZ, Chung SJ, Rhee SG. Thioredoxin-dependent peroxide reductase from yeast. J Biol Chem 1994; 269: 27670-27678.
548. Chae HZ, Robison K, Poole LB, Church G, Storz G, Rhee SG. Cloning and sequencing of thiol-specific antioxidant from mammalian brain: alkyl hydroperoxide reductase and thiol-specific antioxidant define a large family of antioxidant enzymes. Proc Natl Acad Sci U S A 1994; 91: 7017-7021.
549. Harris JR, Schroder E, Isupov MN, Scheffler D, Kristensen P, Littlechild JA, Vagin AA, Meissner U. Comparison of the decameric structure of peroxiredoxin-II by transmission electron microscopy and X-ray crystallography. Biochim Biophys Acta 2001; 1547: 221-234.
550. Wood ZA, Poole LB, Hantgan RR, Karplus PA. Dimers to doughnuts: redox-sensitive oligomerization of 2-cysteine peroxiredoxins. Biochemistry 2002; 41: 5493-5504.
551. Wood ZA, Schroder E, Harris JR, Poole LB. Structure, mechanism and regulation of peroxiredoxins. Trends Biochem Sci 2003; 28: 32-40.
552. Alphey MS, Bond CS, Tetaud E, Fairlamb AH, Hunter WN. The structure of reduced tryparedoxin peroxidase reveals a decamer and insight into reactivity of 2Cys-peroxiredoxins. J Mol Biol 2000; 300: 903-916.
553. Chauhan R, Mande SC. Characterization of the *Mycobacterium tuberculosis* H37Rv alkyl hydroperoxidase AhpC points to the importance of ionic interactions in oligomerization and activity. Biochem J 2001; 354: 209-215.
554. Hofmann B, Hecht HJ, Flohe L. Peroxiredoxins. Biol Chem 2002; 383: 347-364.
555. Choi HJ, Kang SW, Yang CH, Rhee SG, Ryu SE. Crystallization and preliminary X-ray studies of hORF6, a novel human antioxidant enzyme. Acta Crystallogr D Biol Crystallogr 1998; 54: 436-437.
556. Declercq JP, Evrard C. A twinned monoclinic crystal form of human peroxiredoxin 5 with eight molecules in the asymmetric unit. Acta Crystallogr D Biol Crystallogr 2001; 57: 1829-1835.

557. Declercq JP, Evrard C, Clippe A, Stricht DV, Bernard A, Knoops B. Crystal structure of human peroxiredoxin 5, a novel type of mammalian peroxiredoxin at 1.5 Å resolution. J Mol Biol 2001; 311: 751-759.
558. Hirotsu S, Abe Y, Okada K, Nagahara N, Hori H, Nishino T, Hakoshima T. Crystal structure of a multifunctional 2-Cys peroxiredoxin heme-binding protein 23 kDA/proliferation-associated gene product. Proc Natl Acad Sci U S A 1999; 96: 12333-12338.
559. Schroder E, Ponting CP. Evidence that peroxiredoxins are novel members of the thioredoxin fold superfamily. Protein Sci 1998; 7: 2465-2468.
560. Schroder E, Littlechild JA, Lebedev AA, Errington N, Vagin AA, Isupov MN. Crystal structure of decameric 2-Cys peroxiredoxin from human erythrocytes at 1.7 Å resolution. Structure Fold Des 2000; 8: 605-615.
561. Ritz D, Lim J, Reynolds CM, Poole LB, Beckwith J. Conversion of a peroxiredoxin into a disulfide reductase by a triplet repeat expansion. Science 2001; 294: 158-160.
562. Andreesen JR, Wagner M, Sonntag D, Kohlstock M, Harms C, Gursinsky T, Jager J, Parther T, Kabisch U, Grantzdorffer A, Pich A, Sohling B. Various functions of selenols and thiols in anaerobic gram-positive, amino acids-utilizing bacteria. Biofactors 1999; 10: 263-270.
563. Rabilloud T, Heller M, Gasnier F, Luche S, Rey C, Aebersold R, Benahmed M, Louisot P, Lunardi J. Proteomics analysis of cellular response to oxidative stress. Evidence for *in vivo* overoxidation of peroxiredoxins at their active site. J Biol Chem 2002; 277: 19396-19401.
564. Chae HZ, Uhm TB, Rhee SG. Dimerization of thiol-specific antioxidant and the essential role of cysteine 47. Proc Natl Acad Sci U S A 1994; 91: 7022-7026.
565. Flohe L, Jaeger T, Pilawa S, Sztajer H. Thiol-dependent peroxidases care little about homology-based assignments of function. Redox Rep 2003; 8: 256-264.
566. Kwon SJ, Park JW, Choi WK, Kim IH, Kim K. Inhibition of metal-catalyzed oxidation systems by a yeast protector protein in the presence of thioredoxin. Biochem Biophys Res Commun 1994; 201: 8-15.
567. Kang SW, Chae HZ, Seo MS, Kim K, Baines IC, Rhee SG. Mammalian peroxiredoxin isoforms can reduce hydrogen peroxide generated in response to growth factors and tumor necrosis factor-alpha. J Biol Chem 1998; 273: 6297-6302.
568. Rouhier N, Gelhaye E, Sautiere PE, Brun A, Laurent P, Tagu D, Gerard J, de Fay E, Meyer Y, Jacquot JP. Isolation and characterization of a new peroxiredoxin from poplar sieve tubes that uses either glutaredoxin or thioredoxin as a proton donor. Plant Physiol 2001; 127: 1299-1309.
569. Rouhier N, Gelhaye E, Jacquot JP. Glutaredoxin-dependent peroxiredoxin from poplar: Protein-protein interaction and catalytic mechanism. J Biol Chem 2002; 277: 13609-13614.
570. Tartaglia LA, Storz G, Brodsky MH, Lai A, Ames BN. Alkyl hydroperoxide reductase from *Salmonella typhimurium*. Sequence and homology to thioredoxin reductase and other flavoprotein disulfide oxidoreductases. J Biol Chem 1990; 265: 10535-10540.
571. Montemartini M, Kalisz HM, Hecht H-J, Steinert P, Flohe L. Activation of active-site cysteine residues in the peroxiredoxin-type tryparedoxin peroxidase of *Crithidia fasciculata*. European Journal of Biochemistry 1999; 264: 516-524.
572. Bauer H, Kanzok SM, Schirmer RH. Thioredoxin-2 but not thioredoxin-1 is a substrate of thioredoxin peroxidase-1 from *Drosophila melanogaster*: Isolation and characterization of a second thioredoxin in *D. melanogaster* and evidence for distinct biological functions of Trx-1 and Trx-2. J Biol Chem 2002; 277: 17457-17463.
573. Knoops B, Clippe A, Bogard C, Arsalane K, Wattiez R, Hermans C, Duconseille E, Falmagne P, Bernard A. Cloning and characterization of AOEB166, a novel mammalian antioxidant enzyme of the peroxiredoxin family. J Biol Chem 1999; 274: 30451-30458.
574. Seo MS, Kang SW, Kim K, Baines IC, Lee TH, Rhee SG. Identification of a new type of mammalian peroxiredoxin that forms an intramolecular disulfide as a reaction intermediate. J Biol Chem 2000; 275: 20346-20354.
575. Yamashita H, Avraham S, Jiang S, London R, Van Veldhoven PP, Subramani S, Rogers RA, Avraham H. Characterization of human and murine PMP20 peroxisomal proteins that exhibit antioxidant activity *in vitro*. J Biol Chem 1999; 274: 29897-29904.
576. Jeong W, Cha MK, Kim IH. Thioredoxin-dependent hydroperoxide peroxidase activity of bacterioferritin comigratory protein (BCP) as a new member of the thiol-specific antioxidant

protein (TSA)/Alkyl hydroperoxide peroxidase C (AhpC) family. J Biol Chem 2000; 275: 2924-2930.
577. Kong W, Shiota S, Shi Y, Nakayama H, Nakayama K. A novel peroxiredoxin of the plant *Sedum lineare* is a homologue of *Escherichia coli* bacterioferritin co-migratory protein (Bcp). Biochem J 2000; 351: 107-114.
578. Chauhan R, Mande SC. Site-directed mutagenesis reveals a novel catalytic mechanism of *Mycobacterium tuberculosis* alkylhydroperoxidase C. Biochem J 2002; 367: 255-261.
579. Evrard C, Capron A, Marchand C, Clippe A, Wattiez R, Soumillion P, Knoops B, Declercq JP. Crystal structure of a dimeric oxidized form of human peroxiredoxin 5. J Mol Biol 2004; 337: 1079-1090.
580. Kwok LY, Schluter D, Clayton C, Soldati D. The antioxidant systems in *Toxoplasma gondii* and the role of cytosolic catalase in defence against oxidative injury. Mol Microbiol 2004; 51: 47-61.
581. Krnajski Z, Walter RD, Muller S. Isolation and functional analysis of two thioredoxin peroxidases (peroxiredoxins) from *Plasmodium falciparum*. Mol Biochem Parasitol 2001; 113: 303-308.
582. Kang SW, Baines IC, Rhee SG. Characterization of a mammalian peroxiredoxin that contains one conserved cysteine. J Biol Chem 1998; 273: 6303-6311.
583. Choi HJ, Kang SW, Yang CH, Rhee SG, Ryu SE. Crystal structure of a novel human peroxidase enzyme at 2.0 Å resolution. Nat Struct Biol 1998; 5: 400-406.
584. Fujii T, Fujii J, Taniguchi N. Augmented expression of peroxiredoxin VI in rat lung and kidney after birth implies an antioxidative role. Eur J Biochem 2001; 268: 218-225.
585. Fisher AB, Dodia C, Manevich Y, Chen JW, Feinstein SI. Phospholipid hydroperoxides are substrates for non-selenium glutathione peroxidase. J Biol Chem 1999; 274: 21326-21334.
586. Singh AK, Shichi H. A novel glutathione peroxidase in bovine eye. Sequence analysis, mRNA level, and translation. J Biol Chem 1998; 273: 26171-26178.
587. Peshenko IV, Novoselov VI, Evdokimov VA, Nikolaev YV, Kamzalov SS, Shuvaeva TM, Lipkin VM, Fesenko EE. Identification of a 28 kDa secretory protein from rat olfactory epithelium as a thiol-specific antioxidant. Free Radic Biol Med 1998; 25: 654-659.
588. Kawazu S, Tsuji N, Hatabu T, Kawai S, Matsumoto Y, Kano S. Molecular cloning and characterization of a peroxiredoxin from the human malaria parasite *Plasmodium falciparum*. Mol Biochem Parasitol 2000; 109: 165-169.
589. Radyuk SN, Klichko VI, Spinola B, Sohal RS, Orr WC. The peroxiredoxin gene family in *Drosophila melanogaster*. Free Radic Biol Med 2001; 31: 1090-1100.
590. Radyuk SN, Sohal RS, Orr WC. Thioredoxin peroxidases can foster cytoprotection or cell death in response to different stressors - a study of thioredoxin peroxidase under- and over-expression in *Drosophila* cells. Biochem J 2003; Pt 3: 743-752.
591. Altschul SF, Gish W, Miller W, Myers EW, Lipman DJ. Basic local alignment search tool. J Mol Biol 1990; 215: 403-410.
592. Sambrook J, Fritsch EF, Maniatis T. Molecular cloning: a laboratory manual. Cold Spring Harbor: Cold Spring Harbor Laboratory Press; 1989.
593. Barillas-Mury C, Charlesworth A, Gross I, Richman A, Hoffmann JA, Kafatos FC. Immune factor Gambif1, a new rel family member from the human malaria vector, *Anopheles gambiae*. Embo J 1996; 15: 4691-4701.
594. Kurtti TJ, Munderloh UG. Chapter 2: Advances in the definition of culture media for mosquito cells. In: Mitsuhashi J (ed.) Invertebrate Cell Systems Applications, vol. Vol 1: CRC Press, Inc., Boca Raton, FL.; 1989: 21-29.
595. Kozak M. Compilation and analysis of sequences upstream from the translational start site in eukaryotic mRNAs. Nucleic Acids Res 1984; 12: 857-872.
596. Goodin MM, Schlagnhaufer B, Weir T, Romaine CP. Characterization of an RNA-dependent RNA polymerase activity associated with La France isometric virus. J Virol 1997; 71: 2264-2269.
597. Livak KJ. User Belletin #2. In: ABI PRISM 7700 Sequence Detection System; 1997.
598. Aarskog NK, Vedeler CA. Real-time quantitative polymerase chain reaction. A new method that detects both the peripheral myelin protein 22 duplication in Charcot-Marie-Tooth type 1A disease and the peripheral myelin protein 22 deletion in hereditary neuropathy with liability to pressure palsies. Hum Genet 2000; 107: 494-498.

599. Salazar CE, Mills-Hamm D, Kumar V, Collins FH. Sequence of a cDNA from the mosquito *Anopheles gambiae* encoding a homologue of human ribosomal protein S7. Nucleic Acids Res 1993; 21: 4147.
600. Gubler DJ. A method for the *in vitro* cultivation of ovarian and midgut cells from the adult mosquito. Am J Epidemiol 1968; 87: 502-508.
601. Vilcinskas A, Jegorov A, Landa Z, Gotz P, Matha V. Effects of beauverolide L and cyclosporin A on humoral and cellular immune response of the greater wax moth, *Galleria mellonella*. Comp Biochem Physiol C Pharmacol Toxicol Endocrinol 1999; 122: 83-92.
602. Rodriguez J, Agudo M, Van Damme J, Vandekerckhove J, Santaren JF. Polypeptides differentially expressed in imaginal discs define the peroxiredoxin family of genes in *Drosophila*. Eur J Biochem 2000; 267: 487-497.
603. Verdoucq L, Vignols F, Jacquot JP, Chartier Y, Meyer Y. *In vivo* characterization of a thioredoxin h target protein defines a new peroxiredoxin family. J Biol Chem 1999; 274: 19714-19722.
604. Wood ZA, Poole LB, Karplus PA. Peroxiredoxin evolution and the regulation of hydrogen peroxide signaling. Science 2003; 300: 650-653.
605. Flohe L, Budde H, Bruns K, Castro H, Clos J, Hofmann B, Kansal-Kalavar S, Krumme D, Menge U, Plank-Schumacher K, Sztajer H, Wissing J, Wylegalla C, Hecht HJ. Tryparedoxin peroxidase of *Leishmania donovani*: molecular cloning, heterologous expression, specificity, and catalytic mechanism. Arch Biochem Biophys 2002; 397: 324-335.
606. Horling F, König J, Dietz K-J. Type II peroxiredoxin C, a member of the peroxiredoxin family of *Arabidopsis thaliana*: its expression and activity in comparison with other peroxiredoxins. Plant Physiol Biochem 2002; 40: 491-499.
607. Immenschuh S, Iwahara S, Satoh H, Nell C, Katz N, Muller-Eberhard U. Expression of the mRNA of heme-binding protein 23 is coordinated with that of heme oxygenase-1 by heme and heavy metals in primary rat hepatocytes and hepatoma cells. Biochemistry 1995; 34: 13407-13411.
608. Tsuji N, Kamio T, Isobe T, Fujisaki K. Molecular characterization of peroxiredoxin from the hard tick *Heamaphysalis longicornis*. Insect Molecular Biology 2001; 10: 121-129.
609. Das KC, Pahl PM, Guo XL, White CW. Induction of peroxiredoxin gene expression by oxygen in lungs of newborn primates. Am J Respir Cell Mol Biol 2001; 25: 226-232.
610. Iwahara S, Satoh H, Song DX, Webb J, Burlingame AL, Nagae Y, Muller-Eberhard U. Purification, characterization, and cloning of a heme-binding protein (23 kDa) in rat liver cytosol. Biochemistry 1995; 34: 13398-13406.
611. Sherman DR, Sabo PJ, Hickey MJ, Arain TM, Mahairas GG, Yuan Y, Barry CE, 3rd, Stover CK. Disparate responses to oxidative stress in saprophytic and pathogenic mycobacteria. Proc Natl Acad Sci U S A 1995; 92: 6625-6629.
612. Kim H, Lee TH, Park ES, Suh JM, Park SJ, Chung HK, Kwon OY, Kim YK, Ro HK, Shong M. Role of peroxiredoxins in regulating intracellular hydrogen peroxide and hydrogen peroxide-induced apoptosis in thyroid cells. J Biol Chem 2000.
613. Bast A, Wolf G, Oberbaumer I, Walther R. Oxidative and nitrosative stress induces peroxiredoxins in pancreatic beta cells. Diabetologia 2002; 45: 867-876.
614. Akerman SE, Muller S. 2-Cys peroxiredoxin *Pf*Trx-Px1 is involved in the antioxidant defence of *Plasmodium falciparum*. Mol Biochem Parasitol 2003; 130: 75-81.
615. Luckhart S, Li K, Dunton R, Lewis EE, Crampton AL, Ryan JR, Rosenberg R. *Anopheles gambiae* immune gene variants associated with natural *Plasmodium* infection. Molecular & Biochemical Parasitology 2003; 128: 83-86.
616. Sandoval M, Liu X, Mannick EE, Clark DA, Miller MJ. Peroxynitrite-induced apoptosis in human intestinal epithelial cells is attenuated by mesalamine. Gastroenterology 1997; 113: 1480-1488.
617. Szabo C, Wong HR, Salzman AL. Pre-exposure to heat shock inhibits peroxynitrite-induced activation of poly(ADP) ribosyltransferase and protects against peroxynitrite cytotoxicity in J774 macrophages. Eur J Pharmacol 1996; 315: 221-226.
618. Skinner KA, White CR, Patel R, Tan S, Barnes S, Kirk M, Darley-Usmar V, Parks DA. Nitrosation of uric acid by peroxynitrite. Formation of a vasoactive nitric oxide donor. J Biol Chem 1998; 273: 24491-24497.
619. Borderie D, Hilliquin P, Hernvann A, Lemarechal H, Kahan A, Menkes CJ, Ekindjian OG. Inhibition of inducible NO synthase by TH2 cytokines and TGF-β in rheumatoid arthritic synoviocytes: Effects on nitrosothiol production. Nitric Oxide 2002; 6: 271-282.

620. MacMicking JD, North RJ, LaCourse R, Mudgett JS, Shah SK, Nathan CF. Identification of nitric oxide synthase as a protective locus against tuberculosis. Proc Natl Acad Sci U S A 1997; 94: 5243-5248.
621. Corradi M, Montuschi P, Donnelly LE, Pesci A, Kharitonov SA, Barnes PJ. Increased nitrosothiols in exhaled breath condensate in inflammatory airway diseases. Am J Respir Crit Care Med 2001; 163: 854-858.
622. Calabrese V, Scapagnini G, Ravagna A, Bella R, Foresti R, Bates TE, Giuffrida Stella AM, Pennisi G. Nitric oxide synthase is present in the cerebrospinal fluid of patients with active multiple sclerosis and is associated with increases in cerebrospinal fluid protein nitrotyrosine and *S*-nitrosothiols and with changes in glutathione levels. J Neurosci Res 2002; 70: 580-587.
623. Milsom AB, Jones CJ, Goodfellow J, Frenneaux MP, Peters JR, James PE. Abnormal metabolic fate of nitric oxide in Type I diabetes mellitus. Diabetologia 2002; 45: 1515-1522.
624. Tyurin VA, Liu SX, Tyurina YY, Sussman NB, Hubel CA, Roberts JM, Taylor RN, Kagan VE. Elevated levels of *S*-nitrosoalbumin in preeclampsia plasma. Circ Res 2001; 88: 1210-1215.
625. Binkert EF, Kolari OE. The history and use of nitrate and nitrite in the curing of meat. Food Cosmet Toxicol 1975; 13: 655-661.
626. Pedrajas JR, Miranda-Vizuete A, Javanmardy N, Gustafsson JA, Spyrou G. Mitochondria of *Saccharomyces cerevisiae* contain one-conserved cysteine type peroxiredoxin with thioredoxin peroxidase activity. J Biol Chem 2000; 275: 16296-16301.
627. Mongkolsuk S, Loprasert S, Whangsuk W, Fuangthong M, Atichartpongkun S. Characterization of transcription organization and analysis of unique expression patterns of an alkyl hydroperoxide reductase C gene (ahpC) and the peroxide regulator operon ahpF-oxyR-orfX from Xanthomonas campestris pv. phaseoli. J Bacteriol 1997; 179: 3950-3955.
628. Godon C, Lagniel G, Lee J, Buhler JM, Kieffer S, Perrot M, Boucherie H, Toledano MB, Labarre J. The H_2O_2 stimulon in *Saccharomyces cerevisiae*. J Biol Chem 1998; 273: 22480-22489.
629. Tachado SD, Gerold P, McConville MJ, Baldwin T, Quilici D, Schwarz RT, Schofield L. Glycosylphosphatidylinositol toxin of *Plasmodium* induces nitric oxide synthase expression in macrophages and vascular endothelial cells by a protein tyrosine kinase-dependent and protein kinase C-dependent signaling pathway. J Immunol 1996; 156: 1897-1907.
630. Chung YM, Yoo YD, Park JK, Kim YT, Kim HJ. Increased expression of peroxiredoxin II confers resistance to cisplatin. Anticancer Res 2001; 21: 1129-1133.
631. Koo KH, Lee S, Jeong SY, Kim ET, Kim HJ, Kim K, Song K, Chae HZ. Regulation of thioredoxin peroxidase activity by C-terminal truncation. Arch Biochem Biophys 2002; 397: 312-318.
632. Cumming RC, Andon NL, Haynes PA, Park M, Fischer WH, Schubert D. Protein disulfide bond formation in the cytoplasm during oxidative stress. J Biol Chem 2004; 279: 21749-21758.
633. Dietz KJ, Horling F, Konig J, Baier M. The function of the chloroplast 2-cysteine peroxiredoxin in peroxide detoxification and its regulation. J Exp Bot 2002; 53: 1321-1329.
634. Baier M, Dietz KJ. The plant 2-Cys peroxiredoxin BAS1 is a nuclear-encoded chloroplast protein: its expressional regulation, phylogenetic origin, and implications for its specific physiological function in plants. Plant J 1997; 12: 179-190.
635. Kim IH, Kim K, Rhee SG. Induction of an antioxidant protein of *Saccharomyces cerevisiae* by O_2, Fe^{3+}, or 2-mercaptoethanol. Proc Natl Acad Sci U S A 1989; 86: 6018-6022.
636. Yamamoto H, Miyake C, Dietz KJ, Tomizawa K, Murata N, Yokota A. Thioredoxin peroxidase in the *Cyanobacterium Synechocystis* sp. PCC 6803. FEBS Lett 1999; 447: 269-273.
637. Lee SP, Hwang YS, Kim YJ, Kwon KS, Kim HJ, Kim K, Chae HZ. Cyclophilin a binds to peroxiredoxins and activates its peroxidase activity. J Biol Chem 2001; 276: 29826-29832.
638. Banmeyer I, Marchand C, Verhaeghe C, Vucic B, Rees JF, Knoops B. Overexpression of human peroxiredoxin 5 in subcellular compartments of chinese hamster ovary cells: Effects on cytotoxicity and DNA damage caused by peroxides. Free Radic Biol Med 2004; 36: 65-77.
639. Kovach MJ, Carlson JO, Beaty BJ. A *Drosophila* metallothionein promoter is inducible in mosquito cells. Insect Mol Biol 1992; 1: 37-43.
640. Wu CC, Fallon AM. Evaluation of a heterologous metallothionein gene promoter in transfected mosquito cells. Comp Biochem Physiol B Biochem Mol Biol 1997; 116: 353-358.

641. Comtois SL, Gidley MD, Kelly DJ. Role of the thioredoxin system and the thiol-peroxidases Tpx and Bcp in mediating resistance to oxidative and nitrosative stress in *Helicobacter pylori*. Microbiology 2003; 149: 121-129.
642. Nguyen-nhu N, Knoops B. Alkyl hydroperoxide reductase 1 protects *Saccharomyces cerevisiae* against metal ion toxicity and glutathione depletion. Toxicol Lett 2002; 135: 219.
643. Wong CM, Zhou Y, Ng RW, Kung Hf H, Jin DY. (early ejournal version) Cooperation of yeast peroxiredoxins Tsa1p and Tsa2p in the cellular defense against oxidative and nitrosative stress. J Biol Chem 2002; 277: 5385-5394.
644. Isermann K, Liebau E, Roeder T, Bruchhaus I. A peroxiredoxin specifically expressed in two types of pharyngeal neurons is required for normal growth and egg production in *Caenorhabditis elegans*. J Mol Biol 2004; 338: 745-755.
645. Zamore PD, Tuschl T, Sharp PA, Bartel DP. RNAi: double-stranded RNA directs the ATP-dependent cleavage of mRNA at 21 to 23 nucleotide intervals. Cell 2000; 101: 25-33.
646. Bernstein E, Caudy AA, Hammond SM, Hannon GJ. Role for a bidentate ribonuclease in the initiation step of RNA interference. Nature 2001; 409: 363-366.
647. Haley B, Tang G, Zamore PD. *In vitro* analysis of RNA interference in *Drosophila melanogaster*. Methods 2003; 30: 330-336.
648. Zamore PD. Ancient pathways programmed by small RNAs. Science 2002; 296: 1265-1269.
649. Hoa NT, Keene KM, Olson KE, Zheng L. Characterization of RNA interference in an *Anopheles gambiae* cell line. Insect Biochem Mol Biol 2003; 33: 949-957.
650. Levashina EA, Moita LF, Blandin S, Vriend G, Lagueux M, Kafatos FC. Conserved role of a complement-like protein in phagocytosis revealed by dsRNA knockout in cultured cells of the mosquito, *Anopheles gambiae*. Cell 2001; 104: 709-718.
651. Brown AE, Crisanti A, Catteruccia F. Comparative analysis of DNA vectors at mediating RNAi in *Anopheles mosquito* cells and larvae. J Exp Biol 2003; 206: 1817-1823.
652. Clemens JC, Worby CA, Simonson-Leff N, Muda M, Maehama T, Hemmings BA, Dixon JE. Use of double-stranded RNA interference in *Drosophila* cell lines to dissect signal transduction pathways. Proc Natl Acad Sci U S A 2000; 97: 6499-6503.
653. Kennerdell JR, Carthew RW. Use of dsRNA-mediated genetic interference to demonstrate that frizzled and frizzled 2 act in the wingless pathway. Cell 1998; 95: 1017-1026.
654. Schmid A, Schindelholz B, Zinn K. Combinatorial RNAi: a method for evaluating the functions of gene families in *Drosophila*. Trends Neurosci 2002; 25: 71-74.
655. Do HM, Hong JK, Jung HW, Kim SH, Ham JH, Hwang BK. Expression of peroxidase-like genes, H_2O_2 production, and peroxidase activity during the hypersensitive response to *Xanthomonas campestris* pv. vesicatoria in *Capsicum annuum*. Mol Plant Microbe Interact 2003; 16: 196-205.
656. Geiben-Lynn R, Kursar M, Brown NV, Addo MM, Shau H, Lieberman J, Luster AD, Walker BD. HIV-1 antiviral activity of recombinant natural killer cell enhancing factors, NKEF-A and NKEF-B, members of the peroxiredoxin family. J Biol Chem 2003; 278: 1569-1574.
657. Rouhier N, Gelhaye E, Gualberto JM, Jordy MN, De Fay E, Hirasawa M, Duplessis S, Lemaire SD, Frey P, Martin F, Manieri W, Knaff DB, Jacquot JP. Poplar peroxiredoxin Q. A thioredoxin-linked chloroplast antioxidant functional in pathogen defense. Plant Physiol 2004; 134: 1027-1038.
658. Lee KS, Kim SR, Park NS, Kim I, Kang PD, Sohn BH, Choi KH, Kang SW, Je YH, Lee SM, Sohn HD, Jin BR. Characterization of a silkworm thioredoxin peroxidase that is induced by external temperature stimulus and viral infection. Insect Biochem Mol Biol 2005; 35: 73-84.
659. Vierstraete E, Verleyen P, Baggerman G, D'Hertog W, Van den Bergh G, Arckens L, De Loof A, Schoofs L. A proteomic approach for the analysis of instantly released wound and immune proteins in *Drosophila melanogaster* hemolymph. Proc Natl Acad Sci U S A 2004; 101: 470-475.
660. Chen W, Ji J, Xu X, He S, Ru B. Proteomic comparison between human young and old brains by two-dimensional gel electrophoresis and identification of proteins. Int J Dev Neurosci 2003; 21: 209-216.
661. Cho YM, Bae SH, Choi BK, Cho SY, Song CW, Yoo JK, Paik YK. Differential expression of the liver proteome in senescence accelerated mice. Proteomics 2003; 3: 1883-1894.
662. Sohal RS, Arnold L, Orr WC. Effect of age on superoxide dismutase, catalase, glutathione reductase, inorganic peroxides, TBA-reactive material, GSH/GSSG, NADPH/$NADP^+$ and NADH/NAD^+ in *Drosophila melanogaster*. Mech Ageing Dev 1990; 56: 223-235.

663. Berner R, Rudin W, Hecker H. Peritrophic membranes and protease activity in the midgut of the malaria mosquito, *Anopheles stephensi* (Liston) (Insecta: *Diptera*) under normal and experimental conditions. J Ultrastruct Res 1983; 83: 195-204.
664. Dix TA, Fontana R, Panthani A, Marnett LJ. Hematin-catalyzed epoxidation of 7,8-dihydroxy-7,8-dihydrobenzo[*a*]pyrene by polyunsaturated fatty acid hydroperoxides. J Biol Chem 1985; 260: 5358-5365.
665. Dansa-Petretski M, Ribeiro JM, Atella GC, Masuda H, Oliveira PL. Antioxidant role of *Rhodnius prolixus* heme-binding protein. Protection against heme-induced lipid peroxidation. J Biol Chem 1995; 270: 10893-10896.
666. Machado EA, Oliveira PL, Moreira MF, de Souza W, Masuda H. Uptake of *Rhodnius* heme-binding protein (RHBP) by the ovary of *Rhodnius prolixus*. Arch Insect Biochem Physiol 1998; 39: 133-143.
667. Oliveira PL, Kawooya JK, Ribeiro JM, Meyer T, Poorman R, Alves EW, Walker FA, Machado EA, Nussenzveig RH, Padovan GJ, Masuda H. A heme-binding protein from hemolymph and oocytes of the blood-sucking insect, *Rhodnius prolixus*. Isolation and characterization. J Biol Chem 1995; 270: 10897-10901.
668. Immenschuh S, Nell C, Iwahara S, Katz N, Muller-Eberhard U. Gene regulation of HBP 23 by metalloporphyrins and protoporphyrin IX in liver and hepatocyte cultures. Biochem Biophys Res Commun 1997; 231: 667-670.
669. Monteiro G, Pereira GA, Netto LE. Regulation of mitochondrial thioredoxin peroxidase I expression by two different pathways: one dependent on cAMP and the other on heme. Free Radic Biol Med 2002; 32: 278-288.
670. Watabe S, Hiroi T, Yamamoto Y, Fujioka Y, Hasegawa H, Yago N, Takahashi SY. SP-22 is a thioredoxin-dependent peroxide reductase in mitochondria. Eur J Biochem 1997; 249: 52-60.
671. Mitsumoto A, Takanezawa Y, Okawa K, Iwamatsu A, Nakagawa Y. Variants of peroxiredoxins expression in response to hydroperoxide stress. Free Radic Biol Med 2001; 30: 625-635.
672. Woo HA, Kang SW, Kim HK, Yang KS, Chae HZ, Rhee SG. Reversible oxidation of the active site cysteine of peroxiredoxins to cysteine sulfinic acid: Immunoblot detection with antibodies specific for the hyperoxidized cysteine-containing sequence. J Biol Chem 2003.
673. Wagner E, Luche S, Penna L, Chevallet M, Van Dorsselaer A, Leize-Wagner E, Rabilloud T. A method for detection of overoxidation of cysteines: peroxiredoxins are oxidized *in vivo* at the active-site cysteine during oxidative stress. Biochem J 2002; 366: 777-785.
674. Yang KS, Kang SW, Woo HA, Hwang SC, Chae HZ, Kim K, Rhee SG. Inactivation of human peroxiredoxin I during catalysis as the result of the oxidation of the catalytic site cysteine to cysteine-sulfinic acid. J Biol Chem 2002; 277: 38029-38036.
675. Woo HA, Chae HZ, Hwang SC, Yang KS, Kang SW, Kim K, Rhee SG. Reversing the inactivation of peroxiredoxins caused by cysteine sulfinic acid formation. Science 2003; 300: 653-656.
676. Chevallet M, Wagner E, Luche S, van Dorsselaer A, Leize-Wagner E, Rabilloud T. Regeneration of peroxiredoxins during recovery after oxidative stress: only some overoxidized peroxiredoxins can be reduced during recovery after oxidative stress. J Biol Chem 2003; 278: 37146-37153.
677. Jin DY, Chae HZ, Rhee SG, Jeang KT. Regulatory role for a novel human thioredoxin peroxidase in NF-κB activation. J Biol Chem 1997; 272: 30952-30961.
678. Jeong JS, Kwon SJ, Kang SW, Rhee SG, Kim K. Purification and characterization of a second type thioredoxin peroxidase (type II TPx) from *Saccharomyces cerevisiae*. Biochemistry 1999; 38: 776-783.
679. Lim YS, Cha MK, Kim HK, Kim IH. The thiol-specific antioxidant protein from human brain: gene cloning and analysis of conserved cysteine regions. Gene 1994; 140: 279-284.
680. Chae HZ, Kim HJ, Kang SW, Rhee SG. Characterization of three isoforms of mammalian peroxiredoxin that reduce peroxides in the presence of thioredoxin. Diabetes Res Clin Pract 1999; 45: 101-112.
681. Rahlfs S, Becker K. Thioredoxin peroxidases of the malarial parasite *Plasmodium falciparum*. Eur J Biochem 2001; 268: 1404-1409.
682. Cha MK, Yun CH, Kim IH. Interaction of human thiol-specific antioxidant protein 1 with erythrocyte plasma membrane. Biochemistry 2000; 39: 6944-6950.
683. Schroder E, Willis AC, Ponting CP. Porcine natural-killer-enhancing factor-B: oligomerisation and identification as a calpain substrate in vitro. Biochim Biophys Acta 1998; 1383: 279-291.

684. Kitano K, Niimura Y, Nishiyama Y, Miki K. Stimulation of peroxidase activity by decamerization related to ionic strength: AhpC protein from *Amphibacillus xylanus*. J Biochem (Tokyo) 1999; 126: 313-319.
685. Kristensen P, Rasmussen DE, Kristensen BI. Properties of thiol-specific anti-oxidant protein or calpromotin in solution. Biochem Biophys Res Commun 1999; 262: 127-131.
686. Allen DW, Cadman S. Calcium-induced erythrocyte membrane changes. The role of adsorption of cytosol proteins and proteases. Biochim Biophys Acta 1979; 551: 1-9.
687. Plishker GA, Chevalier D, Seinsoth L, Moore RB. Calcium-activated potassium transport and high molecular weight forms of calpromotin. J Biol Chem 1992; 267: 21839-21843.
688. Hillas PJ, del Alba FS, Oyarzabal J, Wilks A, Ortiz De Montellano PR. The AhpC and AhpD antioxidant defense system of *Mycobacterium tuberculosis*. J Biol Chem 2000; 275: 18801-18809.
689. Jung BG, Lee KO, Lee SS, Chi YH, Jang HH, Kang SS, Lee K, Lim D, Yoon SC, Yun DJ, Inoue Y, Cho MJ, Lee SY. A Chinese cabbage cDNA with high sequence identity to phospholipid hydroperoxide glutathione peroxidases encodes a novel isoform of thioredoxin-dependent peroxidase. J Biol Chem 2002; 277: 12572-12578.
690. Schwarz MA, Lazo JS, Yalowich JC, Allen WP, Whitmore M, Bergonia HA, Tzeng E, Billiar TR, Robbins PD, Lancaster JR, Jr., Pitt BR. Metallothionein protects against the cytotoxic and DNA-damaging effects of nitric oxide. Proc Natl Acad Sci U S A 1995; 92: 4452-4456.
691. Wang GW, Schuschke DA, Kang YJ. Metallothionein-overexpressing neonatal mouse cardiomyocytes are resistant to H_2O_2 toxicity. Am J Physiol 1999; 276: H167-175.
692. Sies H, Sharov VS, Klotz LO, Briviba K. Glutathione peroxidase protects against peroxynitrite-mediated oxidations. A new function for selenoproteins as peroxynitrite reductase. J Biol Chem 1997; 272: 27812-27817.
693. Asahi M, Fujii J, Suzuki K, Seo HG, Kuzuya T, Hori M, Tada M, Fujii S, Taniguchi N. Inactivation of glutathione peroxidase by nitric oxide. Implication for cytotoxicity. J Biol Chem 1995; 270: 21035-21039.
694. Stadtman ER. Protein oxidation and aging. Science 1992; 257: 1220-1224.
695. Grune T, Klotz LO, Gieche J, Rudeck M, Sies H. Protein oxidation and proteolysis by the nonradical oxidants singlet oxygen or peroxynitrite. Free Radic Biol Med 2001; 30: 1243-1253.
696. Sayed AA, Williams DL. Biochemical characterization of 2-Cys peroxiredoxins from *Schistosoma mansoni*. J Biol Chem 2004; 279: 26159-26166.
697. Biteau B, Labarre J, Toledano MB. ATP-dependent reduction of cysteine-sulphinic acid by *S. cerevisiae* sulphiredoxin. Nature 2003; 425: 980-984.
698. Chang TS, Jeong W, Woo HA, Lee SM, Park S, Rhee SG. Characterization of mammalian sulfiredoxin and its reactivation of hyperoxidized peroxiredoxin through reduction of cysteine sulfinic acid in the active site to cysteine. J Biol Chem 2004.
699. Woo HA, Jeong W, Chang TS, Park KJ, Park SJ, Yang JS, Rhee SG. Reduction of cysteine sulfinic acid by sulfiredoxin is specific to 2-cys peroxiredoxins. J Biol Chem 2005; 280: 3125-3128.
700. Bartholomay LC, Cho WL, Rocheleau TA, Boyle JP, Beck ET, Fuchs JF, Liss P, Rusch M, Butler KM, Wu RC, Lin SP, Kuo HY, Tsao IY, Huang CY, Liu TT, Hsiao KJ, Tsai SF, Yang UC, Nappi AJ, Perna NT, Chen CC, Christensen BM. Description of the transcriptomes of immune response-activated hemocytes from the mosquito vectors *Aedes aegypti* and *Armigeres subalbatus*. Infect Immun 2004; 72: 4114-4126.
701. Budanov AV, Sablina AA, Feinstein E, Koonin EV, Chumakov PM. Regeneration of peroxiredoxins by p53-regulated sestrins, homologs of bacterial AhpD. Science 2004; 304: 596-600.
702. Koshkin A, Nunn CM, Djordjevic S, Ortiz de Montellano PR. The mechanism of *Mycobacterium tuberculosis* alkylhydroperoxidase AhpD as defined by mutagenesis, crystallography, and kinetics. J Biol Chem 2003; 278: 29502-29508.
703. Wyllie AH, Kerr JF, Currie AR. Cell death: the significance of apoptosis. Int Rev Cytol 1980; 68: 251-306.
704. Sarafian TA, Bredesen DE. Is apoptosis mediated by reactive oxygen species? Free Radic Res 1994; 21: 1-8.
705. Slater AF, Stefan C, Nobel I, van den Dobbelsteen DJ, Orrenius S. Signalling mechanisms and oxidative stress in apoptosis. Toxicol Lett 1995; 82-83: 149-153.

706. Glockzin S, von Knethen A, Scheffner M, Brune B. Activation of the cell death program by nitric oxide involves inhibition of the proteasome. J Biol Chem 1999; 274: 19581-19586.
707. Murphy MP. Nitric oxide and cell death. Biochim Biophys Acta 1999; 1411: 401-414.
708. Ottaviani E, Barbieri D, Malagoli D, Franchini A. Nitric oxide induces apoptosis in the fat body cell line IPLB-LdFB from the insect *Lymantria dispar*. Comp Biochem Physiol B Biochem Mol Biol 2001; 128: 247-254.
709. Zhang P, Liu B, Kang SW, Seo MS, Rhee SG, Obeid LM. Thioredoxin peroxidase is a novel inhibitor of apoptosis with a mechanism distinct from that of Bcl-2. J Biol Chem 1997; 272: 30615-30618.
710. Mu ZM, Yin XY, Prochownik EV. Pag, a putative tumor suppressor, interacts with the Myc Box II domain of c-Myc and selectively alters its biological function and target gene expression. J Biol Chem 2002; 277: 43175-43184.
711. Ichimiya S, Davis JG, O'Rourke DM, Katsumata M, Greene MI. Murine thioredoxin peroxidase delays neuronal apoptosis and is expressed in areas of the brain most susceptible to hypoxic and ischemic injury. DNA Cell Biol 1997; 16: 311-321.
712. Chang TS, Cho CS, Park S, Yu S, Kang SW, Rhee SG. Peroxiredoxin III, a mitochondrion-specific peroxidase, regulates apoptotic signaling by mitochondria. J Biol Chem 2004; 279: 41975-41984.
713. Yuan J, Murrell GA, Trickett A, Landtmeters M, Knoops B, Wang MX. Overexpression of antioxidant enzyme peroxiredoxin 5 protects human tendon cells against apoptosis and loss of cellular function during oxidative stress. Biochim Biophys Acta 2004; 1693: 37-45.
714. Pak JH, Manevich Y, Kim HS, Feinstein SI, Fisher AB. An antisense oligonucleotide to 1-cys peroxiredoxin causes lipid peroxidation and apoptosis in lung epithelial cells. J Biol Chem 2002; 277: 49927-49934.
715. Polyak K, Xia Y, Zweier JL, Kinzler KW, Vogelstein B. A model for p53-induced apoptosis. Nature 1997; 389: 300-305.
716. Wong CM, Chun AC, Kok KH, Zhou Y, Fung PC, Kung HF, Jeang KT, Jin DY. Characterization of human and mouse peroxiredoxin IV: evidence for inhibition by Prx-IV of epidermal growth factor- and p53-induced reactive oxygen species. Antioxid Redox Signal 2000; 2: 507-518.
717. Zhou Y, Kok KH, Chun AC, Wong CM, Wu HW, Lin MC, Fung PC, Kung H, Jin DY. Mouse peroxiredoxin V is a thioredoxin peroxidase that inhibits p53-induced apoptosis. Biochem Biophys Res Commun 2000; 268: 921-927.
718. Sullivan DM, Wehr NB, Fergusson MM, Levine RL, Finkel T. Identification of oxidant-sensitive proteins: TNF-alpha induces protein glutathiolation. Biochemistry 2000; 39: 11121-11128.
719. Butterfield LH, Merino A, Golub SH, Shau H. From cytoprotection to tumor suppression: the multifactorial role of peroxiredoxins. Antioxid Redox Signal 1999; 1: 385-402.
720. Shau H, Huang AC, Faris M, Nazarian R, de Vellis J, Chen W. Thioredoxin peroxidase (natural killer enhancing factor) regulation of activator protein-1 function in endothelial cells. Biochem Biophys Res Commun 1998; 249: 683-686.
721. Budanov AV, Shoshani T, Faerman A, Zelin E, Kamer I, Kalinski H, Gorodin S, Fishman A, Chajut A, Einat P, Skaliter R, Gudkov AV, Chumakov PM, Feinstein E. Identification of a novel stress-responsive gene Hi95 involved in regulation of cell viability. Oncogene 2002; 21: 6017-6031.
722. Henriksson M, Luscher B. Proteins of the Myc network: essential regulators of cell growth and differentiation. Adv Cancer Res 1996; 68: 109-182.
723. Wonsey DR, Zeller KI, Dang CV. The c-Myc target gene PRDX3 is required for mitochondrial homeostasis and neoplastic transformation. Proc Natl Acad Sci U S A 2002; 99: 6649-6654.
724. Tenev T, Zachariou A, Wilson R, Paul A, Meier P. Jafrac2 is an IAP antagonist that promotes cell death by liberating Dronc from DIAP1. Embo J 2002; 21: 5118-5129.
725. Silverman N, Maniatis T. NF-κB signaling pathways in mammalian and insect innate immunity. Genes Dev 2001; 15: 2321-2342.
726. Janssen-Heininger YM, Poynter ME, Baeuerle PA. Recent advances towards understanding redox mechanisms in the activation of nuclear factor kappaB. Free Radic Biol Med 2000; 28: 1317-1327.
727. LaCasse EC, Baird S, Korneluk RG, MacKenzie AE. The inhibitors of apoptosis (IAPs) and their emerging role in cancer. Oncogene 1998; 17: 3247-3259.

728. Xie QW, Kashiwabara Y, Nathan C. Role of transcription factor NF-κB/Rel in induction of nitric oxide synthase. J Biol Chem 1994; 269: 4705-4708.
729. Marshall HE, Stamler JS. Nitrosative stress-induced apoptosis through inhibition of NF-κB. J Biol Chem 2002; 28: 28.
730. Haridas V, Ni J, Meager A, Su J, Yu GL, Zhai Y, Kyaw H, Akama KT, Hu J, Van Eldik LJ, Aggarwal BB. TRANK, a novel cytokine that activates NF-κB and c-Jun N-terminal kinase. J Immunol 1998; 161: 1-6.
731. Simzar S, Ellyin R, Shau H, Sarafian TA. Contrasting antioxidant and cytotoxic effects of peroxiredoxin I and II in PC12 and NIH3T3 cells. Neurochem Res 2000; 25: 1613-1621.
732. Jang HH, Lee KO, Chi YH, Jung BG, Park SK, Park JH, Lee JR, Lee SS, Moon JC, Yun JW, Choi YO, Kim WY, Kang JS, Cheong GW, Yun DJ, Rhee SG, Cho MJ, Lee SY. Two enzymes in one; two yeast peroxiredoxins display oxidative stress-dependent switching from a peroxidase to a molecular chaperone function. Cell 2004; 117: 625-635.
733. Chang TS, Jeong W, Choi SY, Yu S, Kang SW, Rhee SG. Regulation of peroxiredoxin I activity by Cdc2-mediated phosphorylation. J Biol Chem 2002; 277: 25370-25376.
734. Kawazu S, Komaki K, Tsuji N, Kawai S, Ikenoue N, Hatabu T, Ishikawa H, Matsumoto Y, Himeno K, Kano S. Molecular characterization of a 2-Cys peroxiredoxin from the human malaria parasite *Plasmodium falciparum*. Mol Biochem Parasitol 2001; 116: 73-79.
735. Berendji D, Kolb-Bachofen V, Meyer KL, Kroncke KD. Influence of nitric oxide on the intracellular reduced glutathione pool: different cellular capacities and strategies to encounter nitric oxide-mediated stress. Free Radic Biol Med 1999; 27: 773-780.
736. Nikulina MA, Andersen HU, Karlsen AE, Darville MI, Eizirik DL, Mandrup-Poulsen T. Glutathione depletion inhibits IL-1 beta-stimulated nitric oxide production by reducing inducible nitric oxide synthase gene expression. Cytokine 2000; 12: 1391-1394.
737. Saeij JP, van Muiswinkel WB, van de Meent M, Amaral C, Wiegertjes GF. Different capacities of carp leukocytes to encounter nitric oxide-mediated stress: a role for the intracellular reduced glutathione pool. Dev Comp Immunol 2003; 27: 555-568.
738. Folkes LK, Wardman P. Kinetics of the reaction between nitric oxide and glutathione: implications for thiol depletion in cells. Free Radic Biol Med 2004; 37: 549-556.
739. Aslund F, Beckwith J. Bridge over troubled waters: sensing stress by disulfide bond formation. Cell 1999; 96: 751-753.
740. Leyens G, Donnay I, Knoops B. Cloning of bovine peroxiredoxins-gene expression in bovine tissues and amino acid sequence comparison with rat, mouse and primate peroxiredoxins. Comp Biochem Physiol B Biochem Mol Biol 2003; 136: 943-955.
741. Ishii T, Yamada M, Sato H, Matsue M, Taketani S, Nakayama K, Sugita Y, Bannai S. Cloning and characterization of a 23-kDa stress-induced mouse peritoneal macrophage protein. J Biol Chem 1993; 268: 18633-18636.
742. Shau H, Butterfield LH, Chiu R, Kim A. Cloning and sequence analysis of candidate human natural killer-enhancing factor genes. Immunogenetics 1994; 40: 129-134.
743. Kawai S, Takeshita S, Okazaki M, Kikuno R, Kudo A, Amann E. Cloning and characterization of OSF-3, a new member of the MER5 family, expressed in mouse osteoblastic cells. J Biochem (Tokyo) 1994; 115: 641-643.
744. Prosperi MT, Ferbus D, Karczinski I, Goubin G. A human cDNA corresponding to a gene overexpressed during cell proliferation encodes a product sharing homology with amoebic and bacterial proteins. J Biol Chem 1993; 268: 11050-11056.
745. Lim YS, Cha MK, Kim HK, Uhm TB, Park JW, Kim K, Kim IH. Removals of hydrogen peroxide and hydroxyl radical by thiol-specific antioxidant protein as a possible role in vivo. Biochem Biophys Res Commun 1993; 192: 273-280.
746. Chae HZ, Kim IH, Kim K, Rhee SG. Cloning, sequencing, and mutation of thiol-specific antioxidant gene of *Saccharomyces cerevisiae*. J Biol Chem 1993; 268: 16815-16821.
747. Schroder E, Isupov MN, Naran A, Littlechild JA. Crystallization and preliminary X-ray analysis of human thioredoxin peroxidase-B from red blood cells. Acta Crystallogr D Biol Crystallogr 1999; 55 (Pt 2): 536-538.
748. Tsuji K, Copeland NG, Jenkins NA, Obinata M. Mammalian antioxidant protein complements alkylhydroperoxide reductase (ahpC) mutation in *Escherichia coli*. Biochem J 1995; 307 (Pt 2): 377-381.

749. Yamamoto T, Matsui Y, Natori S, Obinata M. Cloning of a housekeeping-type gene (MER5) preferentially expressed in murine erythroleukemia cells. Gene 1989; 80: 337-343.
750. Watabe S, Kohno H, Kouyama H, Hiroi T, Yago N, Nakazawa T. Purification and characterization of a substrate protein for mitochondrial ATP-dependent protease in bovine adrenal cortex. J Biochem (Tokyo) 1994; 115: 648-654.
751. Baker LM, Poole LB. Catalytic mechanism of thiol peroxidase from *Escherichia coli*. Sulfenic acid formation and overoxidation of essential CYS61. J Biol Chem 2003; 278: 9203-9211.
752. Cha MK, Kim HK, Kim IH. Thioredoxin-linked "thiol peroxidase" from periplasmic space of *Escherichia coli*. J Biol Chem 1995; 270: 28635-28641.
753. Wan XY, Zhou Y, Yan ZY, Wang HL, Hou YD, Jin DY. Scavengase p20: a novel family of bacterial antioxidant enzymes. FEBS Lett 1997; 407: 32-36.
754. Kropotov A, Sedova V, Ivanov V, Sazeeva N, Tomilin A, Krutilina R, Oei SL, Griesenbeck J, Buchlow G, Tomilin N. A novel human DNA-binding protein with sequence similarity to a subfamily of redox proteins which is able to repress RNA-polymerase-III-driven transcription of the Alu-family retroposons *in vitro*. Eur J Biochem 1999; 260: 336-346.
755. Park SG, Cha MK, Jeong W, Kim IH. Distinct physiological functions of thiol peroxidase isoenzymes in *Saccharomyces cerevisiae*. J Biol Chem 2000; 275: 5723-5732.
756. Lee J, Spector D, Godon C, Labarre J, Toledano MB. A new antioxidant with alkyl hydroperoxide defense properties in yeast. J Biol Chem 1999; 274: 4537-4544.
757. Fisher AB, Dodia C. Role of phospholipase A2 enzymes in degradation of dipalmitoylphosphatidylcholine by granular pneumocytes. J Lipid Res 1996; 37: 1057-1064.
758. Phelan SA. AOP2 (antioxidant protein 2): structure and function of a unique thiol-specific antioxidant. Antioxid Redox Signal 1999; 1: 571-584.
759. Power JH, Nicholas TE. Immunohistochemical localization and characterization of a rat Clara cell 26-kDa protein (CC26) with similarities to glutathione peroxidase and phospholipase A2. Exp Lung Res 1999; 25: 379-392.
760. Frank S, Munz B, Werner S. The human homologue of a bovine non-selenium glutathione peroxidase is a novel keratinocyte growth factor-regulated gene. Oncogene 1997; 14: 915-921.
761. Iakoubova OA, Pacella LA, Her H, Beier DR. LTW4 protein on mouse chromosome 1 is a member of a family of antioxidant proteins. Genomics 1997; 42: 474-478.
762. Stacy RA, Munthe E, Steinum T, Sharma B, Aalen RB. A peroxiredoxin antioxidant is encoded by a dormancy-related gene, Per1, expressed during late development in the aleurone and embryo of barley grains. Plant Mol Biol 1996; 31: 1205-1216.
763. Sandoval M, Ronzio RA, Muanza DN, Clark DA, Miller MJ. Peroxynitrite-induced apoptosis in epithelial (T84) and macrophage (RAW 264.7) cell lines: effect of legume-derived polyphenols (phytolens). Nitric Oxide 1997; 1: 476-483.
764. Stamler JS. Redox signaling: nitrosylation and related target interactions of nitric oxide. Cell 1994; 78: 931-936.
765. Ascenzi P, Bocedi A, Gentile M, Visca P, Gradoni L. Inactivation of parasite cysteine proteinases by the NO-donor 4-(phenylsulfonyl)-3-((2-(dimethylamino)ethyl)thio)-furoxan oxalate. Biochim Biophys Acta 2004; 1703: 69-77.
766. Bocedi A, Gradoni L, Menegatti E, Ascenzi P. Kinetics of parasite cysteine proteinase inactivation by NO-donors. Biochem Biophys Res Commun 2004; 315: 710-718.
767. Rosenthal PJ, Lee GK, Smith RE. Inhibition of a *Plasmodium vinckei* cysteine proteinase cures murine malaria. J Clin Invest 1993; 91: 1052-1056.
768. Rosenthal PJ, McKerrow JH, Aikawa M, Nagasawa H, Leech JH. A malarial cysteine proteinase is necessary for hemoglobin degradation by *Plasmodium falciparum*. J Clin Invest 1988; 82: 1560-1566.
769. Sherman IW. Biochemistry of *Plasmodium* (malarial parasites). Microbiol Rev 1979; 43: 453-495.
770. Savvides SN, Scheiwein M, Bohme CC, Arteel GE, Karplus PA, Becker K, Schirmer RH. Crystal structure of the antioxidant enzyme glutathione reductase inactivated by peroxynitrite. J Biol Chem 2002; 277: 2779-2784.
771. Sinden RE, Barker GC, Paton MJ, Fleck SL, Butcher GA, Waters A, Janse CJ, Rodriguez MH. Factors regulating natural transmission of *Plasmodium berghei* to the mosquito vector, and the cloning of a transmission-blocking immunogen. Parassitologia 1993; 35 Suppl: 107-112.

772. Dessens JT, Beetsma AL, Dimopoulos G, Wengelnik K, Crisanti A, Kafatos FC, Sinden RE. CTRP is essential for mosquito infection by malaria ookinetes. Embo J 1999; 18: 6221-6227.
773. Dessens JT, Siden-Kiamos I, Mendoza J, Mahairaki V, Khater E, Vlachou D, Xu XJ, Kafatos FC, Louis C, Dimopoulos G, Sinden RE. SOAP, a novel malaria ookinete protein involved in mosquito midgut invasion and oocyst development. Mol Microbiol 2003; 49: 319-329.
774. Sharma A, Mishra NC. Inhibition of a protein tyrosine kinase activity in *Plasmodium falciparum* by chloroquine. Indian J Biochem Biophys 1999; 36: 299-304.
775. Sharma A. Protein tyrosine kinase activity in human malaria parasite *Plasmodium falciparum*. Indian J Exp Biol 2000; 38: 1222-1226.
776. Lobysheva, II, Serezhenkov VA, Vanin AF. Interaction of peroxynitrite and hydrogen peroxide with dinitrosyl iron complexes containing thiol ligands *in vitro*. Biochemistry (Mosc) 1999; 64: 153-158.
777. Wink DA, Cook JA, Pacelli R, DeGraff W, Gamson J, Liebmann J, Krishna MC, Mitchell JB. The effect of various nitric oxide-donor agents on hydrogen peroxide-mediated toxicity: a direct correlation between nitric oxide formation and protection. Arch Biochem Biophys 1996; 331: 241-248.
778. Wink DA, Vodovotz Y, DeGraff W, Cook JA, Pacelli R, Krishna M, Mitchell JB. Chapter 9: Cytoprotective effects of NO against oxidative injury. In: Fang FC (ed.) Nitric Oxide and Infection. New York, NY: Kluwer Academic/Plenum Publishers; 1999: 189-213.
779. Gutierrez HH, Nieves B, Chumley P, Rivera A, Freeman BA. Nitric oxide regulation of superoxide-dependent lung injury: oxidant-protective actions of endogenously produced and exogenously administered nitric oxide. Free Radic Biol Med 1996; 21: 43-52.
780. Sarti P, Avigliano L, Gorlach A, Brune B. Superoxide and nitric oxide--participation in cell communication. Cell Death Differ 2002; 9: 1160-1162.
781. Trujillo M, Radi R. Peroxynitrite reaction with the reduced and the oxidized forms of lipoic acid: new insights into the reaction of peroxynitrite with thiols. Arch Biochem Biophys 2002; 397: 91-98.
782. Kaplan SS, Lancaster JR, Jr., Basford RE, Simmons RL. Effect of nitric oxide on staphylococcal killing and interactive effect with superoxide. Infect Immun 1996; 64: 69-76.

VITA

Tina Marie Loane Peterson was born to Allan and Theresa (Teri) Loane on November 4th, 1974. At the age of nine her family moved from the US to the Netherlands. She earned an International Baccalaureate (IB) Diploma with high level classes in Biology, Chemistry and Mathematics from Genèva, Switzerland in July 1993. Following graduation from the Alberdingk Thijm College in Hilversum, she left "Holland" to attend Virginia Tech. With a Dutch inspired love for dairy, she actively participated in the Dairy Products Evaluation Team under the guidance of Dr. Susan Duncan. She graduated *summa cum laude* with a B.S. in Food Science & Technology and a minor in Biology in May 1997. After working for Nestlé in the QA/QC department, she re-entered Virginia Tech as a Biochemistry doctoral candidate in January 1999. After taking a short time off following the birth of her daughter, she completed the requirements for the Ph.D. in summer 2005.